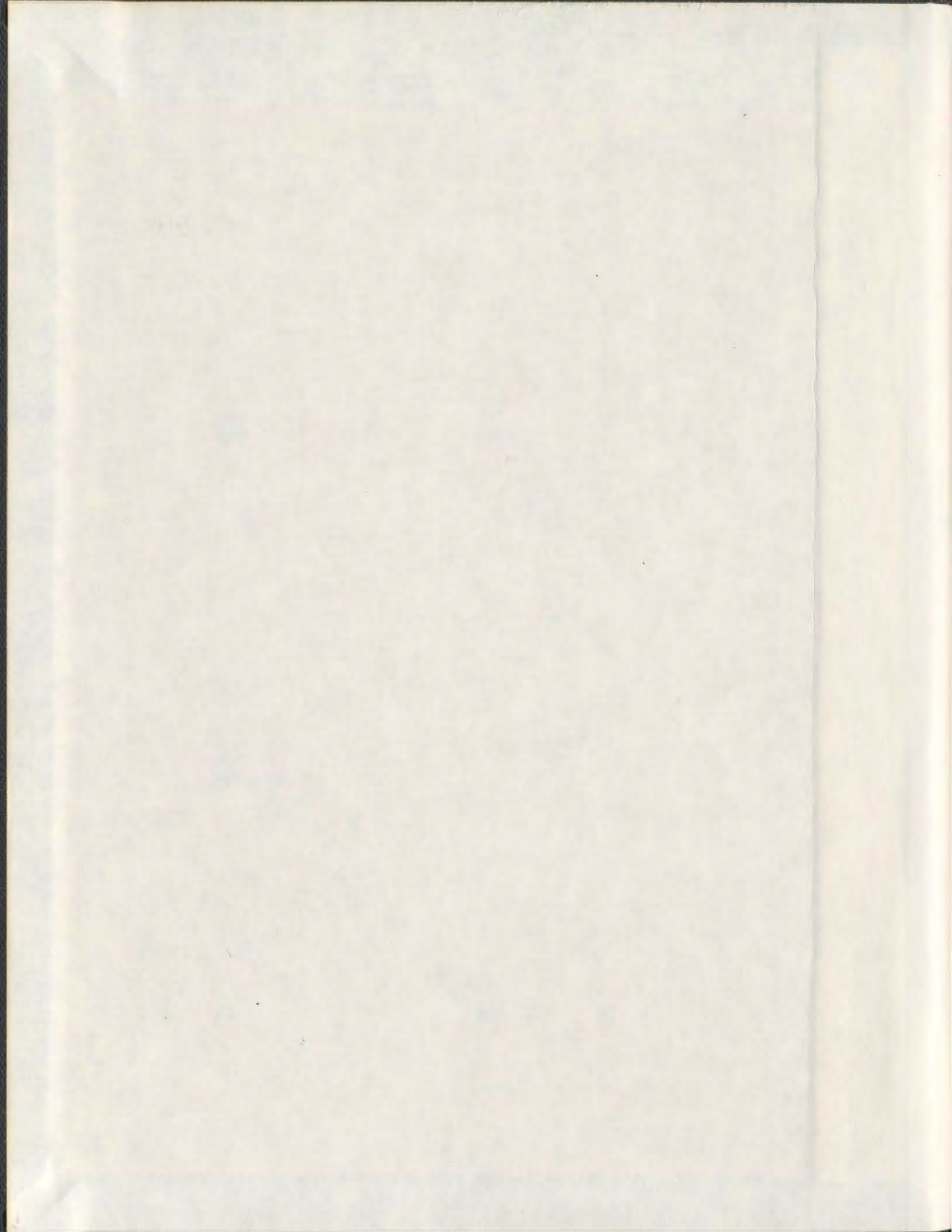


STUDY OF NEW FUNCTIONAL ORGANIC MATERIALS
BASED ON π -CONJUGATED OLIGOMERS AND
[60] FULLERENE

NINGZHANG ZHOU



001311



Study of New Functional Organic Materials Based on π -Conjugated Oligomers and [60]Fullerene

by

© Ningzhang Zhou

A thesis submitted to the
School of Graduate Studies
in partial fulfilment of the
requirements for the degree of
Doctor of Philosophy

Department of Chemistry
Memorial University of Newfoundland

December 2008

St. John's

Newfoundland

Abstract

In recent years, monodisperse and structurally defined π -conjugated oligomers have attracted great attention of materials chemists, owing to their fascinating applications as novel nanoscale building blocks for various molecular based electronic, photonic, and optoelectronic devices. To date, the molecular architectures of functional π -oligomers have evolved beyond the realm of simple one-dimensional (1D) linear conjugation and started to enlist some unique two-dimensional (2D) and three-dimensional (3D) structures. Such progress has opened a new avenue to develop and explore esoteric molecular materials with appealing and unprecedented molecular properties and functions, which can be of great use in various device fabrications, for instance, highly efficient organic light-emitting diodes (OLEDs), field-effect transistors (FETs), photovoltaic (PV) or solar cells, chemical and biological sensors, and so on.

The work of this thesis is primarily dedicated to exploring a class of new hybrid organic materials based on π -conjugated oligomers and Buckminster[60]fullerene (C_{60}), and the detailed studies of which are divided into three major projects. The first project investigates a series of dumbbell shaped C_{60} - π - C_{60} triads, in which the π units are designed to be linear or cruciform shaped OPE/OPV co-oligomers. The second project deals with a series of bifullerene endcapped oligoynes, and the third project embarks on a group of novel H-shaped OPE/OPV co-oligomers. The chemical synthesis of these conjugated oligomers and C_{60} derivatives has been implemented on the basis of various classical and modern organic synthetic methodologies, such as Arbuzov reaction, Horner-Wittig reaction, Sonogashira coupling and Hay coupling.

In particular, an in situ ethynylation protocol has been extensively employed in the synthesis of numerous C_{60} derivatives throughout this thesis work. Subsequent to the synthesis, the compounds obtained are subjected to comprehensive property characterizations using UV-Vis absorption and fluorescence spectroscopy to disclose their π -electronic characteristic, cyclic voltammetry (CV) to probe their redox behavior, differential scanning calorimetry (DSC) to probe their solid-state reactivity, and atomic force microscopy (AFM) to reveal their surface morphologic features at the microscopic level.

In this thesis, a number of efficient synthetic strategies for novel 1D and 2D conjugated OPE/OPV co-oligomers, linear and star-shaped phenylene-oligoynes, and related multiple C_{60} adducts have been successfully established. Insight into the essential structure-property relationships of these novel π -conjugated molecular systems has been gained by comparative studies. Finally, some of the molecules are found to display appealing molecular properties and functions that portend practical uses in organic photovoltaic and nonlinear optical materials as well as molecular sensing devices.

Acknowledgements

Firstly, I would like to express my deep and sincere gratitude to my supervisor, Prof. Yuming Zhao, both for his offering me this precious opportunity to receive a doctoral education and for his guidance during my four-year research and study program at Memorial University of Newfoundland. His perpetual enthusiasm and energy in research have motivated me all the time. He was always accessible and willing to help his students with their research and study. I have to say that I have been so lucky to have a supervisor who cared so much about my work and who responded to my questions and queries always promptly. As a result, research life became smooth and rewarding for me.

I would also like to acknowledge my supervisory committee members, Prof. David Thompson and Prof. Sunil Pansare, for the many helpful suggestions they made during my research work.

I would like to further thank Prof. David Thompson and his graduate student Ms. Li Wang who have provided wonderful collaborations on the property study of my synthesized compounds. I am also grateful to Prof. Erika Merschrod as well, who has been another wonderful collaborator during my research.

It has been a great privilege for me to study at Memorial University. I would like to thank my group members, the organic chemistry division, and all the staff at the general office of the Chemistry Department for their kind assistance.

The help from staff in C-CART in terms of NMR, MS, IR spectroscopic analyses, and the financial support from the department, graduate school, and NSERC are also greatly appreciated.

Finally, I wish to convey my greatest love and gratitude to my parents, my wife and my son. As the parents of four children, my mother and father did their best in raising me and my sisters and brother. During these four years of study, I have been living with my wife, Ying Song, and my son, Ran Zhou. Certainly, parts of my successful achievements during my PhD studies are due to my wife and my son's love and support which have bestowed upon me huge quantities of energy to carry on my PhD program.

Contents

Abstract	ii
Acknowledgements	iv
List of Figures	x
List of Schemes	xv
List of Tables	xx
List of Abbreviations and Symbols	xxi
1 Introduction	1
1.1 An overview of monodisperse π -conjugated oligomers	1
1.1.1 A brief historical account of polymer science	1
1.1.2 The significance of monodisperse π -conjugated oligomers . . .	4
1.1.3 A general survey of conjugated oligomers	10
1.1.3.1 Conjugated oligomers containing aromatic rings . . .	10
1.1.3.2 Conjugated oligomers made up of nonaromatic repeating units	29

1.1.4	Device applications of π -conjugated oligomers	43
1.1.4.1	Organic light-emitting diodes	43
1.1.4.2	Organic field effect transistors	47
1.1.4.3	Organic solar cells	50
1.2	A brief introduction to [60]fullerene C_{60}	55
1.2.1	The discovery of C_{60}	55
1.2.2	The production of C_{60}	57
1.2.3	The structure and chemical properties of C_{60}	58
1.2.4	Major chemical reactions of C_{60}	61
1.2.4.1	Addition of carbon nucleophiles	61
1.2.4.2	Cycloadditions on C_{60}	66
1.3	Outline of the thesis	77
2	OPE/OPV Co-Oligomer Bridged Bisfullerene Triads	80
2.1	Introduction	80
2.2	Results and discussion	87
2.2.1	Synthesis	87
2.2.1.1	Linear-shaped OPE/OPV oligomers and related C_{60} π - C_{60} derivatives	87
2.2.1.2	Cruciform-shaped OPE/OPV oligomers and related C_{60} - π - C_{60} derivatives	91
2.2.1.3	A simple phenylene ethynylene C_{60} model system	97
2.2.2	NMR spectroscopic and electrochemical properties of C_{60} OPE/OPV C_{60} derivatives	100

2.2.2.1	UV-Vis absorption properties	105
2.2.2.2	Excited-state properties	111
2.3	Conclusions	114
2.4	Experimental	116
3	Synthesis and Solid-State Properties of C₆₀ Endcapped Oligoynes	156
3.1	Introduction	156
3.2	Results and discussion	166
3.2.1	Synthesis of C ₆₀ -oligoynes adducts	166
3.2.1.1	Butadiyne-bridged C ₆₀ π C ₆₀ molecular dumbbells	166
3.2.1.2	Hexatriyne-bridged C ₆₀ π C ₆₀ molecular dumbbells	168
3.2.1.3	Octatetrayne-bridged C ₆₀ π C ₆₀ molecular dumbbells	169
3.2.1.4	Dodecahexayne-bridged C ₆₀ π C ₆₀ molecular dumbbells	174
3.2.1.5	Star-shaped tetrafullerene-oligoynes adducts	176
3.2.2	Spectroscopic and microscopic characterizations of thermally induced solid-state polymerization	183
3.2.2.1	Differential scanning calorimetric analysis	183
3.2.2.2	UV-Vis spectroscopic analysis	186
3.2.2.3	Study of morphological properties by atomic force microscopy	192
3.3	Conclusions	196
3.4	Experimental	197
4	Study of 2D Conjugated H-Shaped OPE/OPV Fluorophores	234

4.1	Introduction	234
4.2	Results and discussion	245
4.2.1	Synthesis of OPE/OPV based H-mers	245
4.2.1.1	Synthesis of long H-mer series	245
4.2.1.2	Synthesis of short H-mer series	255
4.2.2	Electronic spectroscopic properties	263
4.2.2.1	Electronic spectroscopic properties of long H-mers	263
4.2.2.2	Electronic spectroscopic properties of short H-mers	265
4.2.3	Molecular sensing properties of functional H-mers	266
4.3	Conclusions	271
4.4	Experimental	275
5	Conclusions and Future Work	318
5.1	Concluding remarks	318
5.2	Future work	321
	Bibliography	325

List of Figures

1.1	Examples of classical synthetic polymers.	3
1.2	Monodisperse oligo(phenylenevinylene)s 1a-g synthesized by Meier and co-workers.	7
1.3	Structural factors determining the bandgap of a π -conjugated oligomer.	8
1.4	Structures of oligo(phenylenevinylene)s 2a-f	8
1.5	Structures of OPs 3a-g	11
1.6	Structure of ladder-type PPP 16	14
1.7	Structures of perfluorinated OPs 22a-d	17
1.8	Structure of molecular wire 33	18
1.9	Soluble OPVs synthesized by Müllen <i>et al.</i>	21
1.10	Structures of <i>cis</i> -OPV 51a-d and <i>trans</i> -OPVs 52a-d	23
1.11	Structures of OPEs 56a-h	25
1.12	Structures of <i>ortho</i> -linked OPEs 57a-e	26
1.13	<i>Meta</i> -OPEs 68a-i (inset, upper left). Also shown is octadecamer 68i in a representative random coil conformation.	28
1.14	Structure of a C_{60} -wheeled nanocar 69	29
1.15	Structures of <i>tert</i> -butyl endcapped oligoenes 77a-c	32

1.16	Oligoenes 78 prepared by Schrock.	32
1.17	Structure of a polymer sp-carbon allotrope, "carbyne" 86	34
1.18	Structures of endcapped polyynes 87-89	34
1.19	Structures of polyynes 90 and 91	35
1.20	Oligoyne 98a-g and the synthesis of oligoynes 98d and 98f based on a modified FBW rearrangement.	38
1.21	Structures of linear and cross-conjugated enyne oligomers.	39
1.22	Oligo(triacetylene)s 122a-g synthesized by Diederich and co-workers.	41
1.23	Isopropylidene based <i>iso</i> -PDAs by Tykwinski and Zhao.	41
1.24	Schematics of the basic structure of an OLED.	44
1.25	Structures of blue-light emitting oligoquinolines 131a-d	46
1.26	Structures of fluoro-substituted oligo(arylenevinylene)s 132	47
1.27	Basic structure of an OFET.	48
1.28	Schematics of an OFET circuit.	49
1.29	Basic structure of an organic solar cell.	52
1.30	Basic principle of organic solar cells.	53
1.31	Structures of C ₆₀ and oligothiophene 135	53
1.32	Structures of compounds 136 and 137	54
1.33	Structures of fullerene-OPE hybrids 138a-b	55
1.34	Structures of corannulene.	56
1.35	Structure of C ₆₀	58
1.36	Bond angle strain of C ₆₀	59
1.37	C ₆₀ isomers of [5,6]-Closed and open, [6,6]-closed and open structures.	60
1.38	A C ₆₀ based X-ray contrast agent reported by Wilson.	65

1.39	Structure of phthalocyanine-fullerene hybrid 183	76
2.1	Carotenoid-functionalized C_{60} derivative 189 reported by Imahori. . .	82
2.2	C_{60} -OPV dyad 190 prepared by Nierengarten <i>et al.</i>	83
2.3	C_{60} -OT dyad 191 and triads 192-193 prepared by Otsubo <i>et al.</i> . . .	84
2.4	Dumbbell-shaped C_{60} - π - C_{60} triads 194-195	85
2.5	C_{60} - π - C_{60} molecular dumbbells 196-198 and related compound 199 targeted in the work described in this chapter.	87
2.6	Structure of OPE/OPV co-oligomer 217	91
2.7	Comparison of ^{13}C NMR spectra for C_{60} -OPE/OPV- C_{60} compounds 196-198 in the region of 135-149 ppm.	102
2.8	Cyclic voltammograms of compounds 196-198	104
2.9	Normalized UV-Vis spectra for short OPE/OPV co-oligomers 212 , 225 , and 238 measured in $CHCl_3$	106
2.10	Normalized UV-Vis spectra for long OPE/OPV co-oligomers 216 , 228 , and 240 measured in $CHCl_3$	107
2.11	Normalized UV-Vis spectra for C_{60} - π - C_{60} triads 196 , 197 , and 198 measured in degassed $CHCl_3$ or toluene.	109
2.12	UV-Vis spectra for C_{60} - π model compound 199 , phenyl acetylene 242 , and pristine C_{60}	110
2.13	Fluorescence spectra of short OPE/OPV co-oligomers 212 , 225 , and 238 measured in degassed $CHCl_3$	112
2.14	Fluorescence spectra for long OPE/OPV oligomers 216 , 228 , and 240 measured in degassed $CHCl_3$	113

2.15	Proposed photoexcitation and deactivation pathways for $C_{60} \pi C_{60}$ hybrids.	116
3.1	Target bisfullerene-oligoynes molecular dumbbells 259 , 260 and 261 in this chapter.	165
3.2	Target star-shaped tetrafullerene-oligoynes adducts 262 in this chapter.	166
3.3	Structures of star-shaped bisfullerene-oligoynes adducts 290a-b	176
3.4	DSC profiles for (A) diyne precursor 265 , (B) tetrayne precursor 280 , (C) short C_{60} diyne C_{60} 259a , (D) short C_{60} tetrayne C_{60} 260a , (E) long C_{60} diyne C_{60} 259b , and (F) long C_{60} tetrayne C_{60} 260b	185
3.5	UV-Vis spectra of short C_{60} diyne C_{60} dumbbell 259a	186
3.6	UV-Vis spectra of long C_{60} diyne C_{60} dumbbell 259b	187
3.7	UV-Vis spectra of short C_{60} tetrayne C_{60} dumbbell 260a	188
3.8	IR spectra for short C_{60} tetrayne C_{60} dumbbell 260a	189
3.9	UV-Vis spectra of long C_{60} tetrayne C_{60} dumbbell 260b	190
3.10	UV-Vis spectra of star-shaped tetrafullerene-diyne adduct 262a	191
3.11	Surface morphology of short C_{60} diyne C_{60} dumbbell 259a on mica measured by AFM.	192
3.12	Surface morphology of long C_{60} diyne C_{60} dumbbell 259b on mica measured by AFM.	193
3.13	Surface morphology of short C_{60} tetrayne C_{60} dumbbell 260a on mica measured by AFM.	194
3.14	Surface morphology of long C_{60} tetrayne C_{60} dumbbell 260b on mica measured by AFM.	195

3.15	Surface morphology of star-shaped tetrafullerene-diyne adduct 262a on mica measured by AFM.	195
4.1	Star-shaped 1,3,5-triazene centered OPV oligomers 314a-c by Meier <i>et al.</i>	236
4.2	Swivel cruciform oligothiophene 315 by Scherf and co-workers.	237
4.3	Swivel cruciform OPV 316 and linear OPV 317	238
4.4	D/A substituted OPE cruciforms developed by Haley <i>et al.</i>	239
4.5	Cruciform OPE/OPV fluorophores developed by Bunz <i>et al.</i> as molecular sensors.	241
4.6	Target 2D conjugated OPE/OPV H-mers 331-339 in this chapter.	244
4.7	UV-Vis absorption spectra of long H-mers 331 335 measured in CHCl ₃	263
4.8	Fluorescence spectra of long H-mers 331 335 measured in degassed CHCl ₃	264
4.9	UV-Vis absorption spectra of short H-mers 336 339 measured in CHCl ₃	266
4.10	Fluorescence spectra of short H-mers 336 339 measured in degassed CHCl ₃	268
4.11	Titration results of H-mer 335 with AgOTf (0-1.3 equiv) in CHCl ₃	270
4.12	Titration results of H-mer 337 in CHCl ₃	272
4.13	Titration results of H-mer 338 in CHCl ₃	273
4.14	Titration results of OPE 389 in CHCl ₃	274

List of Schemes

1.1	Two synthetic routes to soluble OPs developed by Kern <i>et al.</i>	12
1.2	Synthesis of OP 15 by Schlüter <i>et al.</i>	13
1.3	Synthesis of ladder-type OPs 21a-c by one-pot Suzuki coupling.	16
1.4	Synthesis of unsubstituted OTs 24a-e by Steinkopf <i>et al.</i>	16
1.5	Synthesis of undecithiophene 32	18
1.6	Macrocyclic OTs 35-37	20
1.7	Synthetic route to OPVs by Drefahl and Hörhold.	21
1.8	Stepwise synthesis of alkoxy substituted OPVs via an orthogonal approach.	22
1.9	Synthesis of piezochromic OPV fluorophore 55	24
1.10	Synthesis of OPEs through an iterative divergent/convergent approach.	27
1.11	Synthesis of D/A substituted oligoenes 74 and 76	31
1.12	Synthesis of five-membered ring containing oligoenes 78b and 78e	33
1.13	Synthesis of oligoynes 92d and 92e via Hay coupling.	35
1.14	Synthesis of oligoynes via Pd-catalyzed coupling.	39
1.15	Oligo(diacetylene)s 112a-e and the synthesis of 112b	40
1.16	Synthetic route to cyclohexylidene <i>iso</i> -poly(triacetylene)s by Diederich.	42

1.17	A reversible Diels-Alder reaction on pentacene.	50
1.18	Synthesis of [60]fullerene from a polynuclear aromatic precursor.	57
1.19	Addition of carbon nucleophile to C ₆₀	62
1.20	Ethynylation reaction of C ₆₀ developed by Komatsu.	62
1.21	Synthesis of ethynyl bridged oligo(phenothiazine)-C ₆₀ dyads 144	63
1.22	Synthesis of bisfullerene-terminated OPEs 146 by Tour <i>et al.</i>	63
1.23	Cyclopropanation of C ₆₀ with dimethyl bromomalonate.	64
1.24	Examples of reagents and conditions used in Bingel reactions.	66
1.25	[4+2] Cycloadditions of cyclopentadiene and anthracene to C ₆₀	67
1.26	Fluorescence switches based on C ₆₀ -TTF dyads 154	68
1.27	Diels-Alder reaction of C ₆₀ with an <i>in situ</i> generated diene.	69
1.28	Microwave-assisted Diels-Alder reactions of C ₆₀ with heterodienes.	69
1.29	[3+2] Cycloaddition between C ₆₀ and diazo compound.	70
1.30	Synthesis of fullerene-oligopeptide hybrid 169	71
1.31	Synthesis of dendro[60]fullerenes 171 using tosylhydrazones 170	72
1.32	Addition of azides to [60]fullerene.	73
1.33	Synthesis of oligosaccharide-fullerene hybrid 176	73
1.34	[3+2] Cycloaddition of azomethine ylide to C ₆₀	74
1.35	Synthesis of ferrocene-fullerene hybrid 182	75
1.36	[2+1] Cycloadditions of carbenes to C ₆₀	77
2.1	Synthesis of phenyl building blocks 203 and 206	88
2.2	Synthesis of linear OPE-OPV 211 and bisfullerene-OPE-OPV hybrid 196a	90

2.3	Attempted synthesis of compound 196b	91
2.4	Synthesis of long linear OPE/OPV 215 and related bisfullerene hybrid 196b	92
2.5	Synthesis of cruciform building block 223	93
2.6	Synthesis of cruciform OPE/OPV 224 and related bisfullerene hybrid 197a	94
2.7	Synthesis of long cruciform OPE/OPV 227 and related bisfullerene hybrid 197b	95
2.8	Synthesis of phenyl acetylene building block 226	97
2.9	Synthesis of short D-substituted cruciform oligomer 237 and related bisfullerene adduct 198a	98
2.10	Synthesis of long D-substituted cruciform oligomer 239 and related bisfullerene adduct 198b	99
2.11	Synthesis of phenylene ethynylene-C ₆₀ model 199	100
3.1	Topochemical 1,4-addition of conjugated diacetylenes discovered by Wegner.	158
3.2	TTF appended PDA 244 synthesized via a topochemical 1,4-addition reaction by Shimada.	159
3.3	Two possible polymerization pathways for conjugated triynes. (A) 1,4- addition; (B) 1,6-addition.	160
3.4	Topochemical 1,4-addition of conjugated triyne 245 reported by Okada.	160
3.5	Double 1,2-additions of tetraynes 248 and 249 reported by Hakanishi <i>et al.</i>	162

3.6	Preparation of C ₆₀ -containing poly(thiophene)s 255 by Zhang <i>et al.</i> . . .	163
3.7	Preparation of C ₆₀ -containing conjugated polymer 258 by Ramos <i>et al.</i> . . .	164
3.8	Synthesis of C ₆₀ diyne C ₆₀ dumbbell 259a	167
3.9	Synthesis of C ₆₀ diyne C ₆₀ dumbbell 259b	168
3.10	Attempted synthesis of C ₆₀ triyne C ₆₀ dumbbell 274	170
3.11	Attempted synthesis of C ₆₀ tetrayne C ₆₀ dumbbell 260a	171
3.12	Synthesis of C ₆₀ tetrayne C ₆₀ dumbbell 260a	172
3.13	Synthesis of long C ₆₀ tetrayne C ₆₀ dumbbell 260b	173
3.14	Synthesis of C ₆₀ hexayne C ₆₀ dumbbell 261	175
3.15	Attempted synthesis of star-shaped tetrafullerene adduct 290a	178
3.16	Attempted synthesis of star-shaped tetrafullerene adduct 290b	179
3.17	Synthesis of star-shaped diyne-bridged tetrafullerene adduct 262a	181
3.18	Attempted synthesis of star-shaped tetrayne-bridged tetrafullerene adduct 262b	182
4.1	Synthesis of OPV precursor 346	246
4.2	Synthesis of phenylene ethynylene dimers 351 and 356	247
4.3	Synthesis of D/A-substituted H-mers 331 and 332	247
4.4	Synthesis of symmetrically D-A substituted OPEs 358 and 360	249
4.5	Synthesis of D-A substituted long H-mers 333 and 334	250
4.6	Synthesis of unsubstituted long H-mers 335	252
4.7	Synthesis of aldehyde-substituted H-mer 363	253
4.8	Synthesis of D-A substituted H-mer 365	254
4.9	Attempted synthesis of A-substituted short H-mer 336	258

4.10	Synthesis of A-substituted short H-mer 336	259
4.11	Synthesis of D-substituted short H-mer 337	259
4.12	Attempted synthesis of D-A substituted short H-mer 338	260
4.13	Synthesis of D-A substituted short H-mer 338	261
4.14	Synthesis of compounds 339 and 389	262
5.1	Modified method to synthesis of bifullerene endcapped triyne 294 . . .	322
5.2	Compound 396 as potential metal ion sensor	323
5.3	Compound 399 as potential fluorescence probes for carbohydrates . .	324

List of Tables

1.1	Effect of conjugation length on the λ_{\max} of OPVs 1a-g	6
1.2	UV-Vis absorption data (measured in CHCl_3) and color of compounds 2a-f	9
2.1	Summary of cyclic voltammetric data for compounds 196-198 . ^a	103
2.2	Excite-state properties of OPE/OPV co-oligomers and related C_{60} adducts.	115
4.1	Photophysical data for cruciform OPE OPV 327-330	242
4.2	Summary of photophysical data for H-mers 331-339 and OPE 389 . . .	267
4.3	Summary of sensing effectiveness of H-mers 331-339 towards various species.	269

List of Abbreviations and Symbols

1D	one-dimensionally
2D	two-dimensionally
A	acceptor
Å	angstrom
AFM	atomic force microscopy
AM	air mass
APCI	atmospheric pressure chemical ionization
aq	aqueous
Bu	butyl
CA	X-ray contrast agent
calcd	calculated
CIE	Commission Internationale de L'Eclairage
cm	centimeter

CRT	cathode ray tube
CV	cyclic voltammetry
D	donor
d	doublet
DBU	1,8-diazabicyclo[5.4.0]undec-7-ene
dec	decomposed
DFT	density functional theory
DFWM	degenerate four-wave mixing
DIBAL	diisobutylaluminium hydride
DMSO	dimethyl sulfoxide
DSC	differential scanning calorimetry
DTA	differential thermal analysis
ECL	effective conjugation length
E_g	bandgap energy
EL	electroluminescence
Et	ethyl
FBW	Fritsch-Buttenberg-Wiechell

FET	field effect transistor
FMO	frontier molecular orbital
FOLED	flexible organic light-emitting display
FTIR	Fourier transform Infrared
g	gram(s)
h	hour(s)
HOMO	highest occupied molecular orbital
IL	ionic liquid
IR	infrared
IOT	indium tin oxide
LCD	liquid crystal display
LCMS	liquid chromatography-mass spectrometry
LDA	lithium diisopropylamide
LED	light emitting diode
LHMDS	lithium hexamethyldisilazide
LUMO	lowest unoccupied molecular orbital
m	multiplet

m/z	mass to charge ratio
mA	milliampere
MALDI-TOF	matrix assisted laser desorption/ionization time of flight
Me	methyl
mg	milligram(s)
MHz	megahertz
min	minute(s)
mL	milliliter
mmol	millimole
mol	mole
mp	melting point
MS	mass spectrometry
NBS	N-bromosuccinimide
NLO	nonlinear optical
nm	nanometer
NMR	nuclear magnetic resonance
ns	nanosecond

ODCB	<i>ortho</i> -dichlorobenzene
OFET	organic field effect transistor
OLED	organic light emitting diode
OPE	oligo(<i>p</i> -phenyleneethynylene)
OP	oligo(<i>p</i> -phenylene)
OPV	oligo(<i>p</i> -phenylene vinylene)
OT	oligo(α -thiophene)
<i>p</i>	<i>para</i>
PA	poly(acetylene)
PCBM	[6,6]-phenyl C61-butyric acid methyl ester
PCC	pyridinium chlorochromate
PDA	poly(diacetylene)
PDC	pyridinium dichromate
Ph	phenyl
PL	photoluminescence
PPE	poly(<i>p</i> -phenyleneethynylene)
ppm	parts per million

PPP	poly(<i>p</i> -phenylene)
PPV	poly(<i>p</i> -phenylenevinylene)
PTA	poly(triacetylene)
PVC	polyvinyl chloride
s	second or singlet
satd	saturated
SEC	size exclusion chromatography
STC	standard test conditions
t	triplet
TAEB	tetrakis(arylethynyl)benzene
TBAF	tetra- <i>n</i> -butylammonium fluoride
Tf	trifluoromethanesulfonyl
TfOH	trifluoromethanesulfonic acid
THF	tetrahydrofuran
TIPS	triisopropylsilyl
TIPSA	triisopropylsilylacetylene
TLC	thin-layer chromatography

TMEDA	tetramethylethylenediamine
TMS	trimethylsilyl
TMSA	trimethylsilylacetylene
TTF	tetrathiafulvalene
TTFBQ	<i>N,N,N',N'</i> -tetrathiafulvaleneanthraquinone
UV-Vis	ultraviolet-visible
UI	ultrasonic irradiation
UV-Vis-NIR	ultraviolet-visible-near Infrared
V	volt
W	watt
XRD	X-ray diffraction
δ	chemical shift
λ_{em}	maximum emission wavelength
λ_{max}	maximum absorption wavelength

Chapter 1

Introduction

1.1 An overview of monodisperse π -conjugated oligomers

1.1.1 A brief historical account of polymer science

Polymers are an important and indispensable class of materials in present sciences and technologies. A polymer is generally referred to as the substance composed of a collection of individual macromolecules of different molecular weights, where the macromolecular structures are formed by repeating units that connect to one another through covalent chemical bonds.^{1,2} The term, *polymer*, first introduced by a Swedish chemist Berzelius in 1833, is actually derived from the Greek words *poly* for “many” and *meros* for “parts”.³ Long before humans’ efforts to make polymers, nature had already produced a large variety of polymers, such as tar and shellacs, tortoise shell and horns, tree saps, polysaccharides and latex. These natural polymers have been with us

since the beginning of time. The first application of polymers by the human being can be traced back to 1600 BC, at which time the ancient Mesoamerican people in central America, as materials archaeologists recently discovered, had already grasped the knowledge of making rubber. This prehistoric polymer processing actually predated the modern vulcanization process by more than 3500 years!⁴

Chemists began to make use of polymers as early as 1811, when Henri Braconnot did his pioneering work in derivatizing cellulose compounds. This was perhaps the earliest research work on polymers ever documented.⁵ The development of vulcanization later in 1839 by Charles Goodyear was another important milestone in the history of polymer science. Goodyear's method significantly improved the durability of natural polymer rubber and led to the first popularized semi-synthetic polymer.⁶ In 1907, Leo Baekeland for the first time created a complete synthetic polymer Bakelite by reacting phenol with formaldehyde at precisely controlled temperatures and pressures.⁷

Despite these numerous advances in the synthesis and characterization of polymers, a correct understanding of the molecular structure of polymers did not emerge until the 1920s. Before that time, scientists believed that polymers were clusters of small molecules without definite molecular weights and were held together by an unknown force. In 1922, Hermann Staudinger proposed that polymers consist of long chains of atoms held together by covalent bonds, an idea that did not gain wide acceptance for over a decade. Nonetheless, it was for this ingenious idea that Staudinger was ultimately awarded the Nobel Prize in Chemistry in 1953.⁸ After this, the development of polymers was considerably accelerated, and all kinds of new polymers with useful properties were synthesized and applied in various fields. Figure

1.1 lists some landmark discoveries of synthetic polymers, including polyvinyl chloride (PVC) for plumbing pipes and bottles in 1927, polystyrene for cups and packing in 1930, nylon for ropes and clothes in 1938, poly(tetrafluoroethylene), widely known by its trademark *Teflon*, for non-stick pans and igniters of solid-fuel rocket propellants, polyethylene for packing film and toys in 1941, Enkonol for various electronic devices and aircraft engines in 1970, and Kevlar for bullet proof vests and fire proof garments in 1971.^{9,10}

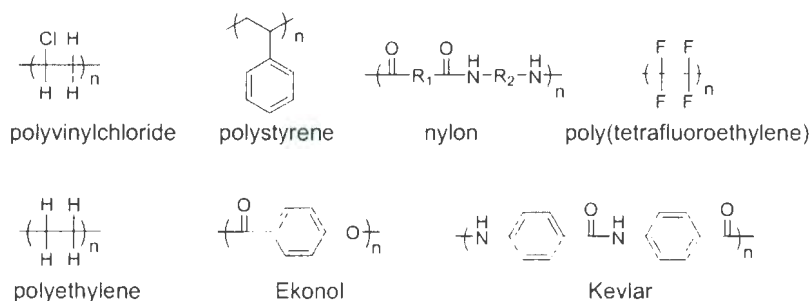


Figure 1.1: Examples of classical synthetic polymers.

Since the 1980s, polymer science has been experiencing another expansion which was mainly triggered by the discovery that π conjugated polymers could exhibit metallic properties upon doping. For example, poly(acetylene)s (PAs) can display an electrical conductivity up to $10^5 \text{ S} \cdot \text{cm}^{-1}$, similar to that of copper, after being doped with iodine.^{11,12} This important discovery has indeed changed the course of research trends in polymer science from the pursuit of high molecular weight polymers with extraordinary temperature tolerance to the survey of polymers with controlled low molecular weights and narrow polydispersity so that their properties can be easily tuned. Three pioneering scientists in this area, A. Heeger, A.

MacDiarmid, and H. Shirakawa, were honored with the Nobel Prize in Chemistry in 2000. It was also among such quests that Holmes and co-workers discovered that poly(*p*-phenylenevinylene)s (PPVs) and related polymers could be used as the active components in organic polymer-based light emitting diodes (OLEDs), and this discovery has turned out to be one of the most significant milestones in the advancement of modern polymer chemistry.¹³

With the ever growing interests in novel π -conjugated materials from both academic and industrial communities, the number of new conjugated polymers for electronic and photonic applications has been rapidly increased and the discipline of π -conjugated polymer chemistry has, in turn, been substantially accelerated. So far, the applications of π -conjugated polymers have encompassed numerous fields, used as, for example, OLEDs,¹⁴ photoconductors,¹⁵ laser dyes, scintillators,¹⁶ switching and signal process,¹⁷ nonlinear optical chromophore, (NLO),^{18,19} and optical data storage media,²⁰ just to name a few. Without any doubt, organic polymers, particularly π -conjugated polymers, will serve as the cornerstone for many future sciences and technologies, such as chemistry, biochemistry, molecular biology, nanotechnology, electronics, medicinal and life sciences, and so on.

1.1.2 The significance of monodisperse π -conjugated oligomers

The demarcation between an oligomer and a polymer is not clearly defined; however, the term of “oligomer” is generally used to refer to the compound similar to a polymer in molecular structure, but with relatively fewer repeating units. When the chemical structures of all the molecules in an oligomer are identical, this oligomer

is then called *monodisperse*. Unlike polymers, oligomers are much easier to be prepared as monodisperse via iterative synthetic methods. There are a large variety of monodisperse oligomers synthesized and investigated in the literature. Among them, monodisperse π -conjugated oligomers with alternating σ and π bonds and precisely defined chain lengths and structures have become particularly attractive to materials chemists for several reasons.

The first reason is that monodisperse conjugated oligomers can provide effective models to probe the structure-property relationships for corresponding conjugated polymers.²¹ Conjugated polymers, as mentioned above, have greatly expanded the application scope of synthetic polymer materials. However, a significant challenge in the study of conjugated polymers lies in how to tailor and optimize the properties of conjugated polymers in a predictable and controllable manner.²²⁻²⁶ Such a task is by no means trivial because the properties of polymers are dependent on various factors such as the degree of polymerization, molecular weight, polydispersity, and others. These factors vary from batch to batch in polymer synthesis and are not readily controllable in many cases.²⁷ The structural heterogeneity, together with other problems arising from the process of polymer synthesis, for example, low solubility, structural defects and synthetic impurities, poses a significant barrier to the acquisition of sound physical data for polymers.

The use of monodisperse oligomers as the model system offers an effective approach (*i.e.* the so-called “oligomer approach”) to solve these problems. In general, all π -conjugated systems would reach an effective conjugation length (ECL) as a result of the convergence of HOMO and LUMO levels with extending π -conjugation.^{28,29} Take the monodisperse oligo(*p*-phenylenevinylene)s (OPVs) series **1a-g** prepared by

Table 1.1: Effect of conjugation length on the λ_{\max} of OPVs **1a-g**.

Compound	n	λ_{\max} [nm]	ϵ [$L \cdot \text{mol}^{-1} \cdot \text{cm}^{-1}$]
1a	1	354	16,800
1b	2	401	40,700
1c	3	431	58,500
1d	4	450	84,800
1e	6	466	117,200
1f	8	475	146,200
1g	11	481	196,300

Meier and co-workers as an example (Figure 1.2).³⁰ These all-*E*-configured dialkoxy substituted OPVs show a considerable bathochromic shift of the $\pi \rightarrow \pi^*$ transition bands in their UV-Vis absorption spectra as the chain length increases from monomer to octamer (see Table 1.1). When the oligomer chain length reaches undecamer ($n = 11$), the longest-wavelength absorption maximum (λ_{\max}) value appears to arrive at a limit of convergence, indicating an ECL index of 11 for these OPVs.³⁰ Besides electronic absorption properties, other physical properties of an oligomer are also believed to be convergent or of little change once its chain length surpasses the ECL. Therefore, an oligomer with a chain length at its ECL can be used as a model compound for the corresponding polymeric species.²⁸⁻³⁰ As a result, the synthesis and characterization of various monodisperse conjugated oligomers has been one of the most intensively investigated fields in conjugated polymer oligomer chemistry over the past few decades.³¹⁻³⁴

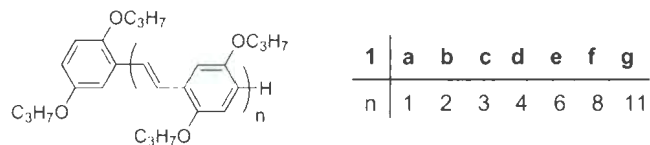


Figure 1.2: Monodisperse oligo(phenylenevinylene)s **1a-g** synthesized by Meier and co-workers.

A second reason why monodisperse π -conjugated oligomers have received so much attention lies in the potential that they may replace their corresponding polymers, with superior function and performance, in various applications. Thanks to progress in organic synthetic methodologies and improvement in analytical techniques for purification and characterization of very large molecules, numerous monodisperse conjugated oligomers that bear different functionalities or feature various stereogenicities can now be obtained without structural defects or impurities via routine multiple-step synthesis. The particular advantage of monodisperse conjugated oligomers over corresponding polymers in terms of structural and compositional purity has thus bestowed them with appealing physical properties. This makes them possess great potential applications in the fabrication of advanced electronic and optoelectronic devices, such as diodes, transistors, LEDs, and so forth (*vide infra*).³⁵

Apart from modifying conjugation length, introducing different substituents of variable electronic nature provides another important approach to finely tune the properties of monodisperse conjugated oligomers. From a practical viewpoint, the bandgap of a conjugated polymer oligomer is a crucial parameter in the design and fabrication of molecular based electronic and optoelectronic devices. In theory, the

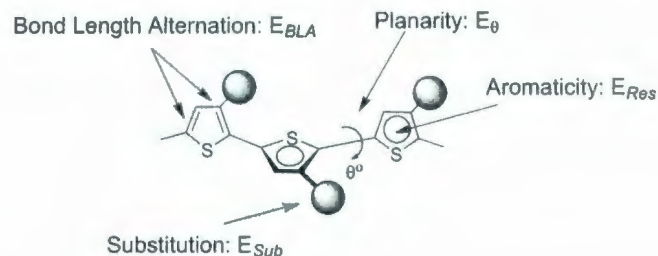


Figure 1.3: Structural factors determining the bandgap of a π -conjugated oligomer.

bandgap energy (E_g) of a linear π -conjugated oligomer is a sum of several structure-related energy components as illustrated in Figure 1.3 and described in Eq. 1.1,

$$E_g = E_{BLA} + E_{Res} + E_{Sub} + E_{\theta} + E_{Int} \quad (1.1)$$

where E_{BLA} denotes the energy contributed by bond length alternation, E_{Res} is the resonance energy, E_{Sub} is the electronic substitution effect, E_{θ} denotes the dihedral angle effect, and E_{Int} refers to the intermolecular interaction energy.³⁶ Recognizing the electronic substitution term (E_{Sub}) as a significant contributor to E_g , Meier and co-workers synthesized and investigated a series of linear, electron “push-pull” phenylenevinylene dimers **2a-f**. By simply adjusting the nature of the electron-withdrawing groups therein, the physical and electronic absorption properties of these oligomers were greatly altered (see Table 1.2 and Figure 1.4).³⁷

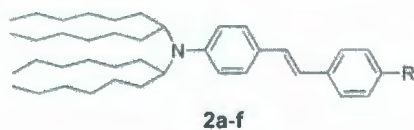


Figure 1.4: Structures of oligo(phenylenevinylene)s **2a-f**.

Table 1.2: UV-Vis absorption data (measured in CHCl_3) and color of compounds **2a-f**.

Compound	R	λ_{max} [nm]	Crystal color
2a	H	366	colorless
2b	CN	401	yellow
2c	CHO	423	orange
2d	NO_2	461	red
2e	HC C(CN) ₂	525	dark red
2f	C(CN) C(CN) ₂	670	blue

Finally, in the advancement of modern nanoscience and nanotechnology, monodisperse π -conjugated oligomers are gradually seizing the central stage. Nanoscience is the study of phenomena and manipulation of materials on the atomic, molecular, or macromolecular scale, while the properties of nanomaterials usually differ dramatically from those on a much larger scale (*i.e.* bulk materials). Nanotechnology is about the design, characterization, production, and application of structures, devices, and systems by controlling shape and size on the nanometer scale—a realm from 100 nm down to the atomic size (*ca.* 0.2 nm).³⁸ Since the molecular size of a conjugated oligomer can now be easily built up to more than 10 nm, which nicely fits the scale of nanoscience and nanotechnology, conjugated oligomers have been extensively employed as key building components in fabricating many kinds of nanoscale devices.^{39,40} At present, it is widely accepted that π -conjugated molecular rods of defined length and molecular structure hold the greatest promise

in realizing some future nanoelectronic and nanophotonic applications, for instance, ultradense and ultrafast information transportation in processing and storage devices. An even more attractive idea for the use of π -conjugated oligomers is to build a computer system based solely on organic molecules. The proposal of “molecular computer”, while still controversial, may eventually lead to new computer systems that surpass the limits of the current computer technology in terms of information storage density and computational speed.⁴¹

Since it is neither intended nor feasible to thoroughly review the recent progress in the study and application of conjugated oligomers within the context of this thesis, the following sections will only highlight several classes of conjugated oligomers that have received most research attention in the recent literature and introduce representative device fabrication based on novel functional conjugated oligomers.

1.1.3 A general survey of conjugated oligomers

1.1.3.1 Conjugated oligomers containing aromatic rings

Oligo(*p*-phenylene)s

As one of the most important branches in the family of π -conjugated oligomers, oligo(*p*-phenylene)s (OPs) have long been investigated and have found numerous applications, such as luminophores for light-emitting materials,^{42,43} semiconductors for field-effect transistors (FETs),⁴⁴ rigid cores for liquid crystalline materials,¹⁵ biomimetic scaffolds for the supramolecular assembly of nanosized barrels, ion channels and amphiphilic materials for biological applications,^{46,47} biomembrane recognition and depolarization,⁴⁸ and so on. The history of research on OPs, if the

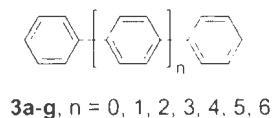
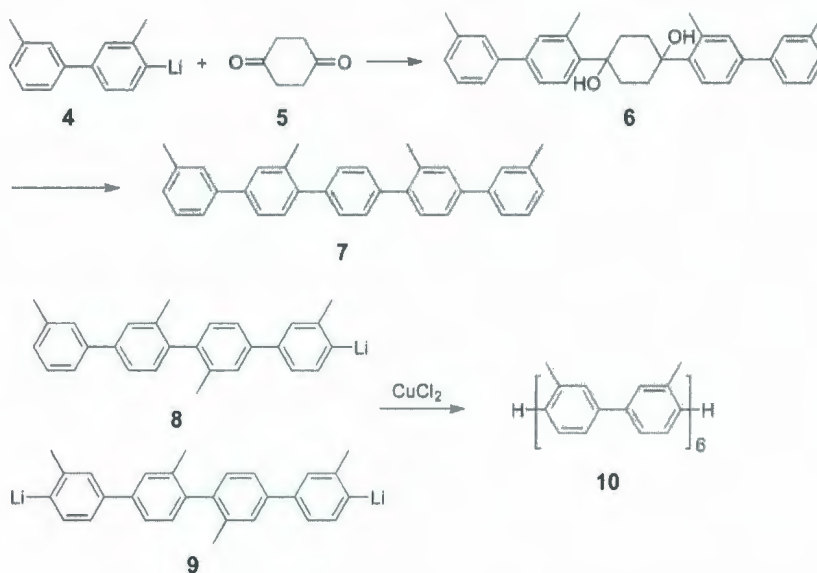


Figure 1.5: Structures of OPs **3a-g**.

well known synthesis of biphenyl by Gattermann is counted as the start, has been almost 120 years.⁴⁹ The first systematic investigation on the synthesis and properties of OPs, however, was undertaken in 1936, at which time Busch and Weber performed a hydrogenation reaction of *p*-dibromobenzene using hydrazine hydrate as the source of hydrogen and palladium as the catalyst under pressurized conditions. A mixture of OPs **3a-g** (see Figure 1.5) with polymerization degrees up to $n = 6$ was obtained as the crude product, from which monodisperse oligomers were isolated and purified by sublimation and crystallization. The solubility of these oligomers was found to decrease dramatically from $440 \text{ g} \cdot \text{L}^{-1}$ for biphenyl to $8.5 \text{ g} \cdot \text{L}^{-1}$ for terphenyl to $0.22 \text{ g} \cdot \text{L}^{-1}$ for quaterphenyl and less than $0.01 \text{ g} \cdot \text{L}^{-1}$ for sexiphenyl. Hampered by the poor solubility, the researchers only determined the melting points of these oligomers, but were not able to verify their chemical structures.^{50,51}

Presently, the properties of these simple unsubstituted OPs (**3a-g**) have been already well studied and understood. UV-Vis spectroscopic analysis discloses that the OPs possess an ECL of $n = 9$.⁵² Time-resolved degenerate four-wave mixing (DFWM) measurements reveal the $\chi^{(3)}$ values for both quaterphenyl and quinquephenyl are less than 1.6×10^{-13} esu, and an enhancement up to 1.7×10^{-12} esu for octiphenyl. These results suggest potential application in nonlinear optical (NLO) materials.⁵³

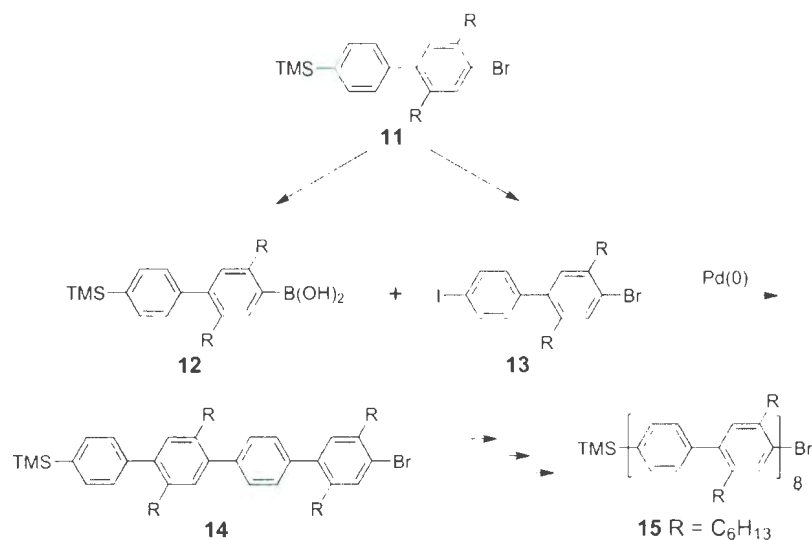
Despite their remarkable thermal stabilities, the unsubstituted OPs are in fact



Scheme 1.1: Two synthetic routes to soluble OPs developed by Kern *et al.*

of limited use in device applications due to their low solubility and intractability.⁵⁴ Therefore, chemical modifications of OPs to improve their solubility and processibility become imperative. The first series of soluble OPs were prepared by Kern and Wirth⁵⁵ and shortly thereafter by Heitz and Ulrich.⁵⁶ The way by which improved solubility was achieved for OPs was to incorporate methyl groups on the phenyl units. As such, monodisperse oligomers up to the hexamer were synthesized. Moreover, the researchers explored a variety of synthetic routes for functionalized OPs, for example, Cu-catalyzed Ullmann coupling, Cu-catalyzed condensation of lithium aryls, and a two-fold addition of organometallic species to cyclohexane-1,4-dione. Eventually, two general methodologies for the preparation of monodisperse alkyl-functionalized OPs were established as outlined in Scheme 1.1. The first method started with addition of an aryl lithium (4) to cyclohexane-1,4-dione (5), followed by aromatization of the resulting diol 6 to give oligo(arylene)s (7). The second method involved the coupling

of mono- and dilithioaryls in one pot under the catalysis of Cu(II) to form a mixture of OPs with different chain lengths. By means of preparative thin-layer chromatographic (TLC) separation, monodisperse phenylene oligomers up to a dodecamer (**10**) were successfully isolated from the product mixture.



Scheme 1.2: Synthesis of OP **15** by Schlüter *et al.*

In recent years, the emergence of modern metal-catalyzed cross-coupling methodologies has enabled numerous extended oligomeric structures to be efficiently assembled via iterative and modular approaches. A general oligomer synthetic strategy involves the repetition of directed protection/coupling/deprotection sequences in a convergent way. Such a convergent protocol is advantageous in terms of minimizing the number of synthetic steps needed. Schlüter *et al.* illustrated the preparation of monodisperse OP rods such as **15**, which contains 16 phenylene repeat units as well as well-defined endcapping groups.⁵⁷ Their synthesis was based on

a convergent (exponential) growth using the Suzuki coupling reaction as the key step. As shown in Scheme 1.2, the iodoarenes tend to couple with their boronic acid counterparts at a much faster rate than the bromoarenes do; as a result, each Suzuki coupling step took place exclusively at the iodo site. The bromo group, however, remained intact during the selective Suzuki coupling reaction and was converted into a boronic acid group afterwards so that further chain length elongation could be fulfilled via another iteration of Suzuki coupling. The C6 alkyl chains attached to every second phenyl unit were designed to improve solubility in common organic solvents, thereby permitting full spectroscopic characterizations of these oligomers.

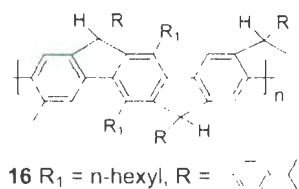


Figure 1.6: Structure of ladder-type PPP **16**.

Ladder-type poly(*p*-phenylene)s (PPPs) such as **16** (Figure 1.6) are polymers of a relatively new kind. The bridging of all the subunits gives rise to a complete flattening of the phenylene backbone and, as a result, allows the π conjugation to reach a maximum degree. Indeed, the ladder type PPPs have shown many intriguing photophysical and optoelectronic properties. For example, the absorption maximum (λ_{max}) of **16** was found to be greatly redshifted (*ca.* 440-450 nm) in comparison to typical PPPs. The photoluminescence (PL) of **16** in solution showed a very intense blue color, with a maximum emission peak (λ_{em}) at 440-450 nm. The extremely

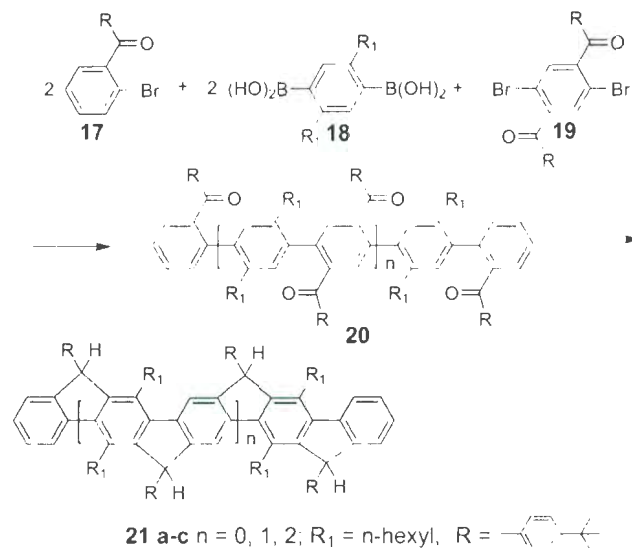
small Stokes shift (*ca.* 150 cm⁻¹) observed was ascribed to the geometric fixation of the chromophore in the ladder structure. In addition, the PL quantum yields, measured as 60-90% in solution and up to 40% in the solid state, are much higher than those of many other phenylene conjugated polymers.^{58,59}

To better understand the structure-property relationships for ladder-type PPPs, Scherf and co-workers prepared a series of ladder-type phenylene oligomers **21a-c** using the synthetic routes outlined in Scheme 1.3. In the synthesis, a one-pot Suzuki coupling between two bifunctional (chain forming) monomers and a monofunctional (endcapping) monomer of a certain amount was performed to afford an oligodisperse mixture of phenylene oligomers with different chain lengths. This mixture was then resolved into its respective monodisperse components by size exclusion chromatography (SEC). With these oligomers as the model for corresponding polymers, the authors drew a conclusion that the ECL of **21** was reached at the stage of dodecamer (*n* = 12).⁶⁰

In 2000, Suzuki and co-workers prepared a series of perfluorinated OPs **22a-d** by using an organocopper-catalyzed cross-coupling method (see Figure 1.7). These oligomers, after train sublimation purification, were applied in OLED devices as the active components. It was discovered that the electron-transport capabilities of these perfluorinated OPs were excellent compared with other perfluorinated compounds. In particular, compound **22a** showed a maximum luminance of 5,540 cd · m⁻² at 17.0 V, while compounds **22b** and **22c** registered at 12,150 cd · m⁻² at 13.7 V. These properties render these oligomers potential application in photovoltaic devices.⁶¹

Oligo(α -thiophene)s

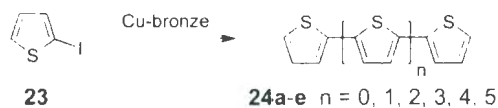
Oligo(α -thiophene)s (OTs) constitute another important class of π conjugated



Scheme 1.3: Synthesis of ladder-type OPs **21a-c** by one-pot Suzuki coupling.

oligomer materials owing to their appealing chemical and electrochemical properties.^{62,63} Over the past decade, OTs have been subjected to intensive investigations in the fields of thin film transistors,^{64,65} electroluminescent diodes,⁶⁶ lasers,⁶⁷ sensors⁶⁸ and photovoltaic cells.^{69,70}

The initial synthesis of OTs can be dated back to the 1930s, when unsubstituted OTs **24a-e** with up to seven repeating units were first prepared, separated, and characterized by Steinkopf and co-workers. The synthetic method that was employed was an Ullmann type reaction of 2-iodothiophene (**23**) catalyzed by copper bronze (Scheme 1.4.)⁷¹⁻⁷³



Scheme 1.4: Synthesis of unsubstituted OTs **24a-e** by Steinkopf *et al.*

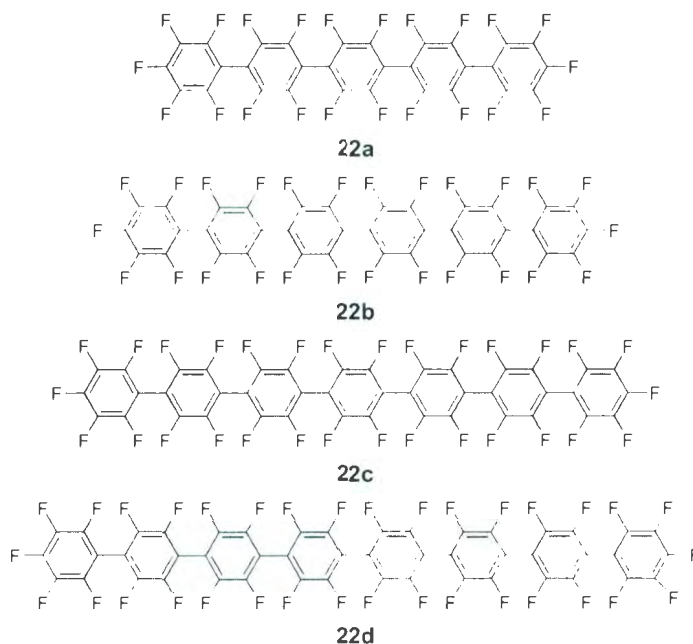
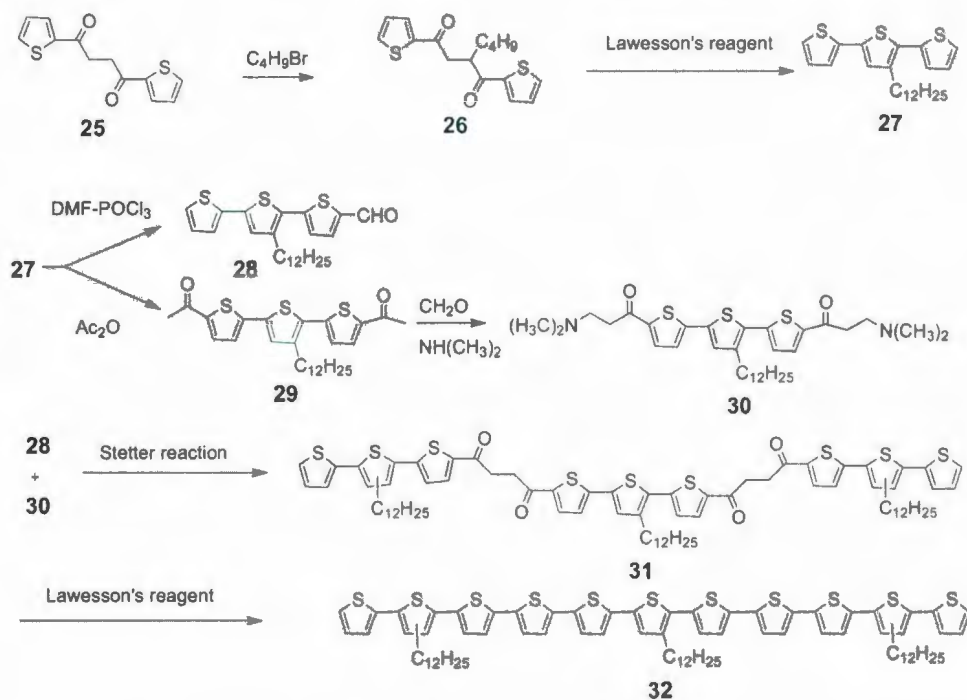


Figure 1.7: Structures of perfluorinated OPs **22a-d**.

In 1991, Wynberg and Hoeve synthesized an OT **32**, the chain length of which was extended up to eleven repeating units. As outlined in Scheme 1.5, their synthesis began with diketone **25**, which was readily alkylated with 1-bromododecane to afford compound **26**. Treating **26** with Lawesson's reagent yielded terthiophene **27**, which underwent a Vilsmeier-Haack reaction to give monoaldehyde **28** and a Friedel-Crafts acylation to give terthiophene derivative **29**. Compound **29** then led to amine **30** via a Mannich reaction. Compounds **28** and **30** reacted through a Stetter reaction⁷⁴ to afford tetraketone **31**. Finally, treating **31** with Lawesson's reagent afforded the desired undecathiophene **32**. This remarkably long OT, complimentary with those short OTs synthesized earlier, then provided an ideal model to probe the structure-property relationships for corresponding poly(thiophene)s.⁷⁵



Scheme 1.5: Synthesis of undecithiophene **32**.

With the advent of various new C-C bond formation reactions, the synthetic access to structurally well-defined OTs has currently become more versatile. For example, a 10 nm long OT **33** (Figure 1.8) was successfully synthesized by Aso and co-workers using a block-coupling protocol based on Stille coupling. In light of its nanometer-sized chain length and highly delocalized π -electronic characteristics, OT **33** has been suggested as a molecular wire for single molecular electronics and related devices.⁷⁶

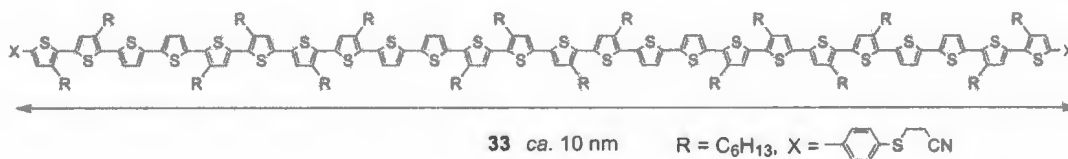
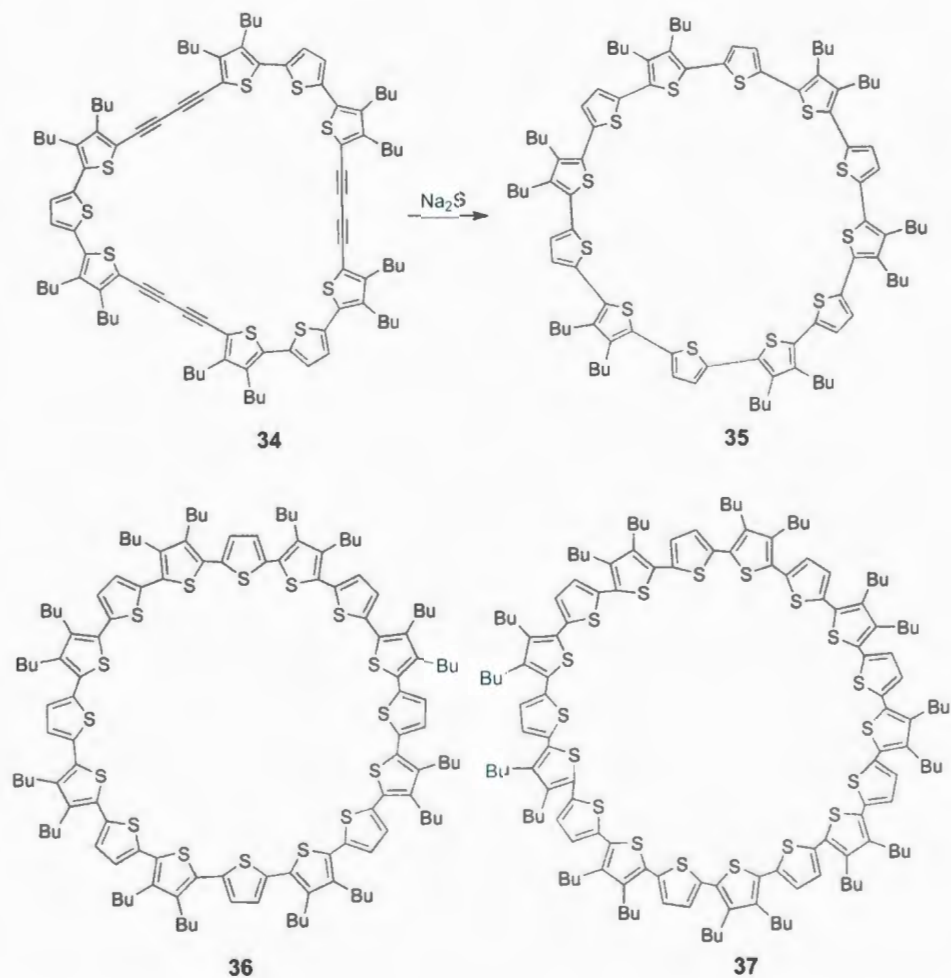


Figure 1.8: Structure of molecular wire **33**.

Apart from linear conjugated OTs, macrocyclic oligomers of thiophenes, such as **35-37** shown in Scheme 1.6, have also attracted considerable interest in recent research. A strategy to construct such conjugated macrocyclic OTs is to react a cyclic butadiyne-bridged OT derivative such as **34** with a sulfur nucleophile, Na₂S, as shown in Scheme 1.6. The three OT macrocycles are stable, bright yellow to red microcrystalline solids that show good solubility in common organic solvents. Although these conjugated macrocycles can be viewed as $4n \pi$ electron (anti-aromatic) systems, their NMR spectra show no evidence for ring current-induced shifts, indicating that a thiophenoid rather than an annulenoid character is in dominance. In view of the unique molecular shape and electronic properties of these molecules, it was anticipated that these cyclic OTs could be used as efficient host molecules to complex with [60]fullerene C₆₀ in a ring/sphere-shaped supramolecular assembly.⁷⁷

Oligo(*p*-phenylenevinylene)s

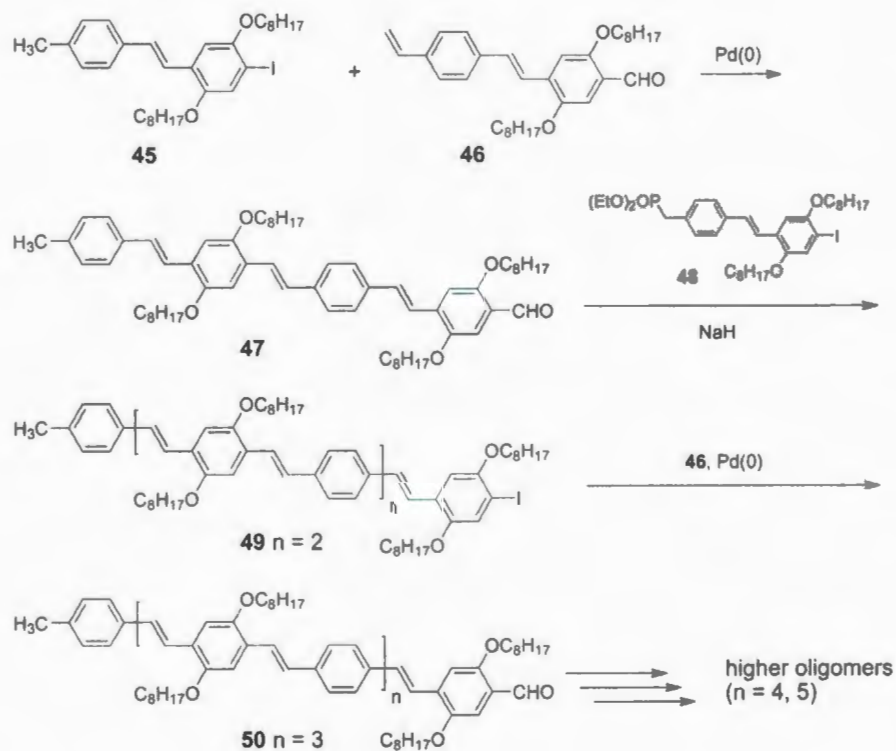
Poly(*p*-phenylenevinylene)s (PPVs) have attracted considerable research interest, ever since Friend, Holmes and co-workers first reported the use of PPVs as emissive layers for light-emitting diodes in 1990.⁷⁸ Today, polymers containing PPV backbones are probably the most widely studied among π -conjugated polymers.^{79,80} An advantageous feature of PPVs lies in the convenient controllability and tunability of their HOMO-LUMO gap by means of chemical modification. Benefited by the rapid advance of modern synthetic chemistry, a large variety of new PPV materials have been synthesized and applied in fabricating electroluminescent devices, such as OLEDs,⁸¹⁻⁸⁴ light-emitting electrochemical cells,⁸⁵ and so on. Even the once difficult-to-realize blue light emitters have been materialized by using PPV based polymers.⁸⁶



Scheme 1.6: Macrocyclic OTs **35-37**.

The first series of unsubstituted oligo(*p*-phenylenevinylene)s (OPVs) was prepared by Drefahl and Hörhold.^{87,88} Starting with benzyltriphenylphosphonium chloride **38** and 4-bromomethylbenzaldehyde **39**, they successfully synthesized OPVs up to an octamer via a strategy involving repetitive Wittig reactions and *in situ* generation of phosphonium functionality (Scheme 1.7).^{87,88}

OPV **43** shows very poor solubility in organic solvents, due to significant $\pi - \pi$ aggregation. Müllen *et al.* solved this problem by means of attaching bulky 3,5-di(*t*-



Scheme 1.8: Stepwise synthesis of alkoxy substituted OPVs via an orthogonal approach.

As such, the OPV chain length could be increased in a modular and rather efficient manner, without the need for any protection/deprotection steps. Outlined in Scheme 1.8 is the detailed synthetic route. These oligomers were found to show a saturation of λ_{max} in the UV-Vis spectrum at the stage of eight aryl rings and seven C=C bonds. In comparison to the corresponding PPVs, these OPVs show much higher fluorescence quantum yields (75-89%) as a result of the elimination of defect sites and impurities.⁹⁰

In 2006, Katayama and co-workers reported the synthesis of a series of all *cis*-OPVs **51a-d** (Figure 1.10) by Suzuki-Miyaura coupling of arylboronic acids with (*Z*)-bromoalkenes. The stereoregularity of the vinylene linkages was found to be over

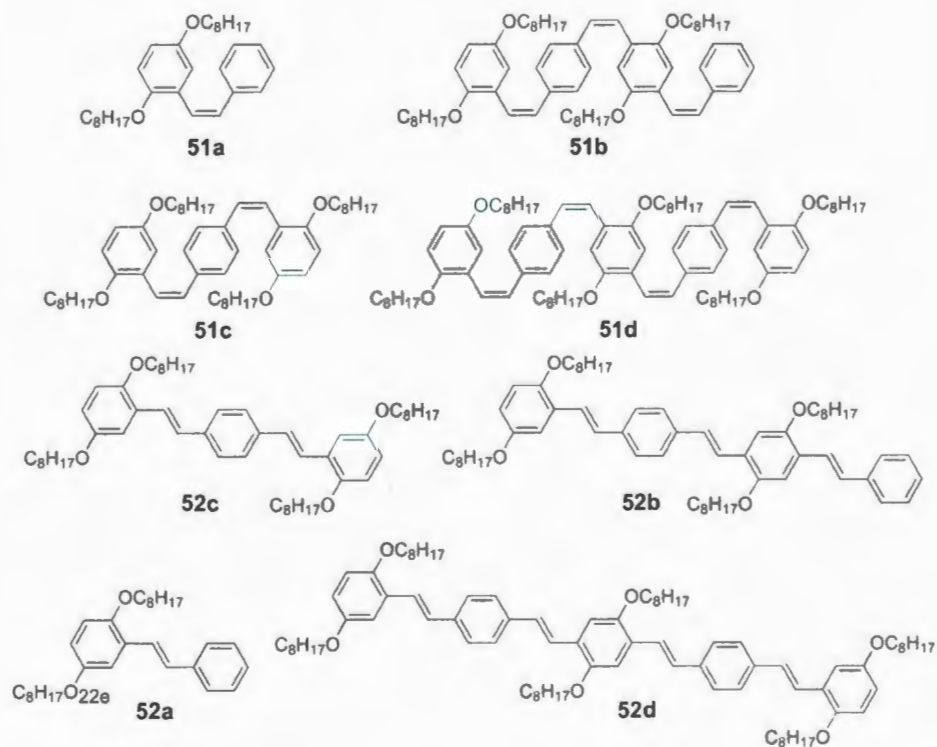
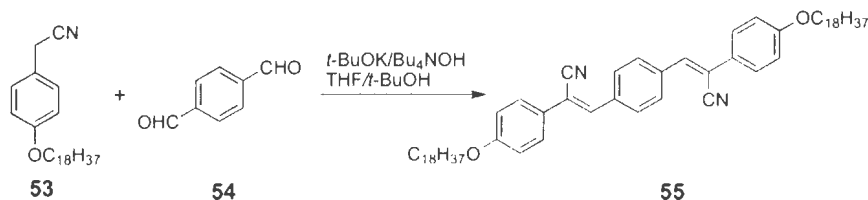


Figure 1.10: Structures of *cis*-OPV 51a-d and *trans*-OPVs 52a-d.

96%. For comparison purposes, the corresponding *all trans*-OPVs 52a-d were also prepared by Hiyama coupling of aryl iodides with (*E*)-alkenylsilanes. The effect of π -conjugation chain length on the photoisomerization behavior of the OPVs was investigated. It was found that phenylene vinylene dimers, 51a and 52a, underwent a two-way isomerization to afford a mixture of *cis* and *trans* isomers at a ratio of 52 : 48, while other higher oligomers, 51b-d and 52b-d, only experienced a quantitative conversion of a one-way isomerization from *cis* to *trans* isomers.⁹¹

Currently, greater attention has been directed toward the functionalization of the OPV backbone with various electron-withdrawing or donating groups so as to modulate or tune the electronic properties. In 2008, Weder and co-workers



Scheme 1.9: Synthesis of piezochromic OPV fluorophore **55**.

reported the synthesis of a cyano-OPV derivative, **55**, which could be used as a piezochromic fluorophore (Scheme 1.9). The emission spectrum measured from the as-prepared powder of **55** shows blue fluorescence at λ_{max} = 481 and 507 nm, which is characteristic of “monomer” emission. After the powder of **55** was subjected to brief compression (1 min at 1,500 psi) or grinding using a mortar and pestle, a significant redshift (λ_{max} = 548 nm) and broadening of the emission band were observed, which was ascribed to the formation of excimers. The “eximer form” remained stable for months under ambient storage. Quickly heating the compressed materials to 130 °C, however, led to full restoration of the original “monomer” form. Such a cycle could be repeated to switch between the two different emission colors. Wide angle X-ray diffraction (XRD) analysis unequivocally revealed the pressure-heat induced changes between different crystalline forms, which were in favor of excimer and monomer respectively.⁹²

Oligo(phenyleneethynylene)s

As the acetylene analogues of PPVs, poly(phenyleneethynylene)s (PPEs) and oligo(phenyleneethynylene)s (OPEs) have received considerable interest over the past two decades. PPEs and OPEs have rigid, rod-like conjugated backbones and show very high photoluminescence efficiencies both in solution and in the solid state. Owing

to their intriguing structural and photophysical properties, PPE based materials have found extensive applications in organic photoluminescent devices and fluorescent chemosensors.^{93,94} In addition, other potential uses of PPEs and OPEs in nanoscience and nanotechnology have been widely explored, including oriented thin films or blends,⁹⁵⁻⁹⁹ single-molecular electronic devices,¹⁰⁰ foldamers mimicking biological macromolecules,¹⁰¹ and molecular machines.^{100,101}

So far, the synthetic strategies for PPEs and OPEs have been almost exclusively based on the well-established Pd/Cu-catalyzed cross-coupling reactions. In 1996, Dixneuf and co-workers prepared a series of monodisperse *para*-OPEs **56a-h** (Figure 1.11) in high yields by stepwise coupling reactions using 4-(trimethylsilylethynyl)-1-iodobenzene as the building block. These unsubstituted OPEs offered useful information as to the essential structure-property relationships.¹⁰²



Figure 1.11: Structures of OPEs **56a-h**.

A set of intriguing *ortho*-OPEs **57a-e** were synthesized by Grubbs and Kratz through Pd-catalyzed cross coupling of diiodo- or dibromobenzene with appropriate ethynylbenzene counterparts (see Figure 1.12). UV-Vis absorption analysis shows a steady redshift of λ_{max} with increasing chain length, which is consistent with what was observed for *para*-OPEs. Cyclic voltammetric characterization of these *ortho*-OPEs shows no electrochemical reduction features, while some of the longer oligomers can

be irreversibly oxidized in CH_2Cl_2 . An X-ray single crystal structure study of **57a** and **57b** revealed that the *ortho*-OPEs adopt a helical structure in the solid state to maximize the intramolecular $\pi - \pi$ stacking of phenyl rings.¹⁰³

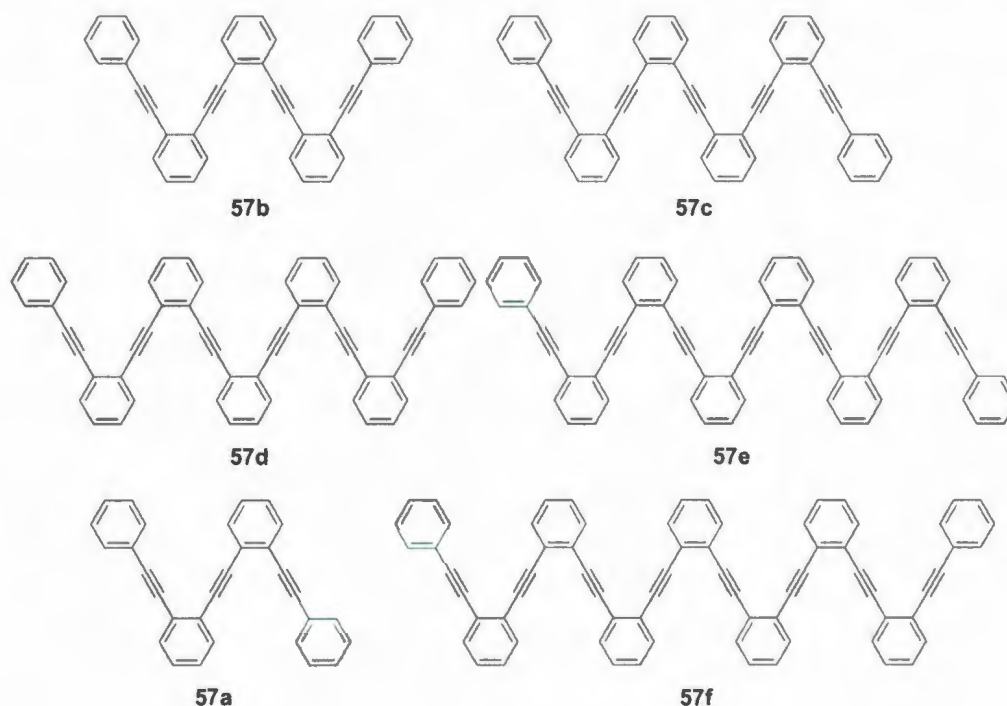
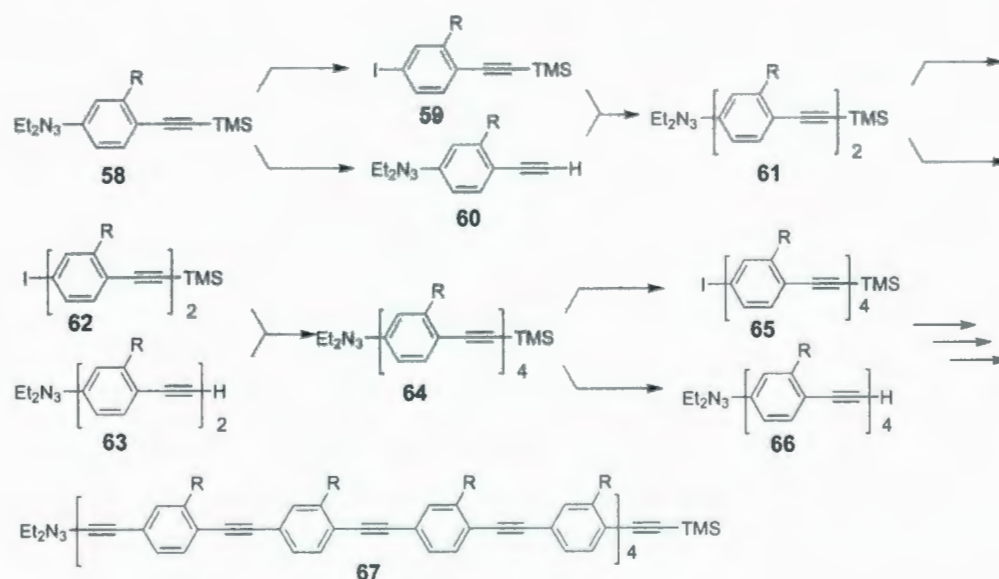


Figure 1.12: Structures of *ortho*-linked OPEs **57a-e**.

The Tour group synthesized a *para*-OPE **67** with 16 repeat units and a span of 128 Å, which holds the record for the longest monodisperse OPE ever made.¹⁰⁴ The synthetic strategy was an iterative divergent/convergent approach as outlined in Scheme 1.10. This method features very high efficiency and simplicity. At each stage in the iteration, the length of the oligomer framework doubles. As such, purification in each coupling step becomes particularly easy due to the dramatic size differences between the product and unreacted starting materials. Moreover,

there are only three sets of reactions—iodonation, protodesilylation, and Pd/Cu-catalyzed cross coupling—involved in the total iterative sequence, which makes this divergent/convergent method a highly efficient and attractive one for constructing long OPE skeletons. UV-Vis spectroscopic studies of these OPEs revealed an ECL at the stage of the octamer. The authors suggested that these rigid, rod-like conjugated oligomers may act as useful molecular wires in nanoscale electronic devices.¹⁰⁴



Scheme 1.10: Synthesis of OPEs through an iterative divergent/convergent approach.

Meta-disubstituted OPEs have been subjected to extensive scrutiny as well, owing to their unique folding/unfolding conformational transformation under different conditions. Moore and co-workers first investigated this phenomenon by examining a series of *meta*-OPEs functionalized with poly(ethylene glycol) methyl ether chains (Figure 1.13).¹⁰⁵ The side chains were designed to bring good solubility to these oligomers in common organic solvents. UV-Vis and ¹H NMR spectroscopic analyses

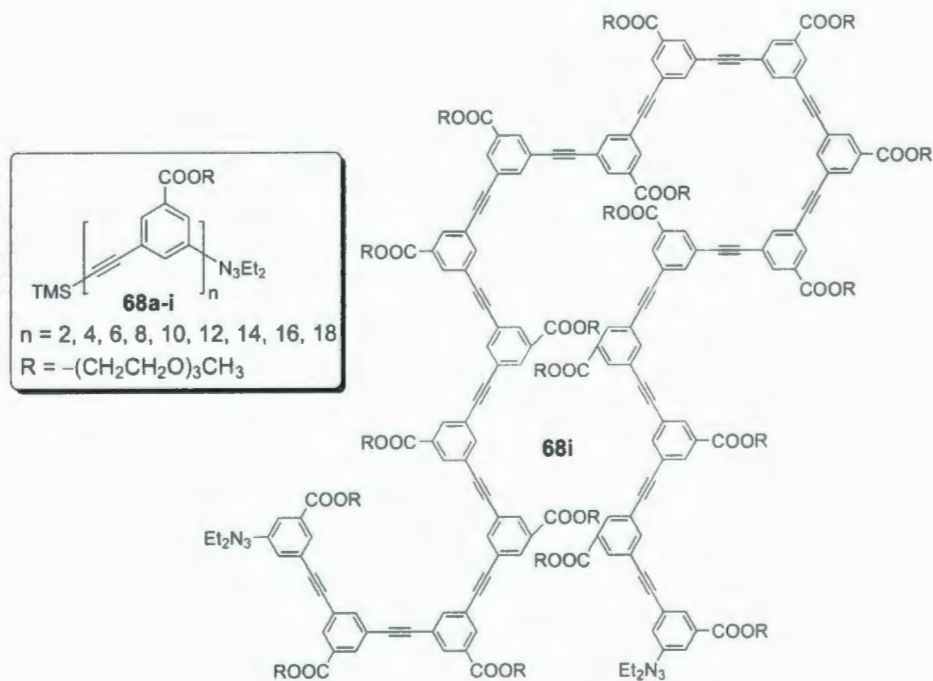


Figure 1.13: *Meta*-OPEs **68a-i** (inset, upper left). Also shown is octadecamer **68i** in a representative random coil conformation.

offered strong evidence that *meta*-OPEs **68e-i** underwent distinctive conformational changes from a helix (folded) in acetonitrile to a random (unfolded) structure in $CHCl_3$. The driving force for the helix formation in a polar solvent, such as acetonitrile, is attributed to solvophobic interactions between the oligomer and solvent molecules. The *meta*-OPEs made by Moore provide a non-biological macromolecular model analogous to biopolymers such as proteins and polynucleotides that commonly fold into well-defined 3-dimensional structures. The studies of *meta*-OPEs in terms of their folding/unfolding properties driven by solvophobicity have allowed the complex interactions and self-organizing forces taking place in biopolymers to be unravelled through a simplified and controllable model system.¹⁰⁵

Most recently, Tour and co-workers prepared a class of surface-rolling molecules such as **69**, termed “nanocars”, the “chassis” of which were constructed by rigid, rod-shaped OPE units, and the “wheels” of which were spherical organic groups, such as [60]fullerene and carborane (Scheme 1.14).¹⁰⁶ This work demonstrates the possibility to control and manipulate directional motion of molecular-sized devices through the so-called “bottom-up approach”, *i.e.* molecular design and tailoring.¹⁰⁶

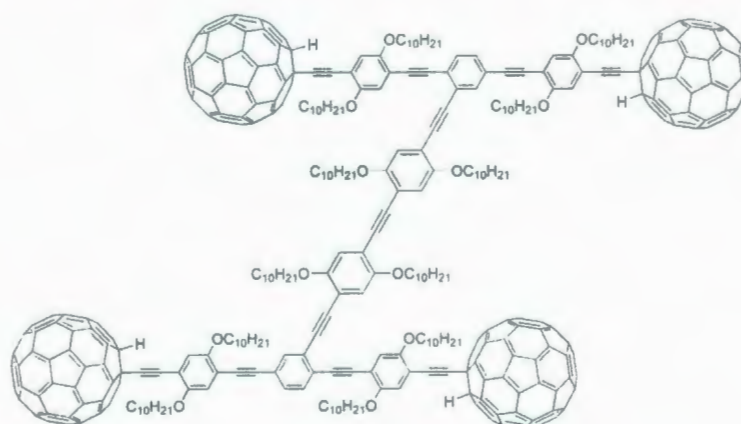


Figure 1.14: Structure of a C_{60} -wheeled nanocar **69**.

1.1.3.2 Conjugated oligomers made up of nonaromatic repeating units

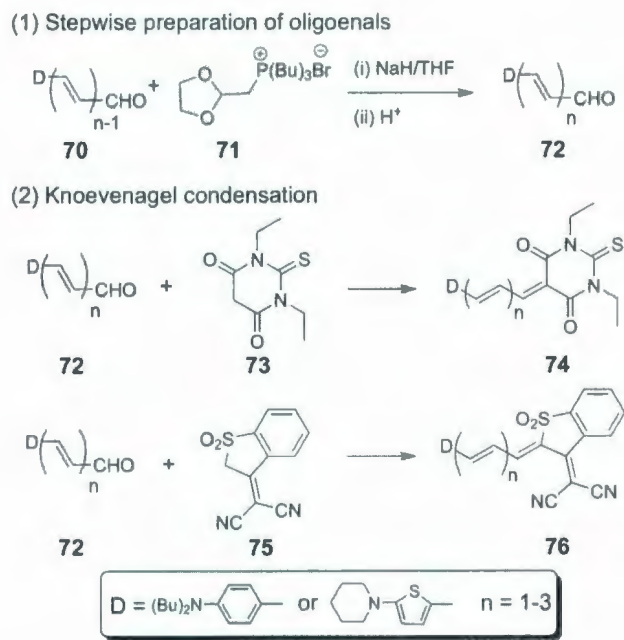
Oligoenes

The polymers whose backbones are made up of alternating C-C and C=C bond are called polyenes or polyacetylenes (PAs). This kind of polymers, normally existing as black powders as a result of extensive delocalization of π electrons, were first discovered by Natta *et al.* in 1958.¹⁰⁷ It was about 20 years later when Chiang and co-workers reported that doped PA films showed intriguingly high conductivities close to

that of metals.¹⁰⁸ Ever since then, PAs have been extensively sought after as organic conductors and NLO materials.¹⁰⁹ The corresponding monodisperse oligomers of PAs, namely oligoenes, have also been extensively investigated in recent years, not only as well-defined model systems for PAs, but as useful materials for various molecular optoelectronic devices.^{110,111}

An important approach to synthesize PAs and oligoenes relies on the use of Wittig-type reactions.^{112,113} One typical example for the synthesis of oligoenes using the Wittig reaction is the work reported by Blanchard-Desce and co-workers in 1997, in which a series of monodisperse oligoenes **74** and **76** with varying chain lengths and D/A end-capping groups were prepared as shown in Scheme 1.11. The oligoene framework was constructed from a D-substituted aldehyde through stepwise repetition of a Wittig reaction followed by acidic hydrolysis. Afterwards, electron withdrawing moieties were attached to the oligoenes via a Knoevenagel condensation reaction. The resulting oligoenes showed very large quadratic hyperpolarizabilities due to the strong electronic communication between the D and A groups via π -conjugation. These properties made them ideal candidates for organic second-order NLO materials.¹¹³

Besides the Wittig reaction, other types of olefination methods have also been employed to synthesize oligoenes. Müllen and co-workers applied the Stille coupling reaction to successfully prepare a homologous series of stable oligoenes **77a-c** (Figure 1.15). These oligoenes show remarkable redox activities as revealed by cyclic voltammetry.¹¹⁰ Oligoene **77c** was observed to undergo seven successive reversible one-electron transfer steps, leading from a tetraanion to a trication in the cyclic voltammetric scan. The electrochemical data also allowed the HOMO-LUMO gaps (ΔE) of **77a-c** to be estimated. By plotting ΔE against $1/n$ (n denotes the number



Scheme 1.11: Synthesis of D/A substituted oligoenes **74** and **76**.

of C=C bonds), a ΔE value of 1.7 eV was extrapolated for PA, which is in agreement with the ΔE value obtained for PA by other experimental means as well as by theoretical calculations.¹¹⁴ The single crystal structure of hexaene **77b** was elucidated by X-ray structure analysis, showing a solid-state packing of oligoenes in layers, where each linear oligoene chain was surrounded by six neighboring *tert*-butyl groups that occupy the spaces between the layers. Such an arrangement is similar to that of *trans*-PAs as determined by X-ray diffraction, which endorses the suitability of using crystalline **77b** as a model for bulk *trans*-PAs.¹¹⁵

In 2006, Schrock and co-workers prepared a series of five-membered ring containing oligoenes **78a-f** (Figure 1.16) through Wittig-type reactions or McMurry coupling involving mono- or bimetallic Mo alkylidene complexes.¹¹⁶ These oligoene products represent portions of the polymers resulting from ring-closing metathesis

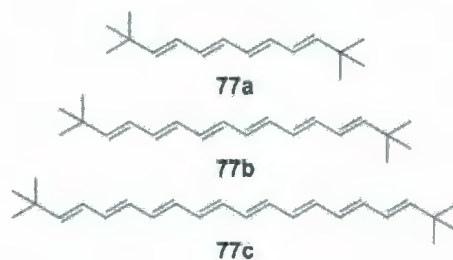


Figure 1.15: Structures of *tert*-butyl endcapped oligoenes **77a-c**.

polymerization (RCMP) of dialkyl dipropargylmalonates.¹¹⁷

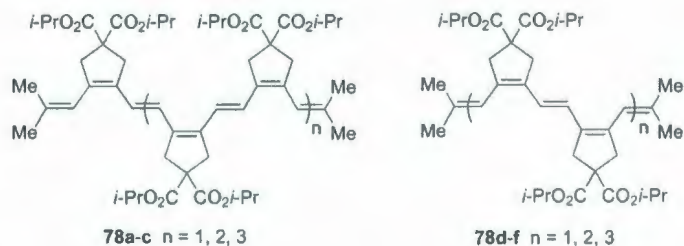
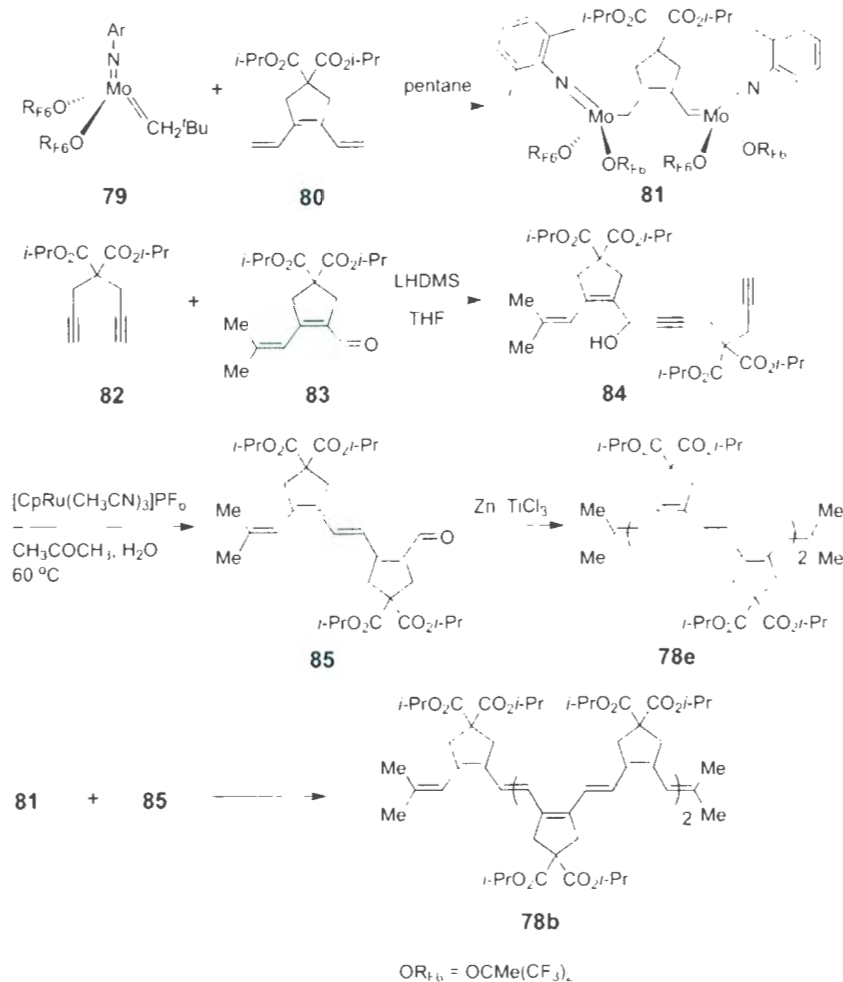


Figure 1.16: Oligoenes **78** prepared by Schrock.

116

Scheme 1.12 illustrates the exemplary synthetic routes to oligoenes **78b** and **78e**. An olefin metathesis reaction between 2,6-dimethylphenylimido ligand **79** and triene **80** gives bimetallic compound **81**. Condensation of 1,6-heptadiyne **82** with dienal **83** then leads to the formation of propargylic alcohol **84**, which is subsequently converted into dimeric aldehyde **85** through a protocol devised by Trost *et al.*¹¹⁸ Finally, compounds **81** and **85** react through a Wittig-type reaction to afford an odd-numbered oligoene, **78b**, while McMurry coupling of **85** produces an even-numbered oligoene, **78e**.



Scheme 1.12: Synthesis of five-membered ring containing oligoynes **78b** and **78e**.

Oligoynes

Carbon-rich compounds and materials are currently an area of active research,¹¹⁹⁻¹²⁵ among which the quest for hypothetical polyynes or oligoynes species remains a challenging goal owing to their unique electronic, optical, and photophysical properties. Of particular interest is the possibility that carbynes (*e.g.* **86** in Figure 1.17) might easily bend and generate other appealing carbon allotropes.^{110,126-131}

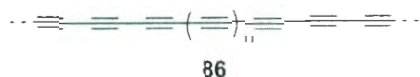


Figure 1.17: Structure of a polymer sp-carbon allotrope, “carbyne” **86**.

The earliest oligoyne synthesized is perhaps diphenylacetylene. As early as in 1869, Carl Glaser at the University of Bonn observed the formation of an oxidatively dimerized product, 1,3-butadiyne, after the copper(I) phenylacetylide was exposed to air.¹³² The first attempt to synthesize long sp-hybridized carbon chains was undertaken by Bohlmann and Jones.¹³³⁻¹³⁵ Driven by an interest in the synthesis of polyynes (di-, tri-, tetra-, and pentayne) containing natural products, they carried out a systematic survey on polyynes **87-89**, the carbon skeletons of which extend up to ten C≡C bonds (Figure 1.18). The synthesis of such polyynes was mainly based on the reaction between an acetylene Grignard reagent and an aldehyde.^{136,137}

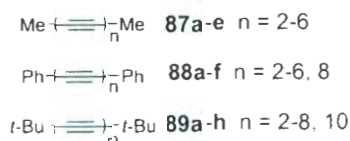


Figure 1.18: Structures of endcapped polyynes **87-89**.

The classical elongation protocol, due to the difficulty encountered in handling the precursors for polyynes, was only of limited scope. The preparation of longer polyyne derivatives was made possible after Walton and co-workers introduced silylation as a protective method in acetylene coupling chemistry.^{138,139} Using triethylsilyl as the protecting group during iterative symmetrical and mixed Hay coupling reactions, a

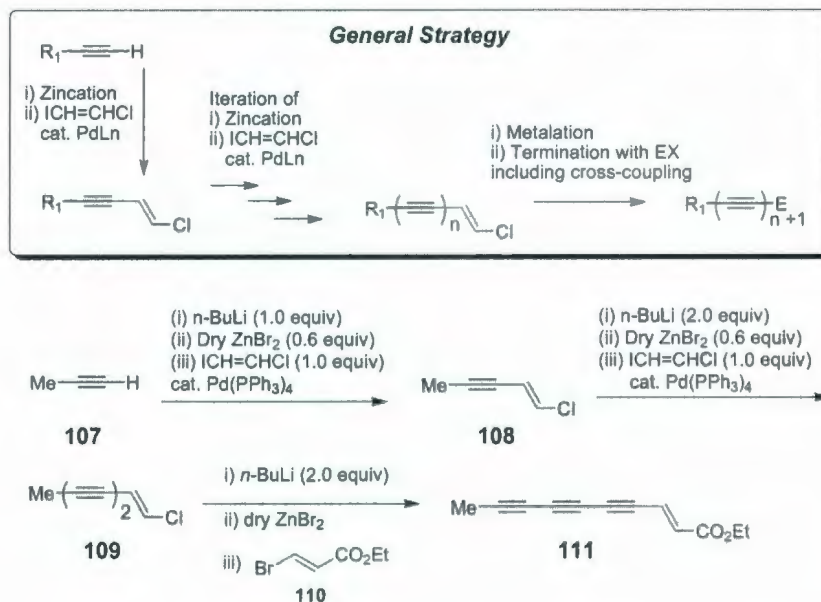
series of unique bis(phosphine) pentafluorophenyl platinum endcapped oligynes **92** in 2003.¹⁴⁰ The synthesis began with a reaction of *trans*-[(C₆F₅)(*p*-tol₃P)₂PtCl] (**93**) and 1,3-butadiyne to yield compound **94**. With **94** in hand, the target oligynes **92d** and **92e** were obtained through Cu-catalyzed oxidative Hay coupling (Scheme 1.13). The oligynes were able to survive extended periods in air and even under heating. The effects of carbon chain length on IR, UV-Vis absorption, and electrochemical redox properties were also investigated. The crystal structure of oligyne **92e** was determined by X-ray analysis, which shows a dramatic, unprecedented degree of chain bending. This finding underscores the geometric flexibility of oligynes and polyynes. It has been envisioned that continued efforts to synthesize extended oligyne compounds would eventually assist in modeling the properties of the one-dimensional polymeric sp carbon allotrope (*i.e.* carbyne). One aim of such studies is to clarify the debate over whether carbyne should feature a backbone with alternating single and triple bonds and a non-zero HOMO LUMO gap.¹⁴⁰

Most recently, a number of new methodologies for the synthesis of structurally well-defined oligynes other than Cu-catalyzed methods have emerged in the literature. Among them, the approach through a modified Fritsch-Buttenberg-Wiechell (FBW) rearrangement, devised by Tykwinski and co-workers, is particularly attractive, due to the easy access to starting materials and facile purification of both intermediates and products, as well as reliably high yields.¹⁴¹⁻¹⁴³ For example, in 2005, the Tykwinski group successfully synthesized a series of triisopropylsilyl endcapped oligynes **98a-g** (n = 2-10) via the modified FBW reaction (Scheme 1.20).¹⁴⁴ Of note is that this method has led to oligyne products in sufficient amounts to allow for a thorough analysis of their structural, physical, and optical properties.

UV-vis spectroscopy shows a consistent lowering of the HOMO LUMO gap (E_g) as a function of the number of acetylenic units (n), fitting well into a power-law relationship, $E_g \propto n^{-0.379 \pm 0.002}$. The authors have also examined the third-order NLO properties of this oligoyne series, the results of which established another power-law relationship between molecular second hyperpolarizabilities (γ) and chain length (n) as $\gamma \propto n^{4.28 \pm 0.13}$. Of great significance is that the exponential factor experimentally obtained for the oligoyne series is much larger than that predicted theoretically. Also, this exponent is larger than those observed for polyenes and polyenyne. These results hence suggest that extended polyynes hold the key to acquire unprecedentedly large third-order NLO susceptibilities. The combined linear and nonlinear optical results have offered concrete support for recent theoretical predictions on polyynes and their effectiveness as models for carbyne. In particular, the ECL of polyynes, which was estimated to be around $n = 32$ based on UV-Vis spectroscopic analysis, is of great value for understanding the characteristics of carbyne.¹⁴⁴

In 2006, Negishi and co-workers reported a highly selective method for the synthesis of conjugated triynes and higher oligoynes based on a Pd-catalyzed alkynyl-alkynyl coupling (Scheme 1.14). The general approach involves an iteration of the Pd-catalyzed coupling between an oligoynyl zincate with (*E*)-ICl (CHCl), followed by metalation and termination with an electrophile (E). Based on this approach, the Negishi group has prepared a variety of conjugated triynes and tetraynes.¹⁴⁵ This Pd-catalyzed coupling method, originally devised for polyyne-containing natural products though, is certainly of great use in preparing various non-naturally existing, unsymmetrically functionalized oligoynes.

Other nonaromatic conjugated oligomers



Scheme 1.14: Synthesis of oligoynes via Pd-catalyzed coupling.

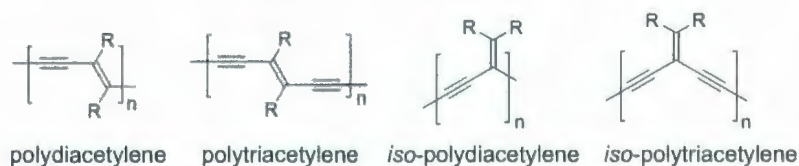
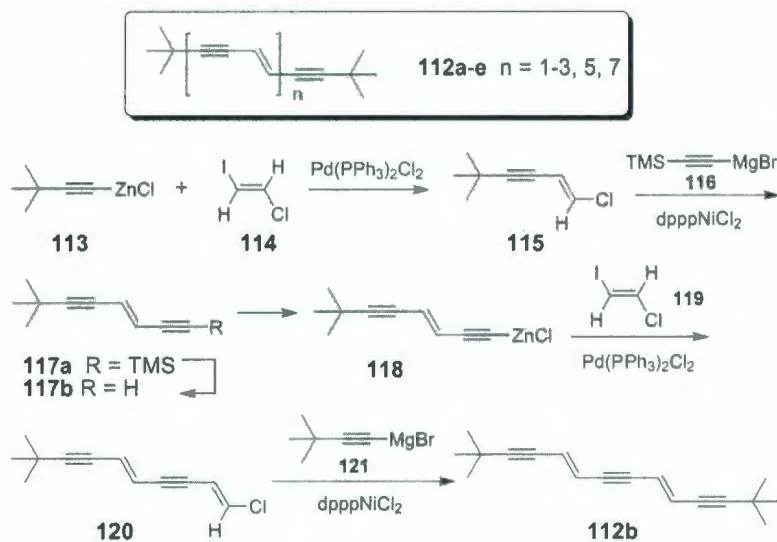


Figure 1.21: Structures of linear and cross-conjugated enyne oligomers.

series, a color change from white to deep yellow, concomitant with a rapid drop of solubility in *n*-hexane or benzene, was observed as the chain length increased from $n = 1$ to 7. The bulky *tert*-butyl endcapping group was found to be essential for maintaining the thermal stability of the oligomers. Unlike oligoenes, these enyne oligomers are quite stable to air and light. Of particular interest is that oligomer **112d** does not react with iodine over a period of more than 24 h, which sharply contrasts the behavior of oligoenes with an identical chain length. Attempts to dope

a film of **112d** with sodium naphthalenide and [18]crown-6 in Et₂O also failed.¹⁵⁰



Scheme 1.15: Oligo(diacetylene)s **112a-e** and the synthesis of **112b**.

The first synthesis of monodisperse PTAs was achieved by a simple oxidative acetylenic coupling protocol in 1994.¹⁵¹ Despite its relatively late arrival, the synthetic methodology for PTAs is more versatile than those for PAs and PDAs in generating functional derivatives. In 1999, Diederich and co-workers prepared a series of monodisperse oligo(triacetylene)s **122a-g** (Figure 1.22) through a rapid and efficient statistical oligomerization protocol.¹⁵² The completion of this PTA series closed the gap between oligomer and polymer analysis. All of the oligomers up to hexadecamer **122g** showed good solubility in nonpolar solvents, allowing for a direct determination of $n_{\text{ECL}} = 10$ by UV-Vis spectroscopy. Raman scattering analysis of oligomers **122a-g** showed an exponential decrease in the stretching frequencies of C \equiv C and C=C bonds with increasing chain length. A plot of $\nu_{(\text{C}\equiv\text{C})}$ versus the number of triple bond also

consistently revealed an ECL of 10 repeat units.

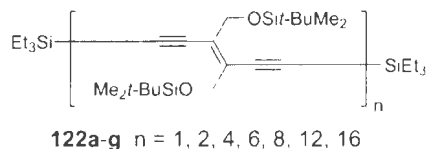


Figure 1.22: Oligo(triacetylene)s **122a-g** synthesized by Diederich and co-workers.

Cross-conjugated molecules are molecules with “three unsaturated groups, two of which although conjugated to a third unsaturated center are not conjugated to each other.”¹⁵³ Cross conjugation can be found in a wide range of molecules, for example, quinones, radialenes, fulvalenes, and fused aromatics.

The first series of cross-conjugated isopropylidene based *iso*-PDAs was synthesized by Tykwinski and Zhao in 1999 (Figure 1.23). Due to the presence of triisopropylsilyl endcapping groups, these oligoenynes showed very good solubility, which allowed for complete spectroscopic characterizations. X-ray structure analysis of trimer **123b** indicated C_2 symmetry and planarity of the molecular framework with a maximum deviation of 0.126 Å from the least-squares plane. The electronic properties of these oligomers were analyzed by UV-Vis spectroscopy in solution and solid thin films, which indicated the ECL is at the nonameric stage ($n = 9$).^{154,155}

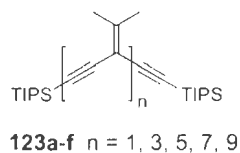
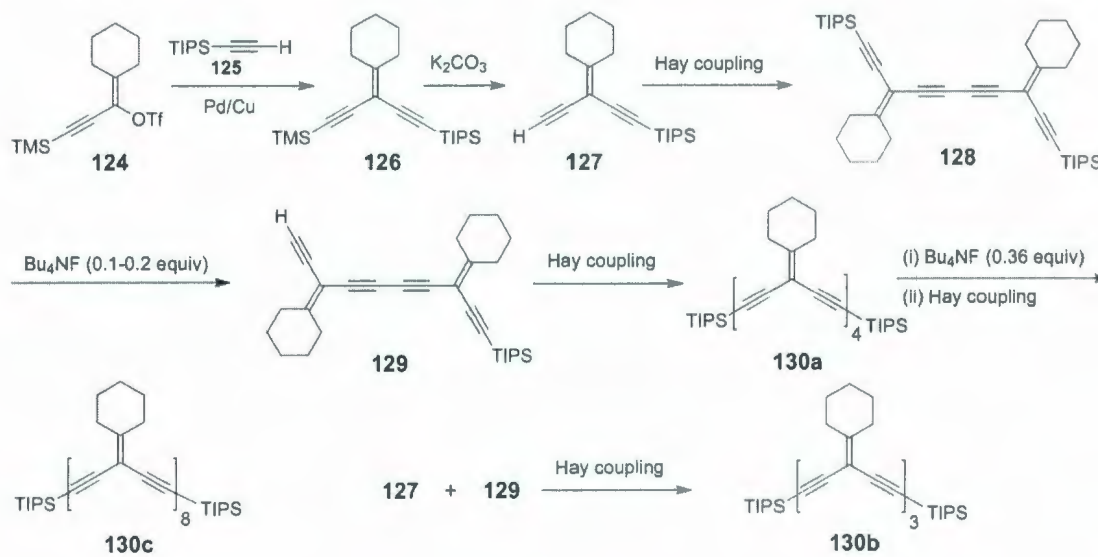


Figure 1.23: Isopropylidene based *iso*-PDAs by Tykwinski and Zhao.

The seminal work on *iso*-PTAs was done by both the Diederich and Tykwinski groups.¹⁵⁶⁻¹⁵⁸ Outlined in Scheme 1.16 is the repetitive synthesis of *iso*-PTAs bearing cyclohexylidene subunits. These *iso*-PTAs have been characterized by NMR, UV-Vis spectroscopy and mass spectrometry, despite their relatively low chemical stability. Oligomer **130c** represents the longest *iso*-PTA prepared to date. A continuous decrease in the HOMO-LUMO gap with an increasing number of repeating units is indicative that there is a certain degree of electronic communications occurring along the cross-conjugated oligomer backbone. The HOMO-LUMO gap energy for an infinitely long *iso*-PTA was thus estimated to be 3.3-3.5 eV by extrapolation. Semi-empirical calculations suggested that *s-trans* *iso*-PTAs prefer a planar conformation, while *s-cis* oligomers favor a slightly twisted "U-shaped" geometry.¹⁵⁶



Scheme 1.16: Synthetic route to cyclohexylidene *iso*-poly(triacetylene)s by Diederich.

1.1.4 Device applications of π -conjugated oligomers

1.1.4.1 Organic light-emitting diodes

Organic light-emitting diodes (OLEDs) are a display technology based on the use of an organic substance as the semiconductor material in LEDs.^{159,160} Ever since Tang's first fabrication of efficient and low-voltage OLEDs from p-n heterostructure devices using thin films of vapor-deposited organic materials in 1987¹⁶¹ and the discovery of electroluminescence from conjugated polymers by Holmes and co-workers in 1990,¹⁶² OLEDs have attracted considerable interests from both academia and industry, owing to their promising applications in making flat-panel displays in lieu of the currently used cathode ray tube (CRT) and liquid crystal display (LCD) technologies.¹⁶³ The advantages of OLEDs for flat-panel displays lie in their high luminous efficiency, full color capability, wide viewing angle, high contrast, low weight, and high flexibility.^{163,164} It is forecasted that some new technologies built on OLEDs, for instance, flexible organic light-emitting displays (FOLEDs), will bring portable, roll-up displays to the consumer market within the next few years.¹⁶⁵

The basic architecture of an OLED device consists of a thin film of organic emitting layer sandwiched between two electrodes^{159,160,163,166} as depicted in Figure 1.24.

In a typical OLED, the active emitting layer is composed of π -conjugated molecules, which are almost electrically insulating in nature. The anode layer is normally made of a transparent conducting material, for example, indium tin oxide (ITO), while the cathode is a reflective metal layer. When a voltage is applied between the two electrodes, opposite charges are injected in the organic material—holes from the anode and electrons from the cathode. The opposite charges move inside the

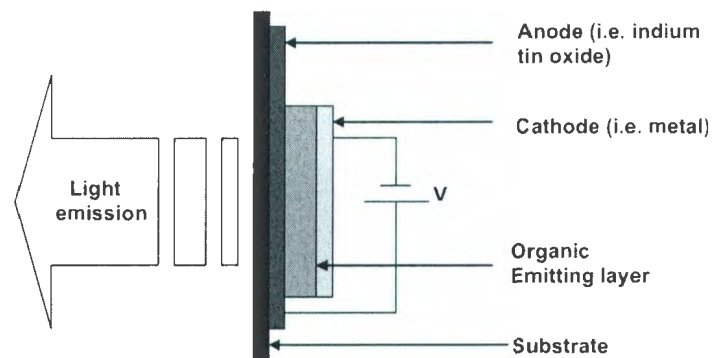


Figure 1.24: Schematics of the basic structure of an OLED.

material and recombine. The recombination of a hole and an electron causes a drop in the energy levels of electrons, accompanied by emission of a photon. Since the wavelength of the photon emitted is tied to the HOMO LUMO energy gap of the electroluminescent molecule, the color of light emanated from an OLED can be easily tuned by modifying the degree of π -conjugation in the emissive organic molecules. The performance of an OLED is usually characterized by several parameters including external quantum efficiency (η_{ext}), current efficiency (η_{L} , $\text{cd} \cdot \text{A}^{-1}$) or luminous efficiency (η_{P} , $\text{lm} \cdot \text{W}^{-1}$), brightness, and turn-on or drive voltage. In a general sense, the higher brightness and lower drive voltage, the better performance an OLED gives.

Currently, various π -conjugated oligomers have been reported useful for OLED fabrications, owing to their high electron carrier mobility, excellent film forming properties (pinhole free), reasonable thermal and oxidative stability, and high color purity (adequate Commission Internationale de L'Eclairage (CIE) coordinates). Moreover, oligomer based materials enable better layer engineering and more sophisticated architectures to be implemented compared with polymer based LED

devices.¹⁶⁷⁻¹⁷³

In 2007, Tonzola and co-workers prepared a series of conjugated dimers **131a-d** based on a 6,6'-bis(4-phenylquinoline) core (Figure 1.25). These oligoquinolines exhibit high glass-transition temperatures ($T_g \geq 133$ °C) and onset decomposition temperatures (T_D between 417–492 °C), which renders them almost the same thermal robustness as conjugated polyquinolines. These features are desirable for OLED materials in view of the inevitable joule heating under OLED operating conditions. The electrochemistry of these oligomers shows reversible reduction processes and high electron affinities (2.68–2.81 eV), which is suggestive that they are good electron-transport materials. Furthermore, these oligomers emit blue photoluminescence with quantum yields of 0.73–0.94 and lifetimes of 1.06–1.42 ns in chloroform solutions. Such properties are essential for developing stable blue OLEDs. Finally, the authors claimed to have achieved high-performance organic light-emitting diodes (OLEDs) with excellent blue chromaticity coordinates from oligoquinolines **131a-d**. In particular, OLEDs employing **131c** as the blue emitter give the best performance with a high brightness (19,740 $\text{cd} \cdot \text{m}^{-2}$ at 8.0 V), high efficiency (7.12 $\text{cd} \cdot \text{A}^{-1}$ and 6.56% external quantum efficiency at 1,175 $\text{cd} \cdot \text{m}^{-2}$), and excellent blue color purity as judged by the CIE coordinates ($x = 0.15$, $y = 0.16$). These results represent the highest efficiency of blue OLEDs, which were built upon neat fluorescent organic emitters.¹⁷⁴

It was also in 2007 that another important advance in OLED materials was made by Li and co-workers.¹⁷⁵ They prepared fluoro-substituted Ph_2N -containing oligo(arylenevinylene) derivatives **132a-k** (Figure 1.26) with an aim to discover new materials for OLEDs. Property characterizations showed that the absorption,

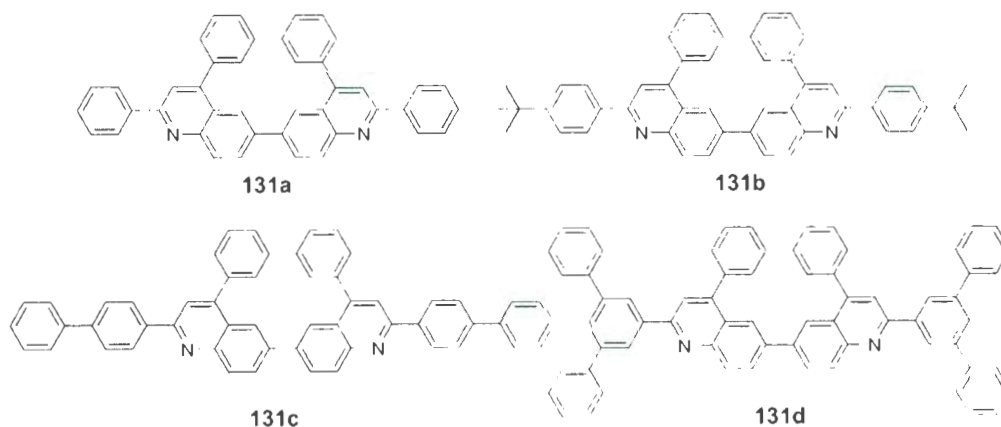


Figure 1.25: Structures of blue-light emitting oligoquinolines **131a-d**.

emission, and electrochemical properties are significantly affected by the position of the fluorine substituents, which provides an effective tool to tune the color of emission from deep blue to orange (a broad wavelength region from 448 to 579 nm in the spectrum). The fluorescence quantum yields of these oligomers are very high (Φ 0.93–0.68). When blue emitter **132a** was tested, a remarkably high external quantum efficiency value (η_{ext} = 4.87%) was attained at J = 20 mA · cm⁻², along with a high luminescence efficiency, 5.91 cd · A⁻¹ at J = 53 mA · cm⁻², a high power efficiency of 3.01 lm · W⁻¹ at J = 21 mA · cm⁻² and the maximum brightness at 10.2 V is 22,506 cd · m⁻² (k = 458 nm; CIE coordinates x = 0.14, y = 0.14) with a full width at half-maximum of 54 nm. The commendable electroluminescent performance of these oligomers has attested to the superiority of these fluoro-containing oligomers in OLED devices.

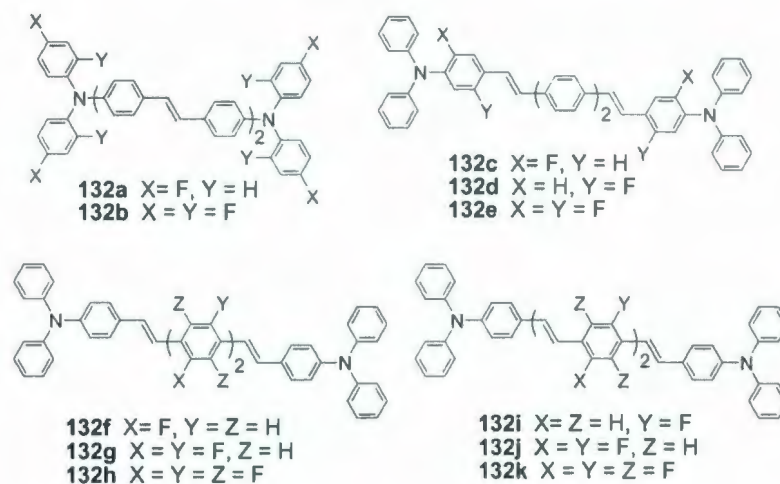


Figure 1.26: Structures of fluoro-substituted oligo(arylenevinylene)s **132**.

1.1.4.2 Organic field effect transistors

A field effect transistor (FET) is a three-electrode device in which the conductance of a thin channel between the source and drain electrodes at the semiconductor-insulator interface can be controlled through a gate bias. As an integral part of computer chips, FETs are playing a prominent role in our everyday life.¹⁷⁶ The first description of the field effect in organic semiconductors can be dated back to 1970.¹⁷⁷ Organic FETs (OFETs), however, have only been identified as potential elements of electronic devices since the report by Koezuka and co-workers in 1987 on electrochemically polymerized poly(thiophene)s.¹⁷⁸ Since then, the performance of OFETs has been continuously improved. One of the most attractive features of OFETs is the possibility of applying liquid-phase techniques such as ink-jet printing or spin coating.¹⁷⁹⁻¹⁸¹ This aspect is regarded as crucial if the transistors are to be implemented on large, flexible substrates in a cost-effective manner. Currently, it is

widely believed that OFETs will be used as integrated circuits for large-area, flexible, and ultra-low-cost electronics such as radiofrequency identification tags and organic active matrix displays.¹⁸²⁻¹⁸⁸ Prototypes of these products have been demonstrated and are now getting close to commercialization.^{189,190}

Depicted in Figure 1.27 is the fundamental architecture of OEFTs.¹⁹¹⁻¹⁹³ In this configuration, the gate electrode is positioned directly on the substrate. Usually a silicon wafer functions as both the substrate and gate. The isolator, often thermally grown silicon dioxide, is laid on top. Above the isolator layer is the organic semiconductor layer, on which the source and drain electrodes are settled.

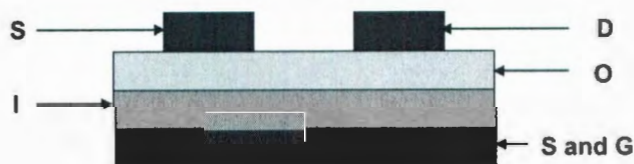


Figure 1.27: Basic structure of an OEFT. S: Source electrode; D: Drain electrode; S and G: Substrate and gate electrode; I: Insulator; O: Organic semiconductor.

The basic circuit of a bottom-gate OFET is shown in Figure 1.28.¹⁹² The source electrode is earthed, and all other voltages are set in reference to this electrode. If a negative voltage U_G is applied to the gate electrode, an electric field is induced perpendicular to the layers. Enhancement in positive charge carriers occurs at the interface between semiconductor and gate insulator as a result. If at the same time a voltage U_G is applied at the drain electrode, holes can be transported from the source electrode to the drain electrode. This conducting situation is called the “on” state, whereas $U_G = 0$ defines the “off” state. The most important parameters gauging the

performance of an OFET are the on/off ratio ($I_{\text{on}}/I_{\text{off}}$) and the charge-carrier mobility (μ_{FET}), both of which need to be tuned as high as possible if better performance is desired.¹⁹⁴

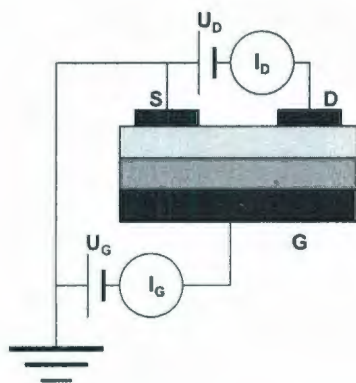
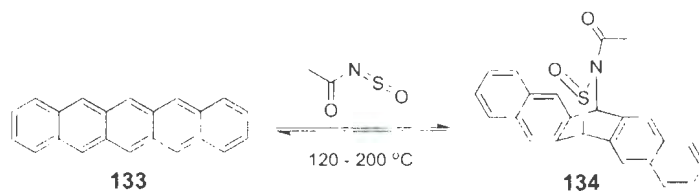


Figure 1.28: Schematics of an OFET circuit. U_D : Drain voltage; I_D : Drain current; S: Source electrode; D: Drain electrode; G: Gate electrode; U_G : Gate voltage; I_G : Gate current.

At present, OFETs can compete with other non-organic thin film transistors such as amorphous silicon devices. The improvements mainly came from the possibility of making highly ordered organic thin films, which are more significant for small molecules than for polymers. The first OFETs based solely on organic materials gave field-effect charge carrier mobilities μ_{FET} less than $10^{-2} \text{ cm}^2 \cdot \text{V}^{-1} \cdot \text{s}^{-1}$, which were considerably inferior to those of the inorganic FETs using amorphous silicon as semiconductor ($\mu_{\text{FET}} = 0.5 - 1 \text{ cm}^2 \cdot \text{V}^{-1} \cdot \text{s}^{-1}$). After 10 years of research, solution-processed OFET components are now approaching the field mobilities of amorphous silicon (maximum mobilities $\mu_{\text{FET}} \sim 0.6 \text{ cm}^2 \cdot \text{V}^{-1} \cdot \text{s}^{-1}$).¹⁹⁵

Among various conjugated oligomers that have been used to constitute the

semiconducting layers in OFETs, oligo(acene)s and oligo(heteroacene)s have been subjected to the most intensive survey, mainly because of their relatively high charge-carrier mobility.¹⁹⁶⁻¹⁹⁹ In 2002, a research group from IBM reported a method of using pentacene to build OFETs. In their work, in order to avert the solubility problem of pentacene, the researchers first converted pentacene to a soluble derivative **134** through a Diels-Alder reaction between pentacene and *N*-sulfinylacetamide (Scheme 1.17). Precursor **134** was able to form a high-quality thin film, which was subsequently restored to pentacene via a retro-Diels-Alder reaction at 120–200 °C. Organic field-effect transistors (OFETs) with pentacene films prepared in this way have shown a charge-carrier mobility of $0.29 \text{ cm}^2 \cdot \text{V}^{-1} \cdot \text{s}^{-1}$ at a drain voltage of $U_D = -20 \text{ V}$ in the linear region of the transfer characteristics plot, a charge-carrier mobility in the saturated region of $0.89 \text{ cm}^2 \cdot \text{V}^{-1} \cdot \text{s}^{-1}$, and an on/off ratio as high as 2×10^7 .



Scheme 1.17: A reversible Diels-Alder reaction on pentacene.

1.1.4.3 Organic solar cells

An organic solar cell is a device that converts light directly into electricity by using organic materials as the active layer.^{200,201} Compared with currently widely used inorganic solar cells, organic solar cells have attracted substantially growing

attention over the past few years, owing to their potential to provide environmentally safe, flexible, lightweight, inexpensive, and efficient solar cells.²⁰²⁻²⁰⁶ Since the breakthrough discovery by Tang's group that donor and acceptor materials could form a heterojunction between holes and electrons in an organic solar cell to give a power conversion efficiency of 1%,²⁰⁷ the efficiencies of so-called "bulk heterojunction organic solar cells" have currently been improved to 5.5%.²⁰⁸⁻²¹¹ The steady increase in efficiency will likely make organic photovoltaic materials a competitive alternative to inorganic materials in future solar cell technology.²¹²

Owing to the high performance, almost all current organic solar cells are fabricated based on the "heterojunction" approach, enlisting [60]fullerene (C_{60}) or its derivatives as acceptors and organic polymers or conjugated oligomers as donors.^{204,205,207} The use of C_{60} as an acceptor in organic solar cells was triggered by the work of Sariciftci *et al.* in 1993,²¹³ which showed that solar cells made from conducting polymers and C_{60} could attain unprecedentedly high device efficiencies. The reason for the use of C_{60} is that, in addition to a high electron affinity, C_{60} features fairly good transparency and electron conductance ($10^{-4} \text{ S} \cdot \text{cm}^{-1}$) as well as an exceedingly large exciton diffusion length.^{212,214} As shown in Figure 1.29, the device is usually built in a planar-layered structure, where the donor/acceptor organic light-absorbing layer is sandwiched between two different electrodes. One of the electrodes must be (semi-)transparent, often indium-tin-oxide (ITO), while the other electrode is aluminium, calcium, magnesium, gold, or other metals.^{202,212,214-216}

Basically, the underlying principle of a light-harvesting organic solar cell is the reverse of that of an OLED, and the developments of these two kinds of devices are somewhat related. Figure 1.30 gives a schematic illustration of the principle

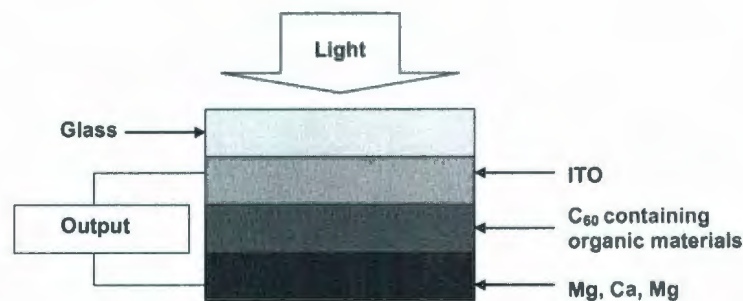


Figure 1.29: Basic structure of an organic solar cell.

based on which an organic solar cell operates. Illumination of the donor through the transparent electrode (ITO) leads to the formation of a photoexcited state of the donor, in which an electron is promoted from the HOMO to the LUMO of the donor (upward arrow). Subsequently, the electron can either return to the HOMO of the donor (downward), yielding luminescence, or be transferred to the LUMO of the adjacent acceptor, resulting in an extra electron on the acceptor ($A^{\bullet-}$) and leaving a hole at the donor ($D^{\bullet+}$). The photogenerated charges are then transported and collected at opposite electrodes. Through an external circuit, a working photovoltaic cell is realized.

There are several parameters that can be used to characterize the quality of organic solar cells, which include fill factor (FF), power conversion efficiency (η), external quantum efficiency (EQE), internal quantum efficiency (IQE), and open-circuit voltage (V_{OC}). All of these values should be obtained under standard test conditions (STC). The STC refers to $1000 \text{ W} \cdot \text{m}^{-2}$ intensity, AM (air mass) 1.5 simulated solar spectrum and the substrate temperature at $25 \text{ }^\circ\text{C}$.²¹⁵

In 2006, Pfeiffer and co-workers fabricated an efficient organic solar cell containing

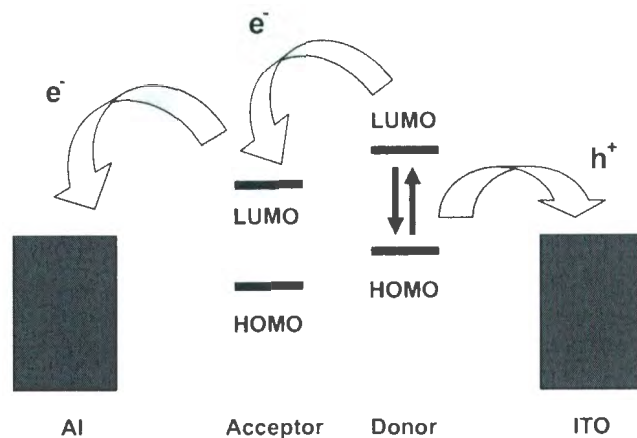


Figure 1.30: Basic principle of organic solar cells.

a novel low-bandgap oligo(othiophene) derivative **135** and C_{60} (Figure 1.31). Compared with other unsubstituted oligo(thiophene)s, the optical bandgap of **135** is considerably reduced (1.77 eV). This is a result of the introduction of electron-accepting dicyanovinyl end groups to form a conjugated A D A molecular motif. The excitons generated on **135** and C_{60} can be efficiently separated at the **135** C_{60} interface. This type of solar cells has achieved a high EQE value of 48% at 570 nm, high photovoltages of 1 V, and a power efficiency of 3.4% under $118 \text{ mW} \cdot \text{cm}^{-2}$ simulated sunlight.²¹⁷

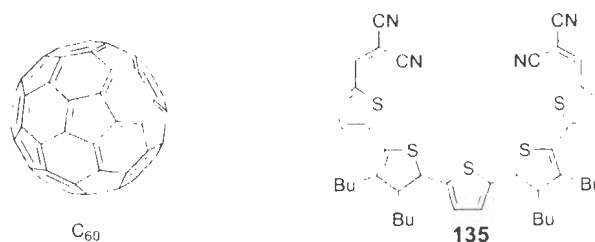


Figure 1.31: Structures of C_{60} and oligothiophene **135**.

In 2008, Nguyen and co-workers prepared a low-bandgap, solution processable oligo(thiophene) derivative **136**, which was functionalized with a highly absorbing chromophoric diketopyrrolopyrrole core (Figure 1.32). Such a molecular design results in optical absorptions that extend to 720 nm in solution and to 820 nm in the solid film, as well as a hole mobility around $10^{-6} \text{ cm}^2 \cdot \text{V}^{-1} \cdot \text{s}^{-1}$. The cyclic voltammogram of **136** shows quasi-reversible oxidation and reduction processes. The bulk heterojunction solar cell employing this oligomer as the donor and [6,6]-phenyl C_{60} -butyric acid methyl ester (PCBM, **137**) as the electron acceptor gives a very high power conversion efficiency, 2.3% under simulated AM 1.5 solar irradiation of $100 \text{ mW} \cdot \text{cm}^{-2}$, when a mixture of 70:30 donor acceptor (by weight) is used as the active layer. To date, this is the highest efficiency achieved among conjugated oligomer-based solution processed bulk heterojunction solar cells.²¹⁸

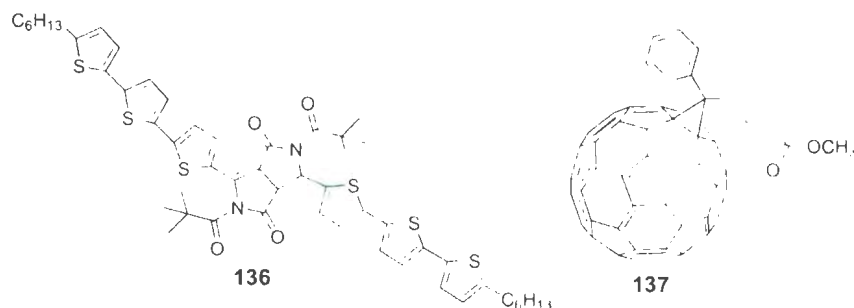


Figure 1.32: Structures of compounds **136** and **137**.

In addition to forming a blend of two different molecules such as the two examples above, the use of a single molecule bearing both donor and C_{60} groups constitutes another widely used method to fabricate the heterojunction organic layers in organic solar cells. Take compounds **138a** and **138b** as an example²¹⁹ (Figure 1.33). These

C_{60} oligomer dyads were synthesized and used to fabricate organic solar cells. Details of this “molecular hybrids” approach will be elaborated in Chapter 2 of this thesis.

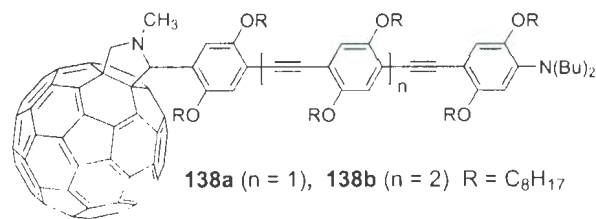


Figure 1.33: Structures of fullerene-OPE hybrids **138a-b**.

1.2 A brief introduction to [60]fullerene C_{60}

1.2.1 The discovery of C_{60}

The investigation on the molecular structure of [60]fullerene (C_{60}) commenced in the 1960s, which was actually earlier than its discovery. In 1966 the possibility of making large hollow carbon cages, structures now called large fullerenes, was proposed by Deadalus alias D. E. H. Jones.²²⁰ Unfortunately, this creative suggestion received no immediate attention from the scientific community. Four years later, in 1970, Osawa first proposed a spherical, football-shaped structure for the C_{60} molecule with an icosahedral (I_h) symmetry – an idea derived from the synthesis of bowl shaped corannulenes.^{221,222} After that, a series of, inter alia, Hückel calculations on C_{60} was reported in theoretical papers by several groups.^{223–225}

In 1984 it was found that large carbon-only clusters C_n with $n = 30–190$ could be produced upon laser vaporization of graphite.²²⁶ Although C_{60} was among these

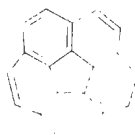


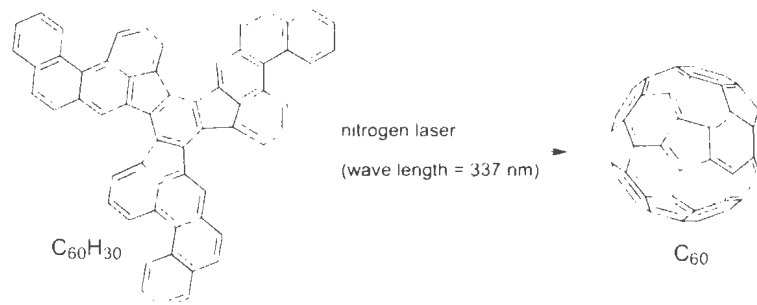
Figure 1.34: Structures of corannulene.

clusters, its identity was not heeded. The milestone achievement in the experimental discovery of C_{60} came in 1985. At that time, Professor Kroto, from the University of Sussex, UK, met Professor Curl, from Rice University, at a conference on molecular structure in Austin, Texas. Kroto went back to Houston with Curl to pay a visit to the laboratory of Rick Smalley. Later they arranged to examine a special kind of refractory carbon clusters, produced by focusing a pulsed laser on graphite in a cluster beam apparatus of Smalley's by using mass spectrometry. In the study, they found that, under specific clustering conditions, the m/z 720 peak attributed to C_{60} exhibited a pronounced intensity in the spectra, suggesting a particularly stable species. After discounting various highly improbable structures, they concluded that the molecule must be in a cage-like shape, and Smalley succeeded in building it out of his paper and tape. The paper describing this work was submitted to *Nature* in September 1985.²²⁷ The extra stability of C_{60} arises from its spherical structure, which is that of a truncated icosahedron with I_h symmetry. They named C_{60} as Buckminsterfullerene because of the similarity of the structure to the geodesic structures credited to a famous American architect, R. Buckminster Fuller. It was because of this ground-breaking work that Kroto, Smalley, and Curl later shared the Nobel Prize in Chemistry in 1996.

1.2.2 The production of C₆₀

For quite a while, the studies of C₆₀ had been conducted by only a small number of research groups due to the high costs and low yields of its production. The research on C₆₀ would not have flourished, had it not been for the breakthrough made by Wolfgang Kratschmer of Heidelberg University and Donald Huffman of the University of Arizona in 1990.²²⁸ The two scientists discovered a truly simple and efficient way to produce solid C₆₀ by arc-vaporization of graphite in a helium environment. Since this discovery, the field of fullerenes has grown rapidly and led to significant impacts in numerous different scientific areas.

Currently, tons of C₆₀ are produced annually by burning toluene under catalytic conditions,²²⁹ aside from vaporization of graphite. Also, with the aims to deduce the mechanisms of fullerene formation and to make specific fullerenes selectively and exclusively, total synthetic routes to C₆₀ fullerene have been explored by several groups, for instance, the reaction shown in Scheme 1.18.²³⁰



Scheme 1.18: Synthesis of [60]fullerene from a polynuclear aromatic precursor.

1.2.3 The structure and chemical properties of C_{60}

As depicted in Figure 1.35, the structure of C_{60} appears like a soccer ball with 12 pentagons and 20 hexagons. The six-membered rings are not aromatic. They are actually of alternating single and double bond character. All the bonds between two six-membered rings (so called 6,6-bonds) are double bonds with a bond length of 1.38 Å. The C-C bonds between six- and five-membered rings (called 5,6-bonds) are actually single bonds with a length of 1.45 Å. Hence, the overall C_{60} structure can be regarded as fused 1,3,5-cyclohexatrienes and [5]-radialenes.

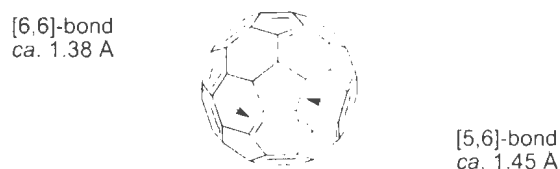


Figure 1.35: Structure of C_{60} .

There is bond angle strain existing on C_{60} .²³¹ The bond angle deviation from the ideal of sp^2 -hybridized carbons at each of the carbons on the C_{60} surface is 11.6° (Figure 1.36). This deviation induces a strain of 8.5 kcal/mol per carbon atom. This is the single largest contribution to the total heat of formation (ΔH_f) of C_{60} (10.16 kcal/mol per carbon atom).²³² Relief of this strain thus provides the major driving force for most of the reactivity of C_{60} .

In terms of its chemical properties, C_{60} is an electronegative molecule that can be easily reduced, but oxidized with difficulty. This is because the negative charge(s) can be significantly stabilized through extensive delocalization on the large spherical

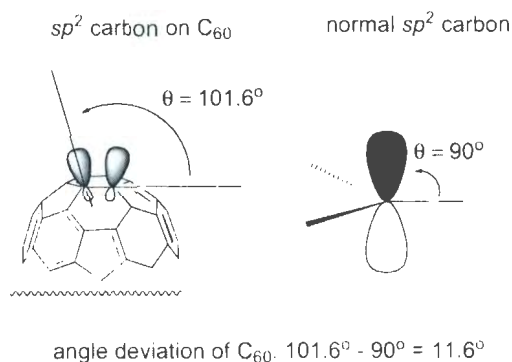


Figure 1.36: Bond angle strain of C_{60} .

surface of the C_{60} cage. Theoretical calculations on C_{60} also indicate that it actually possesses a low-lying triply degenerate LUMO, which bestows C_{60} a very high electron affinity.²³³ Moreover, the high symmetry of the C_{60} cage gives rise to a zero or close to zero molecular dipole moment.

Certain general patterns of its reactivity can be summarized as follows:

1. C_{60} behaves fundamentally as an electron-deficient alkene, not as an aromatic hydrocarbon. Reactions such as cycloadditions, nucleophilic and free radical additions across the bonds between two six-membered rings are therefore its characteristic reactivities. In addition, hydroborations, hydrometallations, hydrogenations, halogenations, and metal complex formation can take place on C_{60} .^{234,235}
2. The driving force for addition reactions is the relief of bond angle strain in the C_{60} cage. Reactions leading to tetrahedral sp^3 hybridized carbon atoms are strongly assisted by the angle strain present in C_{60} . In most cases, addition reactions of C_{60} are exothermic. The exothermicity of subsequent additions

depends on the size and the number of addends already attached to the C_{60} cage, and the favourability of additions decreases at a certain stage. This is because a high degree of addition on C_{60} will result in repulsions among appendant groups as well as strongly disfavored planar cyclohexane rings. Therefore, adducts of C_{60} with a high degree of addition are usually unstable or do not form at all. The interplay of these types of strain determines the number of energetically favorable additions to the C_{60} core.

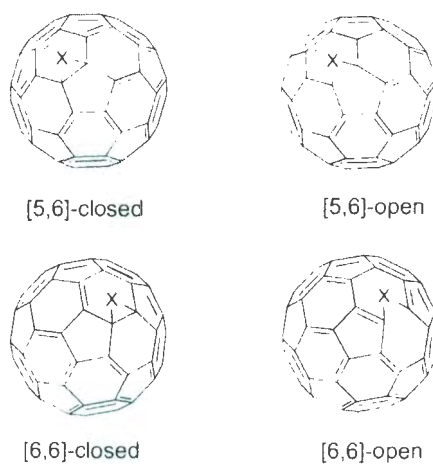


Figure 1.37: C_{60} isomers of [5,6]-Closed and open, [6,6]-closed and open structures.

3. The regioselectivity of addition reactions on C_{60} is controlled by minimization of the number of double bonds in the [5,6]-ring junctions. Double bonds in 5-membered rings are unfavorable, since they tend to increase the strain significantly. As shown in Figure 1.37, each of the additions to [5,6]-double bonds and [6,6]-double bonds leads to two different types of isomeric adducts. Each pair of isomers can be distinguished as open and closed structures. Because

the [5,6]-open and [6,6]-closed structure possess the minimum number of double bonds on 5-membered rings, they are the major products, while the [5,6]-closed and [6,6]-open structures are the minor products. In addition, [5,6]-open adducts are thermodynamically less stable than [6,6]-closed adducts.²³⁶ Isomerization of [5,6]-open to [6,6]-closed adducts promoted by light or heat have been reported.^{237,238}

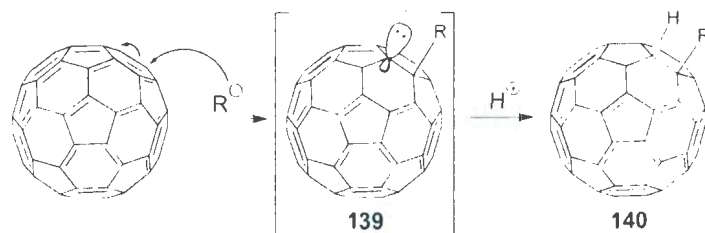
1.2.4 Major chemical reactions of C₆₀

The following section will mainly deal with two types of reactions that have been widely used to prepare functionalized C₆₀ derivatives, namely nucleophilic addition and cycloaddition. Also, in light of the very complicated regiochemistry of multiple addition reactions,²³⁹ only mono addition is discussed in this part.

1.2.4.1 Addition of carbon nucleophiles

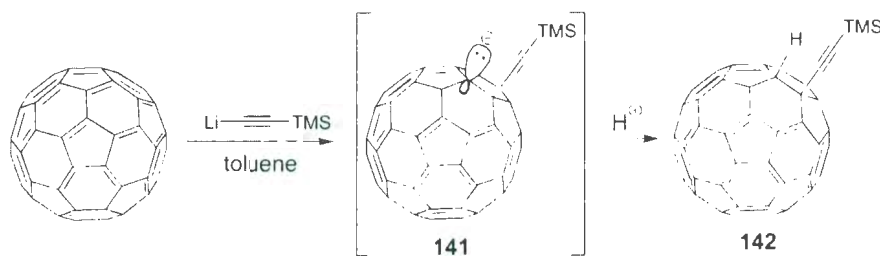
C₆₀ can readily react with many kinds of carbon nucleophilic reagents, including organolithium (RLi) and Grignard (RMgX) reagents (where R can be alkyl, phenyl or alkynyl groups), cyano, deprotonated α -halo esters or ketones.^{234,240-244} In the addition reactions, anions RC₆₀⁻ (**139**) are formed as intermediates, followed by the formation of hydrofullerene derivatives C₆₀HR (**140**) through protonation (Scheme 1.19).

A synthetically useful nucleophilic addition is the reaction between C₆₀ and metal acetylide. In general, metal acetylides are less reactive toward C₆₀ than other organolithium or Grignard compounds, due to their relatively high stability and low nucleophilicity.²⁴⁵ The sluggish reactivity, however, brings better selectivity to



Scheme 1.19: Addition of carbon nucleophile to C_{60} .

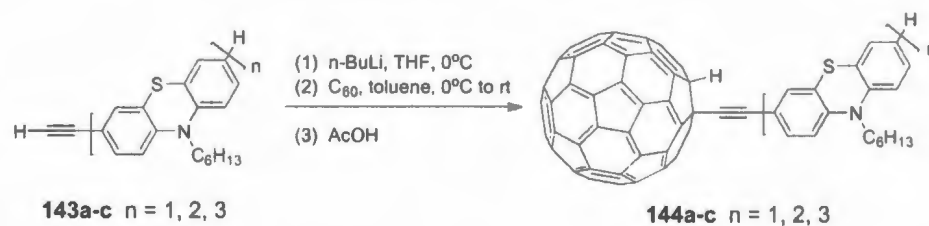
the addition reaction. The first acetylene- C_{60} hybrid was (trimethylsilyl)ethynyl-dihydro[60]fullerene (**142**), synthesized by Komatsu *et al.*²⁴⁵ In this reaction, (trimethylsilyl)ethynyl lithium was reacted with excess C_{60} in toluene at reflux to form an acetylene-fulleride anion intermediate **141**. Quenching the fulleride with an acid then afforded the product (Scheme 1.20).²⁴⁵



Scheme 1.20: Ethynylation reaction of C_{60} developed by Komatsu.

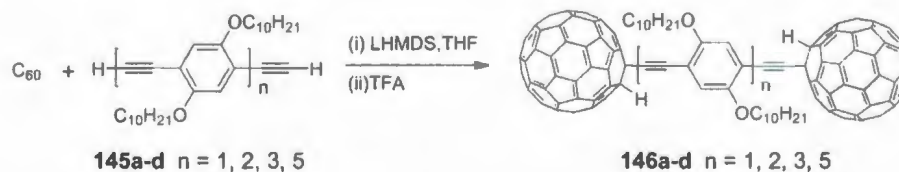
In 2006, Muller and co-workers synthesized a series of ethynyl bridged oligo(phenothiazine)- C_{60} dyads **144a-c** by addition of the corresponding oligophenothiazinyl lithium acetylides to C_{60} followed by protonation with acetic acid (Scheme 1.21). They found that the HOMO-LUMO gap of the resulting C_{60} adduct was lowered by 100 mV per phenothiazine unit attached. Upon UV excitation the phenothiazinyl fluorescence was considerably quenched, presumably due to a charge

separation resulting from an intramolecular photoinduced electron transfer from phenothiazine to the C_{60} group. These properties make this kind of C_{60} derivatives potentially useful materials in molecular optoelectronic devices.²⁴⁶



Scheme 1.21: Synthesis of ethynyl bridged oligo(phenothiazine)- C_{60} dyads **144**.

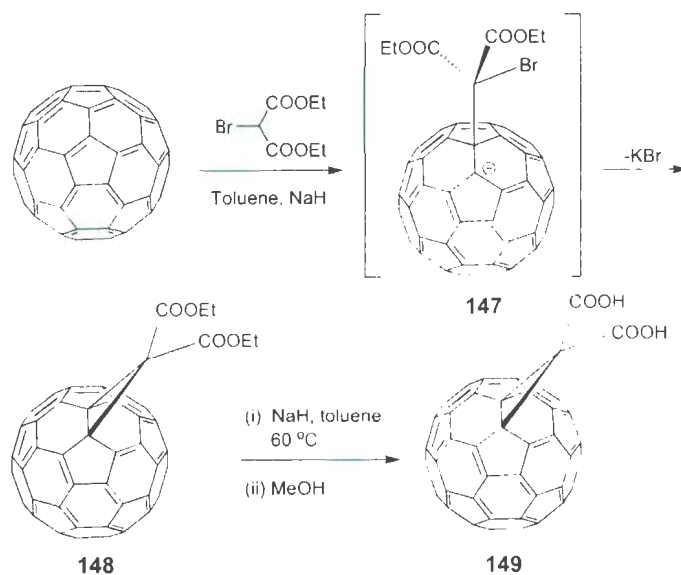
Tour and co-workers recently prepared a series of fullerene-terminated OPEs (**146a-d**) through an *in situ* ethynylation reaction between C_{60} and the corresponding terminal alkynes (Scheme 1.22). In this work, they found that lithium hexamethyldisilazide (LHMDS) was a very efficient base for the one-pot reaction that allowed the attachment of C_{60} to multiple terminal alkynes. The C_{60} -OPE hybrids were envisioned to be useful in organic photovoltaics, third-order NLO materials, and molecular electronics.²⁴⁷



Scheme 1.22: Synthesis of bisfullerene-terminated OPEs **146** by Tour *et al.*

Cyclopropanation of C_{60} , more often referred to as the Bingel reaction, is another important type of nucleophilic addition to C_{60} . The formation of

dihydrofullerene derivatives is achieved by means of intramolecular nucleophilic substitutions as outlined in Scheme 1.23.^{248,249} Here cyclopropanation of C_{60} with diethyl bromomalonate in toluene using NaH as auxiliary base proceeds smoothly at room temperature. 1H and ^{13}C NMR characterization have verified that the nucleophilic addition and subsequent intramolecular nucleophilic substitution took place at a [6,6] double bond of the C_{60} core. The product **148** is readily separable from the reaction mixture by column chromatography. Saponification of **148** can be done by treatment with NaH in toluene at raised temperatures, and subsequent quenching with methanol affords **149**. This method offers an easy access to structurally defined C_{60} derivatives with good solubility in organic solvents such as THF.



Scheme 1.23: Cyclopropanation of C_{60} with dimethyl bromomalonate.

In 2002, Wilson and co-workers reported the first fullerene-based X-ray contrast agent (CA), which was prepared through a modified Bingel reaction. The new CA

(compound **150**, Figure 1.38) is conceptually derived from the contemporary X-ray CAs, all of which use iodine as the X-ray attenuating vehicle and are based on the 2,4,6-triodinated phenyl ring substructure. The detailed synthetic route involved a modified Bingel-type reaction to first prepare a single addend containing six iodine atoms and eight protected hydroxyl groups, followed by the addition of four more adducts each containing four protected hydroxyl groups. The final deprotection step gave the highly water-soluble (> 460 mg/mL), nonionic, heavily-iodinated (24% I) fullerene **150**.²⁵⁰

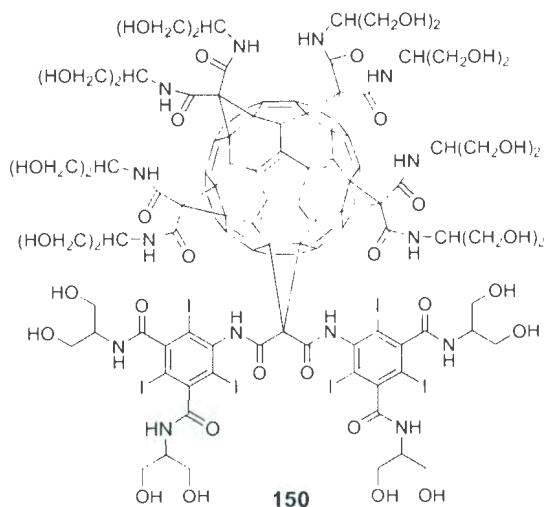
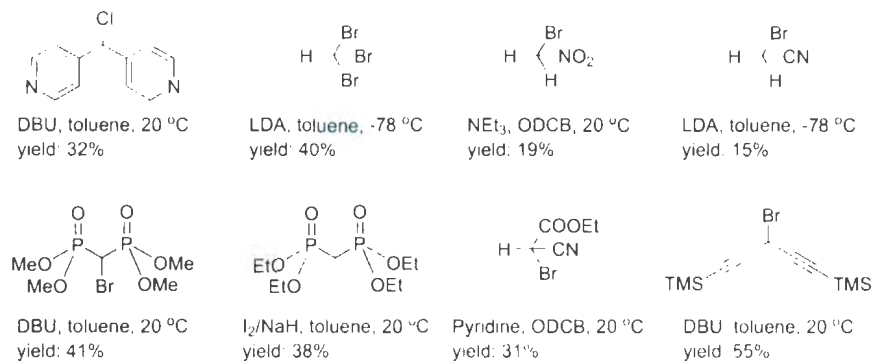


Figure 1.38: A C₆₀ based X-ray contrast agent reported by Wilson.

The Bingel reaction is not restricted to such C-H acidic carbonyl compounds as malonates. Various other substrates have also been used. Selected examples of these C-H acidic compounds are listed in Scheme 1.24.²³⁹



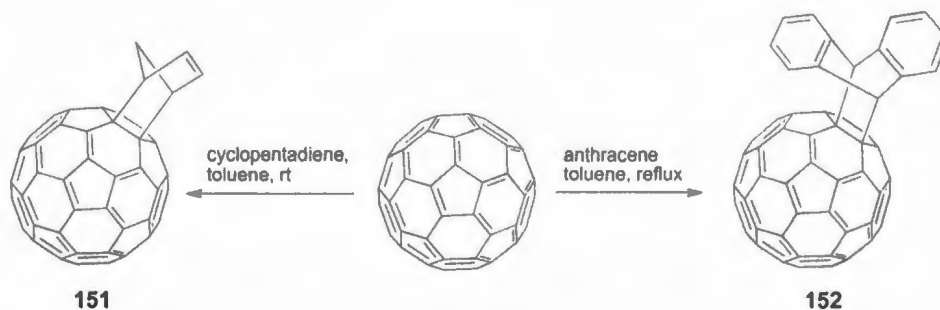
Scheme 1.24: Examples of reagents and conditions used in Bingel reactions.

1.2.4.2 Cycloadditions on C_{60}

[4+2] Cycloadditions

The [6,6] double bonds of C_{60} are dienophilic, which enables the molecule to undergo various Diels-Alder reactions ([4+2] cycloadditions).^{251,252} Mechanistic studies of some cycloadditions on C_{60} have clearly supported a concerted mechanism involving a symmetrical transition state.²⁵³ The dienophilic reactivity of C_{60} is comparable to that of maleic anhydride or *N*-phenylmaleimide.^{254,255} The conditions under which cycloadducts are formed strongly depend on the reactivity of the diene species. Most [4+2] cycloadditions on C_{60} are accomplished under thermal conditions; however, photochemical conditions have also been reported. Microwave irradiation is also efficient as a source of energy for this type of reactions.²⁵⁶ Outlined in Scheme 1.25 are two examples of C_{60} [4+2] cycloaddition.²⁵⁷ In the first reaction, equimolar amounts of cyclopentadiene and C_{60} react at room temperature to give monoadduct **151** in a comparatively high yield, while in the second reaction the formation of the cycloadduct **152** with anthracene needs an excess of the diene in refluxing toluene. Apparently, the reactivity of cycloaddition is directly related to the nature of the

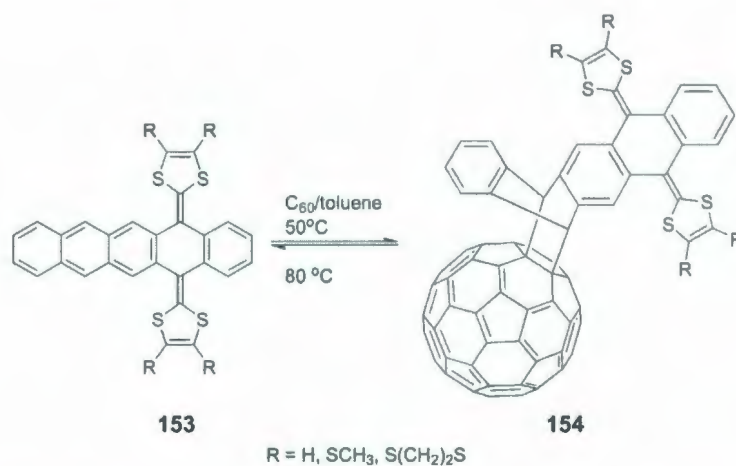
diene counterpart.



Scheme 1.25: [4+2] Cycloadditions of cyclopentadiene and anthracene to C_{60} .

The [4+2] cycloaddition approach can allow a variety of functional groups to be covalently attached to the C_{60} cage, yielding novel C_{60} dyads and polyads. Tetrathiafulvalene (TTF) is a promising candidate for assembling C_{60} based molecular donor-acceptor (D-A) ensembles. TTF is a non-aromatic molecule that can form 1,3-dithiolium cations with aromatic character upon oxidation. The aromaticity gained by TTF in releasing electrons is the key to the design of C_{60} TTF hybrids with long-lived charge-transfer features.²⁵⁸ In 2002, Guldi and co-workers prepared C_{60} TTF dyads **154** by fusing a series of anthracene containing π -extended TTFs to the C_{60} core via the Diels-Alder reaction (Scheme 1.26). Interestingly, these cycloaddition reactions are thermally reversible, enabling such molecular systems to function as fluorescence switches. At 50 °C, the reaction favors the [4+2] cycloaddition direction, forming the dyads which are referred to as the ON-state by the authors since the singlet excited state fluorescence is quenched through activated electron transfer from TTF to C_{60} . When the dyads are heated to 80 °C, a retro-Diels-Alder reaction takes place predominantly, which releases C_{60} and the fluorescent TTF compound. This is

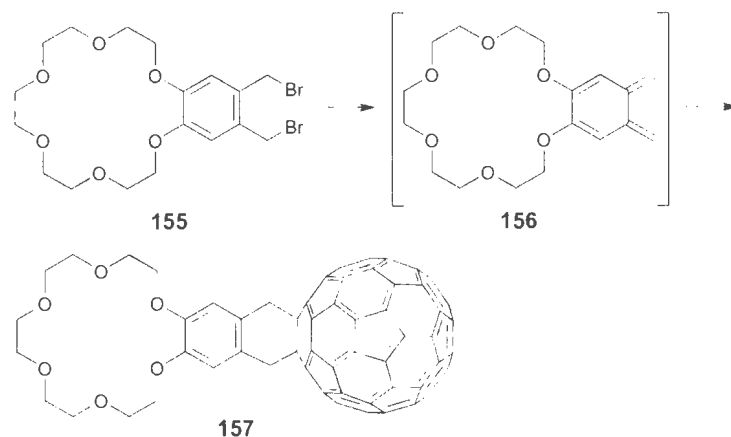
regarded as the OFF-state because the emission is reactivated by stopping electron transfer.²⁵⁹



Scheme 1.26: Fluorescence switches based on C₆₀-TTF dyads **154**.

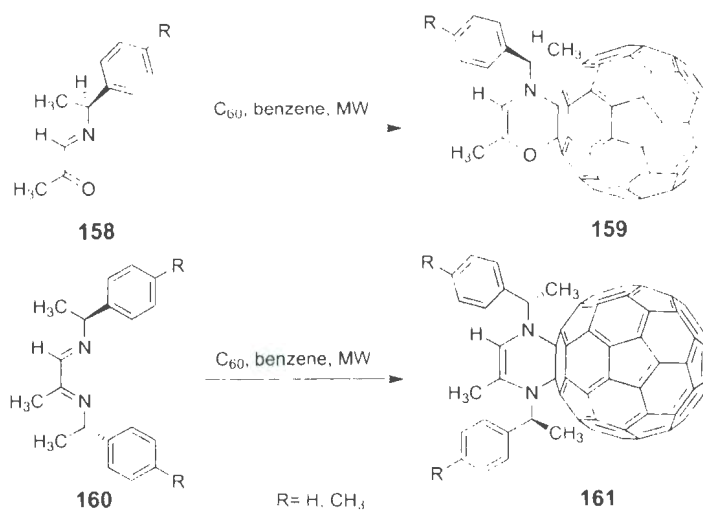
Apart from using a diene directly, compounds that are precursors to dienes can also be applied to [4+2] cycloadditions with C₆₀. Müllen and co-workers discovered an interesting approach to synthesize stable Diels-Alder C₆₀ adducts by making use of an *o*-quinodimethane intermediate **156**, generated *in situ* from an elimination reaction, as the diene to form thermally stable cycloadduct **157** (Scheme 1.27).²⁶⁰ Extraction experiments showed that the complex of **157** with potassium ion was very soluble in protic solvents like MeOH. Using Langmuir-Blodgett (LB) techniques, monolayers of the highly amphiphilic C₆₀-derived crown ether **157** and its potassium ion complex were prepared and investigated.²⁶¹

The [4+2] cycloadditions of C₆₀ occur not only with carbon dienes but also heterodienes. In 2007, Gutierrez and co-workers reported a microwave-assisted synthesis of new C₆₀ adducts **159** and **161** resulting from the Diels-Alder reactions



Scheme 1.27: Diels-Alder reaction of C_{60} with an *in situ* generated diene.

of chiral α -oxo imines **158** and α -diimines **160** with C_{60} (Scheme 1.28).²⁶²

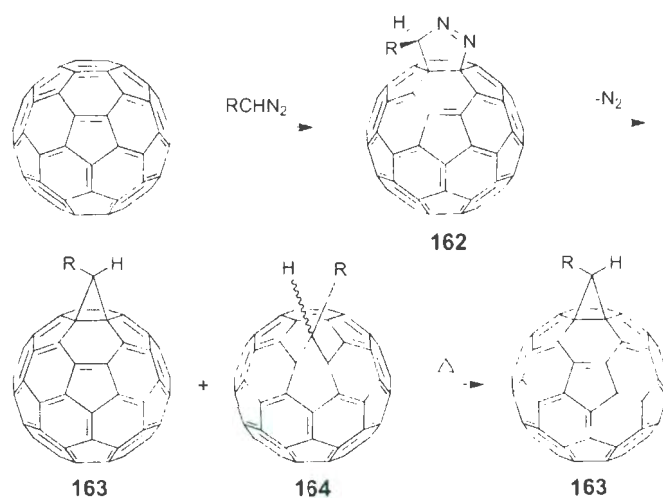


Scheme 1.28: Microwave-assisted Diels-Alder reactions of C_{60} with heterodienes.

[3+2] Cycloadditions

(A) *Addition of diazo compounds.* The product from an addition reaction of a diazo compound with C_{60} is very similar to that of a nucleophilic cyclopropanation

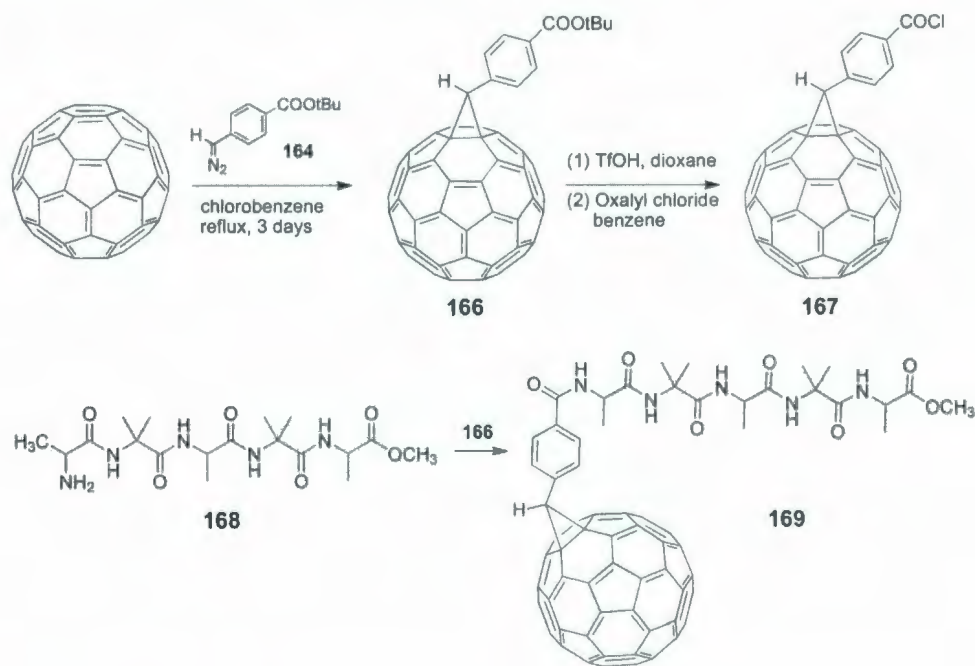
of C_{60} . But the mechanisms of these two types of reactions are markedly different. The product of a diazo addition on C_{60} actually involves three consecutive steps as exemplified in Scheme 1.29: (i) [3 + 2] cycloaddition occurring at a [6,6]-double bond, yielding intermediate **162**, (ii) extrusion of N_2 out of the adduct, affording a mixture of **163** and **164**, and (iii) thermal isomerization of **164** into the more stable product **163**.^{236,263}



Scheme 1.29: [3 + 2] Cycloaddition between C_{60} and diazo compound.

In 1993, Prato and co-workers prepared a C_{60} -oligopeptide hybrid **169** through a 1,3-dipolar cycloaddition reaction. In this work, *tert*-butylcarboxylate **166** was synthesized by the reaction of diazomethylbenzoate **165** with C_{60} . After hydrolysis with trifluoromethanesulfonic acid (TfOH) and chlorination with oxaly chloride, acyl chloride **167** was generated. Compound **167** was then used to acylate pentapeptide **168** to afford the desired C_{60} -oligopeptide hybrid **169** (Scheme 1.30).²⁶⁴ Although this synthetic approach was only tested on a model peptide, it is reasonable to assume

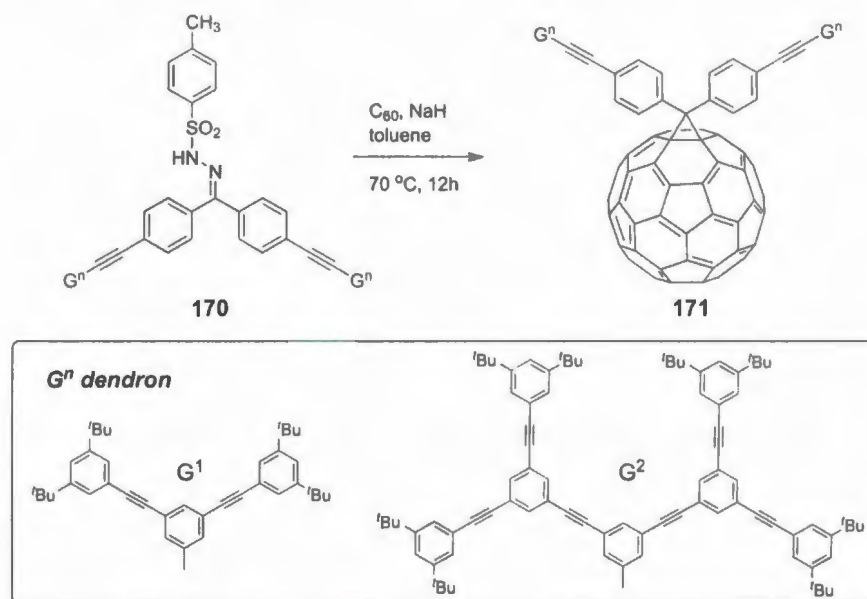
that it will be widely applicable in the preparation of analogous C_{60} adducts derived from other biologically active and water-soluble peptides.



Scheme 1.30: Synthesis of fullerene-oligopeptide hybrid **169**.

In the search of convenient procedures of preparing diazo precursors for C_{60} cycloaddition, Wudl developed a method based on base-induced decomposition of tosylhydrazones.²⁶⁵ This method allows a diazo intermediate to be generated *in situ* to react with C_{60} . Generally, the diazo intermediate can be trapped by C_{60} so rapidly that there is no need for any purification on the intermediate prior to the cycloaddition reaction. Even unstable diazo compounds can be successfully applied in such a facile 1,3-dipolar cycloaddition reaction. Based on this method, Wachter and co-workers later prepared two oligo(arylacetylene) dendron functionalized C_{60} derivatives **171** by

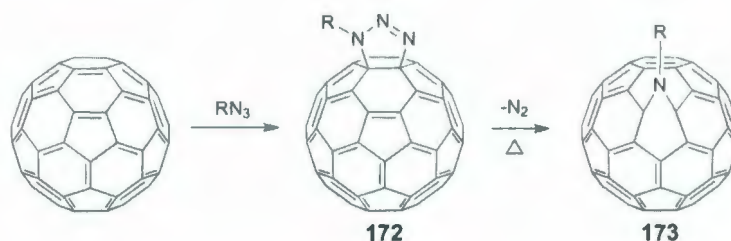
using compounds **170** as precursors (Scheme 1.31).²⁶⁶



Scheme 1.31: Synthesis of dendro[60]fullerenes **171** using tosylhydrazones **170**.

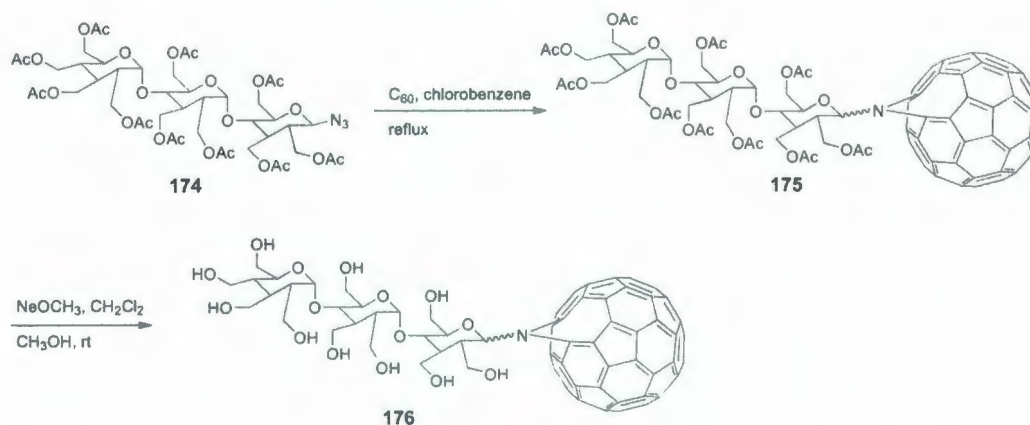
(B) *Addition of azides.* Organic azides can be used as efficient 1,3-dipoles to react with C₆₀ through a [3+2] cycloaddition at the [6,6]-double bond of C₆₀, yielding a [6,6]-triazoline intermediate after mono-addition, for example, **172** in Scheme 1.32. Such adducts sometimes can be detected or even isolated, but in most cases a thermal nitrogen-extrusion quickly follows up to afford aza-bridged fullerenes, with the [5,6]-open isomer, such as **173**, as the major product.^{267–270}

Azides are easily prepared by nucleophilic substitution of alkyl halides with sodium azide (NaN₃), and the yields of azide additions on C₆₀ are generally high. For this reason, functionalization of C₆₀ via the azide cycloaddition has led to a broad range of C₆₀ derivatives. In 1998, Kobayashi and co-workers reported a general



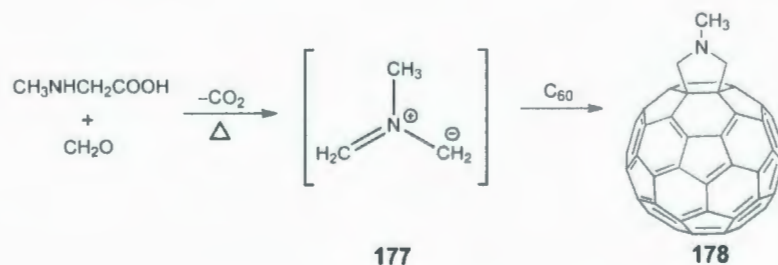
Scheme 1.32: Addition of azides to [60]fullerene.

synthetic route to attach oligosaccharides to C_{60} via azide cycloaddition reactions. Outlined in Scheme 1.33 is a selected example of their work. The cycloaddition was carried out in refluxing chlorobenzene between per-*O*-acetyl glycosyl azide **174** and C_{60} to give a mixture of two inseparable stereoisomers of **175**. Treating **175** with sodium methoxide then generated *N*- β -glycopyranosyl [5,6]-azafulleroid **176** under mild conditions. In view of the unique properties of C_{60} and the biological activities of saccharides attached, this kind of C_{60} -saccharide adducts were envisioned as having potential biological and biomedical applications.²⁷¹



Scheme 1.33: Synthesis of oligosaccharide-fullerene hybrid **176**.

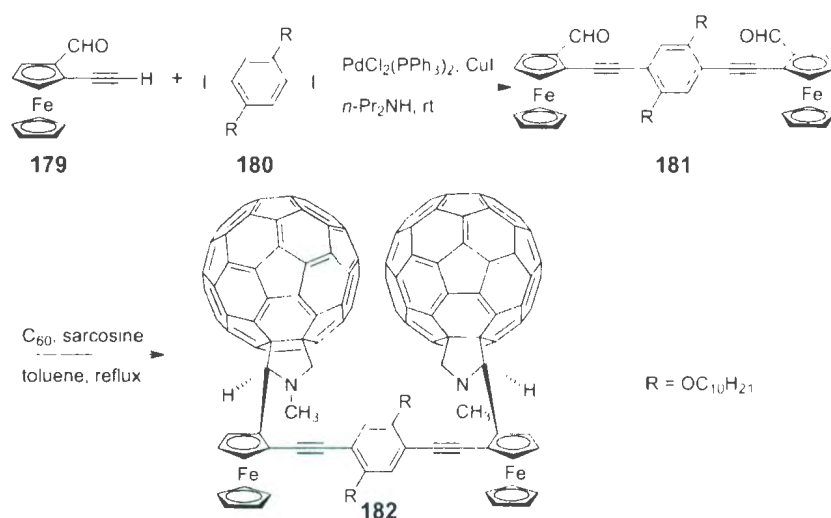
(C) *Addition of azomethine ylides.* Azomethine ylides are very useful 1,3-dipoles to react smoothly with C_{60} in good yields. The product of an azomethine ylide addition on C_{60} is fulleropyrrolidine, for instance, **178** as shown in Scheme 1.34.²⁷²⁻²⁷⁵ This reaction was developed by Prato and Maggini and has become one of the most widely used methods for fullerene functionalization.²⁷² The wide acceptance of this method is due to the good selectivity (only the [6,6]-bond is attacked) and a wide range of addends and functional groups it tolerates. Azomethine ylides can be generated *in situ* from various readily accessible starting materials. One of the easiest approaches to generate an azomethine ylide 1,3-dipole involves the decarboxylation of the immonium salt derived from condensation of an α -amino acid with an aldehyde or ketone.²⁷²⁻²⁷⁴ For example, azomethine ylide **177**, formed *in situ* through decarboxylation of the condensation product of *N*-methylglycine (sarcosine) and paraformaldehyde in refluxing toluene, can react with C_{60} to give *N*-methylpyrrolidine derivative **178** in 41% yield.²⁷²



Scheme 1.34: [3+2] Cycloaddition of azomethine ylide to C_{60} .

In 2001, Riant and Mamane reported the synthesis of an enantiopure ferrocene-fullerene hybrid **182** by using Prato's methodology on a chiral ferrocenyl aldehyde (Scheme 1.35). The synthesis started with a Sonogashira coupling of terminal alkyne

179 with diiodide **180**, giving the C_2 -symmetric dialdehyde **181**, on which lipophilic alkoxy groups were functionalized for better solubility. A two-fold cycloaddition of **181** with sarcosine and C_{60} gave product **182** in a modest yield (21%) with complete diastereoselectivity and good solubility in most common organic solvents. This molecule was designed to show some interesting photophysical properties, owing to its peculiar molecular structure and the presence of photoactive D/A moieties.²⁷⁶



Scheme 1.35: Synthesis of ferrocene-fullerene hybrid **182**.

Recently, a novel dimeric phthalocyanine- C_{60} nanoconjugate **183** (Figure 1.39) was prepared through a [3+2] cycloaddition of azomethine ylide with C_{60} by Guldi and co-workers. Photophysical measurements confirm that an intramolecular electron transfer, from the photoexcited ZnPc moiety to the electron-accepting C_{60} unit, overwhelmingly dominates the overall photoreactivity of the nanoconjugate. Through-space charge-transfer processes facilitated by the close proximity of the ZnPc and the C_{60} moieties play a decisive role in the lifetimes of the charge separated states,

ranging from 10^{-10} to 10^{-9} seconds.²⁷⁴

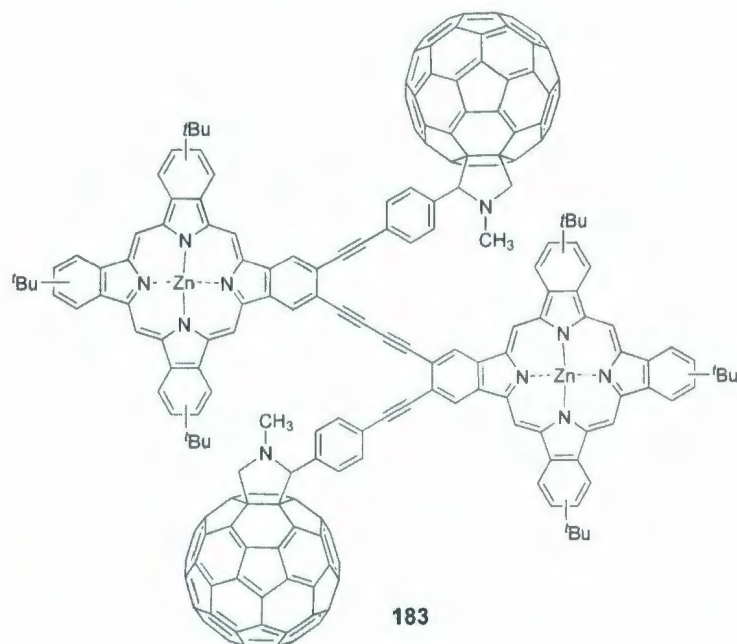
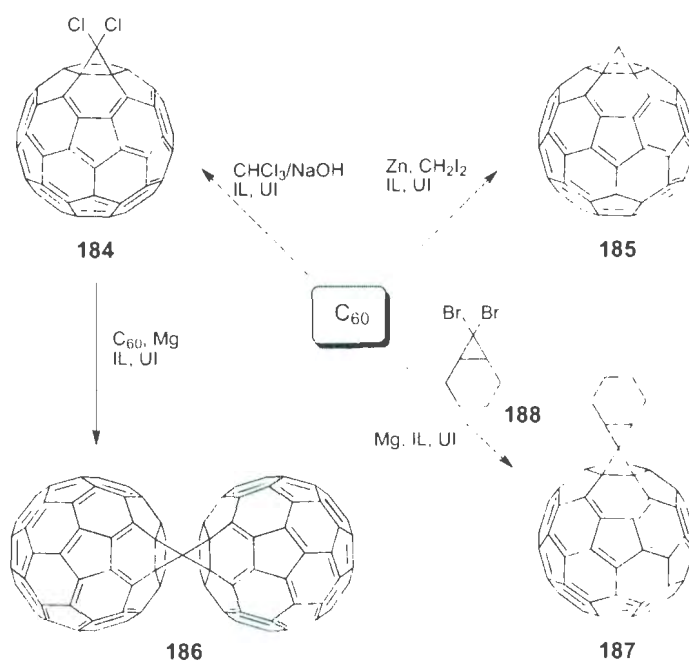


Figure 1.39: Structure of phthalocyanine-fullerene hybrid **183**.

[2+2] and [2+1] Cycloadditions

In addition to the reactions mentioned above, there are various reactive compounds that can react with C_{60} through [2+2] cycloaddition, including benzyne,²⁷⁷ enones,²⁷⁸ alkynes,²⁷⁹ alkenes,²⁸⁰ and ketenes.²⁸¹ [2+1] reactions are also common for C_{60} , which usually proceed through the addition of carbenes or nitrenes onto C_{60} .^{282,283} These two types of cycloadditions both lead predominantly to the formation of closed [6,6]-bridged isomers. In 2003, Zhou and co-workers reported a series of interesting [2+1] cycloaddition reactions of C_{60} and carbenes in ionic liquid (IL) media under ultrasonic irradiation (UI). The synthesis began

with dehalogenation of a polyhalide, for example, CHCl_3 , $\text{C}_{60}(\text{CCl}_2)$, CH_2I_2 , or 7,7-dibromobicyclo(4.1.0)heptane, by treatment with zinc, magnesium or NaOH powder. The resulting carbene intermediate reacted with C_{60} *in situ* in the presence of ultrasonic irradiation. In these reactions, ionic liquid solvents, such as [bmim][PF₆] or [omim][BF₄], were used. [6,6]-Junction cycloaddition products **184-187** were formed as single isomers in 53-79% yields with excellent stereoselectivity (Scheme 1.36).²⁸⁴



Scheme 1.36: [2 + 1] Cycloadditions of carbenes to C_{60} .

1.3 Outline of the thesis

The thesis describes three major projects focusing on the synthesis and property characterization of π -conjugated oligomers and fullerene derivatives. The details of

these studies are elaborated in Chapters 2 to 4.

Chapter 2 introduces the synthesis of a series of dumbbell-shaped $C_{60}-\pi-C_{60}$ triads, in which the π -oligomer units are OPE/OPV based diblock co-oligomers assembled in either a linear or a cruciform shape. Both the ground- and excited-state properties of these novel $C_{60}-\pi-C_{60}$ triad systems have been investigated by spectroscopic and electrochemical analyses. Access to these new C_{60} -oligomers has allowed the roles of the π -oligomer bridge to be better understood, and lent insight into molecular factors such as electron delocalization, conjugation length and dimensionality, and electronic coupling effects. Results of this project indicate that the geometric properties of the oligomer unit deserve serious and judicious considerations in the design of new functional C_{60} -oligomer materials.

In Chapter 3, solid-state polymerization of a series of oligoyne-bridged bisfullerene hybrids are investigated. Specifically, dumbbell-shaped linear bisfullerene-encapped conjugated oligoynes as well as a star-shaped tetrafullerene-oligoyne derivatives are prepared via an *in situ* ethynylation reaction. The solid-state reactivity of these compounds on mica surface at elevated temperatures has been investigated by UV-vis, FT-IR, differential scanning calorimetry (DSC), and XRD techniques. Thermally induced polymerizations of the C_{60} -oligoyne hybrids are monitored by atomic force microscopy (AFM). Relevant structure-property relationships are discussed in this chapter.

Chapter 4 focuses on a new class of two-dimensionally conjugated, H-shaped co-oligomers based on OPE-OPV building blocks, termed H-mers. The synthesis of these H-mers employs Sonogashira coupling and Wittig-Horner reactions. Electronic and spectroscopic properties of the H-mers functionalized with electroactive

substituents are investigated by UV-Vis absorption and fluorescence spectroscopic characterizations. It is found that the electronic and photonic behavior of the H-mers can be flexibly manipulated or finely tuned by chemical functionalization with various electroactive and chromophoric groups at the terminal positions of the H-mers. Moreover, H-mers functionalized with suitable groups (*e.g.* amino) show fluorescence sensing function toward Brønsted acids and selected transition metal ions. The results of this project verify the feasibility of using the conjugated scaffold of H-mers as a versatile fluorophore platform for various fluorescence applications.

Chapter 2

OPE/OPV Co-Oligomer Bridged Bisfullerene Triads

2.1 Introduction

As mentioned in Chapter 1, C_{60} and π -conjugated oligomers are important molecular materials with extensive applications in electronic and optoelectronic devices. Recently, there is an increasing interest in fabricating the so-called “bulk-heterojunction” organic photovoltaic cells using C_{60} and n-type conjugated oligomer materials.^{204,205,207} There are two different approaches to prepare the “heterojunction” in this type of organic photovoltaic cells. The first approach is to simply mix or blend the two active components— C_{60} and conjugated oligomers—into one layer by mechanical means,^{217,218} while the second approach is to synthesize hybrid compounds, in which C_{60} groups and conjugated oligomers are linked to one another through covalent bonds.^{219,285-287} Basically, the two approaches (namely, “blend” and

“molecular”) have essentially the same working principle; that is, the C_{60} moieties function as electron acceptors, and the oligomers as electron donors. In device fabrication, however, the second (*i.e.* molecular) approach tends to exhibit at least two major advantages over the first (blend) one:

1. Severe phase segregation and clustering frequently occur in the blends of C_{60} and conjugated oligomers due to the poor solubility and strong aggregation of pristine C_{60} molecules. This problem is indeed detrimental to the performance of photovoltaic cells. Studies carried out by several groups have clearly confirmed the critical effects of morphological behavior on the quality of the junction and thus on the final output performances of the device. In particular, it has been shown that the limited miscibility of the two components in a C_{60} /conjugated polymer biphasic system can lead to the formation of clusters of C_{60} , which in turn dramatically reduce the efficiency of the device. Hybrid molecules of C_{60} and oligomers can easily avert this problem, as C_{60} moieties and oligomers are bound to one another through strong covalent bonds. Additionally, the C_{60} -oligomer hybrid molecules can be readily tuned to show better solubility and processability than that of blend materials.^{288,289}
2. Structure–property relationships for C_{60} -oligomer hybrids with defined chemical structures can be readily probed and understood by using the systematic approach as described in §1.1.2. As such, key molecular parameters that control the photophysical properties and device performances can be identified and manipulated through rational design and optimization.²⁸⁷

So far, a huge number of C_{60} -oligomer hybrid systems have been reported in the literature, and their photophysical properties have been investigated with the goal to explore their potential uses in photovoltaic devices. An early example of C_{60} -derived linear π -conjugated system **189** was reported in 1995 by Imahori *et al.*, who studied the photochemical properties of a class of carotenoid-functionalized C_{60} derivatives (Figure 2.1).²⁹⁰

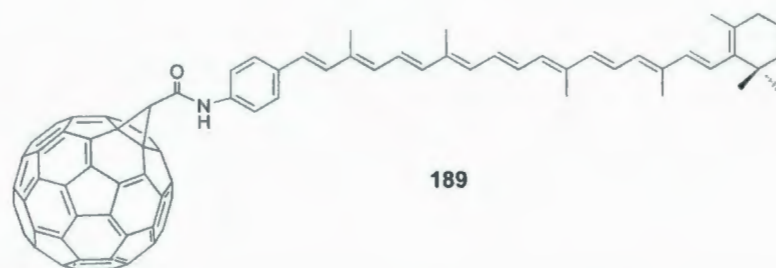


Figure 2.1: Carotenoid-functionalized C_{60} derivative **189** reported by Imahori.

Nierengarten *et al.* in 2000 prepared a fulleropyrrolidine derivative **190**, which contains a short-chain OPV moiety (Figure 2.2). This C_{60} -OPV hybrid can be regarded as the first example of molecular heterojunction specifically designed for photovoltaic purposes. The properties of **190** have been thoroughly investigated. It was found that the electronic absorption envelop of **190** corresponded to the sum of the spectra of the two components, C_{60} and OPV. This result indicates that there are no electronic interactions between the π -conjugated chain and the C_{60} group in the ground state. Nevertheless, a strong quenching of the luminescence of the OPV unit was detected for **190**. A simple photovoltaic device was fabricated, containing a spin-coated film of **190** sandwiched between an indium-tin oxide (ITO) coated glass

electrode and a vacuum evaporated aluminium electrode. This device gave a short circuit current density (J_{SC}) of $10 \mu\text{A} \cdot \text{cm}^{-2}$ and an open circuit voltage (V_{OC}) of 0.46 V under monochromatic irradiation (400 nm , $12 \text{ mW} \cdot \text{cm}^{-2}$). The limited efficiency of this device was attributed to the competition between energy transfer and electron transfer.²⁹¹

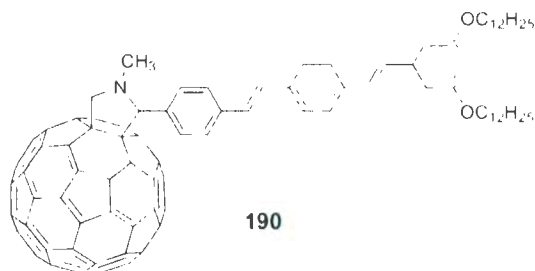


Figure 2.2: C_{60} -OPV dyad **190** prepared by Nierengarten *et al.*

In 2005, Otsubo and co-workers synthesized two oligothiophene-fullerene dyads **191a-b** and two triads **192-193** (Figure 2.3).²⁹² In the triads, quaterthiophene (4T) and octithiophene (8T) are linked by a trimethylene chain and either one is attached to a C_{60} group. The cyclic voltammograms and electronic absorption spectra of these triad compounds show no evidence of electronic interactions among the three electroactive components in the ground state. The emission spectra of **192** and **193** were markedly perturbed by electron transfer and or energy transfer from the oligothiophene to C_{60} . Comparison between the emission spectra of triads (**192** and **193**) and dyads (**191a-b**) suggests that the additionally attached octithiophene or quaterthiophene in the triads is in fact involved in the photodeactivation mechanism. For instance, 8T-4T- C_{60} triad **192** undergoes photoinduced electron transfer after

photoexcitation of the OT moiety, leading to a long-distance charge separated species, $[8T^{+\bullet} - 4T - C_{60}^{-\bullet}]$, the existence of which was confirmed by transient absorption spectroscopy. A sandwich device based on the 8T-4T- C_{60} triad **192** afforded a more effective photovoltaic response to visible light in comparison to the device made of dyad 4T- C_{60} **191a**, owing to the contribution of the additional OT chromophore. On the other hand, the 4T-8T- C_{60} (**193**) based device showed a relatively poorer photovoltaic performance than the 8T- C_{60} (**190b**) device, due to the absence of long-distance charge separation via photoinduced electron transfer.²⁹²

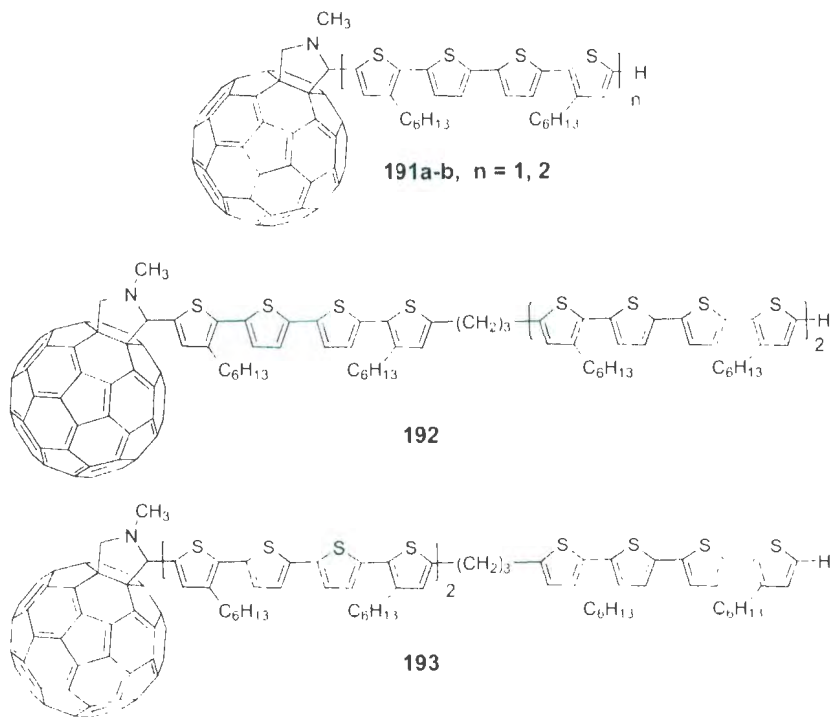


Figure 2.3: C₆₀-OT dyad **191** and triads **192** **193** prepared by Otsubo *et al.*

Apart from the relatively simple dyad motif, triad C_{60} and oligomer derivatives characterized by a symmetric dumbbell-shaped structure, namely $C_{60} \pi C_{60}$, have grown rapidly in number in the recent literature due to their unique structural and photophysical properties. For example, Martín and co-workers prepared a series of C_{60} OPE C_{60} molecules **194**, in which the oligomer chain length was systematically increased from monomer to heptamer.²⁹³ Also, our group recently prepared the first model of a rigid C_{60} TTFAQ C_{60} triad, **195** (see Figure 2.4).²⁹⁴

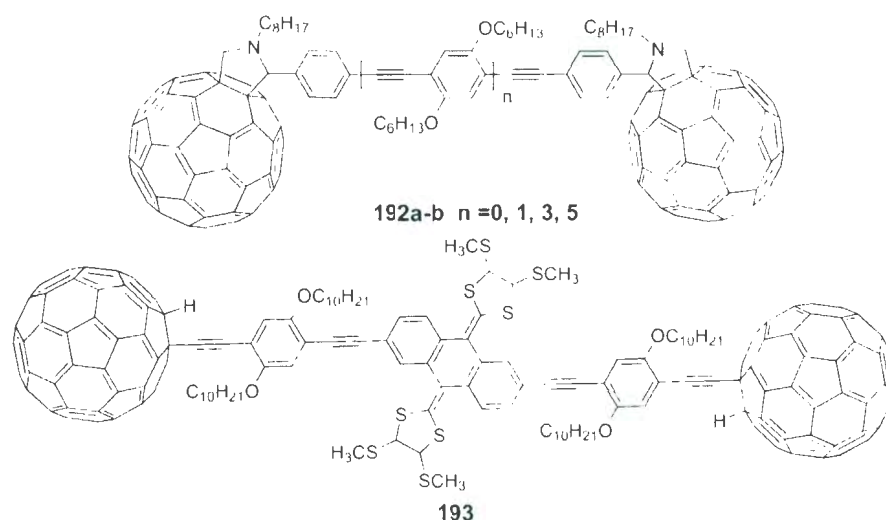


Figure 2.4: Dumbbell-shaped $C_{60} \pi C_{60}$ triads **194** **195**.

In comparison to relatively simple $C_{60} \pi$ dyads, dumbbell-shaped triads are actually not so demanding in synthesis, since the symmetric structure requires no selective strategy to be planned. Moreover, as Martín and co-workers pointed out, the electronic interactions between the two C_{60} cages in either the ground state or the excited state varied significantly depending on the detailed structures and

electronic nature of the bridging π -units incorporated.^{285,295} The presence of a second fullereryl unit into the molecular dumbbell has been reported to significantly influence the photophysical consequences. Such effects presumably arise from the unique stabilization of the photogenerated radical ion pair exerted by the additional C_{60} cage.^{295,296} However, clear understanding of the C_{60} - π - C_{60} system has not yet been fully achieved, while comprehensive property-relationship analyses are still hindered by the relative scarcity of model systems available. To address this issue, a new model system for dumbbell-shaped C_{60} - π - C_{60} triads is synthesized and investigated and the results are reported in this chapter. The oligomer unit of the C_{60} - π - C_{60} model is designed as either a linear (**196**) or a cruciform (**197**) shaped OPE/OPV block co-oligomer, in order to probe the effects of π -conjugation and dimensionality (Figure 2.5). Electron-donor (D) substituted OPE/OPV bridges are prepared in the structure of **198** to elucidate the substituent effect. In addition, a segmental structure of the molecular dumbbells, dyad **199**, is prepared to help better understand the structure-property relationships; particularly, the electronic communication between the phenyl acetylene π -bridge and the C_{60} cage.

The following sections will elaborate on the synthetic methods and property investigations of the C_{60} - π - C_{60} triads and relevant OPE/OPV oligomer precursors.

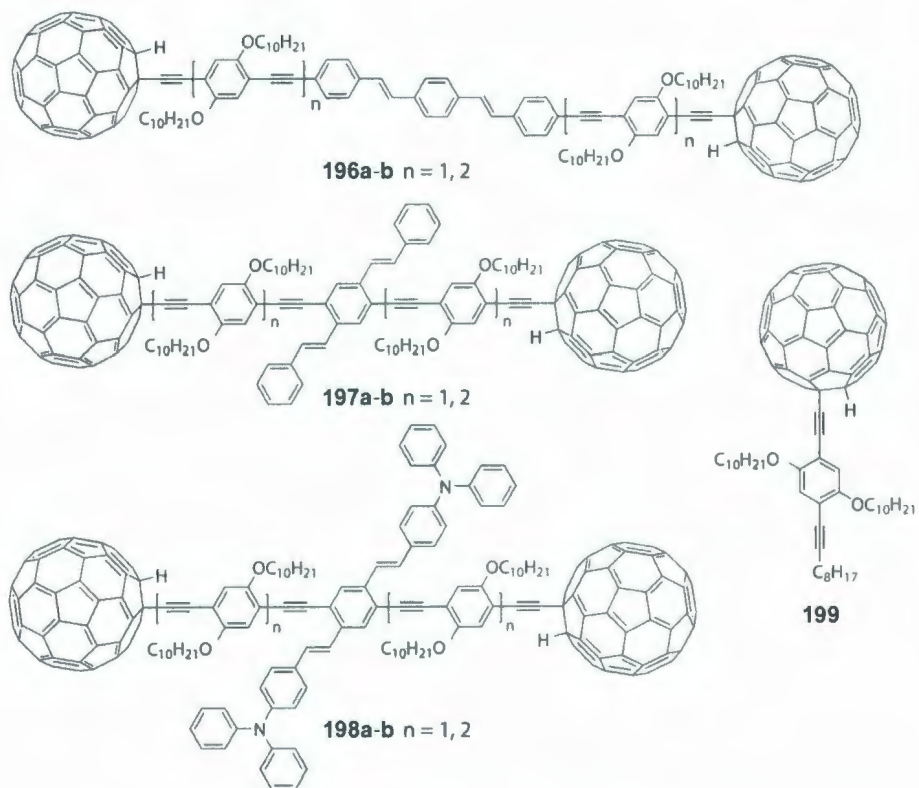


Figure 2.5: $C_{60}-\pi-C_{60}$ molecular dumbbells **196-198** and related compound **199** targeted in the work described in this chapter.

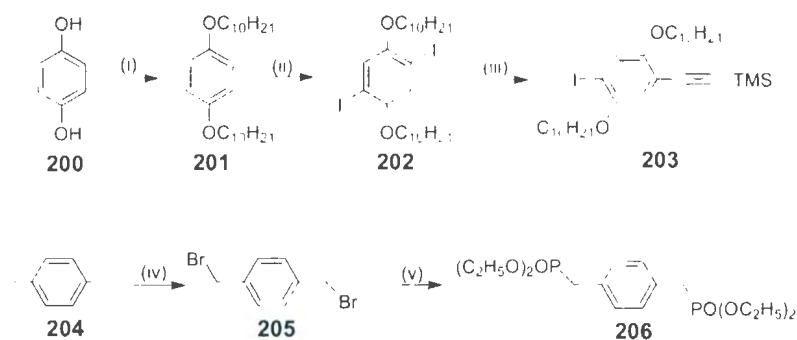
2.2 Results and discussion

2.2.1 Synthesis

2.2.1.1 Linear-shaped OPE/OPV oligomers and related $C_{60}-\pi-C_{60}$ derivatives

To construct the target OPE/OPV oligomers and related bisfullerene derivatives, two essential building blocks **203** and **206** were first prepared as shown Scheme 2.1. 1,4-Dihydroxybenzene (**200**) was alkylated with 1-bromodecane in the presence of KOH

in refluxing EtOH to give 1,4-bis(decyloxy)benzene (**201**), which was then iodinated to afford compound **202** in a yield of 89%. Cross-coupling of **202** with only 0.7 equiv of trimethylsilylacetylene (TMSA) afforded monoiodide **203** as the major product. The synthesis of compound **206** began with a radical bromination of *p*-xylene using NBS, which afforded α, α' -dibromo-*p*-xylene **205** in 53% yield. An Arbuzov reaction between **205** and P(OEt)₃ then afforded **206** in 92% yield.



Scheme 2.1: Synthesis of phenyl building blocks **203** and **206**. Reagents and conditions: (i) C₁₀H₂₁Br, KOH, EtOH, 79%; (ii) Hg(OAc)₂, I₂, CH₂Cl₂, 89%; (iii) TMSA, PdCl₂(PPh₃)₂, CuI, Et₃N, THF, 58%. (iv) NBS, CHCl₃, benzoyl peroxide, 53%; (v) P(OC₂H₅)₃, 92%.

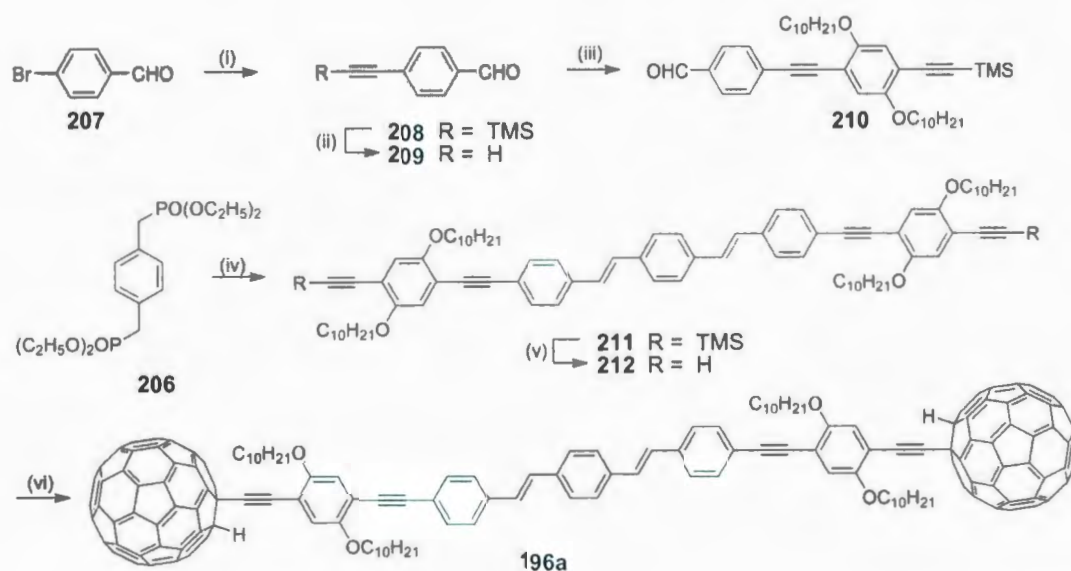
With **203** and **206** in hand, the synthesis continued as outlined in Scheme 2.2. Cross coupling of *p*-bromobenzaldehyde (**207**) with TMSA led to compound **208**, which was desilylated using K₂CO₃ to give terminal alkyne **209**. Compound **209** was cross coupled with **203** under Sonogashira conditions to afford phenyl acetylene **210** in 94% yield. Compound **210** was subjected to a Horner-Wittig reaction with the ylide generated from bis(phosphonate) **206** to complete the first targeted linear

OPE/OPV scaffold. In this reaction, using NaH or *t*-BuOK as the base did not produce the desired oligomer. The use of a stronger lithium base, *n*-BuLi, did lead to the product, but with a very low yield of 15%. After several attempts to optimize the reaction conditions, another lithium base, LHMSD, was found to be the most efficient, giving a yield of 42%.

With linear OPE/OPV **211** in hand, it then came to the fullereryl addition step to finalize the first target C₆₀ π C₆₀ triad **196a**. In this work, an *in situ* ethynylation protocol devised by Tour's group was employed to attach fullereryl groups to the OPE/OPV oligomers,²⁴⁷ due to its high efficiency and reliability. To perform this reaction, oligomer **211** was first desilylated with K₂CO₃ to form oligomer **212**. Slow addition of LHMSD in a well-sonicated mixture of **212** and excess C₆₀ (*ca.* 2 equiv per terminal alkyne) in dry THF under a nitrogen atmosphere resulted in a slurry of dark greenish color. The reaction was quenched with excess trifluoroacetic acid (TFA) to give a brownish slurry. After removal of the solvent under vacuum, the residue was subjected to column chromatographic separation, affording pure **196a** in a yield of 39%.

Subsequent to the synthesis of **196a**, a longer C₆₀ π C₆₀ homologue **196b** was prepared using a similar synthetic strategy. Outlined in Scheme 2.3 is the initially designed route to compound **196b**. Unfortunately, this synthetic route was unsuccessful because the Horner-Wittig reaction between **206** and **214** failed to produce oligomer **215**, despite the numerous attempts.

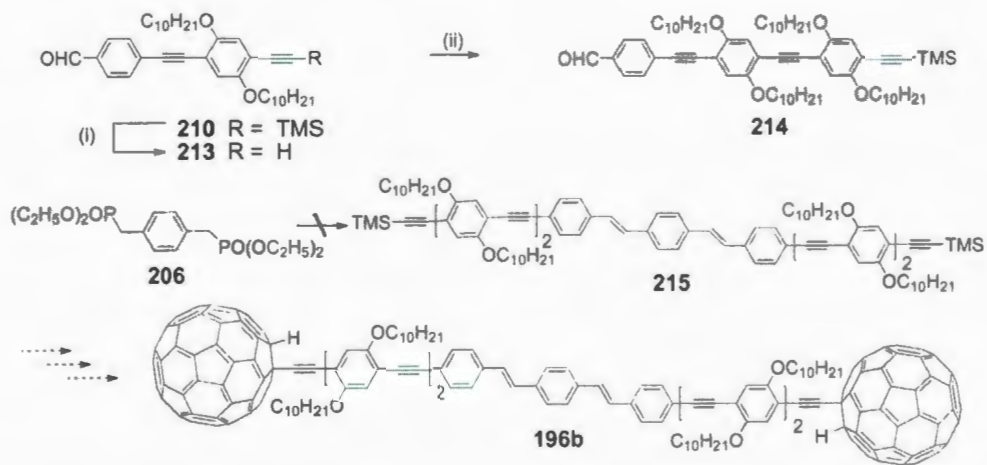
An alternative synthetic route was therefore explored as shown in Scheme 2.4, which proved to be more effective than the previous one. In this approach, the short linear OPE/OPV **212** was further elongated by cross-coupling with iodoarene **203**



Scheme 2.2: Synthesis of linear OPE/OPV **211** and bisfullerene-OPE/OPV hybrid **196a**. Reagents and conditions: (i) TMSA, PdCl₂(PPh₃)₂, CuI, DBU, benzene, 65%; (ii) K₂CO₃, CH₃OH, THF, 95%; (iii) **203**, PdCl₂(PPh₃)₂, CuI, Et₃N, THF, 94%; (iv) LHMDS then **210** at -78 °C, 42%; (v) K₂CO₃, CH₃OH, THF, 100%; (vi) C₆₀, LHMDS, THF then TFA 39%.

under Sonogashira conditions, yielding long linear OPE/OPV co-oligomer **215** in 60% yield. Desilylation of **215** followed by an *in situ* ethynylation reaction with excess C₆₀ then furnished the desired long bisfullerene-OPE/OPV hybrid **196b**.

It is worth mentioning that in the coupling reaction that led to oligomer **215**, another long OPE/OPV co-oligomer **217** (Figure 2.6) was obtained as a byproduct. The formation of **217** can be accounted for by a sequence of combined homo- and cross-coupling reactions. The mixed coupling reactions became particularly prominent, with a yield of 24%, when the exhaustive oxygen removal step was omitted in the beginning of the reaction. To our best knowledge, compound **217** represents



Scheme 2.3: Attempted synthesis of compound **196b**. Reagents and conditions: (i) TBAF, THF, 56%; (ii) **203**, PdCl₂(PPh₃)₂, CuI, Et₃N, 80%.

the longest OPE/OPV based monodisperse block co-oligomer ever made.

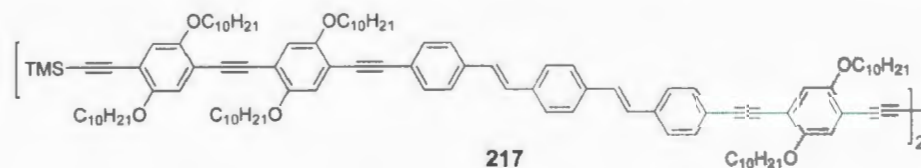
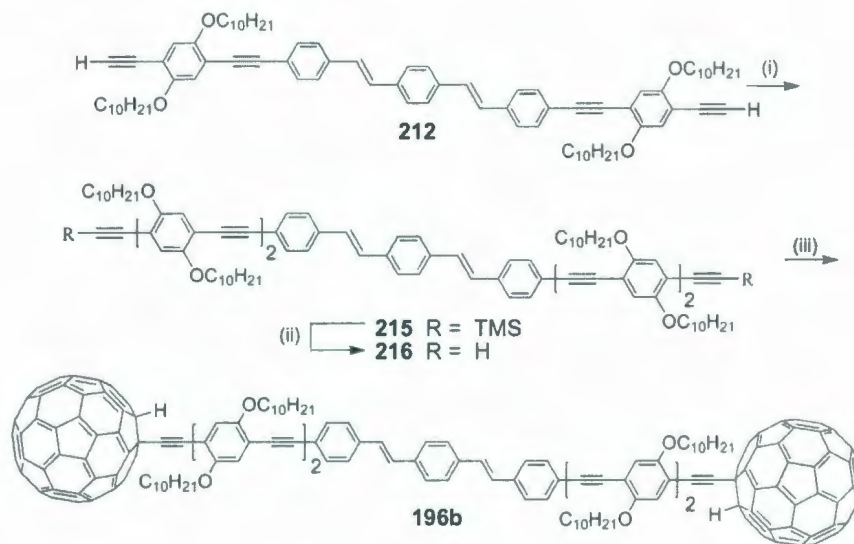


Figure 2.6: Structure of OPE/OPV co-oligomer **217**.

2.2.1.2 Cruciform-shaped OPE/OPV oligomers and related C₆₀-π-C₆₀ derivatives

The target cruciform-shaped OPE/OPV and related bisfullerene derivatives are actually structural isomers of the linear OPE/OPV compounds introduced in the previous subsection. The synthesis of the cruciform oligomers began with *p*-xylene as the starting material. As shown in Scheme 2.5, oxidative iodination of *p*-xylene

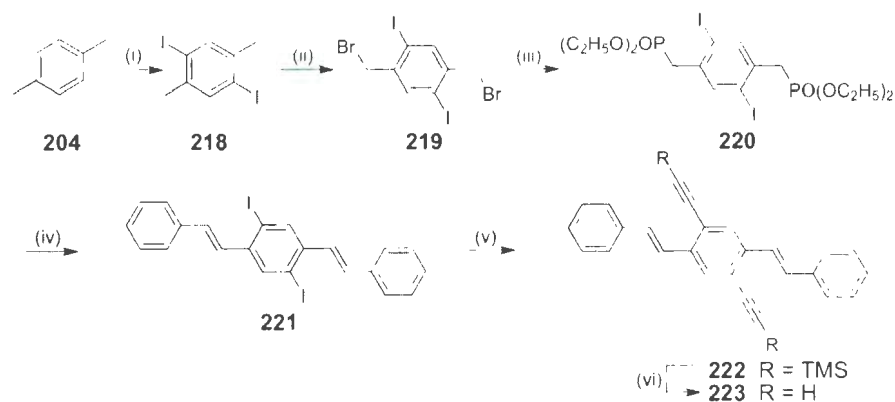


Scheme 2.4: Synthesis of long linear OPE/OPV **215** and related bisfullerene hybrid **196b**. Reagents and conditions: (i) **203**, PdCl₂(PPh₃)₂, CuI, Et₃N, 60%; (ii) K₂CO₃, CH₃OH, THF, 61%; (iii) C₆₀, LHMDS, THF then TFA, 41%.

(**204**) afforded 2,5-diiodo-1,4-dimethylbenzene (**218**). The synthesis of compound **219** demanded much effort. Compound **219** is commercially available, but with a price of 250 Euro per 100 mg as quoted from a UK company at the time of this work. Therefore, it was not economical to buy this compound as a starting material for multistep synthesis.

Bunz and co-workers previously reported the synthesis of **219**; however, the product was isolated along with *ca.* 10% inseparable byproducts.²⁹⁷ In order to acquire pure product of **219**, an alternative route was scrutinized, in which *p*-xylene was first brominated by treating with NBS and then subjected to an iodination. This approach unfortunately did not lead to the desired product. So, the attention returned to Bunz's method again. Eventually, with a slight modification on the workup step

of Bunz's method, pure compound **219** was attained. During the workup, instead of adding sodium sulfite at first, the reaction mixture was let to stand overnight at room temperature. This allowed product **219** to co-crystallize with succinimide, while other bromination byproducts remained in the solution. Succinimide could be removed completely by water rinsing, leaving almost pure **219** as the crude product. Further purification of **219** was done by recrystallization from CHCl_3 and hexanes.

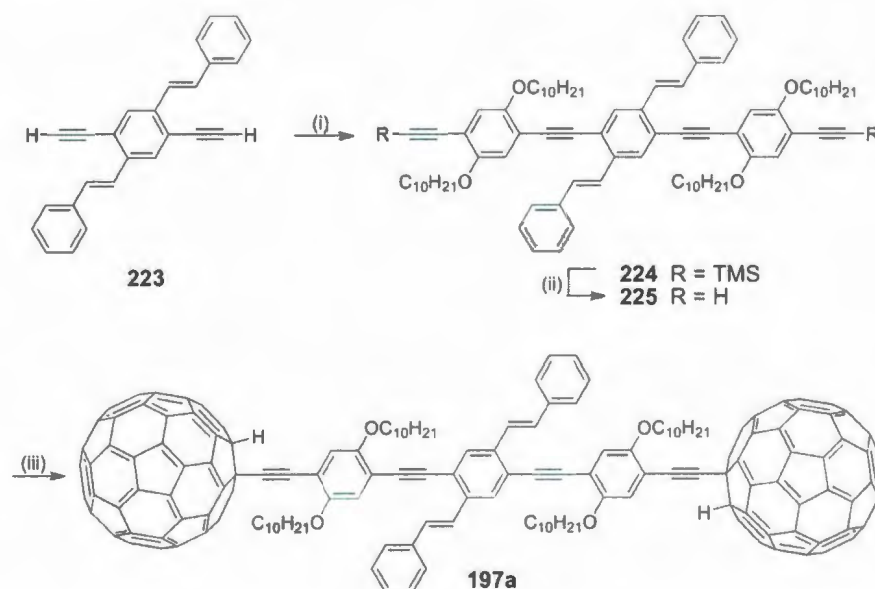


Scheme 2.5: Synthesis of cruciform building block **223**. Reagents and conditions: (i) I_2 , H_5IO_6 , H_2O , AcOH , H_2SO_4 , 69%; (ii) NBS, CHCl_3 , benzoyl peroxide, 13%; (iii) $\text{P}(\text{OC}_2\text{H}_5)_3$, 88%; (iv) NaH, THF then benzaldehyde, 63%; (v) TMSA, $\text{PdCl}_2(\text{PPh}_3)_2$, CuI, Et_3N , THF, 87%; (vi) K_2CO_3 , CH_3OH , THF, 86%.

Pure compound **219** was then subjected to an Arbuzov reaction with $\text{P}(\text{OEt})_3$, giving 2,5-diiodo-1,4-bis(diethylphosphonomethyl)benzene (**220**) in a yield of 88%. A Horner-Wittig reaction between **220** and benzaldehyde in the presence of NaH afforded phenylenevinylene trimer **221** as yellow crystalline solid. Treating **221** with TMSA under the catalysis of Pd-Cu in a mixed solvent of Et_3N and THF then gave

oligomer **222** in a yield of 86%. Removal of the TMS groups in **222** with K_2CO_3 finally led to the formation of the key cruciform building block, oligomer **223**.

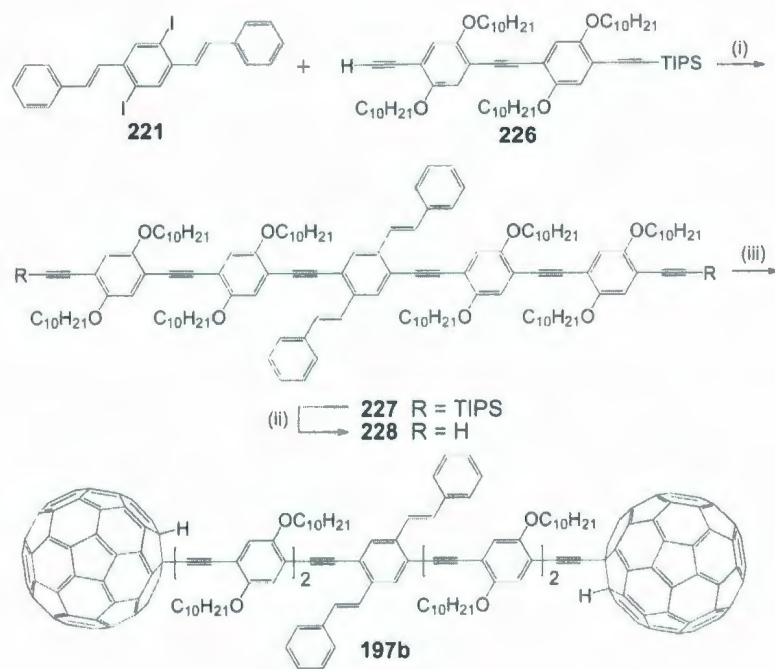
Cruciform OPE/OPV co-oligomers **224** and **225** were obtained by Sonogashira coupling of **223** with **203** followed by desilylation as outlined in Scheme 2.6. With oligomer **225**, bisfullerene-cruciform OPE/OPV hybrid **197a** was synthesized in a yield of 41% through the *in situ* ethynylation reaction.



Scheme 2.6: Synthesis of cruciform OPE/OPV **224** and related bisfullerene hybrid **197a**. Reagents and conditions: (i) **203**, $PdCl_2(PPh_3)_2$, CuI , Et_3N , THF, 59%; (ii) K_2CO_3 , CH_3OH , THF, 81%; (iii) C_{60} , LHMDS, THF then TFA, 41%.

Using a similar strategy to that in the synthesis of compound **197a**, a long cruciform OPE/OPV precursor **228** and related bisfullerene hybrid **197b** were prepared. Synthetic details are outlined in Scheme 2.7. Sonogashira coupling between compound **221** and **226** first produced long cruciform oligomer **227** in 97%

yield. After deprotection of **227** with TBAF, the resulting terminal alkyne **228** was functionalized with two fullereryl groups using the *in situ* ethynylation reaction to give bisfullerene adduct **197b**.

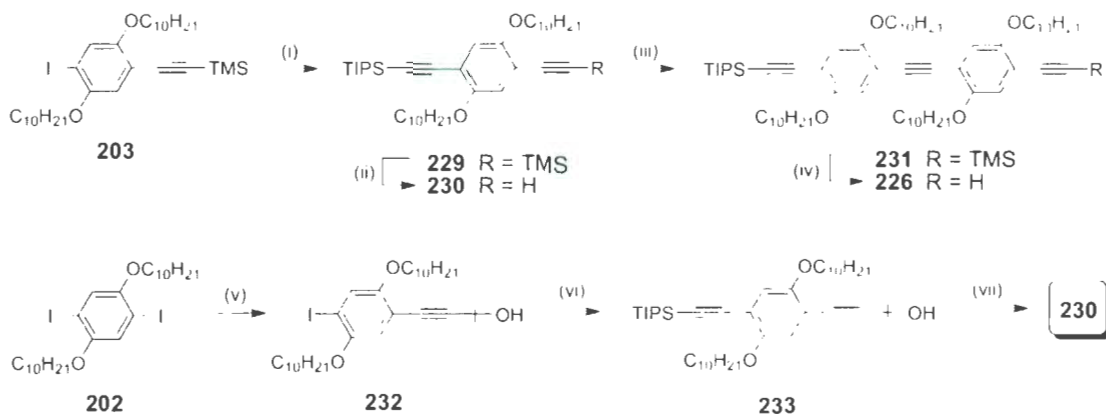


Scheme 2.7: Synthesis of long cruciform OPE/OPV **227** and related bisfullerene hybrid **197b**. Reagents and conditions: (i) $\text{PdCl}_2(\text{PPh}_3)_2$, CuI , Et_3N , THF, 97%; (ii) TBAF, THF, 82%; (iii) C_{60} , LHMDS, THF then TFA, 21%.

In the above synthesis, a mono terminal alkynylarene **226** serves as an essential building block for the elongation of the OPE oligomer chain. The synthesis of **226** can be readily achieved by a Sonogashira coupling reaction between iodoarene **203** and an unsymmetrically protected bisalkynylbenzene precursor **230** as described in Scheme 2.8. There are two approaches that can be used to prepare compound

230. The first one started with a standard Sonogashira cross coupling between iodoarene **203** and triisopropylsilylacetylene (TIPSA), giving compound **229** in a yield of 93%. Compound **229** was treated with K_2CO_3 to selectively remove the TMS group, affording compound **230** in 79% yield. While this route is relatively concise and efficient, the involvement of two costly silyl-protected acetylene reagents (TMSA and TIPSA) in the synthesis is indeed not favorable for large-scale preparation. To reduce the usage of silyl reagents, an alternative route to **230** was adopted, in which diiodoarene **202** was first cross-coupled with one equiv of 1,1-dimethylpropargyl alcohol under Sonogashira conditions. The resulting product **232** was cross-coupled with TIPSA under Pd/Cu catalysis to form **233**. Compound **233** was then deprotected by NaOH in refluxing toluene to afford the desired product **230** in a yield of 76%.

The unique shape of the 2D cruciform OPE/OPV skeleton also enables versatile modifications or substitutions at the four terminal positions of the oligomer. In our work, a strong electron-donating (D) and chromophoric group, *N,N*-diphenylamino, was selected to be attached to the OPV branch of the cruciform. Such functionalization has allowed the substitution effect to be examined on the oligomers and related bisfullerene adducts. The synthesis of two short D-substituted cruciform OPE/OPV oligomers, **237** and **238**, as well as a related bisfullerene adduct, **198a**, is described in Scheme 2.9. It began with a Horner-Wittig reaction between **220** and *N,N*-diphenylaminobenzaldehyde, yielding D-functionalized OPV **234** in a yield of 80%. Sonogashira reaction between **234** and TMSA gave the key intermediate **235**, which was converted to **236** via desilylation in 90% yield. Afterwards, another Pd-catalyzed cross coupling was performed between **236** and iodoarene **203**, leading to



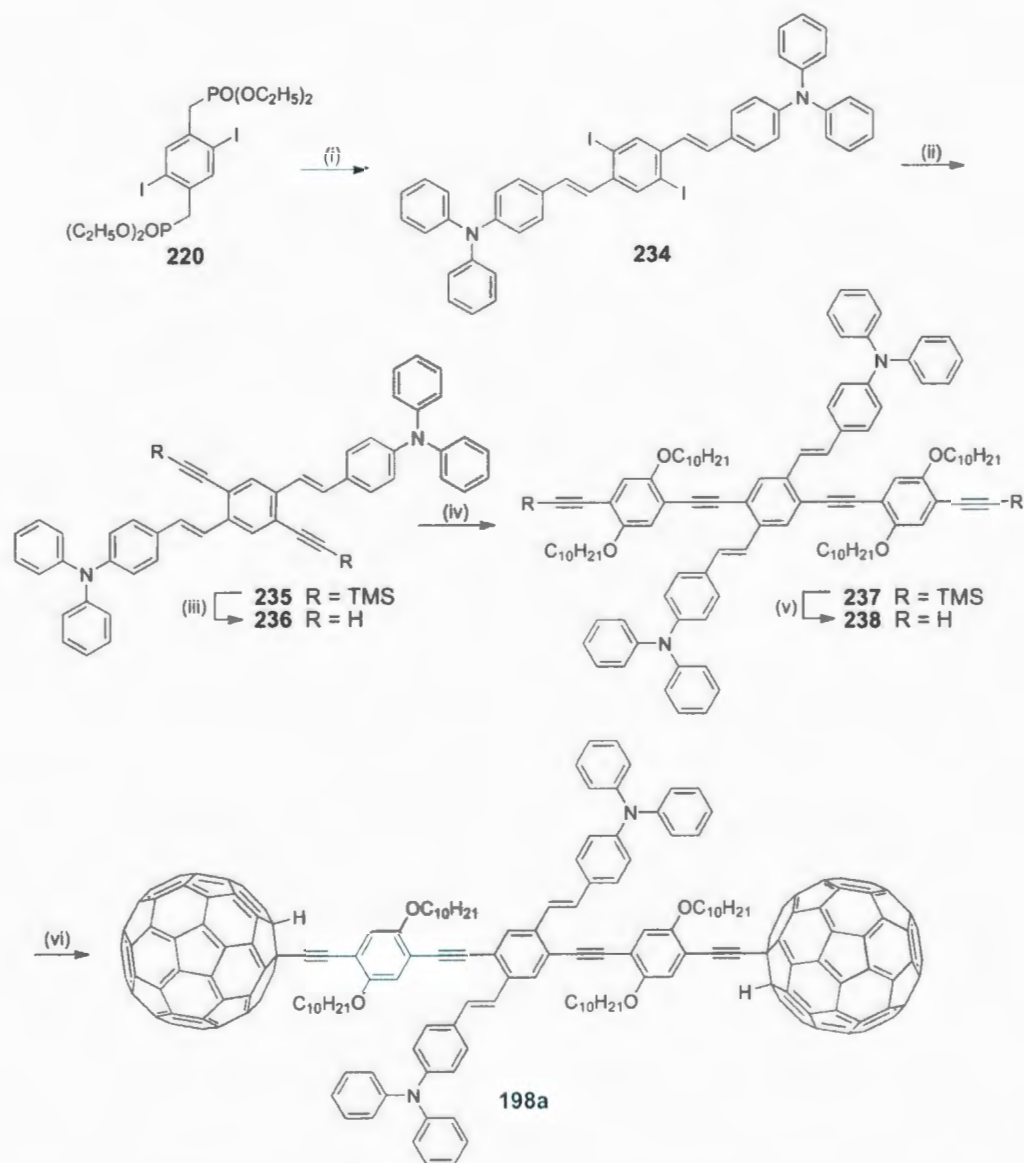
Scheme 2.8: Synthesis of phenylacetylene building block **226**. Reagents and conditions: (i) TIPSA, PdCl₂(PPh₃)₂, CuI, Et₃N, 93%; (ii) K₂CO₃, CH₃OH, THF, 92%; (iii) **203**, PdCl₂(PPh₃)₂, CuI, Et₃N, THF, 98%; (iv) K₂CO₃, CH₃OH, THF, 96%; (v) 1,1-dimethylpropargyl alcohol, PdCl₂(PPh₃)₂, CuI, Et₃N, 54%; (vi) TIPSA, PdCl₂(PPh₃)₂, CuI, Et₃N, 100%; (vii) NaOH, toluene, reflux, 76%.

the formation cruciform OPE/OPV **237**. Treating **237** with TBAF gave the terminal alkyne-substituted cruciform **238**, which was subjected to an *in situ* ethynylation to afford the cruciform shaped bisfullerene-oligomer adduct **198a** in a yield of 23%.

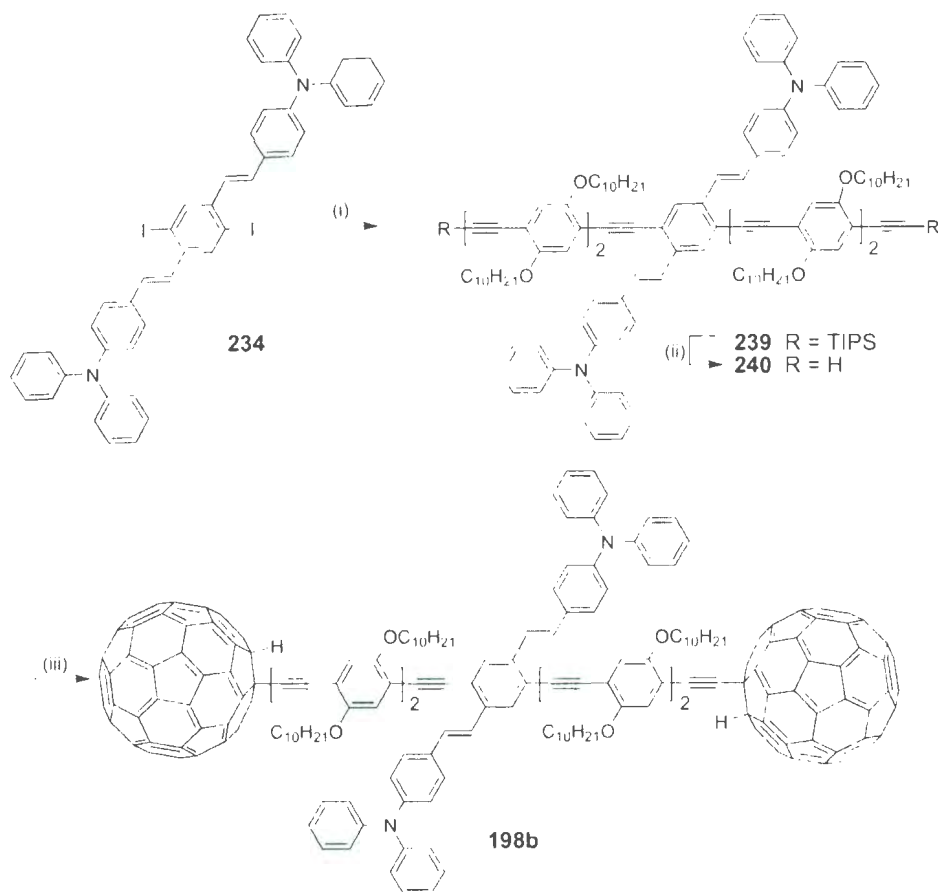
Following the same strategy as used in the synthesis of **198a**, long D-substituted OPE/OPV cruciform **239** and related bisfullerene adduct **198b** were successfully prepared. The synthetic details are given in Scheme 2.10.

2.2.1.3 A simple phenylene ethynylene C₆₀ model system

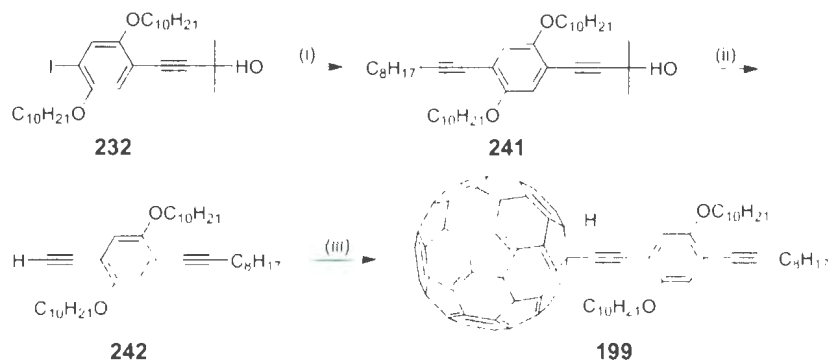
Apart from the complex dumbbell-shaped C₆₀ OPE/OPV C₆₀ triads synthesized in the previous two subsections, a simple phenylene ethynylene-C₆₀ dyad, **199**, was also prepared in the work of this chapter (Scheme 2.11). The purpose of making this



Scheme 2.9: Synthesis of short D-substituted cruciform oligomer **237** and related bisfullerene adduct **198a**. Reagents and conditions: (i) (a) NaH, THF; (b) *N,N*-biphenylaminobenzaldehyde, 80%; (ii) TMSA, PdCl₂(PPh₃)₂, CuI, Et₃N, THF, 76%; (iii) K₂CO₃, CH₃OH, THF, 90%; (iv) **203**, PdCl₂(PPh₃)₂, CuI, Et₃N, THF, 79%; (v) TBAF, THF, 92%; (vi) C₆₀, LHMDS, THF then TFA, 23%.



Scheme 2.10: Synthesis of long D-substituted cruciform oligomer **239** and related bisfullerene adduct **198b**. Reagents and conditions: (i) **226**, $\text{PdCl}_2(\text{PPh}_3)_2$, CuI , Et_3N , 46%; (ii) TBAF, THF, 80%; (iii) C_{60} , LHMDS, THF then TFA, 17%.



Scheme 2.11: Synthesis of phenylene ethynylene- C_{60} model **199**. Reagents and conditions: (i) 1-decyne, $\text{PdCl}_2(\text{PPh}_3)_2$, CuI , Et_3N , 86%; (ii) NaOH , toluene, reflux, 90%; (iii) C_{60} , LHMDS , THF then TFA, 76%.

molecule is to use it as a model to examine the electronic communication between the C_{60} group and the adjacent π conjugated system it is attached to. Since compound **199** can be regarded as a common segment of the C_{60} -OPE-OPV- C_{60} triads prepared in this chapter, understanding the properties of **199** will be of great assistance in elucidating the structure-property relationships for more complex C_{60} -OPE-OPV- C_{60} systems. Detailed discussions in this respect will be made in later sections.

2.2.2 NMR spectroscopic and electrochemical properties of C_{60} -OPE/OPV- C_{60} derivatives

All the C_{60} -OPE-OPV- C_{60} compounds and their corresponding OPE-OPV precursors have been characterized by IR, ^1H and ^{13}C NMR spectroscopy and mass spectrometry, the results of which offer convincing proof of their molecular structures and purities. Particularly remarkable is the ^{13}C NMR spectroscopic data for the six dumbbell-shaped bisfullerene compounds **196-198**. The centrosymmetric molecular

structure of these dumbbell-shaped compounds makes the two fullereryl groups in each molecule chemically equivalent. In addition, each of the C_{60} cages possesses a mirror symmetry plane bisecting itself. Theoretically 30 distinctive signals should appear in the region of 135–149 ppm corresponding to all the sp^2 carbons on the two-fold symmetric C_{60} cage.²⁴⁷ Experimentally, well-resolved ^{13}C NMR spectra were observed for all the six bisfullerene adducts in this region as shown in Figure 2.7. Of the 30 different sp^2 carbons, there are 26 signals for **196a**, 26 signals for **196b**, 28 signals for **197a**, 26 signals for **197b**, 24 signals for **198a**, and 27 signals for **198b** observed in the spectra.

From the comparison of the ^{13}C NMR resonances in Figure 2.7, it is clear that the different electronic properties of the oligomer π -bridges cause no significant changes in the chemical shifts of each type of sp^2 carbons on the C_{60} cage. This observation indicates that the electronic communication between the C_{60} cage and the π -bridge in the ground state is rather insignificant, although the two π -segments are closely linked to each other through only one sp^3 carbon.

Electrochemical properties for the six bisfullerene molecular dumbbells **196-198** were probed using cyclic voltammetry (CV). Detailed redox potential data are summarized in Table 2.1, and cyclic voltammograms are given in Figure 2.8.

The cyclic voltammograms of bisfullerene hybrids bearing cruciform OPE/OPV π -bridges (**197a** and **197b**) show no noticeable redox features in the region of positive potentials, but their linear shaped isomers **196a** and **196b** do show distinctive quasi-reversible redox wave pairs of a similar shape in this region, which can be assigned to the oxidations on the linear OPE/OPV π -bridges. These results indicate that the linear OPE/OPV co-oligomers possess better electron-donating ability than

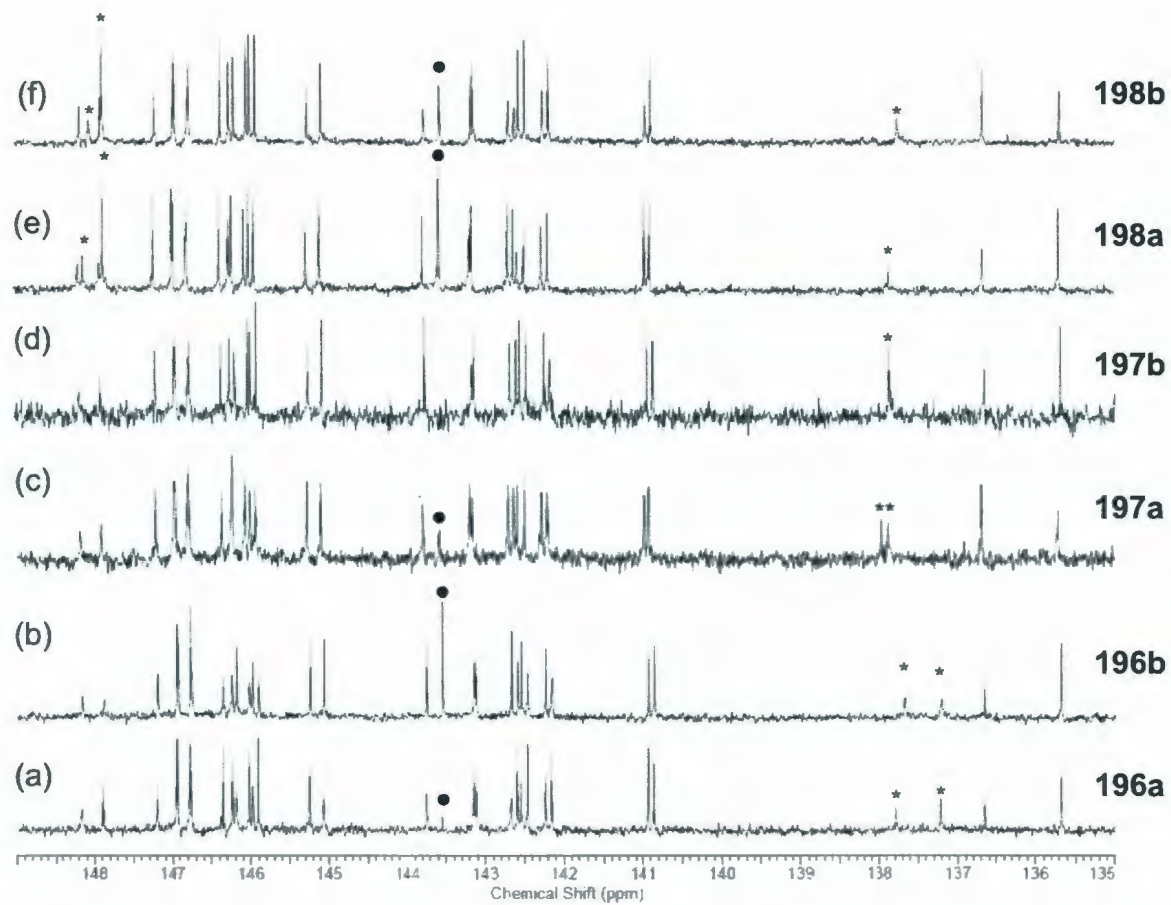


Figure 2.7: Comparison of ^{13}C NMR spectra for C_{60} -OPE/OPV- C_{60} compounds 196-198 in the region of 135-149 ppm. Signals labeled with * are due to aromatic carbons in the oligomer bridges. Signals labeled with • are due to unreacted C_{60} .

Table 2.1: Summary of cyclic voltammetric data for compounds **196-198**.^a

Entry	Oxidation (V)			Reduction (V)	
	E_{pa}	E_{pc}	E_{pa}	E_{pc}	
196a	1.27	1.18	-0.47, -0.83, -1.10, -1.40	-0.59, -0.79, -0.99, -1.24, -1.51, -1.97	
196b		1.10	-0.35, -1.10, -1.34	-0.69, -0.80	
197a			-0.38, -0.84, -1.12, -1.27	-0.59, -1.00, -1.24, -1.52, -1.73	
197b			-1.03, -1.27	-0.29, -0.60, -0.80, -1.00, -1.51	
198a				-0.37, -0.84, -1.04, -1.28, -1.74	
198b				-0.59, -0.85, -0.99, -1.16, -1.42, -1.52	

^aCyclic voltammetric experiments were performed at room temperature. Data were recorded in solutions of *o*-dichlorobenzene-CH₃CN (4:1, v/v). Bu₄NBF₄ (0.1 M) as the supporting electrolyte, glassy carbon as the working electrode, and Pt wire as the counter electrode. Potentials are given in Volts versus a Ag/AgCl reference electrode. Scan rate: 100 mV · s⁻¹.

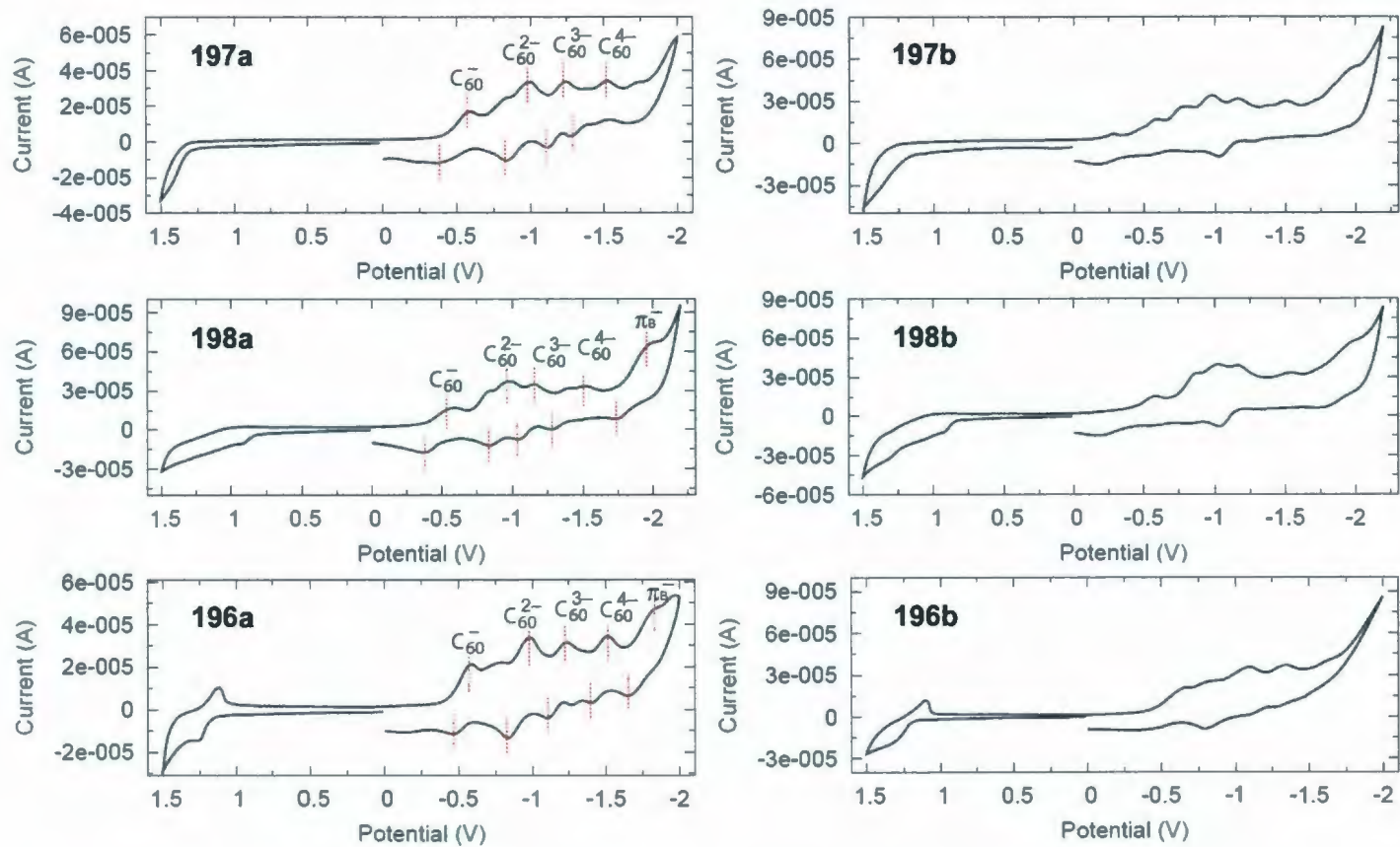


Figure 2.8: Cyclic voltammograms of compounds 196-198.

do the cruciforms, presumably as a result of their greater degree of π electron delocalization and relatively higher-lying HOMOs. For the bisfullerene adducts with D-functionalized cruciform OPE/OPV bridges, **198a** and **198b**, the oxidation on each of the π -bridges in their cyclic voltammograms exhibits irreversible features. Also notable is that the onsets of the oxidation peaks for **198a** and **198b** are much lower than those of **196a** and **196b**, indicating significantly raised HOMO energies in **198a** and **198b** as a result of the donor group (NPh_2) effect via π conjugation.

When scanning cathodically, four quasi-reversible reduction steps characteristic of the sequential single-electron transfers on the C_{60} cage from C_{60} to C_{60}^{4-} can be observed in each of the cyclic voltammograms of compounds **196a**, **197a**, and **198a**, which contain short OPE/OPV π -bridges. Moreover, a single-electron reduction process on the oligomer bridge (denoted π_{B}) can be seen in the voltammograms of **196a** and **198a**. For the bisfullerene adducts that contain long OPE/OPV π bridges (**196b**, **197b**, and **198b**), redox envelopes in the negative potential region show undefined, irreversible patterns that are too complex to make specific assignments.

2.2.2.1 UV-Vis absorption properties

(A) *OPE/OPV based co-oligomers.* UV-Vis absorption spectra for the prepared linear and cruciform OPE/OPV co-oligomers were measured in chloroform at room temperature and are shown in Figures 2.9 and 2.10.

From Figure 2.9, it can be seen that the UV-Vis spectrum of short linear OPE/OPV **212** shows two distinctive $\pi \rightarrow \pi^*$ transition bands at 401 and 293 nm. The low-energy absorption peak at 401 nm can be attributed to electron transition from the HOMO to the LUMO, while the peak at 293 nm is likely due to

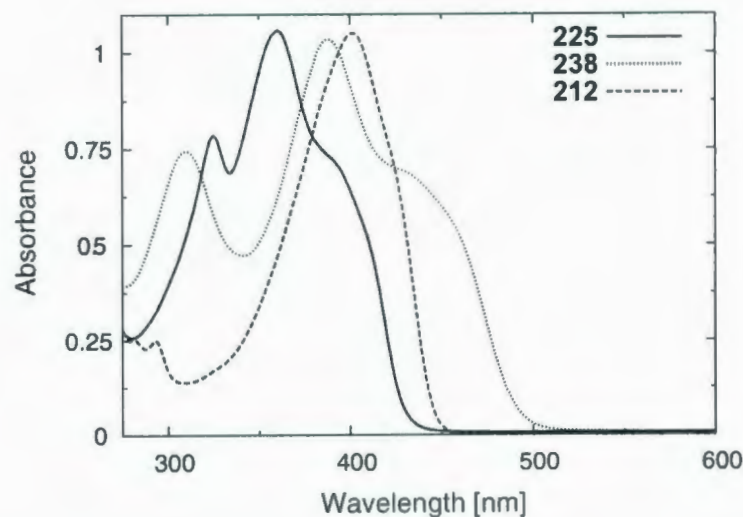


Figure 2.9: Normalized UV-Vis spectra for short OPE/OPV co-oligomers **212**, **225**, and **238** measured in CHCl_3 .

mixed contribution of HOMO-1 \rightarrow LUMO+1 and HOMO \rightarrow LUMO+2 transitions as suggested by our recent time-dependent density functional theory (TD-DFT) calculations.²⁹⁸

The UV-Vis spectrum of short OPE/OPV cruciform **225**, a structural isomer of **212** though, exhibits a quite different spectral envelop than that of **212**. There are three distinctive absorption bands observed at 390, 360, and 324 nm, respectively. Notice that the lowest-energy absorption peak of short cruciform **225** (390 nm) is blueshifted by *ca.* 11 nm relative to that of short linear **212** (401 nm). This indicates that the linear oligomer features a relatively narrower HOMO-LUMO gap and more delocalized π -characteristics than its cruciform cousin. This result is in line with an empirical estimation that the π -framework of a linear OPE/OPV is more planar than a cruciform due to less steric hindrance encountered at the central phenyl ring. The observation that cruciform **225** shows more intense absorptions at 360 and 324 nm

than its linear isomer **212** suggests that the shape of π -conjugation is an important factor governing the electronic absorption behavior OPE/OPV based co-oligomers.

The UV-Vis spectrum of D-functionalized cruciform **238** shows two low-energy absorption bands similar in shape to those of cruciform **225**, but they are considerably redshifted to 435 and 387 nm (see Figure 2.9) due to the presence of two electron donor groups attached to the termini of the OPV branch. These D-substituents push electrons toward the OPV branch through direct π -conjugation, which should in principle elevate the energy level of the HOMO in **238** and reduce the energy gaps for respective $\pi \rightarrow \pi^*$ electron transitions.

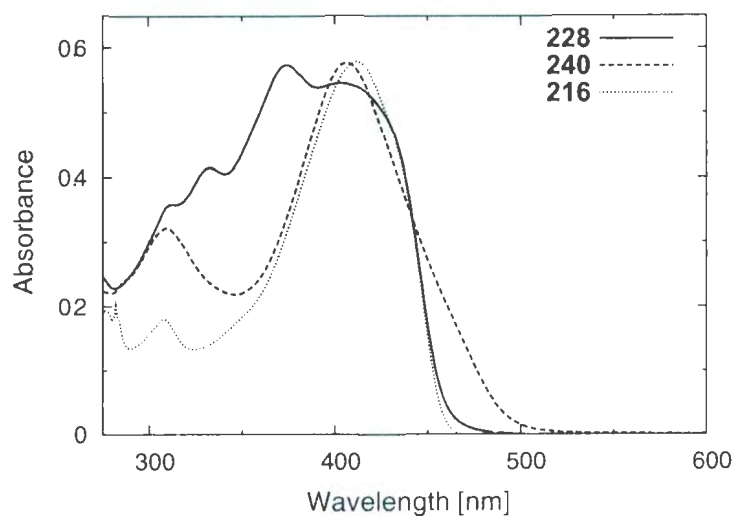


Figure 2.10: Normalized UV-Vis spectra for long OPE/OPV co-oligomers **216**, **228**, and **240** measured in CHCl_3 .

Figure 2.10 shows the spectra of long OPE/OPV oligomers **216**, **228**, and **240**. Notably, the two bands corresponding to HOMO \rightarrow LUMO transitions on the long linear OPE/OPV **216** and long cruciform OPE/OPV **228** appear at a nearly

identical wavelength around 410 nm. This observation indicates that the degree of π -delocalization for the two long OPE:OPV oligomers – linear and cruciform – are similar to each other. Such spectral features differ drastically from those of the short OPE:OPV series, which can be ascribed to the extension of the OPE branch in the oligomer backbone. As with short cruciform OPE:OPV **225**, long cruciform **228** also shows two strong high-energy absorption peaks at 372 and 330 nm respectively. The absorption of long linear OPE:OPV **216** in this spectral range, however, appears much weaker in intensity as a result of different shape and dimensionality of π -conjugation. In addition, both the long linear and long cruciform oligomers feature a high-energy band at similar wavelengths, 308 nm for **216** and 312 nm for **228**. The physical origin of this band is not clear yet and awaits further theoretical investigations.

For D-substituted long OPE:OPV cruciform **240**, the HOMO \rightarrow LUMO transition gives rise to a pronounced absorption shoulder extending from *ca.* 450 to 500 nm, which can be ascribed to a charge-transfer (CT) band. The most intense peak in the spectrum of **240** is centered at 406 nm, a wavelength that is considerably redshifted in comparison to the band of the same electronic origin observed in the spectrum of long cruciform **228** (372 nm). Unlike the scenarios observed in the short OPE:OPV series, the high-energy absorption band at 309 nm in the spectrum of D-functionalized long cruciform **240** shows no significant shift compared to the spectra of unfunctionalized long cruciform OPE:OPV **228** (312 nm) and long linear **216** (308 nm).

(B) C_{60} :OPE:OPV- C_{60} hybrids. Electronic absorption properties of C_{60} : π - C_{60} triads **196-198** in the ground state were characterized by UV-Vis spectroscopy, and

detailed spectral profiles are shown in Figure 2.11.

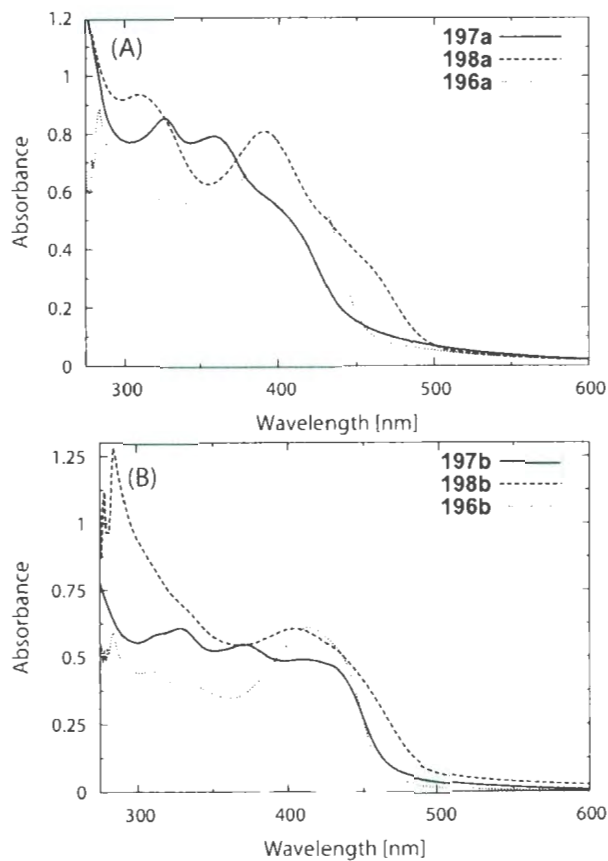


Figure 2.11: Normalized UV-Vis spectra for $C_{60} \pi C_{60}$ triads **196**, **197**, and **198** measured in degassed $CHCl_3$ or toluene.

In these spectra, the $\pi \rightarrow \pi^*$ transitions of the OPE-OPV bridges give rise to the dominating spectral features. Also, the characteristic absorptions of C_{60} can be clearly seen as a band at *ca.* 300-350 nm and a weak tail beyond 500 nm. The $\pi \rightarrow \pi^*$ absorption bands due to the bridging OPE-OPV moieties show no significant spectral shifts in comparison to the spectra of their corresponding OPE-OPV precursors.

indicating that the electronic communication between the fullereryl groups and the π -oligomer units is rather insignificant in the ground state. These results are consistent with the UV-Vis data reported for some analogous C_{60} -OPE- C_{60} systems in previous literature.^{217,299}

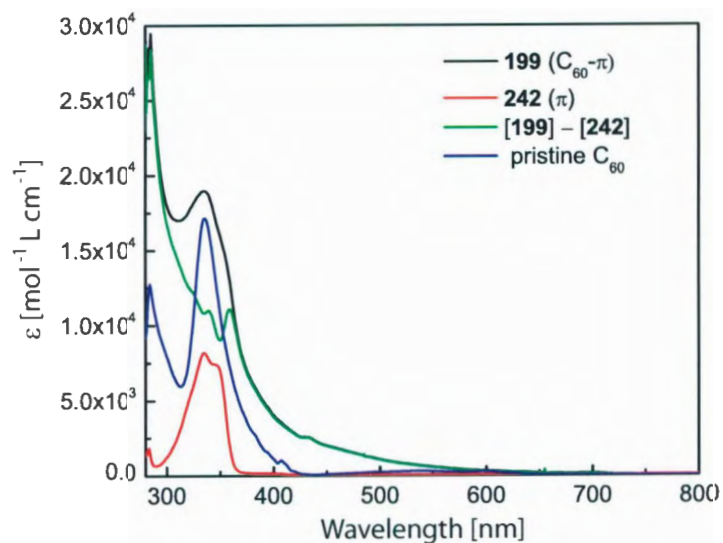


Figure 2.12: UV-Vis spectra for C_{60} - π model compound **199**, phenyl acetylene **242**, and pristine C_{60} .

To further understand the subtle electronic interplay between the fullereryl groups and π -conjugated oligomers in C_{60} - π - C_{60} triads, a simplified model compound **199** and its constituent moieties— phenyl acetylene **242** and pristine C_{60} — were investigated by UV-Vis spectroscopic analysis. Figure 2.12 plots the extinction coefficients (ϵ) of these compounds versus absorption wavelength. In a general sense, the model compound **199** can be viewed as a C_{60} - π dyad, in which the phenyl

acetylene (π) and C_{60} group are connected through an acetylene linkage. In the spectra, compounds **199** (C_{60} - π), **242** (π), and pristine C_{60} all show a very similar λ_{max} at 340 nm. Once again, comparative UV-Vis analysis on the simple model system confirms there is no significant electronic communication taking place between C_{60} and the phenyl acetylene units in the ground state. If otherwise, the λ_{max} for (C_{60} - π), **199** and phenyl acetylene **242** would have shown detectable differences.

The green trace in Figure 2.12 was generated by subtracting the UV-Vis trace of **242** (π) from that of **199** (C_{60} - π). The resulting curve can be deemed as the absorption contribution from the fullereryl group. Note that this calculated trace is markedly different from that of pristine C_{60} , particularly, in that there is a pronounced absorption tail from 400 to 600 nm in the calculated trace. The spectral variation is believed to arise from the introduction of a sp^3 hybridized carbon atom that breaks the I_h symmetry of the fullerene cage upon chemical functionalization.

2.2.2.2 Excited-state properties

(A) *OPE OPV based co-oligomers.* The OPE:OPV based oligomers are highly emissive upon photo-excitation. To gain insight into the properties of their first excited states, steady-state fluorescence spectroscopic measurements were carried out. Figure 2.13 shows the fluorescence spectra of short OPE:OPV co-oligomers **212**, **225**, and **238**.

The emission spectral profile of short linear OPE:OPV co-oligomer **212** can be assigned to the $S_1 \rightarrow S_0$ transition featuring three distinctive vibronic modes. The spacing of vibrational progression is measured to be 1432 cm^{-1} , which largely corresponds to the C-C bond vibration. The intensity distribution along the

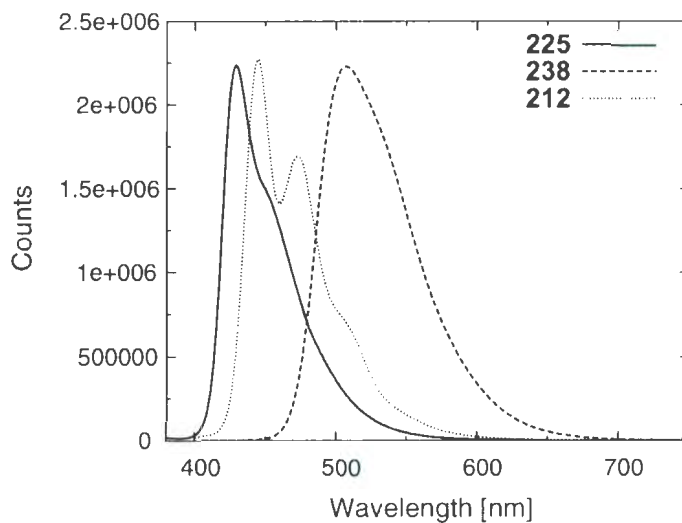


Figure 2.13: Fluorescence spectra of short OPE/OPV co-oligomers **212**, **225**, and **238** measured in degassed CHCl_3 .

vibrational progression is observed as a skewed shape, with the 0-0 band (445 nm) being the strongest. Such a distribution pattern is indicative that the changes of nuclear coordinates between the ground and the first electronic excited states are very small.

The emission bands of short cruciform **225** are blueshifted relative to those of linear oligomer **212**, which is in agreement with the conclusion drawn from previous UV-Vis analysis; that is, the short linear oligomer possess a narrower HOMO-LUMO gap than does its cruciform isomer due to a higher degree of planarity. Unlike linear oligomer **212**, however, there are only two vibronic bands discernible in the spectrum of **225** and their lineshapes are relatively broader compared to linear **212**. The different emission behavior of the two isomers **212** and **225** can be ascribed to their different π -conjugation motifs.

The fluorescence spectrum of D-functionalized cruciform OPE/OPV **238** shows a substantially redshifted maximum emission wavelength $\lambda_{em} = 507$ nm relative to that of cruciform **225**, along with a barely discernible emission shoulder at 530 nm. The spectral shifts are likely due to the donor effect that raises the energy level of the HOMO through π -conjugation. The emission bands of **238** show a broad bell-shaped distribution, which alludes to a dramatic geometry change between the two equilibria in the first excited (S_1) and the ground electronic (S_0) states. In addition, the considerable lineshape broadening suggests a rapid equilibrium among a multitude of rotamers in the relaxed first excited state.

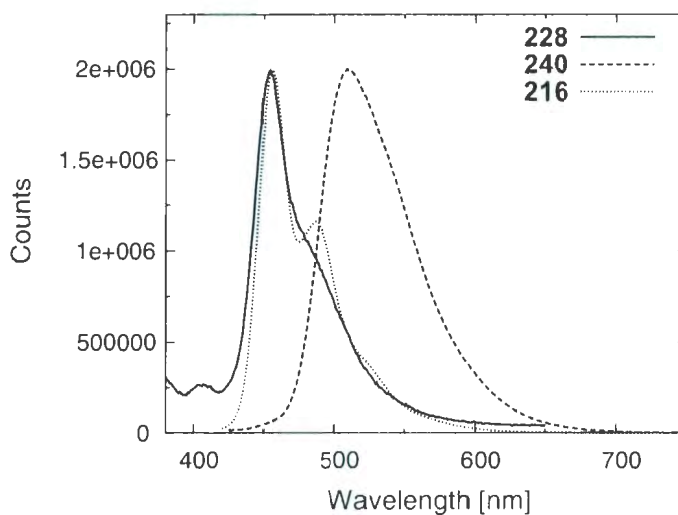


Figure 2.14: Fluorescence spectra for long OPE/OPV oligomers **216**, **228**, and **240** measured in degassed CHCl_3 .

The fluorescence spectra of long OPE/OPV oligomers **216**, **228**, and **240** are shown in Figure 2.14, from which it can be clearly observed that linear **216** and cruciform **228** show maximum emission peaks λ_{em} at an almost identical wavelength.

This phenomenon is presumably due to the effect of increased π -pathways in the OPE branch and is in agreement with their electronic absorption data. The emission of D-functionalized long oligomer **240** behaves similarly to its short homologue **238**, exhibiting greatly redshifted λ_{em} and much broader lineshapes in comparison to those of unsubstituted long OPE 'OPV' oligomers..

(B) C_{60} OPE 'OPV' C_{60} hybrids. After having electron-accepting C_{60} groups attached to them, the fluorescence of the OPE 'OPV' co-oligomers in the spectra of C_{60} π C_{60} derivatives **196** **198** was found to be substantially quenched by more than two orders of magnitude. Table 2.2 summarizes the fluorescence quantum yields (Φ_f) and lifetimes (τ) measured for C_{60} π C_{60} triads **196** **198** and respective OPE 'OPV' co-oligomers. The dramatic quenching effect can be explained on the basis of a proposed photodeactivation mechanism²⁵² shown in 2.15, in which very fast photoinduced energy/electron transfers compete effectively with radiative decay pathways. Detailed photophysics and photodynamics are under investigation by our collaborating group (Prof. D. W. Thompson, Memorial University) using transient absorption spectroscopy, and the results will be disclosed in due course.

2.3 Conclusions

In this chapter, a series of dumbbell-shaped C_{60} - π - C_{60} triads, in which the π units are OPE 'OPV' based diblock co-oligomers assembled in either a linear or a cruciform shape, was prepared. A simple phenylene ethynylene- C_{60} dyad was also synthesized with the aim to use it as the model to examine the electronic communication between the C_{60} group and adjacent π -conjugated systems. The synthesis of these

Table 2.2: Excite-state properties of OPE/OPV co-oligomers and related C_{60} adducts.

Entry	Description	Φ_f	τ (ns)
212	short linear OPE/OPV	0.63	1.2
196a	short linear C_{60} - π - C_{60}	6.0×10^{-3}	1.6
216	long linear OPE/OPV	0.89	0.50
196b	long linear C_{60} - π - C_{60}	$\leq 10^{-3}$	1.0
225	short cruciform OPE/OPV	0.96	2.7
197a	short cruciform C_{60} - π - C_{60}	<i>ca.</i> 10^{-3}	2.6
228	long cruciform OPE/OPV	0.96	1.1
197b	long cruciform C_{60} - π - C_{60}	0.01	1.0
238	short D-cruciform OPE/OPV	0.80	1.8
198a	short D-cruciform C_{60} - π - C_{60}	1.3×10^{-3}	4.8
240	long D-cruciform OPE/OPV	0.46	N/A
198b	long D-cruciform C_{60} - π - C_{60}	$\leq 10^{-3}$	4.8
199	model C_{60} - π	2.6×10^{-3}	2.6

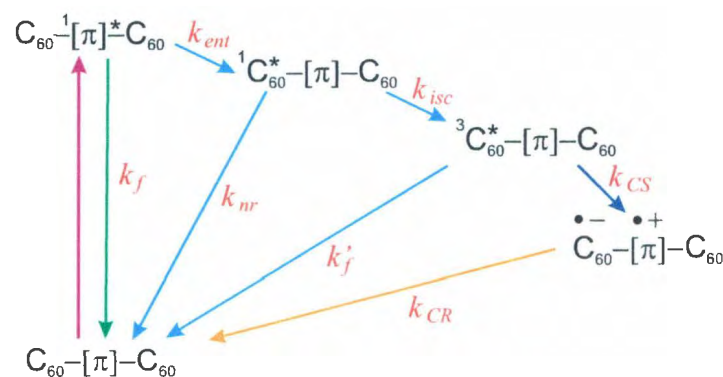


Figure 2.15: k_f : fluorescent emission; k_{ent} : energy transfer; k_{nr} : non-radiative decay; k_{isc} : intersystem crossing; k_{CS} : charge separation; k_{CR} : charge recombination.

fullerene oligomer hybrids were mainly based on Horner-Wittig reaction, transition metal catalyzed coupling reactions and an *in situ* ethynylation reaction. Both the ground- and excited-state properties for these novel C_{60} - π - C_{60} triads systems have been investigated by spectroscopic and electrochemical analysis such as UV-vis, fluorescence and cyclic voltammetry. It has been found that various molecular factors such as electron delocalization, conjugation length and dimensionality, and electronic coupling effects exerted influences on the electronic characteristic of the π -oligomers and C_{60} groups. These results offer useful guiding principles for the design of novel functional C_{60} -oligomer materials.

2.4 Experimental

General procedures and methods

Chemicals and reagents were purchased from commercial suppliers and used without further purification. [60]Fullerene (purity 99.5+%) was purchased from MTR Ltd.

Tetrabutylammonium fluoride (1 M in THF) and lithium hexamethyldisilazide (1 M in THF) were purchased from Aldrich. THF was distilled from sodium benzophenone. Et₃N and toluene were distilled from LiH. Catalysts, Pd(PPh₃)₄ and Pd(PPh₃)₂Cl₂, were prepared from PdCl₂ according to standard procedures. All reactions were performed in standard, dry glassware under an inert atmosphere of N₂ unless otherwise noted. Evaporations and concentrations were done at H₂O aspirator pressure. Flash column chromatography was carried out with silica gel 60 (230-400 mesh) from VWR International. Thin-layer chromatography (TLC) was carried out with silica gel 60 F254 covered on plastic sheets and visualized by UV light or KMnO₄ stain. Melting points (Mp) were measured with a Fisher-Johns melting point apparatus and are uncorrected. ¹H and ¹³C NMR spectra were measured on a Bruker Avance 500 MHz spectrometer. Chemical shifts are reported in ppm downfield from the signal of the internal reference SiMe₄. Coupling constants (*J*) are given in Hz. The coupling constants of some aryl proton signals are reported as pseudo first-order spin systems, even though they are second-order spin systems. Infrared spectra (IR) were recorded on a Bruker Tensor 27 spectrometer. UV-Vis spectra were recorded on an Agilent 8453 UV-Vis or a Cary 6000i UV-Vis-NIR spectrophotometer. APCI mass spectra were measured on an Agilent 1100 series LCMSD spectrometer, and high-resolution MALDI-TOF mass spectra on an Applied Biosystems Voyager instrument with dithranol as the matrix. Cyclic voltammetric experiments were performed on an Epsilon electrochemical analyzer. Fluorescence spectra were measured in CHCl₃ at ambient temperature using a Quantamaster 10000 fluorometer.

Compound 196a. To an oven-dried round-bottomed flask equipped with a magnetic stirrer were added compound **212** (38 mg, 0.033 mmol), C₆₀ (118 mg, 0.160 mmol), and dry THF (180 mL). The mixture was sonicated at 0 °C for 5 h to form a brownish suspension. Lithium hexamethyldisilazide (LHMDS) (0.160 mL, 1 M, 0.160 mmol) was added dropwise at rt under N₂ protection. The mixture was further stirred at rt for 1 h and then trifluoroacetic acid (TFA) (0.1 mL) was added to the suspension to quench the reaction. Removal of the solvent *in vacuo* followed by silica flash column chromatography (hexanes/toluene, 3:1) afforded compound **196a** (33 mg, 0.013 mmol, 39%) as a brown solid. IR (KBr) 3025, 2922, 2851, 2199, 2089, 1631, 1514, 1494, 1464 cm⁻¹; ¹H NMR (CDCl₃/CS₂, 500 MHz) δ 7.53–7.52 (m, 12H, Ar-H), 7.25 (s, 2H, C₆₀-H), 7.18 (s, 2H, Ar-H), 7.15 (s, br, 4H, C=C-H, AB system), 7.11 (s, 2H, Ar-H), 4.18 (t, *J* = 6.0 Hz, 4H, OCH₂), 4.14 (t, *J* = 6.5 Hz, 4H, OCH₂), 1.99–1.91 (m, 8H, OCH₂CH₂), 1.71–1.60 (m, 8H, OCH₂CH₂CH₂), 1.47–1.22 (m, 48H), 0.91 (t, *J* = 6.3 Hz, 6H, CH₃), 0.85 (t, *J* = 6.3 Hz, 6H, CH₃); ¹³C NMR (CDCl₃/CS₂, 125 MHz) δ 155.0, 154.2 (two Ar-O carbons), 152.1, 151.9, 148.2, 147.9, 147.2, 146.9, 146.8, 146.4, 146.23, 146.19, 146.02, 145.97, 145.9, 145.2, 145.1, 143.8, 143.2, 143.1, 142.7, 142.6, 142.55, 142.46, 142.23, 142.16, 140.94, 140.87, 137.8, 137.2, 136.7, 135.7 (Of 30 different *sp*² carbons in the C_s symmetrical C₆₀ core, 28 signals are discernible in this region, peaks at 137.8 and 137.2 ppm are signals due to the oligomer unit), 132.5, 129.6, 128.5, 127.6, 127.0, 123.1, 117.5, 117.2, 115.5, 113.4, 98.1, 96.2, 87.8, 81.0 (four alkynyl carbons), 70.2, 70.0 (two OCH₂), 62.5 (tertiary *sp*³ CH on the C₆₀ core), 56.0 (quaternary *sp*³ carbon on the C₆₀ core), 32.6, 60.6, 30.5, 30.41, 30.38, 30.3, 30.2, 30.1, 27.2, 26.8, 23.46, 23.45, 14.8 (CH₃); MALDI-TOF MS *m/z* calcd for C₂₀₂H₁₀₆O₄ 2596.82, found 2597.91 [M + H]⁺.

Compound 196b. Compound **196b** (33 mg, 0.0096 mmol, 41%) was obtained as a brownish solid by the same *in situ* ethynylation protocol as described in the synthesis of **196a**, using compound **216** (47 mg, 0.024 mmol), C₆₀ (86 mg, 0.12 mmol), LHMDS (0.12 mL, 1 M, 0.120 mmol) and dry THF (100 mL). IR (KBr) 3026, 2923, 2852, 2203, 2151, 1636, 1559, 1540, 1501, 1463 cm⁻¹; ¹H NMR (CDCl₃/CS₂, 500 MHz) δ 7.51–7.48 (m, 12H, Ar-H), 7.23 (s, 2H, C₆₀-H), 7.16 (s, 2H, Ar-H), 7.12 (s, br, 4H, C–C-H), 7.08 (s, 2H, Ar-H), 7.000 (s, 2H, Ar-H), 6.998 (s, 2H, Ar-H), 4.15–4.11 (m, 8H, OCH₂), 4.08–4.02 (m, 8H, OCH₂), 1.96–1.81 (m, 16H, OCH₂CH₂), 1.69–1.51 (m, 16H, OCH₂CH₂CH₂), 1.41–1.20 (m, 96H), 0.89–0.82 (m, 24H, CH₃); ¹³C NMR (CDCl₃/CS₂, 125 MHz) δ 154.6, 153.8, 153.6 (2 ×) (three signals out of four Ar-O carbons observed, one coincidental peak overlapped), 151.7, 151.6, 147.8, 147.5, 146.8, 146.6, 146.4, 146.0, 145.9, 145.8, 145.7, 145.6, 145.5, 144.9, 144.7, 143.4, 143.2, 142.78, 142.76, 142.3, 142.22, 142.17, 142.1, 141.9, 141.8, 140.6, 140.5, 137.3, 136.8, 136.3, 135.3 (Of 30 different *sp*² carbons in the C_s symmetrical C₆₀ core, 29 signals are discernible in this region, peaks at 137.3 and 136.8 ppm are signals due to the oligomer unit), 132.1, 129.2, 128.2, 127.2, 126.5, 122.8, 117.4, 117.2, 117.0, 115.4, 114.4, 113.0 (two coincidental peaks due to the oligomer *sp*² carbons not observed), 97.7, 95.6, 92.3, 91.8, 87.6, 80.7 (six alkynyl carbons), 69.9, 69.8, 69.6, 69.2 (four OCH₂), 62.1 (tertiary *sp*³ CH on the C₆₀ core), 55.7 (quaternary *sp*³ carbon on the C₆₀ core), 32.2, 30.2, 30.03, 29.99, 29.8, 29.7, 26.8, 26.6, 26.4, 23.1, 14.4 (CH₃); MALDI-TOF MS *m/z* calcd for C₂₅₈H₁₉₄O₈ 3421.5, found 3421.7 [M]⁺.

Compound 197a. Compound **197a** (28 mg, 0.011 mmol, 41%) was obtained as a brownish solid by the same *in situ* ethynylation protocol as described in the

synthesis of **196a**, using compound **225** (30 mg, 0.026 mmol), C₆₀ (102 mg, 0.142 mmol), LHMDS (0.142 mL, 1 M, 0.142 mmol) and dry THF (130 mL). IR (KBr) 2922, 2851, 2199, 2087, 1630, 1499 cm⁻¹; ¹H NMR (CDCl₃, 500 MHz) δ 7.92 (s, 2H, central Ar-H), 7.75 (d, *J* = 16.5 Hz, 2H, C=C-H), 7.59 (d, *J* = 7.5 Hz, 4H, styryl Ar-H), 7.36 (t, *J* = 7.5 Hz, 4H, styryl Ar-H), 7.30–7.25 (m, 6H, C=C-H, Ar-H, and C₆₀-H), 7.16 (s, 2H, Ar-H), 7.14 (s, 2H, Ar-H), 4.16 (t, *J* = 5.5 Hz, 4H, OCH₂), 4.13 (t, *J* = 6.5 Hz, 4H, OCH₂), 1.98–1.92 (m, 4H, OCH₂CH₂), 1.84–1.79 (m, 4H, OCH₂CH₂), 1.70–1.63 (m, 4H, OCH₂CH₂CH₂), 1.50–1.42 (m, 4H, OCH₂CH₂CH₂), 1.41–1.18 (m, 48H), 0.89–0.81 (m, 12H, CH₃); ¹³C NMR (CDCl₃/CS₂, 125 MHz) δ 155.0, 154.2, 152.0, 151.9 (four Ar-O carbons), 148.2, 147.9, 147.2, 147.0, 146.8, 146.4, 146.2, 146.1, 146.0, 145.9, 145.3, 145.1, 143.8, 143.6, 143.2, 142.7, 142.62, 142.57, 142.5, 142.3, 142.2, 141.0, 140.9, 138.0, 137.9, 136.7, 135.7 (Of the 30 different *sp*² carbons in the *C_s* symmetrical C₆₀ core, 27 signals are discernible in this region), 131.2, 129.3, 129.2, 128.5, 127.6, 126.5, 123.2, 117.7, 117.1, 115.4, 113.9 (11 aromatic and olefinic carbons), 98.3, 94.5, 93.3, 81.2 (four alkynyl carbons), 70.4, 69.9 (two OCH₂), 62.6 (tertiary *sp*³ CH on the C₆₀ core), 56.1 (quaternary *sp*³ carbon on the C₆₀ core), 33.5, 32.7, 32.6, 30.7, 30.6, 30.5 (br), 30.4, 30.3 (br), 30.2 (br), 30.1 (br), 30.0, 27.3, 26.8, 23.6, 14.9 (CH₃); MALDI-TOF MS *m/z* calcd for C₂₀₂H₁₀₆O₄ 2596.82, found 2597.98 [M + H]⁺.

Compound 197b. Compound **197b** (22 mg, 0.0064 mmol, 21%) was obtained as a brownish solid by the same *in situ* ethynylation protocol as described in the synthesis of **196a**, using compound **228** (60 mg, 0.030 mmol), C₆₀ (109 mg, 0.152 mmol), LHMDS (0.15 mL, 1 M, 0.15 mmol) and dry THF (180 mL). IR (KBr) 2922,

2851, 2201, 2089, 1630, 1586, 1506, 1464 cm^{-1} ; ^1H NMR (CDCl_3 , 500 MHz) δ 7.91 (s, 2H, central Ar-H), 7.75 (d, $J = 15.5$ Hz, 2H, C \equiv C-H), 7.59 (d, $J = 8.5$ Hz, 4H, styryl Ar-H), 7.36 (t, $J = 7.0$ Hz, 4H, styryl Ar-H), 7.29–7.25 (m, 6H, C \equiv C-H, Ar-H, and C_{60} -H), 7.17 (s, 2H, Ar-H), 7.10 (s, 2H, Ar-H), 7.07 (s, 2H, Ar-H), 7.06 (s, 2H, Ar-H), 4.16–4.05 (m, 16H, OCH_2), 1.97–1.87 (m, 16H, OCH_2), 1.80–1.75 (m, 8H, OCH_2CH_2), 1.70–1.64 (m, 8H, OCH_2CH_2), 1.61–1.54 (m, 16H, $\text{OCH}_2\text{CH}_2\text{CH}_2$), 1.50–1.10 (m, 96H), 0.90–0.82 (m, 24H, CH_3); ^{13}C NMR (CDCl_3 , CS_2 , 125 MHz) δ 154.67, 153.88, 153.73 (three Ar-O carbons, one coincidental peak not observed), 151.8, 151.7, 147.8, 147.6, 146.9, 146.6, 146.5, 146.0, 145.93, 145.86, 145.70, 145.65, 145.59, 144.9, 144.8, 143.4, 142.82, 142.80, 142.4, 142.3, 142.2, 142.1, 141.9, 141.8, 140.6, 140.5, 137.6, 136.3, 135.4 (Of 30 different sp^2 carbons in the C_s symmetrical C_{60} core, 29 signals are discernible in this region), 130.8, 128.9, 128.8, 128.1, 127.1, 122.8, 117.5, 117.4, 117.2, 117.1, 115.4, 114.8, 114.3, 113.1 (14 aromatic and olefinic carbons, three coincidental peaks not observed), 97.8, 93.7, 92.8, 92.2, 91.9, 80.7 (six alkynyl carbons), 70.0, 69.94, 69.87, 69.7 (four OCH_2 carbons), 62.2 (tertiary sp^3 CH on the C_{60} core), 55.7 (quaternary sp^3 carbon on the C_{60} core), 32.23 (br), 32.18, 30.2 (br), 30.11, 30.08, 30.04, 29.97, 29.90, 29.86, 29.82 (br), 29.80, 29.73 (br), 29.69 (br), 29.65, 29.61 (br), 29.5, 26.9, 26.4, 26.3, 23.0, 14.4 (CH_3); MALDI-TOF MS m/z calcd for $\text{C}_{258}\text{H}_{194}\text{O}_8$ 3421.48, found 3423.60 $[\text{M} + \text{H}]^+$.

Compound 198a. Compound **198a** (31.5 mg, 0.0108 mmol, 23%) was obtained as a brownish solid by the same *in situ* ethynylation protocol as described in the synthesis of **196a**, using compound **238** (70 mg, 0.047 mmol), C_{60} (170 mg, 0.242 mmol), LHMDS (0.24 mL, 1 M, 0.24 mmol), and dry THF (200 mL). IR (KBr) 2922,

2851, 2197, 2086, 1627, 1590, 1507, 1493, 1464 cm^{-1} ; ^1H NMR (CDCl_3 , CS_2 , 500 MHz) δ 7.91 (s, 2H, central Ar-H), 7.67 (d, $J = 15.5$ Hz, 2H, C' C-H), 7.48 (d, $J = 8.0$ Hz, 4H, styryl Ar-H), 7.26–7.21 (m, 12H, Ar-H, NPh-H, C' C'-H, and C'₆₀-H), 7.16 (d, $J = 5.5$ Hz, 4H, styryl Ar-H), 7.10 (d, $J = 7.5$ Hz, 8H, NPh-H), 7.06 (s, 2H, Ar-H), 7.05 (s, 2H, Ar-H), 7.02 (t, $J = 7.5$ Hz, 4H, NPh-H), 4.16–4.12 (m, 8H, OCH_2), 1.93–1.81 (m, 8H, OCH_2CH_2), 1.67–1.61 (m, 4H, $\text{OCH}_2\text{CH}_2\text{CH}_2$), 1.50–1.45 (m, 4H, $\text{OCH}_2\text{CH}_2\text{CH}_2$), 1.38–1.19 (m, 48H), 0.85–0.81 (m, 12H, CH_3); ^{13}C NMR (CDCl_3 , CS_2 , 125 MHz) 154.6, 153.8 (two Ar-O carbons), 151.7, 151.5, 147.8, 147.7, 147.5, 147.4, 146.8, 146.5, 146.4, 146.0, 145.85, 145.81, 145.65, 145.60, 145.5, 141.9, 144.7, 143.4, 142.77, 142.75, 142.29, 142.21, 142.2, 142.1, 141.9, 141.8, 140.6, 140.5, 137.5, 136.3, 135.3 (Of 30 different sp^2 carbons in the C_s symmetrical C'₆₀ core, 28 signals are discernible in this region, peaks at 147.7, 147.4, and 137.5 ppm are signals due to the oligomer unit), 131.6, 130.0, 129.4, 128.5, 128.0, 124.7, 124.3, 123.3, 122.5, 117.4, 116.7, 115.1, 113.3, (one coincidental carbon signal due to the oligomer unit not observed), 97.9, 94.2, 92.5, 80.7 (four alkynyl carbons), 70.0, 69.6 (two OCH_2), 62.1 (tertiary sp^3 CH on the C'₆₀ core), 55.6 (quaternary sp^3 carbon on the C'₆₀ core), 32.24, 32.21, 30.2, 30.14, 30.06, 30.03, 30.00, 29.95, 29.91, 29.8, 29.72, 29.70, 29.5, 26.8, 26.3, 23.10, 23.07, 14.5 (CH_3); MALDI-TOF MS m/z calcd for $\text{C}_{226}\text{H}_{124}\text{N}_2\text{O}_4$ 2930.96, found 2932.01 $[\text{M} + \text{H}]^+$.

Compound 198b. Compound **198b** (17 mg, 0.0045 mmol, 17%) was obtained as a brownish solid by the same *in situ* ethynylation protocol as described in the synthesis of **196a**, using compound **240** (60 mg, 0.026 mmol), C'₆₀ (109 mg, 0.150 mmol), LHMDs (0.15 mL, 1 M, 0.15 mmol), and dry THF (180 mL). IR (KBr) 2922.

2851, 2199, 2088, 1627, 1592, 1508, 1493, 1465 cm^{-1} ; ^1H NMR (CDCl_3 , CS_2 , 500 MHz) δ 7.93 (s, 2H, central Ar-H), 7.68 (d, $J = 16.5$ Hz, 2H, C=C-H), 7.49 (d, $J = 9.0$ Hz, 4H, styryl Ar-H), 7.30–7.23 (m, 12H, Ar-H, NPh-H, C=C-H, and C_{60} -H), 7.19–7.05 (m, 24H, Ar-H), 4.18–4.15 (m, 8H, OCH_2), 4.10–4.06 (m, 8H, OCH_2), 1.97–1.78 (m, 16H, OCH_2CH_2), 1.71–1.45 (m, 16H, $\text{OCH}_2\text{CH}_2\text{CH}_2$), 1.43–1.19 (m, 96H), 0.90–0.82 (m, 24H, CH_3); ^{13}C NMR (CDCl_3 , CS_2 , 125 MHz) δ 155.0, 154.1, 154.0 (2 \times) (three signals out of four Ar-O carbons observed, one coincidental peak overlapped), 152.1, 152.0, 148.2, 148.0, 147.8, 147.2, 146.95, 146.93, 146.8, 146.4, 146.3, 146.2, 146.03, 145.98, 145.9, 145.2, 145.1, 143.8, 143.15, 143.12, 142.7, 142.6, 142.54, 142.47, 142.23, 142.16, 140.94, 140.87, 137.8, 136.7, 135.7 (Of 30 different sp^2 carbons in the C, symmetrical C_{60} core, 28 signals are discernible in this region, peaks at 148.0, 147.8, and 137.8 ppm are signals due to the oligomer unit), 132.0, 129.83, 129.78, 128.4, 128.3, 125.1, 124.7, 123.75, 123.66, 122.9, 117.8, 117.5, 117.4, 115.7, 115.0, 114.7, 113.4 (one coincidental carbon signal due to the oligomer unit not observed), 98.1, 94.3, 93.0, 92.6, 92.2, 81.0 (six alkynyl carbons), 70.4, 70.3, 70.2, 70.0 (four OCH_2), 62.4 (tertiary sp^3 CH on the C_{60} core), 56.0 (quaternary sp^3 carbon on the C_{60} core), 32.4, 31.3, 30.4, 30.3, 30.2, 30.15, 30.12, 30.07, 30.04, 30.00, 29.9, 29.8, 29.7, 27.0, 26.5, 23.1, 14.6 (CH_3); MALDI-TOF MS m/z calcd for $\text{C}_{282}\text{H}_{212}\text{N}_2\text{O}_8$ 3756.63, found 3757.93 $[\text{M} + \text{H}]^+$.

Compound 199. Compound **199** (70 mg, 0.055 mmol, 76%) was obtained as a brownish solid by the same *m situ* ethynylation protocol as described in the synthesis of **196a**, using compound **242** (40 mg, 0.0725 mmol), C_{60} (131 mg, 0.181 mmol), LHMS (0.18 mL, 1 M, 0.18 mmol), and dry THF (150 mL). IR (KBr) 2923, 2852,

2224, 2090, 1638, 1617, 1499, 1464 cm^{-1} ; ^1H NMR ($\text{CDCl}_3/\text{CS}_2$, 500 MHz) δ 7.23, 7.17, 7.02 (three singlet signals, 3H, two Ar-H and one C_{60} -H), 4.12 (t, $J = 7.0$ Hz, 2H, OCH_2), 4.08 (t, $J = 6.5$ Hz, 2H, OCH_2), 2.51 (t, $J = 7.0$ Hz, 2H, CH_2 next to alkynyl bond), 1.94-1.85 (m, 4H), 1.70-1.61 (m, 4H), 1.57-1.49 (m, 4H), 1.42-1.19 (m, 32H), 0.93-0.88 (m, 6H), 0.83 (t, $J = 6.5$ Hz, 3H); ^{13}C NMR ($\text{CDCl}_3/\text{CS}_2$, 125 MHz) δ 154.8, 153.9 (two carbons of Ar-O), 151.9, 151.8, 147.9, 147.6, 147.0, 146.7, 146.5, 146.1, 146.0, 145.9, 145.7, 145.6, 145.0, 144.8, 143.5, 142.88, 142.85, 142.4, 142.33, 142.28, 142.2, 141.96, 141.89, 140.7, 140.6, 136.4, 135.5 (Of 30 different sp^2 carbons in the C_s symmetrical C_{60} core, 27 signals are discernible in this region), 117.4, 116.0, 112.1 (three Ar carbons), 97.3, 96.9, 80.6 (three of the four alkynyl carbons), 70.0, 69.8 (two OCH_2), 62.2 (tertiary sp^3 CH on the C_{60} core), 55.8 (quaternary sp^3 carbon on the C_{60} core), 32.2, 30.1, 30.0, 29.9, 29.6, 29.51, 29.46, 29.2, 29.0, 26.8, 26.3, 22.9, 20.1, 14.4 (CH_3); MALDI-TOF MS m/z calcd for $\text{C}_{98}\text{H}_{62}\text{O}_2$ 1270.47, found 1271.84 $[\text{M} + \text{H}]^+$.

1,4-Bis(decyloxy)benzene (201). 1-Bromodecane (17.7g, 0.08 mol), 1,4-dihydroquinone (4.4g, 0.040 mol) and KOH (5.62g, 0.100 mol) were added into EtOH (100 mL) and stirred at 90 °C for 60 h. The reaction was cooled down. Water (150 mL) and CH_2Cl_2 (150 mL) were added. The organic layer was isolated, washed by brine, and dried over MgSO_4 . After the solvent was removed *in vacuo*, a pale brown solid was obtained. The solid was recrystallized from methanol to give **201** as white flakes (12.4 g, 0.0316 mol, 79%). Mp 69–70 °C. ^1H NMR (CDCl_3 , 500 MHz) δ 6.85 (s, 4H, Ar-H), 3.93 (t, $J = 7.0$ Hz, 4H), 1.81-1.76 (m, 4H), 1.50-1.44 (m, 4H), 1.39-1.31 (m, 24H), 0.92 (t, $J = 6.0$ Hz, 6H); ^{13}C NMR (CDCl_3 , 125 MHz) δ 153.4 (Ar-O carbons),

115.6 (Ar carbons), 68.9, 32.1, 29.81, 29.79, 29.6, 29.5, 26.3, 22.9, 14.3.

1,4-Bis(decyloxy)-2,5-diiodobenzene (202). To a round bottomed flask equipped with a magnetic stirrer was added compound **201** (13.6 g, 34.8 mmol), Hg(OAc)₂ (30.9 g, 97.0 mmol), I₂ (24.5 g, 96.5 mmol), and CH₂Cl₂ (300 mL). The reaction mixture was stirred overnight at rt, then the formed slurry was filtered through a MgSO₄ pad. The MgSO₄ pad was rinsed with CH₂Cl₂. The filtrate was washed with Na₂S₂O₃ (10% aq), NaHCO₃ (satd), water, brine, and dried over MgSO₄. The solvent was removed *in vacuo* and the crude product was recrystallized from ethanol to afford product **202** as colorless flakes (20 g, 31.2 mmol, 89%). Mp 50-51 °C; ¹H NMR (CDCl₃, 500 MHz) δ 7.18 (s, 2H, Ar-H), 3.93 (t, *J* = 6.5 Hz, 4H), 1.83-1.76 (m, 4H), 1.54-1.47 (m, 4H), 1.36-1.29 (m, 24H), 0.89 (t, *J* = 7.0 Hz, 6H); ¹³C NMR (CDCl₃, 125 MHz) δ 153.3 (Ar-O carbons), 123.3 (Ar carbons), 86.8 (Ar-I carbons), 70.8 (two CH₂O), 32.3, 30.0, 29.8, 29.7, 29.6, 26.5, 23.1, 14.5.

1,4-Bis(decyloxy)-2-iodo-5-(trimethylsilylethynyl)benzene (203). Compound **202** (6.5 g, 0.010 mol), trimethylsilylacetylene (1 mL, 7 mmol), PdCl₂(PPh₃)₂ (350 mg, 0.500 mmol), CuI (190 mg, 1.00 mmol), and Et₃N (20 mL) were added to THF (60 mL). The solution was bubbled by N₂ at rt for 5 min and then stirred at 45 °C under N₂ protection overnight. After the reaction was complete as checked by TLC analysis, the solvent was removed *in vacuo*. To the obtained residue was added chloroform, and the mixture was filtered through a MgSO₄ pad. The filtrate was sequentially washed with aq HCl (10%) and brine. The organic layer was dried with MgSO₄ and concentrated under vacuum to afford the the crude product, which

was then purified by silica flash column chromatography (hexanes/CH₂Cl₂, 90:10) to yield compound **203** (3.6 g, 5.8 mmol, 58%) as light yellowish solid. Mp 35–36 °C. IR (neat) 2924, 2854, 2158, 1586, 1485, 1465, 1374 cm⁻¹; ¹H NMR (CDCl₃, 500 MHz) δ 7.25 (s, 1H, Ar-H), 6.83 (s, 1H, Ar-H), 3.94 (t, *J* = 6.5 Hz, 2H, CH₂O), 3.93 (t, *J* = 6.5 Hz, 2H, CH₂O), 1.81-1.77 (m, 4H), 1.53-1.48 (m, 4H), 1.34-1.27 (m, 24H), 0.88 (t, *J* = 6.5 Hz, 6H, CH₃), 0.25 (s, 9H, Si(CH₃)₃); ¹³C NMR (CDCl₃, 125 MHz) δ 155.3, 152.1, 124.3, 116.7, 113.9, 101.2, 99.8, 88.3 (six aromatic carbons and two alkynyl carbons), 70.5, 70.2 (two CH₂O), 32.34, 32.33, 30.07, 30.02, 30.0, 29.9, 29.8, 29.7, 29.6, 26.5, 26.4, 23.1, 14.5, 0.38; APCI-MS *m/z* calcd for C₃₁H₅₂IO₂Si 612.3, found 612.3 [M]⁺

α, α'-Dibromo-*p*-xylene (205). *p*-Xylene (6.00 g, 56.5 mol), NBS (20.1 g, 113 mmol) and benzoylperoxide (20 mg) in 200 mL of CHCl₃ were heated to reflux under a bright light. After 8 h of refluxing, the solution was cooled down to rt. The generated succinimide was filtered off. The yellow solution was concentrated to give the crude product which was purified by silica flash column chromatography (hexanes) to yield compound **205** (7.92 g, 30 mmol, 53%) as a white solid. Mp 144–145 °C; ¹H NMR (CDCl₃, 500 MHz) δ 7.37 (s, 4H), 4.47 (s, 4H); ¹³C NMR (CDCl₃, 125 MHz) δ 138.2, 129.7, 33.0; GC-MS *m/z* (%) 264 ([M]⁺, 12), 184 ([M-Br]⁺, 95), 104 ([M-2Br]⁺, 100).

Tetraethyl 1,4-phenylenebis(methylene)diphosphonate (206). 1,4-Bis(bromomethyl)benzene (**205**) (0.13 g, 0.49 mmol) and triethylphosphite (1 mL) were placed in a round-bottomed flask and heated to reflux for 12 h. The mixture was cooled to rt, yielding colorless crystals. The bulk unreacted triethylphosphite was

carefully decanted. The remaining white solid was washed three times with hexanes, and then was stirred under heating in hexanes to extract residual triethylphosphite. The mixture was cooled to rt again. Compound **206** was isolated after filtration as a white solid (0.172 g, 0.455 mmol, 92%). Mp 81–83 °C; ^1H NMR (CDCl_3 , 500 MHz) δ 7.35 (s, 4H, Ar-H), 4.03 (m, 8H, OCH_2), 3.12 (d, $J_{P,H}$ = 20.6 Hz, 4H, Bz-H), 1.24 (t, J = 7.5 Hz, 12H, (CH_3)); ^{13}C NMR (CDCl_3 , 125 MHz) δ 130.0, 129.7, 62.4 (OCH_2), 55.3 (d, $J_{P,C}$ = 138.5 Hz, Bz-C), 16.5 (CH_3); APCI-MS m/z calcd for $\text{C}_{16}\text{H}_{28}\text{O}_6\text{P}_2$ 378.1, found 379.1 $[\text{M} + \text{H}]^+$.

4-(Trimethylsilylethynyl)benzaldehyde (208). 4-Bromobenzaldehyde (925 mg, 5.00 mmol), TMSA (1.4 mL, 10 mmol), $\text{PdCl}_2(\text{PPh}_3)_2$ (9.50 mg, 0.05 mmol), CuI (17.6 mg, 0.0250 mmol) and DBU (0.91g, 6.1 mmol) were added to benzene (20 mL). The solution was bubbled by N_2 at rt for 5 min and then stirred under reflux and N_2 protection for 1 h. After the reaction was complete as checked by TLC analysis, the solvent was removed *in vacuo*. To the obtained residue was added CH_2Cl_2 . The mixture was filtered through a MgSO_4 pad. Then it was sequentially washed by aq HCl (10%) and brine. The organic layer was dried over MgSO_4 and concentrated under vacuum. The crude product was purified by silica flash column chromatography (hexane) to yield compound **208** (660 mg, 3.26 mmol, 65%) as a white solid. mp 76–77 °C; ^1H NMR (CDCl_3 , 500 MHz) δ 10.00 (s, 1H), 7.82 (d, J = 7.5 Hz, 2H), 7.60 (d, J = 7.5 Hz, 2H), 0.27 (s, 9H); GC-MS m/z (%) 202 ($[\text{M}]^+$, 60), 187 ($[\text{M}-\text{CH}_3]^+$, 100).

4-Ethynylbenzaldehyde (209). To a solution of compound **208** (200 mg, 0.990 mmol) in 1:1 MeOH THF (10 mL) was added K_2CO_3 (50 mg, 0.36 mmol). After being stirred at rt for 0.5 h, the solvent was removed under vacuum. The residue was dissolved in chloroform and sequentially washed by aq HCl (10%) and brine. The organic layer was dried over $MgSO_4$. Filtration to remove $MgSO_4$ followed by evaporation under vacuum afforded the crude product, which was purified by silica flash column chromatography (hexanes, EtOAc, 95:5) to yield compound **209** as a white solid (122 mg, 0.941 mmol, 95%). Mp 94–95 °C; IR (neat) 3223, 2839, 2102, 1704, 1689, 1606, 1563, 1390 cm^{-1} ; 1H NMR ($CDCl_3$, 500 MHz) δ 10.03 (s, 1H), 7.85 (d, $J = 8.5$ Hz, 2H), 7.65 (d, $J = 8.5$ Hz, 2H), 3.30 (s, 1H); ^{13}C NMR ($CDCl_3$, 125 MHz) δ 191.6 (CHO), 136.2, 132.9, 129.7, 128.5 (four Ar carbons), 82.8, 81.3 (two alkynyl carbons); GC-MS m/z (%) 130 ($[M]^+$, 98), 129 ($[M-H]^+$, 100), 101 ($[M-CHO]^+$, 78).

4-((2,5-Bis(decyloxy)-4-(trimethylsilylethynyl)phenyl)ethynyl)benzaldehyde (210). 4-Ethynylbenzaldehyde (**209**) (113 mg, 0.872 mmol), **203** (532 mg, 0.870 mmol), $PdCl_2(PPh_3)_2$ (31 mg, 0.044 mmol), and CuI (16 mg, 0.087 mmol) were added to Et_3N (20 mL). The mixture was bubbled by N_2 at rt for 5 min and then stirred at rt under N_2 protection for 4 h. After the reaction was complete as checked by TLC analysis, the solvent was removed under vacuum. The obtained residue was diluted with $CHCl_3$ and then was sequentially washed by aq HCl (10%) and brine. The resulting organic layer was dried over $MgSO_4$ and concentrated under vacuum. The crude product was purified by silica flash column chromatography (hexanes CH_2Cl_2 , 4:1) to yield compound **210** (502 mg, 0.816 mmol, 94%) as a pale yellow wax. IR

(KBr) 2954, 2921, 2852, 2207, 2153, 1696, 1599, 1560, 1509 cm^{-1} ; ^1H NMR (CDCl_3 , 500 MHz) δ 10.0 (s, 1H, CHO), 7.85 (d, $J = 9.0$ Hz, 2H, Ar-H), 7.65 (d, $J = 8.5$ Hz, 2H, Ar-H), 6.97 (s, 2H, Ar-H), 6.96 (s, 2H, Ar-H), 4.00 (t, $J = 6.5$ Hz, 2H, OCH_2), 3.98 (t, $J = 6.5$ Hz, 2H, OCH_2), 1.85–1.79 (m, 4H, OCH_2CH_2), 1.54–1.50 (m, 4H, $\text{OCH}_2\text{CH}_2\text{CH}_2$), 1.37–1.24 (m, 24H), 0.90–0.85 (m, 6H, CH_3), 0.27 (s, 9H, $\text{Si}(\text{CH}_3)_3$); ^{13}C NMR (CDCl_3 , 125 MHz) δ 191.5 (CHO), 154.3, 154.0 (two Ar-O carbons), 135.6, 132.2, 130.0, 129.7, 117.4, 117.1, 114.9, 113.5 (eight aromatic carbons), 101.2, 100.8, 94.0, 90.4 (four alkynyl carbons), 69.75, 69.73 (two OCH_2), 32.1, 29.9, 29.80, 29.76, 29.64, 29.60, 29.57, 29.5, 26.3, 26.2, 22.9, 14.3 (CH_3), 0.2 ($\text{Si}(\text{CH}_3)_3$); APCI MS m/z calcd for $\text{C}_{40}\text{H}_{58}\text{O}_3\text{Si}$ 614.4, found 615.4 $[\text{M} + \text{H}]^+$.

1,4-Bis(4-((2,5-bis(decyloxy)-4-(trimethylsilylethynyl)phenyl)ethynyl)-*E*-styryl)benzene (211). To an oven-dried flask purged with nitrogen was added compound **206** (112 mg, 0.589 mmol), LHMDS (0.91 mL, 0.91 mmol), and dry THF (15 mL) at -78 °C. After stirring for 1 h the solution turned into a red color. Then aldehyde **210** (362 mg, 0.589 mmol) dissolved in dry THF (20 mL) was added in small portions over a period of 1 h via a syringe. The reaction was allowed to proceed at rt overnight. Afterwards, the excess LHMDS was quenched with water and the mixture was extracted three times with CHCl_3 . The organic layer was washed with brine and dried over MgSO_4 . Removal of the solvent under vacuum afforded the crude product of **211**, which was purified by silica flash column chromatography (hexanes/ CH_2Cl_2 , 7:3) to yield compound **211** (160 mg, 0.123 mmol, 42%) as a yellow solid. Mp 121–122 °C; IR (KBr) 3029, 2956, 2924, 2854, 2152, 1602, 1517, 1494, 1468, 1413 cm^{-1} ; ^1H NMR (CDCl_3 , 500 MHz) δ 7.53–7.50 (m, 12H, Ar-H), 7.16–7.09 (m, 4H, C=C-H),

6.97 (s, 2H, Ar-H), 6.95 (s, 2H, Ar-H), 4.01 (t, $J = 6.5$ Hz, 4H, OCH₂), 3.99 (t, $J = 6.0$ Hz, 4H, OCH₂), 1.86–1.80 (m, 8H, OCH₂CH₂), 1.55–1.50 (m, 8H, OCH₂CH₂CH₂), 1.39–1.26 (m, 48H), 0.90–0.86 (m, 12H, CH₃), 0.27 (s, 18H, Si(CH₃)₃); ¹³C NMR (CDCl₃, 125 MHz) δ 154.4, 153.7 (two Ar-O carbons), 137.5, 136.9, 132.1, 129.3, 128.3, 127.2, 126.6, 122.7, 117.5, 117.1, 114.5, 114.0 (10 aromatic and two alkenyl carbons), 101.4, 100.3, 95.3, 87.2 (four alkynyl carbons), 69.9, 69.8 (two OCH₂), 32.14, 32.12, 29.89, 29.88, 29.8, 29.7, 29.60, 29.56, 26.32, 26.27, 22.93, 22.91, 14.35, 14.34 (CH₃), 0.2 (Si(CH₃)₃); MALDI-TOF MS m/z calcd for C₈₈H₁₂₂O₄Si₂ 1299.89, found 1299.94 [M]⁺.

1,4-Bis(4-((2,5-bis(decyloxy)-4-ethynylphenyl)ethynyl)-*E*-styryl)benzene (212). To a solution of compound **211** (160 mg, 0.123 mmol) in 1:1 THF/MeOH (18 mL) was added K₂CO₃ (50 mg). The mixture was stirred at rt for 30 min, then the solvent was removed by rotary evaporation. The residue was diluted in CHCl₃ and sequentially washed by aq HCl (10%) and brine. The organic layer was dried over MgSO₄ and concentrated under vacuum. The crude product was purified by silica flash column chromatography (hexanes/CH₂Cl₂, 7:3) to yield compound **212** (148 mg, 0.123 mmol, 100%) as a yellow solid. Mp 122–123 °C; IR (KBr) 3314, 3294, 3028, 2923, 2853, 2106, 1516, 1494, 1468 cm⁻¹; ¹H NMR (CDCl₃, 500 MHz) δ 7.53–7.49 (m, 12H, Ar-H), 7.16–7.09 (m, 4H, C=C-H), 7.00 (s, 2H, Ar-H), 6.98 (s, 2H, Ar-H), 4.03–3.99 (m, 8H, OCH₂), 3.34 (s, 2H, alkynyl H), 1.86–1.81 (m, 8H, OCH₂CH₂), 1.55–1.47 (m, 8H, OCH₂CH₂CH₂), 1.40–1.28 (m, 48H), 0.90–0.86 (m, 12H, CH₃); ¹³C NMR (CDCl₃, 125 MHz) δ 154.4, 153.7 (two Ar-O carbons), 137.5, 136.9, 132.1, 129.3, 128.2, 127.2, 126.6, 122.6, 118.0, 117.0, 114.9, 112.8 (10 aromatic

and two alkenyl carbons), 95.4, 87.1, 82.5, 80.3 (four alkynyl carbons), 69.9 (two OCH₂ overlapped), 32.1, 29.9, 29.82, 29.80, 29.77, 29.7, 29.60, 29.58, 29.4, 26.3, 26.1, 22.92, 22.91, 14.3 (CH₃); MALDI-TOF MS *m/z* calcd for C₈₂H₁₀₆O₄ 1154.81, found 1155.92 [M + H]⁺.

4-((2,5-Bis(decyloxy)-4-ethynylphenyl)ethynyl)benzaldehyde (213). To a solution of compound **210** (447 mg, 0.728 mmol) in THF (15 mL) was added TBAF (0.1 mL). The mixture was stirred at rt for 10 min, and then the solvent was removed by rotary evaporation. The residue was diluted in chloroform and sequentially washed by aq HCl (10%) and brine. The organic layer was dried over MgSO₄ and concentrated under vacuum. The crude product was purified by silica flash column chromatography (EtOAc/hexanes, 1:99) to yield compound **213** (220 mg, 0.406 mmol, 56%) as a yellow solid. Mp 42–43 °C; IR (KBr) 3289, 2924, 2871, 2852, 2211, 2106, 1701, 1639, 1602, 1562, 1510, 1495, 1469 cm⁻¹; ¹H NMR (CDCl₃, 500 MHz) δ 10.03 (s, 1H, CHO), 7.87 (d, *J* = 8.5 Hz, 2H, Ar-H), 7.67 (d, *J* = 8.5 Hz, 2H, Ar-H), 7.01 (s, 2H, Ar-H), 7.00 (s, 2H, Ar-H), 4.02 (t, *J* = 6.5 Hz, 2H, OCH₂), 4.01 (t, *J* = 6.5 Hz, 2H, OCH₂), 3.37 (s, 1H, CC-H) 1.87–1.80 (m, 4H, OCH₂CH₂), 1.57–1.44 (m, 4H, OCH₂CH₂CH₂), 1.40–1.25 (m, 24H), 0.90–0.86 (m, 6H, CH₃); ¹³C NMR (CDCl₃, 125 MHz) δ 191.5 (CHO), 154.4, 154.0 (two Ar-O carbons), 135.6, 132.2, 130.0, 129.8, 118.0, 117.2, 113.9, 113.8 (eight aromatic carbons), 94.1, 90.2, 82.9, 80.1 (four alkynyl carbons), 70.0, 69.8 (two OCH₂), 32.1, 32.09, 29.9, 29.80, 29.6, 29.5, 29.4, 26.3, 26.1, 22.9, 14.3 (CH₃); APCI MS *m/z* calcd for C₃₇H₅₀O₃ 542.4, found 543.3 [M + H]⁺.

4-((4-((2,5-Bis(decyloxy)-4-(trimethylsilyl)ethynyl)phenyl)ethynyl)-2,5-bis(decyloxy)phenyl)ethynyl)benzaldehyde (214). Compound **213** (220 mg, 0.406 mmol), **203** (248 mg, 0.410 mmol), PdCl₂(PPh₃)₂ (15 mg, 0.022 mmol), and CuI (8.0 mg, 0.04 mmol) were added to Et₃N (15 mL). The mixture was bubbled by N₂ at rt for 5 min and then stirred at rt under N₂ protection for 2 h. After the reaction was complete as checked by TLC analysis, the solvent was removed by rotary evaporation. The residue obtained was diluted with CHCl₃ and then was sequentially washed by aq HCl (10%) and brine. The resulting organic layer was dried over MgSO₄ and concentrated under vacuum. The crude product was then purified by silica flash column chromatography (hexanes:CH₂Cl₂, 2:3) to yield compound **214** (337 mg, 0.327 mmol, 80%) as a yellow solid. Mp 68–69 °C; ¹H NMR (CDCl₃, 500 MHz) δ 10.06 (s, 1H, CHO), 7.90 (d, *J* = 7.5 Hz, 2H, Ar-H), 7.70 (d, *J* = 7.5 Hz, 2H, Ar-H), 7.05 (s, 2H, Ar-H), 7.00 (s, 1H, Ar-H), 6.98 (s, 1H, Ar-H), 4.09–4.00 (m, 8H, OCH₂), 1.91–1.82 (m, 8H, OCH₂CH₂), 1.58–1.52 (m, 8H, OCH₂CH₂CH₂), 1.43–1.28 (m, 48H), 0.93–0.89 (m, 12H, CH₃), 0.30 (s, 9H, Si(CH₃)₃); ¹³C NMR (CDCl₃, 125 MHz) δ 191.5 (CHO), 154.4, 154.2, 152.7, 153.6 (four Ar-O carbons), 135.6, 132.2, 130.1, 129.8, 117.7, 117.5, 117.3, 117.2, 115.5, 114.7, 114.2, 113.2 (eight aromatic carbons), 101.4, 100.4, 94.1, 92.1, 91.5, 90.6 (six alkynyl carbons), 70.1, 70.0, 69.8, 69.7 (four OCH₂), 32.13, 32.12, 29.9, 29.85, 29.80, 29.7, 29.59, 29.57, 26.4, 26.3, 26.2, 22.9, 14.3(CH₃), 0.19 (Si(CH₃)₃); APCI MS *m/z* calcd. for C₆₈H₁₀₂O₅Si 1026.75, found 1027.7 [M + H]⁺.

1,4-Bis(4-((4-((2,5-bis(decyloxy)-4-(trimethylsilyl)ethynyl)phenyl)ethynyl)-2,5-bis(decyloxy)phenyl)ethynyl)-*E*-styryl)benzene (215). Compound

212 (148 mg, 0.128 mmol), **203** (314 mg, 0.513 mmol), PdCl₂(PPh₃)₂ (8.98 mg, 0.0128 mmol), CuI (4.86 mg, 0.0256 mmol) were added to Et₃N (20 mL). The solution was cooled to -78 °C and degassed under vacuum and then stirred at rt under N₂ protection for 4 h. After the reaction was complete as checked by TLC analysis, the solvent was removed by rotary evaporation. The residue obtained was diluted with CHCl₃, and then sequentially washed by aq HCl (10%) and brine. The organic layer was dried over MgSO₄ and concentrated under vacuum to afford the crude product of **215**, which was purified by silica flash column chromatography (hexanes/CH₂Cl₂, 7:3) to yield compound **215** (164 mg, 0.0772 mmol, 60%) as a yellow solid. Mp 76–77 °C; IR (KBr) 2924, 2854, 2152, 1620, 1502, 1468 cm⁻¹; ¹H NMR (CDCl₃, 500 MHz) δ 7.54–7.50 (m, 12H, Ar-H), 7.18–7.11 (m, 4H, C=C-H, second-order AB system), 7.02 (s, 2H, Ar-H), 7.01 (s, 2H, Ar-H), 6.97 (s, 2H, Ar-H), 6.95 (s, 2H, Ar-H), 4.07–3.97 (m, 16H, OCH₂), 1.87–1.80 (m, 16H, OCH₂CH₂), 1.58–1.49 (m, 16H, OCH₂CH₂CH₂), 1.41–1.26 (m, 96H), 0.91–0.87 (m, 24H, CH₃), 0.28 (s, 18H, Si(CH₃)₃); ¹³C NMR (CDCl₃, 125 MHz) δ 154.5, 154.0, 153.8, 153.7 (four Ar-O carbons), 137.5, 137.0, 132.2, 129.3, 128.3, 127.2, 126.7, 122.9, 117.9, 117.5, 117.4, 114.9, 114.7, 114.4, 114.1 (15 signals discernible out of 14 aromatic and 2 alkenyl carbons in this region, one coincidental peak not observed), 101.5, 100.3, 95.4, 91.8, 91.7, 87.4 (six alkynyl carbons), 70.1, 70.0, 69.9, 69.8 (four OCH₂), 32.2, 29.9, 29.8, 29.7, 29.6, 26.4, 26.3, 26.2, 22.9, 14.3 (CH₃), 0.2 (Si(CH₃)₃); MALDI-TOF MS *m/z* calcd for C₁₄₄H₂₁₀O₈Si₂ 2124.56, found 2126.93 [M + H]⁺.

1,4-Bis(4-((4-((2,5-bis(decyloxy)-4-ethynylphenyl)ethynyl)-2,5-bis(decyloxy) phenyl)ethynyl)-*E*-styryl)benzene (216). To a solution of compound

215 (164 mg, 0.0772 mmol) in 1:1 MeOH/THF (20 mL) was added K_2CO_3 (50 mg, 0.36 mmol). The mixture was stirred at rt for 1 h, then the solvent was removed by rotary evaporation. The residue was diluted in chloroform and sequentially washed by aq HCl (10%) and brine. The organic layer was dried over $MgSO_4$ and then concentrated under vacuum to afford the crude product of **216**, which was purified by silica flash column chromatography (hexanes/ CH_2Cl_2 , 65:35) to yield compound **216** as a yellow solid (93 mg, 0.045 mmol, 61%). Mp 124–125 °C; IR (KBr) 3315, 3027, 2954, 2923, 2853, 2203, 2104, 1630, 1604, 1515, 1505, 1468 cm^{-1} ; 1H NMR ($CDCl_3$, 500 MHz) δ 7.54–7.49 (m, 12H, Ar-H), 7.17–7.10 (m, 4H, C=C-H), 7.02 (s, 2H, Ar-H), 7.01 (s, 2H, Ar-H), 6.99 (s, 2H, Ar-H), 6.98 (s, 2H, Ar-H), 4.06–3.98 (m, 16H, OCH_2), 3.34 (s, 2H, alkynyl H), 1.88–1.79 (m, 16H, OCH_2CH_2), 1.57–1.45 (m, 16H, $OCH_2CH_2CH_2$), 1.42–1.25 (m, 96H), 0.90–0.83 (m, 24H, CH_3); ^{13}C NMR ($CDCl_3$, 125 MHz) δ 154.4, 153.9, 153.8, 153.6 (four Ar-O carbons), 137.5, 137.0, 132.2, 129.3, 128.3, 127.2, 126.6, 122.8, 118.3, 117.4, 117.33, 117.27, 115.3, 114.5, 114.4, 112.8 (14 aromatic and two alkenyl carbons), 95.4, 91.8, 91.5, 87.4, 82.5, 80.3 (six alkynyl carbon signals), 70.02, 69.99, 69.8 (three OCH_2 signals, one coincidental peak not observed), 32.2, 29.94, 29.92, 29.9, 29.83, 29.80, 29.72, 29.69, 29.66, 29.59, 29.56, 29.4, 26.4, 26.22, 26.20, 22.9, 14.3 (CH_3); MALDI-TOF MS m/z calcd for $C_{138}H_{194}O_8$ 1980.48, found 1981.72 $[M + H]^+$.

Oligomer 217. Oligomer **217** was isolated as a byproduct during the synthesis of **215**. 1H NMR ($CDCl_3$, 500 MHz) δ 7.54–7.49 (m, 24H, styryl Ar-H), 7.17–7.10 (m, 8H, C=C-H), 7.02 (s, 2H, Ar-H), 7.01 (s, 2H, Ar-H), 7.00 (s, 4H, Ar-H), 6.97 (s, 2H, Ar-H), 6.95 (s, 2H, Ar-H), 4.06–3.96 (m, 24H, OCH_2), 1.87–1.79 (m, 24H,

OCH₂CH₂), 1.57–1.49 (m, 24H, OCH₂CH₂CH₂), 1.38–1.27 (m, 144H), 0.90–0.84 (m, 36H, CH₃), 0.27 (s, 18H, Si(CH₃)₃); ¹³C NMR (CDCl₃, 125 MHz) δ 155.3, 154.5, 153.9, 153.82, 153.79, 153.6 (six Ar-O carbons), 137.6, 137.5, 137.0, 136.9, 132.19, 132.14, 129.4, 129.3, 128.31, 128.25, 127.2, 126.6, 122.8, 122.7, 118.0, 117.9, 117.5, 117.4, 117.2, 115.5, 114.9, 114.6, 114.4, 114.0, 112.9 (25 signals discernible out of 24 aromatic and four alkenyl carbons in this region), 101.5, 100.3, 96.0, 95.4, 91.8, 91.7, 87.4, 87.2, 79.9, 79.6 (ten alkynyl carbons), 70.09, 70.07, 70.02, 69.93, 69.91, 69.8 (six OCH₂ carbons), 32.2, 29.91, 29.85, 29.7, 29.6, 29.4, 26.39, 26.35, 26.31, 26.25, 26.23, 26.20, 22.9, 14.3 (CH₃), 0.2 (Si(CH₃)₃); MALDI-TOF MS *m/z* calcd for C₂₂₆H₃₁₄O₁₂Si₂ 3278.36, found 3280.93 [M + H]⁺.

2,5-Diiodo-*p*-xylene (218). To a round-bottomed flask equipped with a condenser, *p*-xylene (**204**) (10.0 g, 94.2 mmol), H₅IO₆ (8.95 g, 39.3 mmol), iodine (19.1 g, 75.1 mmol), water (37.5 mL), H₂SO₄ (5.5 mL), and acetic acid (185 mL) were added, and the mixture was heated at 80–100 °C under stirring for 4 h. Water (250 mL) was then added and the flask was cooled in ice water to promote crystallization of the product. The crude product was filtered off, washed with water, and recrystallized from acetone to give compound **218** as a white solid (23.3 g, 62.9 mmol, 69%). Mp 106–107 °C; ¹H NMR (CDCl₃, 500 MHz) δ 7.65 (s, 2H, Ar-H), 2.34 (s, 6H, PhCH₃); ¹³C NMR (CDCl₃, 125 MHz) δ 140.8, 139.4, 100.8, 27.1 (CH₃).

1,4-Bis(bromomethyl)-2,5-diiodobenzene (219). Compound **218** (10.0 g, 0.0280 mol), NBS (22.0 g, 0.124 mol), and benzoylperoxide (0.500 g, 2.06 mmol) were dissolved in 250 mL of chloroform and then heated to reflux under a bright light

irradiation. After 8 h of refluxing, the solution was allowed to stand over night at rt for a complete crystallization of the product. The product was filtered off together with the succinimide byproduct. Removal of the succinimide by water rinsing afforded the crude product, which was further purified by recrystallization from chloroform and hexane to yield compound **219** as a white solid (1.90 g, 3.68 mmol, 13%). Mp 230-231 °C; ¹H NMR (CDCl₃, 500 MHz) δ 7.90 (s, 2H, Ar-H), 4.48 (s, 4H, PhCH₂); ¹³C NMR (CDCl₃, 125 MHz) δ 142.5, 141.2, 99.8, 36.5 (CH₂).

1,4-Bis(diethylphosphoromethyl)-2,5-diiodobenzene (220). Compound **219** (1.85 g, 3.59 mmol) and triethylphosphite (5.6 mL, 35 mmol) were added to a round-bottomed flask and heated to reflux for 12 h. Colorless crystals were formed while cooling the mixture to rt. The excess triethylphosphite was decanted, and the remaining white solid was washed by hexanes three times at rt and once at boiling temperature to completely remove the unreacted triethylphosphite. The resulting solid was filtered off after cooling to rt, affording compound **220** as a white solid (1.99 g, 3.16 mmol, 88%). Mp 170-171 °C; ¹H NMR (CDCl₃, 500 MHz) δ 7.88 (d, *J* = 2.5 Hz, 2H, Ar-H), 4.11-4.05 (m, 8H, O-CH₂), 3.30 (d, *J*_{H,P} = 20.5 Hz, 4H, PhCH₂), 1.29 (t, *J* = 7.0 Hz, 12H, CH₂CH₃); ¹³C NMR (CDCl₃, 125 MHz) δ 141.0 (d, ²*J*_{C,P} = 28.1 Hz), 136.4, 100.9 (Ar C-I), 62.6 (OCH₂), 37.6 (d, ¹*J*_{C,P} = 138.3 Hz), 16.6 (CH₃).

1,4-Bis((*E*)-2-styryl)-2,5-diiodobenzene (221). To an oven-dried flask protected under N₂ atmosphere were added compound **220** (0.45 g, 0.71 mmol), NaH (0.043 g, 1.8 mmol), and dry THF (15 mL). Upon gentle heating at *ca.* 40 °C,

the solution gradually turned into a vivid purple-red color. Benzaldehyde (0.17 mL, 1.56 mmol) dissolved in THF (5 mL) was added in small portions over a period of 1 h through a syringe. The reaction was kept under stirring and heating for another 30 min before work-up. The small excess NaH was carefully quenched with water and the mixture was extracted three times with chloroform. The chloroform layer was washed by brine, dried over MgSO₄, and concentrated to precipitation. The residual was crystallized from hexanes to yield compound **221** as yellow crystals (0.24 g, 0.45 mmol, 63%). mp 230–231 °C; ¹H NMR (CDCl₃, 500 MHz) δ 8.09 (s, 2H, Ar-H), 7.55 (d, *J* = 7.5 Hz, 4H, Ar-H), 7.38 (t, *J* = 7.3 Hz, 4H, Ar-H), 7.30 (t, *J* = 7.15 Hz, 2H, Ar-H), 7.20 (d, *J* = 16.0 Hz, 2H, C=C-H), 6.99 (d, *J* = 16.1 Hz, 2H, C=C-H); ¹³C NMR (CDCl₃, 125 MHz) δ 140.8, 136.5, 136.3, 135.4, 130.5, 128.8, 128.4, 127.0, 100.3.

1,4-Bis(*E*-styryl)-2,5-bis(trimethylsilylethynyl)benzene(222). Compound **221** (130 mg, 0.24 mmol), trimethylsilylacetylene (0.17 mL, 1.2 mmol), PdCl₂(PPh₃)₂ (8.6 mg, 0.012 mmol), CuI (4.6 mg, 0.024 mmol), and Et₃N (3 mL) were added to THF (3 mL). The solution was bubbled by N₂ at rt for 5 min, and then stirred at 45 °C under N₂ protection overnight. After the reaction was complete as checked by TLC analysis, the solvent was removed *in vacuo*. The resulting residue was diluted with CHCl₃, and then was filtered through a MgSO₄ pad. The solution obtained was sequentially washed by aq HCl (10%) and brine. The organic layer was dried over MgSO₄ and concentrated under vacuum to give a crude product of **222**. The crude product was then purified by silica flash column chromatography (hexanes/CH₂Cl₂, 95:5) to give compound **222** (100 mg, 0.212 mmol, 87%) as a

yellowish solid. Mp 267–268 °C; IR (neat) 2958, 2154, 1633, 1594, 1574 cm^{-1} ; ^1H NMR (CDCl_3 , 500 MHz) δ 7.81 (s, 2H, central Ar-H), 7.59 (d, $J = 16.0$ Hz, 2H, C=C-H), 7.53 (d, $J = 7.5$ Hz, 4H, Ar-H), 7.37 (t, $J = 6.5$ Hz, 4H, Ar-H), 7.28 (t, $J = 7.5$ Hz, 2H, Ar-H), 7.21 (d, $J = 16.0$ Hz, 2H, C=C-H), 0.33 (s, 18H, $\text{Si}(\text{CH}_3)_3$); ^{13}C NMR (CDCl_3 , 125 MHz) δ 137.8, 137.5, 130.8, 129.01, 128.95, 128.2, 126.9, 125.8, 122.5, 103.4, 101.4, 0.2; APCI-MS m/z calcd for $\text{C}_{32}\text{H}_{34}\text{Si}_2$ 474.8, found 475.1 $[\text{M}]^+$.

1,4-Diethynyl-2,5-di-(E)-styrylbenzene (223). To a solution of compound **222** (120 mg, 0.253 mmol) in 1:1 MeOH/THF (15 mL) was added K_2CO_3 (200 mg, 1.45 mmol). After being stirred at rt for 1h, the solvent was removed through rotary evaporation. The residue was dissolved in CHCl_3 and sequentially washed by aq HCl (10%) and brine. The organic layer was dried over MgSO_4 and then concentrated under vacuum to afford a crude product of **223**, which was further purified by silica flash column chromatography (hexanes CH_2Cl_2 , 95:5) to yield compound **223** as a yellow solid (72 mg, 0.22 mmol, 86%). Mp 166 °C (dec); IR (neat) 3296, 3042, 2925, 2101, 1632, 1593, 1575 cm^{-1} ; ^1H NMR (CDCl_3 , 500 MHz) δ 7.88 (s, 2H, central Ar-H), 7.58 (d, $J = 16.0$ Hz, 2H, C=C-H), 7.55 (d, $J = 6.5$ Hz, 4H, Ar-H), 7.39 (t, $J = 6.5$ Hz, 4H, Ar-H), 7.30 (t, $J = 6.5$ Hz, 2H, Ar-H), 7.19 (d, $J = 16.0$ Hz, 2H, C=C-H), 3.48 (s, 2H, $\text{C}\equiv\text{C-H}$); Meaningful ^{13}C NMR spectrum was not obtained because of poor solubility; APCI-MS m/z calcd for $\text{C}_{26}\text{H}_{18}$ 330.1, found 331.1 $[\text{M} + \text{H}]^+$.

1,4-Di(E-styryl)-2,5-bis(2,5-bis(decyloxy)-4-trimethylsilylethynylphenylethynyl) benzene (224). Compound **223** (70 mg, 0.21 mmol), **203** (560 mg, 0.917 mmol), $\text{PdCl}_2(\text{PPh}_3)_2$ (14.7 mg, 0.0210 mmol), CuI (7.98 mg, 0.0423 mmol) and

Et₃N (12 mL) were added to THF (8 mL). The solution was bubbled by N₂ at rt for 5 min, and then stirred at 45 °C under N₂ protection for 24 h. After the reaction was complete as checked by TLC analysis, the solvent was removed by rotary evaporation. To the resulting residue was diluted with CHCl₃ and then filtered through a MgSO₄ pad. The solution obtained was sequentially washed by aq HCl (10%) and brine. The organic layer was dried over MgSO₄ and concentrated under vacuum. The crude product was then purified by silica flash column chromatography (hexanes-CH₂Cl₂, 10:1) to yield compound **224** (160 mg, 0.123 mmol, 59%) as a yellowish solid. Mp 137–138 °C; IR (neat) 2922, 2852, 2211, 2150, 1632, 1601, 1503, 1468 cm⁻¹; ¹H NMR (CDCl₃, 500 MHz) δ 7.91 (s, 2H, central Ar-H), 7.73 (d, *J* = 16.5 Hz, 2H, C=C-H), 7.57 (d, *J* = 6.5 Hz, 4H, Ar-H), 7.35 (t, *J* = 7.5 Hz, 4H, Ar-H), 7.29–7.24 (m, 4H, overlap of a doublet and a triplet, C=C-H and Ar-H), 7.02 (s, 2H, Ar-H), 6.99 (s, 2H, Ar-H), 4.02 (t, *J* = 7.0 Hz, 4H, OCH₂), 4.00 (t, *J* = 6.5 Hz, 4H, OCH₂), 1.82 (m, 4H), 1.73 (m, 4H), 1.53 (m, 4H), 1.41–1.16 (m, 48H), 0.88 (t, *J* = 7.0 Hz, 6H, CH₃), 0.84 (t, *J* = 8.0 Hz, 6H, CH₃), 0.61 (s, 18H, Si(CH₃)₃); ¹³C NMR (CDCl₃, 125 MHz) δ 154.4, 153.8, 137.6 (overlap of two signals), 130.8, 128.9, 128.8, 128.1, 127.1, 126.1, 122.7, 117.7, 117.0, 114.4, 114.3, 101.4, 100.5, 93.5, 92.6, 70.0, 69.7, 32.11, 32.10, 29.9, 29.82, 29.77, 29.73, 29.68, 29.6, 29.5, 29.3, 26.3, 26.1, 22.90, 22.88, 14.3, 0.19; MALDI-TOF MS *m/z* calcd for C₈₈H₁₂₂O₁Si₂ 1298.89, found 1300.94 [M + H]⁺.

1,4-Bis(*E*-styryl)-2,5-bis(2,5-bis(decyloxy)-4-ethynylphenylethynyl)benzene (225). To a solution of compound **224** (140 mg, 0.108 mmol) in 1:1 MeOH/THF (15 mL) was added K₂CO₃ (200 mg, 1.45 mmol). After being stirred at rt for 2 h, the reaction solvent was removed by rotary evaporation. The residue

was dissolved in chloroform and sequentially washed by aq HCl (10%) and brine. The organic layer was dried over MgSO₄. Filtration to remove MgSO₄, followed by evaporation under vacuum, afforded a crude product of **225** which was further purified by silica flash column chromatography (hexanes/CH₂Cl₂, 85:15) to yield compound **225** as a yellow solid (100 mg, 0.0866 mmol, 81%). Mp 132–133 °C; IR (neat) 3310, 3283, 2920, 2851, 2201, 2103, 1601, 1504, 1466 cm⁻¹; ¹H NMR (CDCl₃, 500 MHz) δ 7.91 (s, 2H, central Ar-H), 7.74 (d, *J* = 16.5 Hz, 2H, C=C-H), 7.57 (d, *J* = 7.5 Hz, 4H, Ar-H), 7.35 (t, *J* = 7.5 Hz, 4H, Ar-H), 7.29–7.24 (m, 4H, overlap of a doublet and a triplet, C=C-H and Ar-H), 7.06 (s, 2H, Ar-H), 7.02 (s, 2H, Ar-H), 4.03–4.00 (m, 8H, OCH₂), 3.37 (s, 2H, C=C-H), 1.86–1.80 (m, 4H), 1.76–1.70 (m, 4H), 1.53–1.16 (m, 48H), 0.88 (t, *J* = 7.5 Hz, 6H, CH₃), 0.84 (t, *J* = 6.0 Hz, 6H, CH₃); ¹³C NMR (CDCl₃, 125 MHz) δ 154.6, 154.0 (two Ar-O carbons), 137.9, 137.8, 131.1, 129.2, 129.1, 128.4, 127.4, 126.3, 123.0, 118.4, 117.3, 115.0, 113.4, 93.8, 92.6, 82.9, 80.5, 70.3, 70.1, 32.4, 32.3, 30.2, 30.1, 30.04, 30.01, 29.98, 29.82, 29.80, 29.75, 29.7, 29.6, 26.41, 26.36, 23.2, 23.1, 14.6; MALDI-TOF MS *m/z* calcd for C₈₂H₁₀₆O₄ 1154.81, found 1156.77 [M + H]⁺.

((4-((2,5-Bis(decyloxy)-4-ethynylphenyl)ethynyl)-2,5-bis(decyloxy)phenyl)ethynyl)triisopropylsilane (226). To a solution of compound **231** (0.659 g, 0.610 mmol) in 1:1 MeOH/THF (30 mL) was added K₂CO₃ (100 mg). After being stirred at rt for 4 h, the reaction solvent was removed under vacuum. The residue was dissolved in chloroform and sequentially washed by aq HCl (10%) and brine. The organic layer was dried over MgSO₄. Filtration to remove MgSO₄ followed by evaporation under vacuum afforded compound **226** as a yellow solid which was pure

enough for next synthetic step (0.590 g, 0.586 mmol, 96%). Mp 54–55 °C; IR (KBr) 3317, 2922, 2851, 2150, 2108, 1602, 1536, 1496, 1467, 1419, 1387 cm^{-1} ; ^1H NMR (CDCl_3 , 500 MHz) δ 6.99 (s, 1H, Ar-H), 6.98 (s, 1H, Ar-H), 6.95 (s, 1H, Ar-H), 6.94 (s, 1H, Ar-H), 4.04–3.98 (m, 6H), 3.96 (t, $J = 6.0$ Hz, 2H), 3.34 (s, 1H), 1.85–1.81 (m, 8H), 1.50–1.47 (m, 8H), 1.37–1.25 (m, 48H), 1.16 (s, 21H), 0.91–0.87 (m, 12H); ^{13}C NMR (CDCl_3 , 125 MHz) δ 154.5, 154.3, 153.48, 153.45 (four Ar-O carbons), 118.095, 118.057, 117.1, 116.6, 115.2, 114.4, 114.2, 112.7 (eight aromatic carbons), 103.2, 96.6, 91.8, 91.2, 82.5, 80.2 (six alkynyl carbons), 70.0, 69.9, 69.7, 69.3 (four CH_2O carbons), 32.1, 29.9, 29.85, 29.81, 29.78, 29.76, 29.71, 29.70, 29.6, 29.5, 29.4, 26.4, 26.2, 26.17, 22.9, 18.9, 14.3, 11.6; APCI-MS m/z calcd for $\text{C}_{67}\text{H}_{110}\text{O}_4\text{Si}$ 1006.8, found 1007.9 [$\text{M} + \text{H}$] $^+$.

1,4-Bis(*E*-styryl)-2,5-bis(2,5-bis(decyloxy)-4-(2,5-bis(decyloxy)-4-triisopropylsilylethynylphenylethynyl)phenylethynyl)benzene (227). Compound **226** (202 mg, 0.200 mmol), **221** (53.4 mg, 0.100 mmol), $\text{PdCl}_2(\text{PPh}_3)_2$ (14.4 mg, 0.0200 mmol), CuI (7.6 mg, 0.040 mmol) were added to Et_3N (20 mL). The solution was bubbled by N_2 at rt for 5 min and then stirred at 45 °C under N_2 protection for 36 h. After the reaction was complete as checked by TLC analysis, the solvent was removed by rotary evaporation. The residue obtained was diluted with CHCl_3 . The mixture was filtered through a MgSO_4 pad, and then was sequentially washed by aq HCl (10%) and brine. The organic layer was dried over MgSO_4 and concentrated under vacuum. The crude product was purified by silica flash column chromatography (hexanes CH_2Cl_2 , 3:1) to yield compound **227** (223 mg, 0.0972 mmol, 97%) as a yellowish solid. Mp 104–105 °C; IR (KBr) 2956, 2925, 2855, 2150, 1629, 1510 cm^{-1} ;

^1H NMR (CDCl_3 , 500 MHz) δ 7.98 (s, 2H, central Ar-H), 7.81 (d, $J = 16.0$ Hz, 2H, C=C-H), 7.64 (d, $J = 8.0$ Hz, 4H, styryl Ar-H), 7.41 (t, $J = 8.0$ Hz, 4H, styryl Ar-H), 7.35–7.25 (m, 4H, overlap of styryl Ar-H and C=C-H), 7.13 (s, 2H, Ar-H), 7.11 (s, 2H, Ar-H), 7.02 (s, 2H, Ar-H), 7.00 (s, 2H, Ar-H), 4.12–4.00 (m, 16H, OCH_2), 1.93–1.88 (m, 8H), 1.87–1.79 (m, 8H), 1.59–1.54 (m, 16H), 1.46–1.16 (m, 138H), 0.93–0.87 (m, 24H, CH_3); ^{13}C NMR (CDCl_3 , 125 MHz) δ 154.6, 154.0, 153.8, 153.5 (four Ar-O carbon signals), 137.64, 137.62, 130.9, 129.0, 128.9, 128.2, 127.2, 126.2, 122.8, 118.2, 117.5, 117.3, 116.8, 115.0, 114.6, 114.3, 114.1 (17 aromatic and alkenyl carbon signals), 103.3, 96.8, 93.6, 92.7, 92.1, 91.5 (six alkynyl carbon signals), 70.1, 70.03, 70.01, 69.5 (four OCH_2 signals), 32.1, 29.92, 29.87, 29.81, 29.80, 29.7, 29.6, 29.5, 29.4, 26.5, 26.3, 26.23, 26.21, 22.9, 19.0, 14.3, 11.6; MALDI-TOF MS m/z calcd for $\text{C}_{156}\text{H}_{231}\text{O}_8\text{Si}_2$ 2292.75, found 2293.43 $[\text{M} + \text{H}]^+$.

1,4-Bis(*E*-styryl)-2,5-bis(2,5-bis(decyloxy)-4-(2,5-bis(decyloxy)-4-ethynylphenylethynyl)phenylethynyl)benzene (228). To a solution of compound **227** (223 mg, 0.0920 mmol) in THF (30 mL) was added TBAF (0.4 mL, 1M in THF, 0.4 mmol). The content was stirred at rt for 5 h, and the solvent was removed by rotary evaporation. The residue was diluted in CHCl_3 and sequentially washed by aq HCl (10%) and brine. The organic layer was dried over MgSO_4 and concentrated under vacuum to afford a crude product of **228** which was further purified by silica flash column chromatography (hexanes/ CH_2Cl_2 , 7:3) to yield compound **228** (168 mg, 0.0848 mmol, 82%) as a yellow solid. Mp 140–141 $^\circ\text{C}$; IR (KBr) 3314, 3288, 2955, 2923, 2853, 2209, 2104, 1628, 1604, 1510, 1467 cm^{-1} ; ^1H NMR (CDCl_3 , 500 MHz) δ 7.94 (s, 2H, central Ar-H), 7.77 (d, $J = 16.0$ Hz, 2H, C=C-H), 7.60 (d, J

8.0 Hz, 4H, styryl Ar-H), 7.37 (t, $J = 7.5$ Hz, 4H, styryl Ar-H), 7.31–7.26 (m, 4H, overlap of styryl Ar-H and C=C-H), 7.09 (s, 2H, Ar-H), 7.07 (s, 2H, Ar-H), 7.02 (s, 2H, Ar-H), 7.00 (s, 2H, Ar-H), 4.08–3.99 (m, 16H, OCH₂), 3.35 (s, 2H, alkynyl H), 1.91–1.73 (m, 16H), 1.56–1.45 (m, 16H), 1.44–1.16 (96H), 0.91–0.83 (m, 24H, CH₃); ¹³C NMR (CDCl₃, 125 MHz) δ 154.4, 154.0, 153.8, 153.6 (four Ar-O carbon signals), 137.6, 130.8, 129.0, 128.9, 128.2, 127.2, 126.2, 122.8, 118.3, 117.5, 117.33, 117.29, 115.2, 114.8, 114.2, 112.9 (two coincidental aromatic carbon peaks not observed), 93.6, 92.7, 91.74, 91.67, 82.5, 80.3 (six alkynyl carbon signals), 70.03, 70.01, 69.9 (one coincidental OCH₂ carbon signal not observed), 32.14, 32.10, 29.91, 29.85, 29.82, 29.80, 29.77, 29.69, 29.67, 29.58, 29.56, 29.5, 29.43, 29.41, 26.24, 26.19, 22.9, 14.3; MALDI-TOF MS m/z calcd for C₁₃₈H₁₉₄O₈ 1980.48, found 1980.44 [M]⁺.

((2,5-Bis(decyloxy)-4-((triisopropylsilyl)ethynyl)phenyl)ethynyl)trimethylsilane (229). Compound **203** (1.23g, 2.01 mmol), triisopropylsilylacetylene (0.94 mL, 2.2 mmol), PdCl₂(PPh₃)₂ (60 mg, 0.085 mmol) and CuI (30 mg, 0.16 mmol) were added to Et₃N (40 mL). The solution was bubbled by N₂ at rt for 5 min and then stirred at 45 °C under N₂ protection for 12 h. After the reaction was complete as checked by TLC analysis, the solvent was removed by rotary evaporation. To the obtained residue was added chloroform. The mixture was filtered over a MgSO₄ pad. Then it was sequentially washed by aq HCl (10%) and brine. The organic layer was dried over MgSO₄ and concentrated under vacuum. The crude product was then purified with silica flash column chromatography (hexanes/CH₂Cl₂, 90:10) to yield compound **229** (1.25 g, 1.87 mmol, 93%) as a light yellow solid. Mp 66–67 °C; IR (KBr) 2942, 2927, 2896, 2867, 2853, 2153, 1617, 1537, 1499, 1469, 1405, 1388 cm⁻¹;

^1H NMR (CDCl_3 , 500 MHz) δ 6.88 (s, 1H, Ar-H), 6.87 (s, 1H, Ar-H), 3.96 (t, J 6.5 Hz, 2H, CH_2O), 3.93 (t, J 6.5 Hz, 2H, CH_2O), 1.82-1.73 (m, 4H), 1.52-1.43 (m, 4H), 1.27 (br, 24H), 1.14 (s, 21H, $\text{Si}(\text{CH}(\text{CH}_3)_3)$), 0.90-0.87 (m, 6H), 0.26 (s, 9H, $\text{Si}(\text{CH}_3)_3$); ^{13}C NMR (CDCl_3 , 125 MHz) δ 154.4, 154.2 (two Ar-O carbons), 117.9, 116.9, 114.5, 114.0 (four aromatic carbons), 103.2, 101.5, 100.0, 96.7 (four alkynyl carbons), 69.9, 69.5 (two CH_2O), 32.1, 29.9, 29.8, 29.7, 29.62, 29.56, 26.4, 26.3, 22.9, 19.1, 18.9, 14.3, 11.6, 0.20; APCI-MS m/z calcd for $\text{C}_{12}\text{H}_{74}\text{O}_2\text{Si}_2$ 666.5, found 667.5 $[\text{M} + \text{H}]^+$.

((2,5-Bis(decyloxy)-4-ethynylphenyl)ethynyl)triisopropylsilane (230).

Method 1: To a solution of compound **229** (1.76 g, 2.64 mmol) in 1:1 MeOH-THF (40 mL) was added K_2CO_3 (200 mg, 1.45 mmol). After being stirred at rt for 4 h, the reaction solvent was removed by rotary evaporation. The residue was diluted in chloroform and sequentially washed by aq HCl (10%) and brine. The organic layer was dried over MgSO_4 . Filtration to remove MgSO_4 followed by evaporation under vacuum afforded the crude product which was purified with silica flash column chromatography (hexanes/ CH_2Cl_2 90:10) to yield compound **230** as white solid (1.45 g, 2.44 mmol, 92%).

Method 2: To a solution of compound **233** (560 mg, 0.857 mmol) in toluene (30 mL) was added NaOH (50 mg, 1.3 mmol). After being stirred under reflux for 4 h, the reaction solvent was removed by rotary evaporation. The residue was diluted in CH_2Cl_2 and sequentially washed by aq HCl (10%) and brine. The organic layer was dried over MgSO_4 . Filtration to remove MgSO_4 followed by evaporation under vacuum afforded the crude product. The crude product was then purified by silica

flash column chromatography (hexanes CH_2Cl_2 , 90:10) to yield compound **230** (395 mg, 0.664 mmol, 77%) as a white solid. Mp 48-49 °C; IR (KBr) 3286, 2922, 2851, 2145, 1617, 1501, 1470, 1387 cm^{-1} ; ^1H NMR (CDCl_3 , 500 MHz) δ 6.919 (s, 1H, Ar-H), 6.916 (s, 1H, Ar-H), 3.99 (t, J = 6.5 Hz, 2H), 3.93 (t, J = 6.5 Hz, 2H), 3.32 (s, 1H), 1.83-1.74 (m, 4H), 1.54-1.44 (m, 4H), 1.32-1.28 (m, 24H), 1.15 (s, 21H), 0.89 (t, J = 6.5 Hz, 6H); ^{13}C NMR (CDCl_3 , 125 MHz) δ 15-1.6, 154.4, 118.1, 117.7, 115.1, 113.1, 103.2, 97.1, 82.5, 80.5, 70.2, 69.7, 32.3, 30.0, 29.99, 29.98, 29.92, 29.9, 29.8, 29.6, 26.6, 26.3, 23.1, 19.1, 14.5, 11.8; APCI-MS m/z calcd for $\text{C}_{39}\text{H}_{66}\text{O}_2\text{Si}$ 594.5, found 595.5 $[\text{M} + \text{H}]^+$.

((4-((2,5-Bis(decyloxy)-4-((triisopropylsilyl)ethynyl)phenyl)ethynyl)-2,5-bis(decyloxy)phenyl)ethynyl)trimethylsilane (231). Compound **230** (0.73 g, 1.2 mmol), **203** (0.76 g, 1.2 mmol), $\text{PdCl}_2(\text{PPh}_3)_2$ (40 mg, 0.057 mmol), CuI (16 mg, 0.084 mmol) were added to Et_3N (20 mL). The solution was bubbled by N_2 at rt for 5 min and then stirred at 45 °C under N_2 protection for 36 h. After the reaction was complete as checked by TLC analysis, the solvent was removed by rotary evaporation. To the residue obtained was added chloroform. The mixture was filtered through a MgSO_4 pad, and then then was sequentially washed by aq HCl (10%) and brine. The organic layer was dried over MgSO_4 and concentrated under vacuum. The crude product was purified by silica flash column chromatography (hexanes CH_2Cl_2 , 80:20) to yield compound **231** (1.30 g, 1.20 mmol, 98%) as a yellowish solid. Mp 55-56 °C; IR (KBr) 2957, 2922, 2852, 2149, 1617, 1506, 1468, 1423, 1390 cm^{-1} ; ^1H NMR (CDCl_3 , 500 MHz) δ 6.96 (s, 1H, Ar-H), 6.940 (s, 2H, Ar-H), 6.936 (s, 1H, Ar-H), 4.02-3.95 (m, 8H, CH_2O), 1.84-1.79 (m, 8H), 1.55-1.48 (m, 8H), 1.35-1.25 (m, 48H),

1.16 (s, 21H, Si(CH(CH₃)₂)₃), 0.91-0.87 (m, 12H), 0.27 (s, 9H, (Si(CH₃)₃)); ¹³C NMR (CDCl₃, 125 MHz) δ 154.8, 154.6, 153.8, 153.7 (four Ar-O carbons), 118.4, 117.9, 117.4, 116.9, 115.1, 114.8, 114.5, 114.1 (eight aromatic carbons), 103.5, 101.7, 100.4, 96.9, 92.0, 91.6 (six alkynyl carbons), 70.3, 70.1, 69.9, 69.7 (four C₂H₂O), 32.3, 30.7, 30.5, 30.099, 30.056, 29.97, 29.94, 29.91, 29.89, 29.86, 29.8, 26.7, 26.5, 26.44, 26.42, 23.1, 19.1, 14.5, 11.8, 0.4 (Si(CH₃)₃); APCI-MS *m/z* calcd for C₇₀H₁₁₈O₄Si₂ 1078.9, found 1080.0 [M + H]⁺.

4-(2,5-Bis(decyloxy)-4-iodophenyl)-2-methylbut-3-yn-2-ol (232). Compound **202** (3.84 g, 5.98 mol), 1,1-dimethylpropargyl alcohol (0.63 mL, 6.3 mmol), PdCl₂(PPh₃)₂ (210 mg, 0.299 mmol), CuI (114 mg, 0.600 mmol) and Et₃N (20 mL) were added to THF (20 mL). The solution was bubbled by N₂ at rt for 5 min and then stirred at 45 °C under N₂ protection for 3 h. After the reaction was complete as checked by TLC analysis, the solvent was removed by rotary evaporation. To the obtained residue was added chloroform. The mixture was filtered over a MgSO₄ pad. Then it was sequentially washed by aq HCl (10%) and brine. The organic layer was dried over MgSO₄ and concentrated under vacuum. The crude product was then purified by silica flash column chromatography (hexanes/EtOAc, 95:5) to yield compound **232** (1.92 g, 3.21 mmol, 54%) as a yellowish solid. Mp 52–53 °C; IR (neat) 3387 (br), 2924, 2854, 2227, 1588, 1486, 1466, 1437, 1378 cm⁻¹; ¹H NMR (CDCl₃, 500 MHz) δ 7.26 (s, 1H, Ar-H), 6.81 (s, 1H, Ar-H), 3.94 (t, *J* = 6.3 Hz, 4H), 2.02 (s, 1H), 1.84-1.76 (m, 4H), 1.64 (s, 6H), 1.57-1.45 (m, 4H), 1.28 (br, 24H), 0.90 (t, *J* = 6.3 Hz, 6H); ¹³C NMR (CDCl₃, 125 MHz) δ 154.6, 152.0, 124.0, 116.4, 113.3, 98.8, 87.7, 78.4, 70.3, 69.9, 66.0, 32.114, 32.105, 31.6, 29.8, 29.78, 29.76, 29.6, 29.5, 29.4,

26.3, 26.2, 22.9, 14.3; APCI-MS m/z calcd for $C_{31}H_{51}IO_3$ 598.3, found 599.2 $[M + H]^+$.

4-(2,5-Bis(decyloxy)-4-((triisopropylsilyl)ethynyl)phenyl)-2-methylbut-3-yn-2-ol (233). Compound **232** (508 mg, 0.848 mmol), triisopropylsilylacetylene (0.188 mL, 0.848 mmol), $PdCl_2(PPh_3)_2$ (15 mg, 0.021 mmol) and CuI (8.1 mg, 0.042 mmol) were added to Et_3N (30 mL). The solution was bubbled by N_2 at rt for 5 min and then stirred at rt under N_2 protection for 12 h. After the reaction was complete as checked by TLC analysis, the solvent was removed by rotary evaporation. To the residue obtained was added chloroform. The mixture was filtered through a $MgSO_4$ pad. Then it was sequentially washed by aq HCl (10%) and brine. The organic layer was dried over $MgSO_4$ and concentrated under vacuum. The crude product was then purified by silica flash column chromatography (hexanes:EtOAc, 95:5) to yield compound **233** (553 mg, 0.848 mmol, 100%) as a colorless oil. IR (neat) 3416 (br), 2925, 2862, 2151, 2063, 1617, 1499, 1467, 1409, 1385 cm^{-1} ; 1H NMR ($CDCl_3$, 500 MHz) δ 6.89 (s, 1H, Ar-H), 6.84 (s, 1H, Ar-H), 3.95 (t, $J = 6.5$ Hz, 2H), 3.93 (t, $J = 6.5$ Hz, 2H), 2.25 (s, 1H), 1.82-1.74 (m, 4H), 1.63 (s, 6H), 1.53-1.44 (m, 4H), 1.28 (br, 24H), 0.90 (t, $J = 6.5$ Hz, 3H), 0.89 (t, $J = 7.0$ Hz, 3H); ^{13}C NMR ($CDCl_3$, 125 MHz) δ 154.5, 153.6, 117.9, 116.8, 114.2, 113.7, 103.1, 99.2, 96.4, 78.8, 69.8, 69.5, 65.9, 32.1, 31.8, 30.2, 29.83, 29.79, 29.71, 29.7, 29.6, 29.56, 26.4, 26.2, 22.9, 19.2, 18.9, 14.3, 11.6; APCI-MS m/z calcd for $C_{12}H_{72}O_3Si$ 652.5, found 653.4 $[M + H]^+$.

1,4-Bis(*E*-4-*N,N*-diphenylaminostyryl)-2,5-diiodobenzene (234). An oven-dried flask under N_2 protection was charged with compound **220** (616 mg, 0.978

mmol), NaH (59 mg, 2.5 mmol), and dry THF (25 mL). Upon gentle heating at *ca.* 40 °C, the solution turned into a vivid purple-red color. 4-*N,N*-diphenylaminobenzaldehyde (0.68 g, 2.5 mmol) in dry THF was added in small portions over a period of 1 h via a syringe. The reaction was stirred under heating for another 30 min before work-up. The small excess NaH was quenched with H₂O and the mixture was extracted with CHCl₃ three times. The organic layer was washed by brine, dried over MgSO₄, and concentrated to precipitation. The resulting solid was recrystallized from hexanes to yielded **234** as bright yellow crystals (680 mg, 0.783 mmol, 80%). Mp 292–293 °C; IR (neat) 3035, 1588, 1509, 1492 cm⁻¹; ¹H NMR (CDCl₃, 500 MHz) δ 8.05 (s, 2H, central Ar-H), 7.42 (d, *J* = 8.5 Hz, 4H, Ar-H), 7.28 (t, *J* = 7.8 Hz, 8H, NPh-H), 7.13 (d, *J* = 7.5 Hz, 8H, NPh-H), 7.09–7.05 (m, 10H), 6.92 (d, *J* = 16.0 Hz, 2H, C=C-H.); a meaningful ¹³C NMR spectrum was not obtained because of poor solubility; APCI-MS *m/z* calcd for C₄₆H₃₄I₂N₂ 868.1, found 869.1 [M + H]⁺.

1,4-Bis(*E*-4-*N,N*-diphenylaminostyryl)-2,5-bis(trimethylsilylethynyl)benzene (235). Compound **234** (400 mg, 0.460 mmol), trimethylsilylacetylene (0.327 mL, 2.30 mmol), PdCl₂(PPh₃)₂ (16 mg, 0.023 mmol), CuI (8.78 mg, 0.0459 mmol) and Et₃N (10 mL) were added to THF (10 mL). The solution was bubbled by N₂ at rt for 5 min and then heated to 45 °C under stirring and N₂ protection overnight. After the reaction was complete as checked by TLC analysis, the solvent was removed by rotary evaporation. The resulting residue was diluted with chloroform. The mixture was filtered through a MgSO₄ pad. The solution obtained was sequentially washed by aq HCl (10%) and brine. The organic layer was dried over MgSO₄ and concentrated

under vacuum to give the crude product of **235**, which was further purified by silica flash column chromatography (hexanes:CH₂Cl₂, 4:1) to yield compound **235** (281 mg, 0.347 mmol, 76%) as a yellow solid. Mp 228–229 °C; IR (neat) 3034, 2956, 2148, 1588, 1508, 1490 cm⁻¹; ¹H NMR (CDCl₃, 500 MHz) δ 7.77 (s, 2H, central Ar-H), 7.47 (d, *J* = 16.5 Hz, 2H, C=C-H), 7.27 (t, *J* = 7.5 Hz, 8H, NPh-H), 7.15 (d, *J* = 16.0 Hz, 2H, C=C-H), 7.12 (d, *J* = 6.5 Hz, 8H, NPh-H), 7.06–7.02 (m, 8H, Ar-H), 0.30 (s, 18H, Si(CH₃)₃); ¹³C NMR (CDCl₃, 125 MHz) δ 147.9, 147.7, 137.7, 131.5, 130.0, 129.5, 128.7, 127.8, 124.9, 123.9, 123.6, 123.4, 122.2, 103.6 (alkynyl C), 101.0 (alkynyl C), 0.3 (Si(CH₃)₃); APCI-MS *m/z* calcd for C₅₆H₅₂N₂Si₂ 808.4, found 809.3 [M + H]⁺.

1,4-Bis(*E*-4-*N,N*-diphenylaminostyryl)-2,5-diethynylbenzene (236). To a solution of compound **235** (270 mg, 0.334 mmol) in 1:1 MeOH:THF (6 mL) was added K₂CO₃ (100 mg, 0.724 mmol). The mixture was stirred at rt for 30 min, then the reaction solvent was removed by rotary evaporation. The residue was diluted in CHCl₃ and sequentially washed by aq HCl (10%) and brine. The organic layer was dried over MgSO₄ and concentrated under vacuum to afford the crude product of **236**, which was further purified by silica flash column chromatography (hexanes:CH₂Cl₂, 85:15) to yield compound **236** (198 mg, 0.298 mmol, 90%) as a yellowish solid. Mp 275 °C (dec); IR (neat) 3285, 3035, 1589, 1508, 1487 cm⁻¹; ¹H NMR (CDCl₃, 500 MHz) δ 7.82 (s, 2H, central Ar-H), 7.44 (d, *J* = 16.5 Hz, 2H, C=C-H), 7.42 (d, *J* = 9.5 Hz, 4H, Ar-H), 7.27 (t, *J* = 8.0 Hz, 8H, NPh-H), 7.14–7.11 (m, 10H, overlap of C=C-H and NPh-H), 7.06–7.03 (m, 8H, Ar-H), 3.43 (s, 2H, C=C-H); Meaningful ¹³C NMR spectrum was not obtained due to poor solubility; APCI-MS *m/z* calcd for

C₅₀H₃₆N₂ 664.3, found 665.4 [M + H]⁺.

1,4-Bis(*E*-4-*N,N*-diphenylaminostyryl)-2,5-bis(2,5-bis(decyloxy)-4-trimethylsilylethynylphenyl)benzene (237). Compound **236** (30 mg, 0.045 mmol), **203** (138 mg, 0.226 mmol), PdCl₂(PPh₃)₂ (1.6 mg, 0.0023 mmol), CuI (0.86 mg, 0.0045 mmol), and Et₃N (4 mL) were mixed into THF (4 mL). The solution was bubbled by N₂ at rt for 5 min and then stirred at 45 °C under N₂ protection for 24 h. After the reaction was complete as checked by TLC analysis, the solvent was removed by rotary evaporation. To the residue obtained was added CHCl₃. The mixture was filtered through a MgSO₄ pad, then the solution was sequentially washed by aq HCl (10%) and brine. The organic layer was dried over MgSO₄ and concentrated under vacuum to afford the crude product of **237**, which was then purified by silica flash column chromatography (hexanes/CH₂Cl₂, 85:15) to yield compound **237** (58 mg, 0.035 mmol, 79%) as a pale yellow wax. IR (neat) 3034, 2925, 2854, 2152, 1591, 1508, 1494 cm⁻¹; ¹H NMR (CDCl₃, 500 MHz) δ 7.87 (s, 2H, central Ar-H), 7.63 (d, *J* = 17.0 Hz, 2H, C=C-H), 7.44 (d, *J* = 8.0 Hz, 4H, Ar-H), 7.26 (t, *J* = 8.0 Hz, 8H, NPh-H), 7.20 (d, *J* = 16.5 Hz, 2H, C=C-H), 7.11 (d, *J* = 7.5 Hz, 8H, NPh-H), 7.04 (t, *J* = 7.0 Hz, 4H, NPh-H), 7.01 (s, 2H, Ar-H), 6.96 (s, 2H, Ar-H), 4.00 (t, *J* = 7.0 Hz, 4H, OCH₂), 3.98 (t, *J* = 6.0 Hz, 4H, OCH₂), 1.80-1.73 (m, 8H, OCH₂CH₂), 1.54-1.48 (m, 4H), 1.43-1.37 (m, 4H), 1.31-1.16 (m, 48H), 0.88 (t, *J* = 7.0 Hz, 6H, CH₃), 0.83 (t, *J* = 6.5 Hz, 6H, CH₃), 0.27 (s, 18H, Si(CH₃)₃); ¹³C NMR (CDCl₃, 125 MHz) δ 154.4, 153.7, 147.9, 147.7, 137.5, 131.7, 130.0, 129.5, 128.6, 128.0, 124.8, 124.4, 123.5, 123.4, 122.5, 117.8, 117.0, 114.5, 114.2 (19 aromatic and alkenyl carbon signals), 101.4, 100.5, 93.7, 92.3 (four alkynyl carbon signals), 70.1, 69.7 (two OCH₃),

32.1, 29.92, 29.87, 29.83, 29.79, 29.75, 29.7, 29.6, 29.5, 29.4, 26.3, 26.2, 22.90, 22.88, 14.3 (CH₃), 0.2 (Si(CH₃)₃); MALDI-TOF MS *m/z* calcd for C₁₁₂H₁₄₀N₂O₁Si₂ 1634.0, found 1632.9 [M]⁺.

1,4-Bis(*E*-4-*N,N*-diphenylaminostyryl)-2,5-bis(2,5-bis(decyloxy)-4-ethynylphenyl) benzene (238). To a solution of compound **237** (102 mg, 0.0624 mmol) in THF (10 mL) was added TBAF (0.036 mL, 1 M in THF, 0.036 mmol). After stirring at rt for 40 min, the reaction solvent was removed by rotary evaporation. The residue was diluted in chloroform and sequentially washed by aq HCl (10%) and brine. The organic layer was dried over MgSO₄ and then concentrated under vacuum to afford **238** (86 mg, 0.058 mmol, 92%) as a yellowish wax. IR (neat) 2926, 2854, 2200, 2105, 1625, 1591, 1494 cm⁻¹; ¹H NMR (CDCl₃, 500 MHz) δ 7.89 (s, 2H, central Ar-H), 7.63 (d, *J* = 15.5 Hz, 2H, C=C-H), 7.44 (d, *J* = 8.5 Hz, 4H, Ar-H), 7.26 (t, *J* = 8.0 Hz, 8H, NPh-H), 7.17 (d, *J* = 14.0 Hz, 2H, C=C-H), 7.11 (d, *J* = 7.5 Hz, 8H, NPh-H), 7.05–7.02 (m, 10H, Ar-H), 6.98 (s, 2H, Ar-H), 4.00 (t, *J* = 6.0 Hz, 8H, OCH₂), 3.34 (s, 2H, C≡C-H), 1.81–1.72 (m, 8H, OCH₂CH₂), 1.48–1.44 (m, 4H), 1.43–1.37 (m, 4H), 1.33–1.16 (m, 48H), 0.87 (t, *J* = 6.5 Hz, 6H, CH₃), 0.83 (t, *J* = 7.0 Hz, 6H, CH₃); ¹³C NMR (CDCl₃, 125 MHz) δ 154.4, 153.7 (two Ar-O carbons), 147.9, 147.7 (two Ar-N carbons), 137.6, 131.6, 130.1, 129.5, 128.6, 128.0, 124.8, 124.3, 123.44, 123.41, 122.5, 118.3, 117.0, 114.9, 113.1 (19 aromatic and alkenyl carbon signals), 93.7, 92.3, 82.6, 80.2 (four alkynyl carbon signals), 70.1, 69.7 (two OCH₃), 32.12, 32.09, 29.8, 29.6, 29.4, 29.2, 26.2, 22.9, 14.3 (CH₃); MALDI-TOF MS *m/z* calcd for C₁₀₆H₁₂₄N₂O₄ 1489.96, found 1490.41 [M]⁺.

1,4-Bis(*E*-4-*N,N*-diphenylaminostyryl)-2,5-bis(2,5-bis(decyloxy)-4-(2,5-bis(decyloxy)-4-triisopropylsilylethynylphenylethynyl)phenylethynyl)benzene (239). Compound **234** (90 mg, 0.10 mmol), **226** (215 mg, 0.213 mmol), PdCl₂(PPh₃)₂ (14 mg, 0.020 mmol), and CuI (8 mg, 0.04 mmol) were added to Et₃N (15 mL). The solution was bubbled by N₂ at rt for 5 min and then stirred at 45 °C under N₂ protection for 24 h. After the reaction was complete as checked by TLC analysis, the solvent was removed by rotary evaporation. To the residue obtained was diluted with chloroform, and the mixture was filtered through a MgSO₄ pad. The resulting solution was sequentially washed by aq HCl (10%) and brine. The organic layer was dried over MgSO₄ and concentrated under vacuum. The crude product was then purified by silica flash column chromatography (hexanes/CH₂Cl₂, 3:1) to yield compound **239** (126 mg, 0.0479 mmol, 46%) as a pale yellow wax. IR (KBr) 2925, 2856, 2150, 1625, 1593, 1509, 1494 cm⁻¹; ¹H NMR (CDCl₃, 500 MHz) δ 7.90 (s, 2H, central Ar-H), 7.66 (d, *J* = 17.0 Hz, 2H, C=C-H), 7.47 (d, *J* = 9.5 Hz, 4H, Ar-H), 7.28 (t, *J* = 8.0 Hz, 8H, NPh-H), 7.23 (d, *J* = 15.5 Hz, 2H, C=C-H), 7.13 (d, *J* = 7.5 Hz, 8H, NPh-H), 7.07–7.04 (m, 10H, NPh-H, Ar-H, and C=C-H), 6.96 (s, 2H, Ar-H), 6.95 (s, 2H, Ar-H), 4.06–4.03 (m, 12H, OCH₂), 3.98 (t, *J* = 7.0 Hz, 4H, OCH₂), 1.85–1.76 (m, 16H, OCH₂CH₂), 1.52–1.40 (m, 16H), 1.39–1.17 (m, 120H), 0.92–0.82 (m, 24H, CH₃); ¹³C NMR (CDCl₃, 125 MHz) δ 154.8, 154.1, 154.0, 153.7 (four Ar-O carbon signals), 148.1, 147.9, 137.7, 131.9, 130.2, 129.7, 128.8, 128.2, 125.0, 124.6, 123.7, 123.6, 122.7, 118.5, 117.7, 117.5, 117.0, 115.1, 114.8, 114.5, 114.4 (19 aromatic and two olefinic carbon signals are all discernible), 103.5, 96.9, 94.0, 92.7, 92.2, 91.7 (six alkynyl carbon signals), 70.3, 70.24, 70.18, 69.7 (four OCH₂), 32.3, 30.09, 30.06, 30.03, 29.99, 29.95, 29.9, 29.79, 29.75, 29.7, 26.7, 26.43, 26.41, 23.1, 19.2 (*i*-Pr), 14.5

(CH₃), 11.8 (*i*-Pr); MALDI-TOF MS *m, z* calcd for C₁₈₀H₂₅₂N₂O₈Si₂ 2626.89, found 2628.57 [M + H]⁺.

1,4-Bis(*E*-4-*N,N*-diphenylaminostyryl)-2,5-bis(2,5-bis(decyloxy)-4-(2,5-bis(decyloxy)-4-ethynylphenylethynyl)phenylethynyl)benzene (240). To a solution of compound **239** (20 mg, 0.076 mmol) in THF (10 mL) was added TBAF (0.05 mL, 1M in THF, 0.05 mmol). The mixture was stirred at rt for 12 h, then the reaction solvent was removed by rotary evaporation. The residue was diluted with chloroform and then was sequentially washed by aq HCl (10%) and brine. The organic layer was dried over MgSO₄ and concentrated under vacuum. The crude product was then purified by silica flash column chromatography (hexanes, CH₂Cl₂, 7:3) to yield compound **240** (14 mg, 0.0060 mmol, 80%) as a pale yellow wax. IR (KBr) 2924, 2853, 2205, 2104, 1631, 1593, 1510, 1494 cm⁻¹; ¹H NMR (CDCl₃, 500 MHz) δ 7.91 (s, 2H, central Ar-H), 7.66 (d, *J* = 17.5 Hz, 2H, C=C-H), 7.47 (d, *J* = 8.5 Hz, 4H, Ar-H), 7.27 (t, *J* = 7.0 Hz, 8H, NPh-H), 7.23 (d, *J* = 15.5 Hz, 2H, C=C-H), 7.13 (d, *J* = 8.0 Hz, 8H, NPh-H), 7.07–7.03 (m, 10H, NPh-H, Ar-H, and C=C-H), 7.01 (s, 2H, Ar-H), 6.99 (s, 2H, Ar-H), 4.06–4.00 (m, 16H, OCH₂), 3.35 (s, 2H, alkynyl H), 1.87–1.75 (m, 16H, OCH₂CH₂), 1.55–1.42 (m, 16H), 1.40–1.18 (m, 120H), 0.91–0.82 (m, 24H, CH₃); ¹³C NMR (CDCl₃, 125 MHz) δ 154.4, 153.9, 153.8, 153.6 (four Ar-O carbon signals), 147.9, 147.7, 137.5, 131.7, 130.1, 129.5, 128.6, 128.0, 124.8, 124.4, 123.5, 123.4, 122.5, 118.3, 117.6, 117.3, 115.2, 114.7, 114.4, 112.9 (20 signals out of 19 aromatic and two olefinic carbon signals are discernible, one coincidental peak missing), 93.8, 92.4, 91.8, 91.6, 82.5, 80.3 (six alkynyl carbon signals), 70.04, 70.01, 69.97, 69.8 (four OCH₂), 32.13, 32.11, 29.89, 29.85, 29.83, 29.79, 29.7, 29.64, 29.61,

29.58, 29.55, 29.51, 29.44, 26.23, 26.19, 22.9, 14.3 (CH₃); MALDI-TOF MS *m/z* calcd for C₁₆₂H₂₁₂N₂O₈ 2314.6, found 2316.1 [M + H]⁺.

4-(4-(Dec-1-ynyl)-2,5-bis(decyloxy)phenyl)-2-methylbut-3-yn-2-ol (241).

Compound **232** (266 mg, 0.444 mmol), dec-1-yne (92 mg, 0.12 mL, 0.67 mmol), PdCl₂(PPh₃)₂ (15 mg, 0.022 mmol), CuI (8.4 mg, 0.044 mmol) and Et₃N (10 mL) were added to THF (10 mL). The solution was bubbled by N₂ at rt for 5 min and then stirred at rt under N₂ protection for 6 h. After the reaction was complete as checked by TLC analysis, the solvent was removed by rotary evaporation. To the residue obtained was added CH₂Cl₂. The mixture was filtered through a MgSO₄ pad. Then it was sequentially washed by aq HCl (10%) and brine. The organic layer was dried over MgSO₄ and concentrated under vacuum. The crude product was then purified with silica flash column chromatography (hexanes/EtOAc, 90:10) to yield compound **241** (232 mg, 0.381 mmol, 86%) as a light yellowish solid. Mp 64–65 °C; IR (KBr) 3432, 2955, 2920, 2852, 2233, 1638, 1618, 1533, 1505, 1468, 1412, 1392 cm⁻¹; ¹H NMR (CDCl₃, 500 MHz) δ 6.84 (s, 2H, Ar-H), 3.93 (t, *J* = 6.5 Hz, 4H), 2.53 (s, 1H, OH), 2.47 (t, *J* = 7.0 Hz, 2H), 1.80–1.74 (m, 4H), 1.63 (s, 6H), 1.49–1.45 (m, 6H), 1.31–1.28 (m, 34H), 0.90–0.88 (m, 9H); ¹³C NMR (CDCl₃, 125 MHz) δ 153.7, 153.6 (two Ar-O carbons), 117.4, 117.3, 115.1, 112.6 (four Ar carbons), 98.9, 96.1, 78.7, 76.9 (four alkynyl carbons), 69.7, 69.6 (two OCH₂ carbons), 65.8 (one OC(CH₃)₂ carbon), 32.09, 32.07, 31.6, 29.84, 29.80, 29.77, 29.75, 29.6, 29.57, 29.50, 29.49, 29.42, 29.4, 29.1, 29.0, 26.19, 26.17, 22.8, 19.9, 14.2; APCI-MS *m/z* calcd. for C₄₁H₆₈O₃ 608.52, found 609.4 [M + H]⁺.

1-(Dec-1-ynyl)-2,5-bis(decyloxy)-4-ethynylbenzene (242). To a solution of compound **241** (211 mg, 0.347 mmol) in toluene (20 mL) was added NaOH (50 mg, 1.3 mmol). After being stirred at reflux for 16 h, the solvent was removed by rotary evaporation. The residue was dissolved in CH₂Cl₂ and sequentially washed by aq HCl (10%) and brine. The organic layer was dried over MgSO₄. Filtration to remove MgSO₄ followed by evaporation under vacuum afforded the crude product. The crude product was purified with silica flash column chromatography (hexanes/CH₂Cl₂, 70:30) to yield compound **242** (171 mg, 0.311 mmol, 90%) as a light yellowish solid. Mp 42–44 °C; IR (KBr) 3290, 2955, 2925, 2869, 2851, 2237, 2107, 1627, 1535, 1502, 1469, 1429, 1406, 1389 cm⁻¹; ¹H NMR (CDCl₃, 500 MHz) δ 6.93 (s, 1H, Ar-H), 6.88 (s, 1H, Ar-H), 3.98–3.93 (m, 4H, OCH₂), 3.30 (s, 1H), 2.46 (t, *J* = 7.0 Hz, 2H), 1.82–1.77 (m, 4H), 1.66–1.58 (m, 2H), 1.49–1.44 (m, 6H), 1.33–1.29 (m, 34H), 0.91–0.88 (m, 9H); ¹³C NMR (CDCl₃, 125 MHz) δ 154.4, 153.6 (two Ar-O carbons), 118.0, 117.4, 115.8, 111.8 (four Ar carbons), 96.5, 81.9, 80.3, 76.8 (four alkynyl carbons), 69.85, 69.80 (two OCH₂ carbons), 32.1, 29.86, 29.81, 29.78, 29.75, 29.6, 29.56, 29.54, 29.53, 29.5, 29.40, 29.38, 29.2, 29.0, 26.2, 26.1, 22.9, 20.0, 14.3; APCI-MS *m/z* calcd. for C₃₈H₆₂O₂ 550.47, found 551.4 [M + H]⁺.

Chapter 3

Synthesis and Solid-State Properties of C₆₀ Endcapped Oligoynes

3.1 Introduction

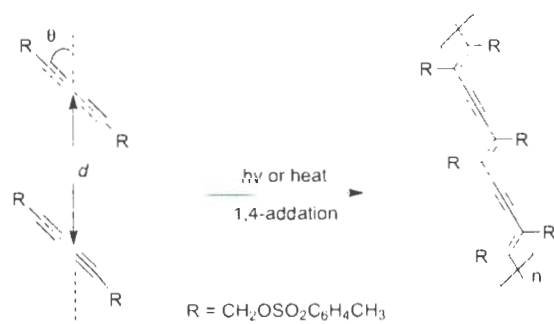
Solid-state polymerization, commonly induced by ionizing radiations (X- and γ -rays) or other energetic conditions such as heat, pressure, and UV irradiation, constitutes a powerful synthetic approach to produce novel macromolecular structures.^{300,301} According to the starting monomers and polymerization conditions applied, the structural uniqueness of the products from solid-state polymerization reactions can be manipulated at three different levels, that is, morphological, crystallographic, and molecular.³⁰⁰ The first report on radiation-induced solid-state polymerization was presented by Schmitz and Lawton in 1951, describing the formation of a polymeric product from solid ethylene glycol dimethacrylate through irradiation with electron beams.³⁰² Numerous investigations ensued from this discovery afterwards, which

have greatly fueled the development of this research topic. A couple of early milestones in this area include: the irradiation-induced solid-state polymerization of acrylamide studied by Mesrobian *et al.*³⁰³ and Henglein *et al.*,³⁰⁴ the polymerization of hexamethylcyclotrisiloxane in the solid state scrutinized by Lawton, Grubb and Balwit,³⁰⁵ and the investigation of several vinyl monomers undertaken by Restaino *et al.*³⁰⁶ in respect to their solid-state polymerization behavior.

So far there are a variety of organic compounds which have been found with intriguing solid-state polymerization reactivities. Among them, conjugated polyynes and oligoynes are a class of substrates particularly useful for generating novel conjugated materials in the solid phase or at interfaces. Generally, solid-state polymerization of oligoynes can be induced by external incentives such as moderate heating or UV-Vis irradiation, owing to the high reactivity of conjugated C≡C bonds.^{307,308} Also, the structures and morphology of the products of oligoyne polymerization are tied to the orientation and packing geometry of the oligoyne molecules before polymerization. Functional groups that are capable of directing the solid-state packing of oligoynes, *e.g.*, through hydrogen bonding and π - π stacking, have been widely used to pre-organize oligoynes for this purpose.³⁰⁹ Furthermore, the use of surfactants, templates, and other mechanisms can also exert some control over the polymerization of oligoynes in the solid state.

Conjugated 1,3-butadiynes, also called diacetylenes, have received the most intensive investigations among other conjugated oligoynes or polyynes due to the abundant availability of diyne precursors and easy controllability over polymerization outcomes.^{310,311} The interest in polymerization of diacetylenes began by Wegner's pioneering work about two and a half decades ago, wherein Wegner first identified the

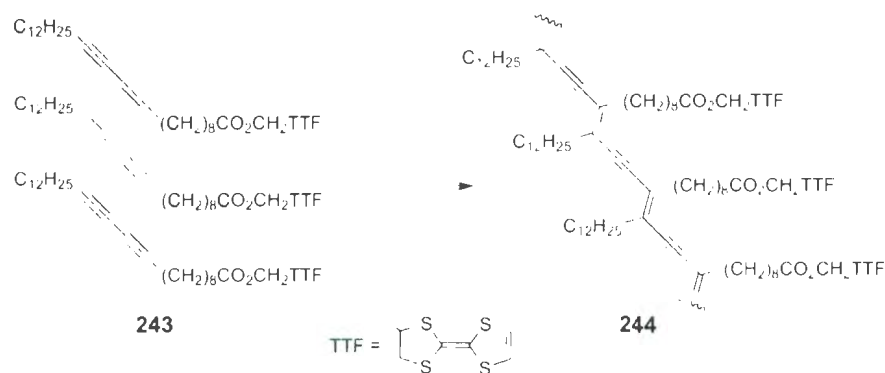
polymerization of a diacetylene containing $\text{CH}_2\text{OSO}_2\text{C}_6\text{H}_4\text{CH}_3$ as a topochemically controlled 1,4-addition reaction³¹² (see Scheme 3.1). Note that a special term *topochemically* was used here, because when the monomeric diynes in the crystal are packed in an appropriate geometry—that is, the distance d and the angle θ are about 5 Å and 45° respectively—the single crystal of diynes can be polymerized into the single crystal of poly(diacetylene)s (PDAs) in its entirety. Due to the unique one-dimensional orientation and highly polarizable conjugated π -electron density, PDAs produced from this topochemical reaction have demonstrated great potential in photovoltaic³¹³ and NLO materials.^{314,315}



Scheme 3.1: Topochemical 1,4-addition of conjugated diacetylenes discovered by Wegner.

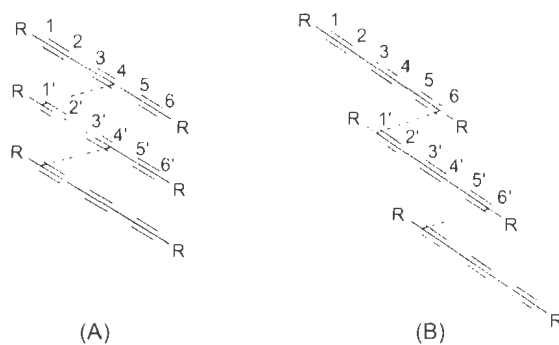
In order to control and modify the electronic and optical properties of PDA materials, a strategy of attaching various functional side chains (such as aryl, alkynyl groups and heteroatoms) to the terminal *sp* carbons of diacetylene monomers have been explored.^{316–318} For instance, Shimada and co-workers prepared a diacetylene derivative **243** bearing TTF groups in one of the two terminal substituents in 1995 (Scheme 3.2). Such a molecular design features both a conjugated diyne main chain

and an electron-donating side chain. When the light yellow crystal of **243** was subjected to UV irradiation generated by a low-pressure mercury lamp or a γ -ray bombardment emanating from ^{60}Co , a dark blue crystal of polymer **244** was obtained. Such kind of electroactive PDAs were expected by the authors to show interesting electronic and optical properties. In particular, the excellent electron-donating ability imparted by the TTF groups may lead to highly conductive charge-transfer complexes, which under controlled conditions can achieve superconductivity.³¹⁹



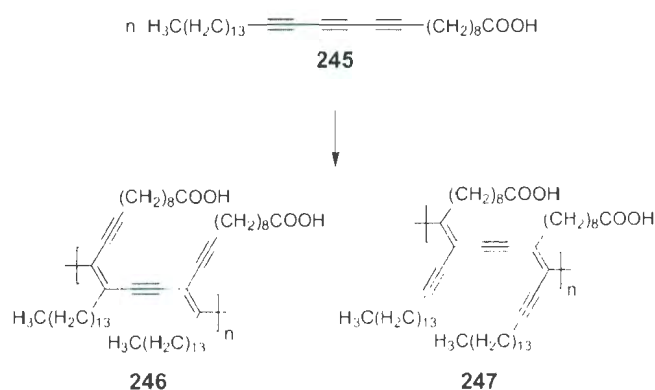
Scheme 3.2: TTF appended PDA **244** synthesized via a topochemical 1,4-addition reaction by Shimada.

Conjugated oligoynes longer than diacetylenes (*e.g.* 1,3,5-hexatriynes and 1,3,5,7-octatetraynes) can lead to highly extended poly(enyne) frameworks with enhanced conjugation and rich π -electronic characteristics. However, control over the structure of the polymeric products resulting from long oligoynes tends to be much more difficult than that of diynes, since a multitude of polymerization pathways may be involved. For example, the solid of triynes $\text{R}(\text{C}\equiv\text{C})_3\text{R}$ can be polymerized via either a 1,4-addition or a 1,6-addition motif, or a combination of both as shown in Scheme 3.3.³⁰⁰



Scheme 3.3: Two possible polymerization pathways for conjugated triynes. (A) 1,4-addition; (B) 1,6-addition.

In 1991, Okada and co-workers prepared a long-alkyl substituted triyne **245**. By means of solid-state ^{13}C NMR spectroscopy, 1,4-addition was identified as the major reaction pathway for the topochemical polymerization of **245**, and two novel PDA products **246** and **247** were obtained (Scheme 3.4).³²⁰



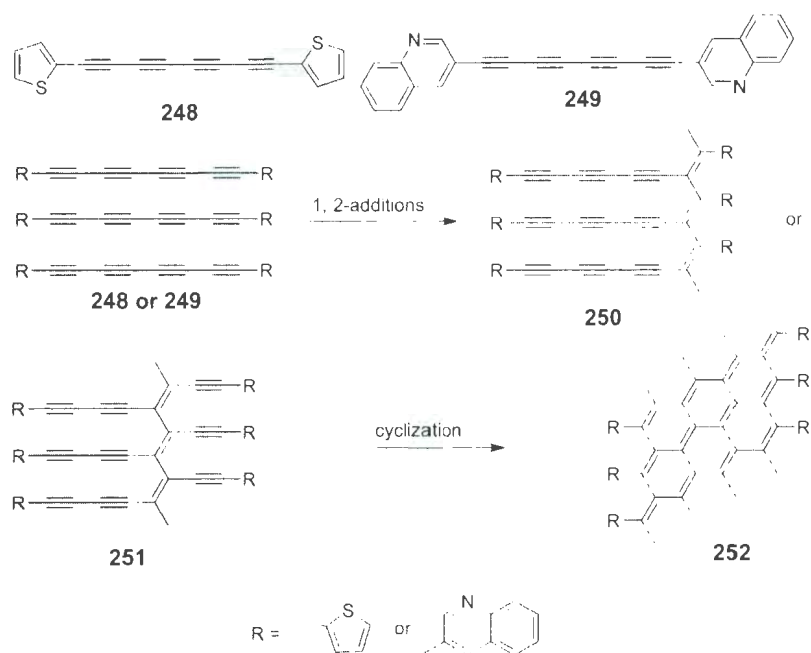
Scheme 3.4: Topochemical 1,4-addition of conjugated triyne **245** reported by Okada.

The possible pathways for topochemical polymerization of conjugated tetraynes are numerous, including 1,4-, 1,6-, 1,8-, 3,6-additions and other possibilities. Which of

these pathways would prevail? The answer is dependent on the packing geometry with which tetrayne molecules are oriented in a particular phase, as the geometry is directly related to the atom displacements involved in the polymerization. In 1998, Hakanishi and co-workers prepared two octatetraynes **248** and **249** which are directly linked to aromatic side groups.³²¹ The bright yellow colored crystalline solids of **248** and **249** reacted in the solid state at 150 and 198 °C, respectively, to afford polymers within a few minutes, as revealed by thermal studies based on differential scanning calorimetry (DSC) and differential thermal analysis/thermogravimetric analysis (DTA/TGA). X-ray diffraction analysis indicates that the resulting polymers are largely amorphous. X-ray crystallographic data show that **248** are packed in parallel stacks with $d = 3.9 \text{ \AA}$ and $\theta = 71^\circ$, a geometry not suitable for a 1,4-addition reaction. FT-IR and solid state ^{13}C NMR spectroscopic data also corroborate that there are no acetylenic moieties present in the products. Based on the acquired experimental data, the authors proposed a mechanism involving first a 1,2-addition followed by cyclization for the polymerization process, which yielded an irregular cycloaromatized polymeric structure **252**.³²¹

Despite the increasing body of knowledge on the solid-state polymerization of aryl and alkyl functionalized oligoynes, the use of C_{60} endcapped oligoynes remains unexplored; in particular, to our best knowledge, there had been no precedent of using C_{60} functionalized oligoynes to make C_{60} -containing polymer materials through solid-state polymerization, prior to the work conducted in this chapter.

Recently, there is a growing interest in the preparation of C_{60} -containing polymers. When a suitable amount of C_{60} moieties are integrated into a polymer matrix, a number of optoelectronic properties (*e.g.* photoconductivity, optical limiting,

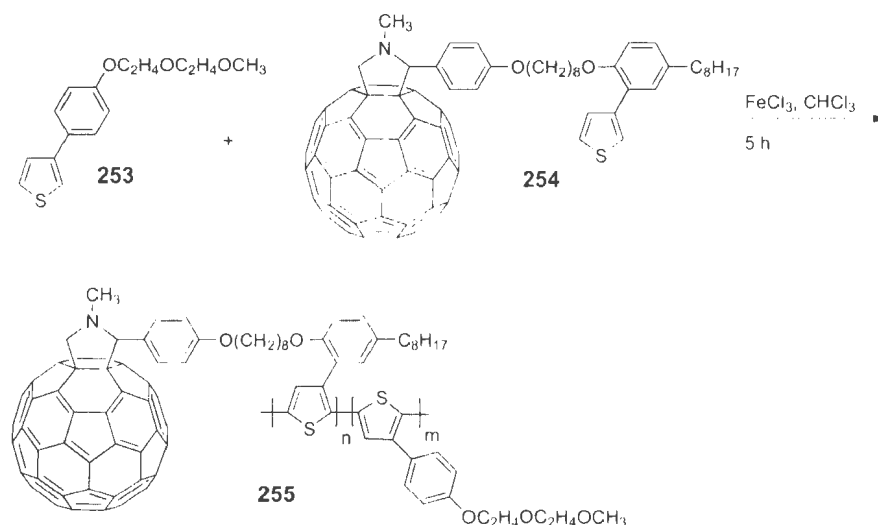


Scheme 3.5: Double 1,2-additions of tetraynes **248** and **249** reported by Hakanishi *et al.*

etc.) of the polymers can be substantially enhanced.^{322,323} In the meantime, the drawbacks of using pristine C₆₀ in large-scale applications, such as insolubility and low compatibility, can be readily overcome by the presence of soluble polymer components.³²⁴⁻³²⁷ It has been reported that conjugated polymer-C₆₀ composites can give rise to very good photoconductivity, as a result of intimate association of donors and acceptors in the photoconductive domain.³²²

Zhang and co-workers recently investigated a class of C₆₀ functionalized polythiophene derivatives.³²⁸ In their work, soluble conjugated copolymer **255** was obtained from co-polymerization of two monomers, **253** and **254** (Scheme 3.6). Because of the solubilizing ether side chains, the copolymer showed very good

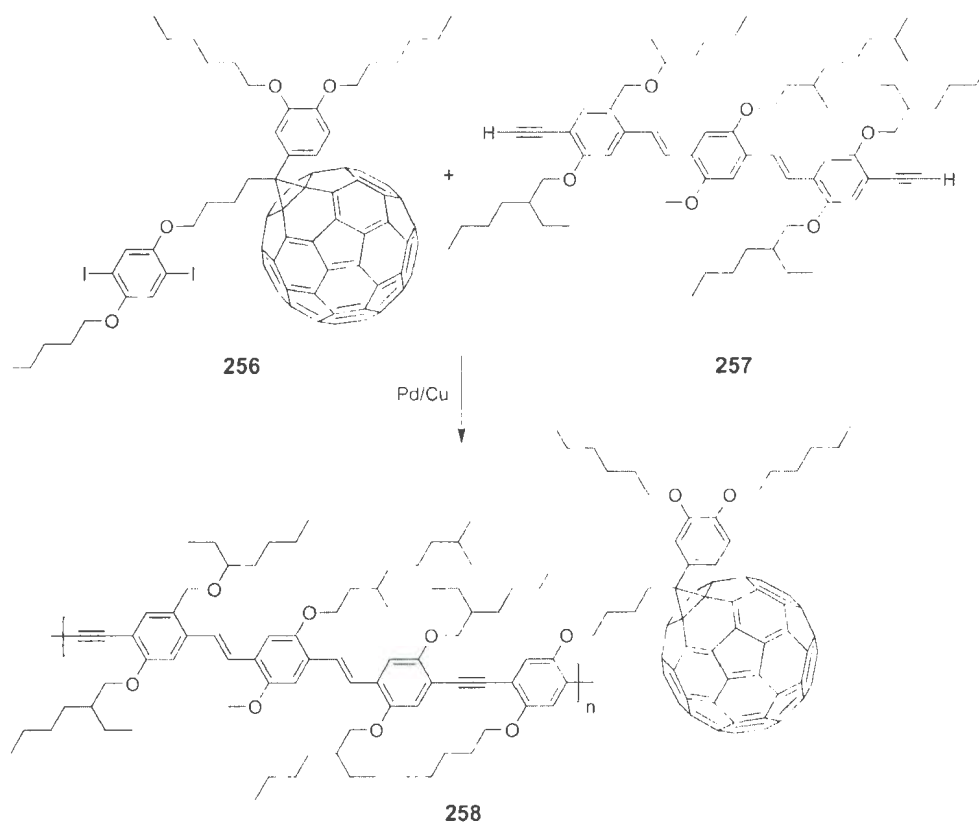
processability for device applications. Photodiodes prepared by spin-coating the solution of this copolymer in chloroform were characterized to function as rectifying junctions. In addition, the photodiodes showed extended spectral coverage up to 700 nm, although the external quantum efficiencies were moderate.



Scheme 3.6: Preparation of C₆₀-containing poly(thiophene)s **255** by Zhang *et al.*

Ramos *et al.* prepared a processable π -conjugated polymer **258** through Sonogashira coupling of C₆₀-containing diiodobenzene **256** and terminal alkyne substituted oligo(*p*-phenylenevinylene) **257** (Scheme 3.7).³²⁹ With this polymer, a plastic solar cell was fabricated, in which the donor domain was constituted by π -conjugated phenylenevinylene chains, the C₆₀ groups covalently linked to the polymer backbone functioned as the acceptor. The authors claimed that photoexcitation of this C₆₀-containing polymer resulted in an electron-transfer reaction from the conjugated backbone to the pendant C₆₀ moiety. This type of C₆₀ bearing polymers form bicontinuous networks of donors and acceptors that are confined to a molecular

scale. As such, the troublesome phase segregation or clustering phenomena as commonly observed in the blends of polymers and pristine C_{60} can be avoided. The successful testing of polymer **258** in solar cell devices thus opened a new avenue for the design of efficient organic photovoltaic materials.³²⁹



Scheme 3.7: Preparation of C_{60} -containing conjugated polymer **258** by Ramos *et al.*

In view of the current trends in oligoyne solid-state chemistry and C_{60} -containing polymer materials, as well as armed with the success in synthesizing C_{60} -OPE, OPV- C_{60} derivatives described in Chapter 1, we subsequently set out a quest for another class of rigid, dumbbell-shaped bisfullerene adducts **259-261**, in which the central

π -bridging units are made up of conjugated oligoynes (diyne, tetrayne, and hexayne) (see Figure 3.1). In addition, a series of star-shaped tetrafullerene adducts **262** that consist of a central oligoyne linkage was pursued in our work (Figure 3.2). For all the target compounds in this chapter, the exceptional solid-state reactivity of oligoynes is envisioned to provide a new dimension to generate novel C_{60} -appended carbon-rich poly(enyne) frameworks. Detailed synthesis and solid-state properties of these new compounds are described in the following context.

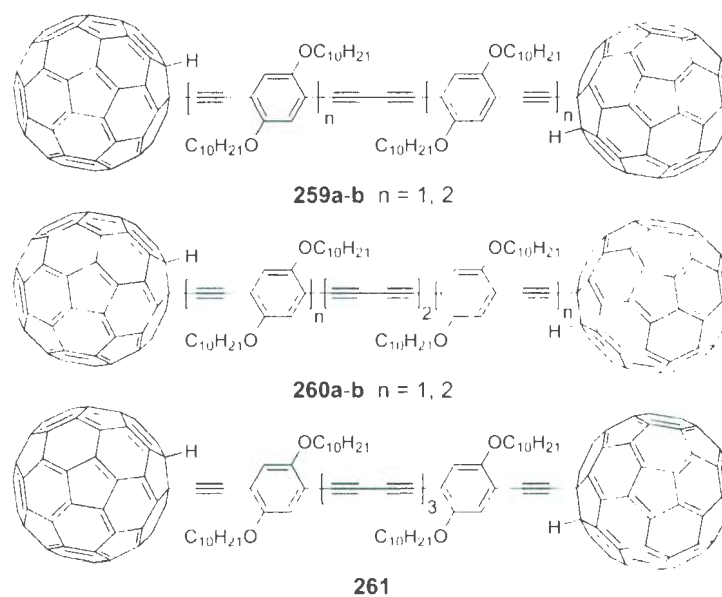


Figure 3.1: Target bisfullerene-oligoyne molecular dumbbells **259**, **260** and **261** in this chapter.

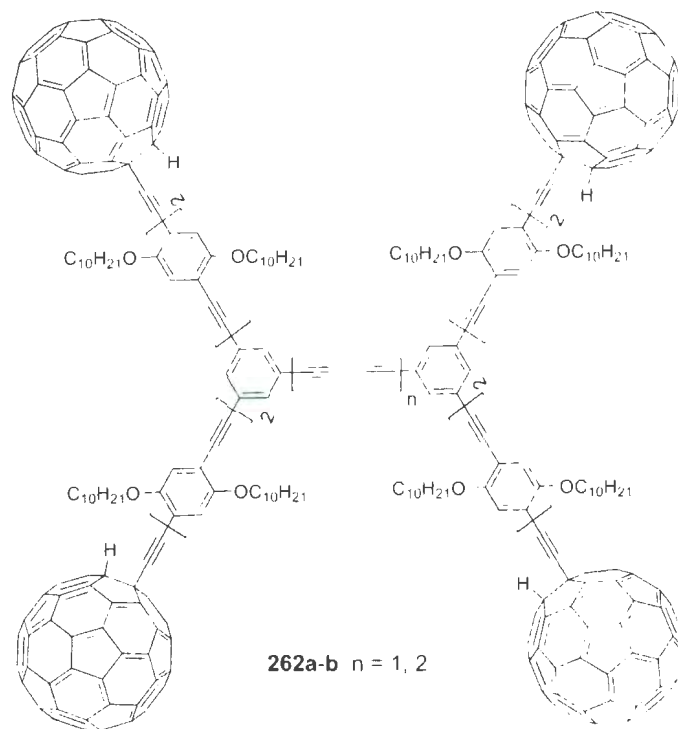


Figure 3.2: Target star-shaped tetrafullerene-oligoyne adducts **262** in this chapter.

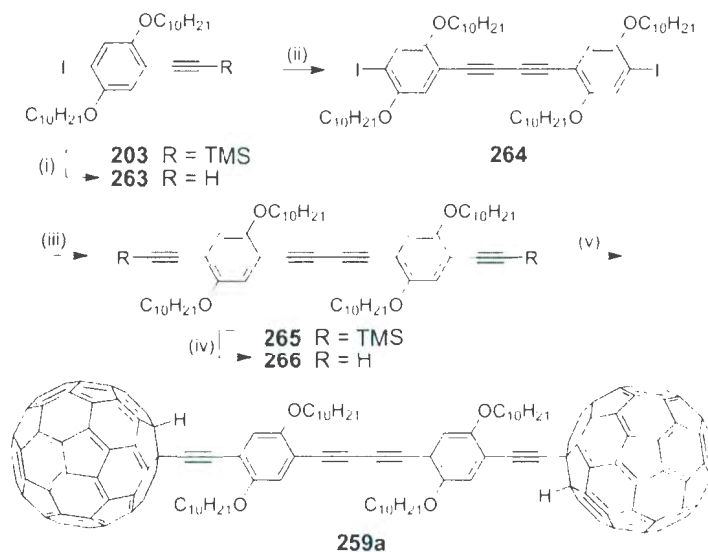
3.2 Results and discussion

3.2.1 Synthesis of C_{60} -oligoyne adducts

3.2.1.1 Butadiyne-bridged $C_{60} \pi C_{60}$ molecular dumbbells

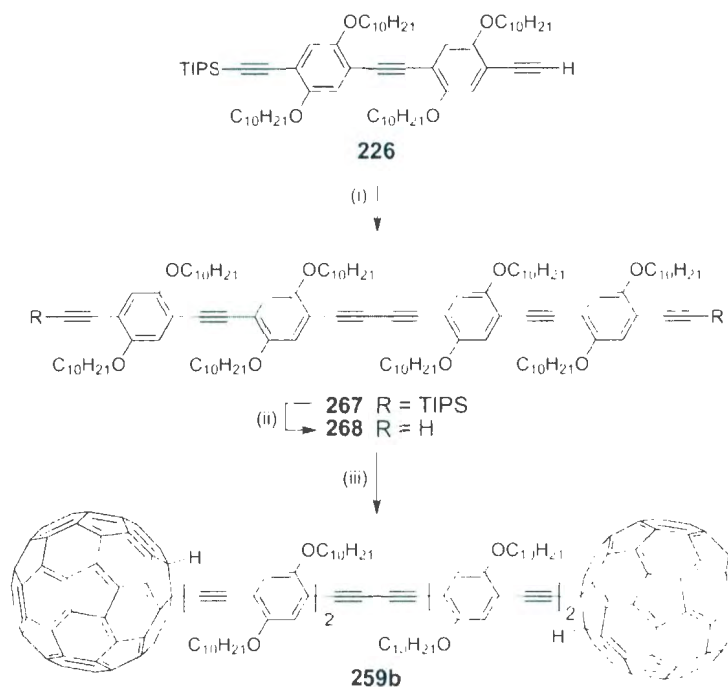
The synthesis of butadiyne-bridged $C_{60} \pi C_{60}$ molecular dumbbell **259a** is outlined in Scheme 3.8. Desilylation of compound **203** with K_2CO_3 afforded terminal alkyne **263** in 99% yield. Hay coupling of **263** generated butadiyne **264** with a yield of 75%. Treating **264** with TMSA under the catalysis of Pd-Cu yielded compound **265**, which was subsequently converted into terminal diyne **266** via protodesilylation. Compound **266** was subjected to an *in situ* ethynylation with C_{60} using LHMDS as the base.

followed by TFA quenching, which provided the target C_{60} diyne C_{60} dumbbell **259a** in 24% yield.



Scheme 3.8: Synthesis of C_{60} diyne C_{60} dumbbell **259a**. Reagents and conditions: (i) K_2CO_3 , CH_3OH , THF, 99%; (ii) $CuCl/TMEDA$, air, acetone, 75%; (iii) TMSA, $PdCl_2(PPh_3)_2$, CuI , Et_3N , THF, 86%; (iv) K_2CO_3 , CH_3OH , THF, 96%; (v) C_{60} , LHMDS, THF then TFA, 24%.

In a similar manner, a longer C_{60} diyne C_{60} dumbbell **259b** was prepared through the synthetic route shown in Scheme 3.9. The synthesis commenced with a Hay homocoupling of **226** to give diyne **267** in 43% yield. Removal of the TIPS groups in **267** with TBAF gave oligomer **268**, which was then converted into target compound **259b** via an *in situ* alkylation reaction as described above.



Scheme 3.9: Synthesis of C_{60} diyne C_{60} dumbbell **259b**. Reagents and conditions: (i) CuCl/TMEDA , air, acetone, 43%; (ii) TBAF , THF, 82%; (iii) C_{60} , LHMDS , THF then TFA , 33%.

3.2.1.2 Hexatriyne-bridged $\text{C}_{60}-\pi-\text{C}_{60}$ molecular dumbbells

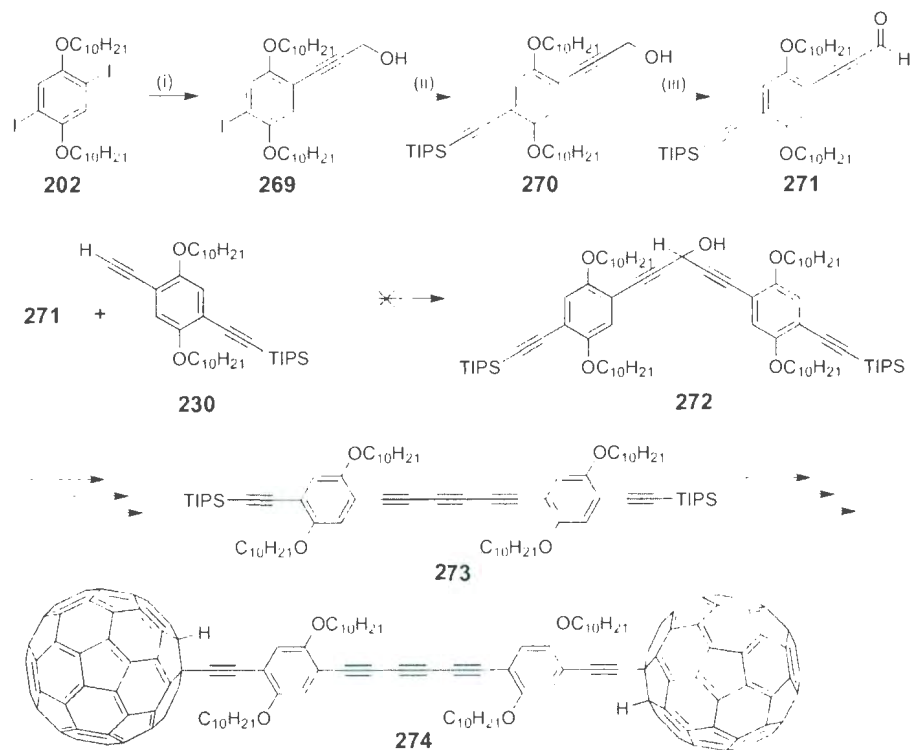
Subsequent to the success in preparing butadiyne-bridged C_{60} dumbbells, the synthesis of homologous hexatriyne-bridged dumbbells was explored. Scheme 3.10 depicts the preliminary efforts to synthesize this type of compounds. Unlike the oligoynes with an even number of conjugated $\text{C}\equiv\text{C}$ bonds, triynes or other oligoynes with an odd number of $\text{C}\equiv\text{C}$ bonds turn out to be more challenging to prepare, since oxidative homocoupling reactions are of no or quite limited use in the synthesis.

In this work, a triyne precursor **273** was first targeted and it was planned to be made by using a modified Fritsch-Buttenberg-Wiechell rearrangement protocol

recently developed by Tykwinski's group¹⁴¹⁻¹⁴³ (see Scheme 3.10). Starting from diiodoarene **202**, aldehyde **271** was readily prepared through two steps of selective cross couplings and a Swern oxidation. Compound **271** was then expected to react with **230** under basic conditions to afford intermediate **272**. However, after numerous attempts employing different bases such as LDA, LHMDS, EtMgBr, BuLi, this seemingly straightforward reaction failed to yield the desired product **272**, despite that nucleophilic additions of this kind have been abundantly reported in the literature. A possible reason for our misfortune here could be grounded on the significant steric hindrance exerted by the long alkyl chains adjacent to the aldehyde group in **271**, which impeded the acetylide anion from attacking the carbonyl group. The difficulty in obtaining intermediate **272** thus temporarily thwarted the efforts to acquire the target C₆₀-triyne-C₆₀ dumbbell **274** in this thesis work. Nonetheless, there are no major flaws in the designed synthetic strategy, and it is envisioned that some structural modifications, *e.g.* using shorter alkyl chains, should adequately address the problem in the future work.

3.2.1.3 Octatetrayne-bridged C₆₀- π -C₆₀ molecular dumbbells

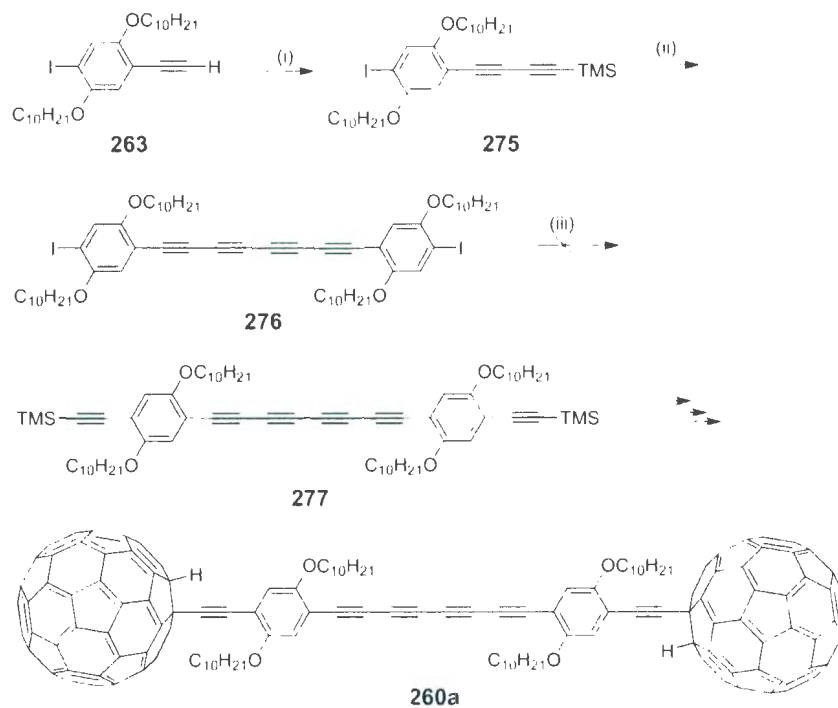
In this work, a bisfullerene-encapped linearly conjugated 1,3,5,7-octatetrayne **260a** was first targeted, and the initial synthetic route to it is outlined in Scheme 3.11. Herein tetrayne **277** was planned to be the essential precursor to the target molecule. To make it, compound **275** was first prepared via a Hay coupling between the terminal alkyne **263** with excess TMSA. Desilylation of **275** followed by another Hay coupling afforded the desired diiodo tetrayne **276**. With compound **276** in hand, tetrayne **277** was expected to be readily prepared by a Sonogashira coupling with TMSA.



Scheme 3.10: Attempted synthesis of C_{60} triyne C_{60} dumbbell **274**. Reagents and conditions: (i) propargyl alcohol, $PdCl_2(PPh_3)_2$, CuI , Et_3N , THF, 56%; (ii) TIPS, $PdCl_2(PPh_3)_2$, CuI , Et_3N , THF, 100%; (iii) oxalyl chloride, DMSO, CH_2Cl_2 then Et_3N , 80%.

However, this coupling reaction conducted under typical Sonogashira conditions (*i.e.* $Pd(PPh_3)_2Cl_2 \cdot CuI$ in a mixture of Et_3N and THF) only resulted in an intractable mixture rather than the desired product. The synthetic effort for compound **260a** was therefore quickly diverted to another route.

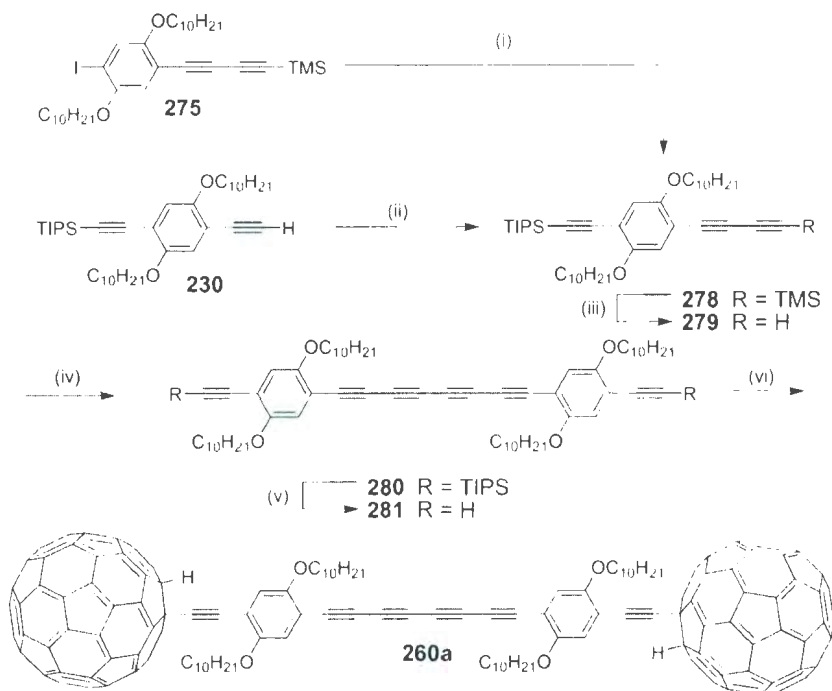
In Scheme 3.12, a diyne building block **278** was first prepared from either compound **275** or compound **230**. Selective removal of the TMS group in **278** with K_2CO_3 followed by a Hay coupling afforded tetrayne **280**. Compound **280**



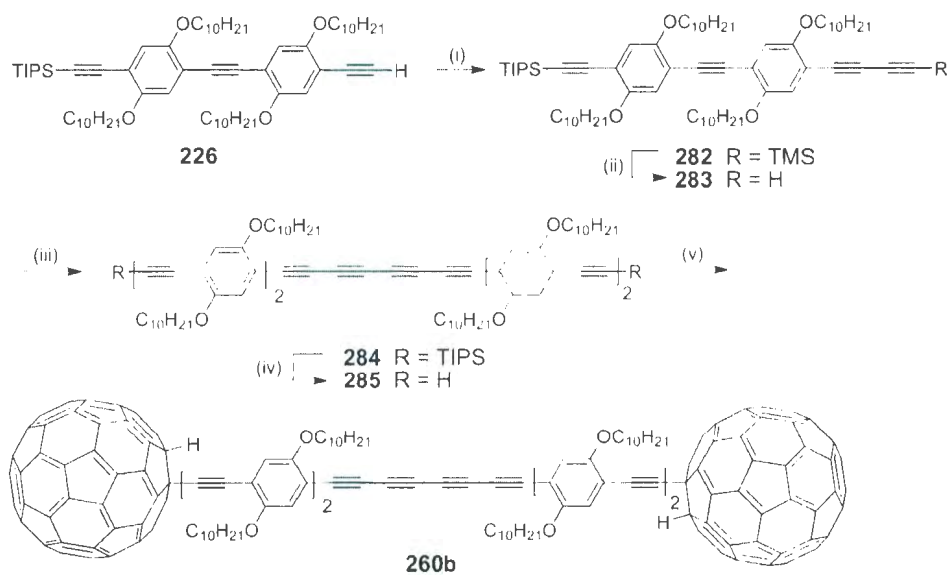
Scheme 3.11: Attempted synthesis of C₆₀ tetrayne C₆₀ dumbbell **260a**. Reagents and conditions: (i) TMSA, CuCl·TMEDA, air, acetone, 68%; (ii) (a) K₂CO₃, CH₃OH, THF, (b) CuCl·TMEDA, air, acetone, 53%; (iii) TMSA, PdCl₂(PPh₃)₂, CuI, Et₃N, THF.

was desilylated with TBAF gave compound **281**, which was subjected to an *in situ* alkylation with C₆₀ to successfully yield target compound **260a** in 31% yield.

Using a strategy similar to above, another tetrayne-bridged dumbbell **260b** containing further extended phenylacetylene segments was prepared as shown in Scheme 3.13.



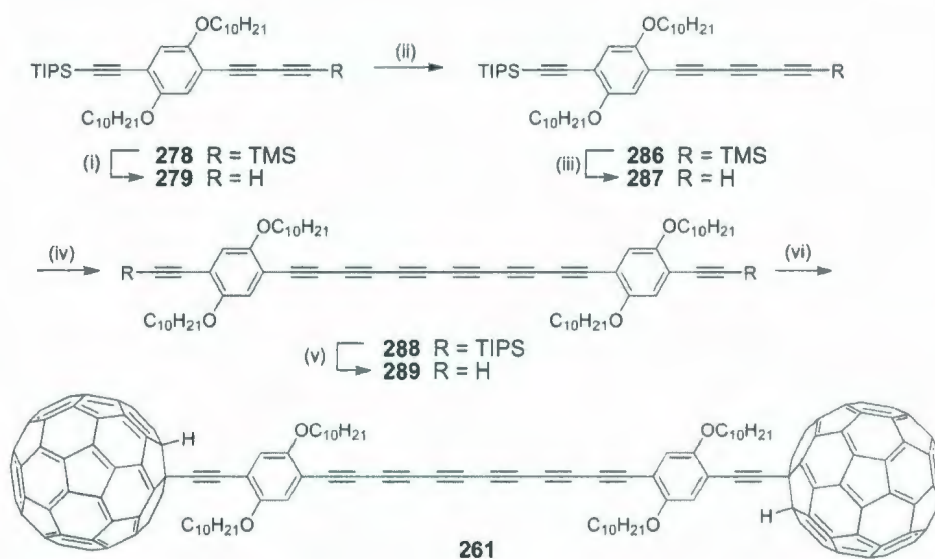
Scheme 3.12: Synthesis of C_{60} tetrayne C_{60} dumbbell **260a**. Reagents and conditions: (i) TIPSA, $\text{PdCl}_2(\text{PPh}_3)_2$, CuI , Et_3N , THF, 86%; (ii) TMSA, CuCl/TMEDA , air, acetone, 71%; (iii) K_2CO_3 , CH_3OH , THF; (iv) CuCl/TMEDA , air, acetone, 53% from **278** to **280**; (v) TBAF, THF, 77%; (vi) C_{60} , LHMDS, THF then TFA, 31%.



Scheme 3.13: Synthesis of long C_{60} tetrayne C_{60} dumbbell **260b**. Reagents and conditions: (i) TMSA, CuCl/TMEDA, air, acetone, 79%; (ii) K_2CO_3 , CH_3OH , THF, (iii) CuCl/TMEDA, air, acetone, 85% over two steps; (iv) TBAF, THF, 83%; (v) C_{60} , LHMDS, THF then TFA, 35%.

3.2.1.4 Dodecahexayne-bridged $C_{60}-\pi-C_{60}$ molecular dumbbells

The use of oligoynes longer than tetraynes to bridge bisfullerene dumbbells was also explored in this thesis work, although the increasing instability of higher oligoynes was anticipated as a potential trouble beforehand. Outlined in Scheme 3.14 is the synthesis of a C_{60} hexayne C_{60} dumbbell **261**. Through two iterative desilylation and oxidative Hay coupling processes, hexayne **288** was prepared and isolated as a brownish wax with moderate chemical stability. Treating **288** with TBAF led to terminal diyne **289**. Since the stability of deprotected hexayne **289** was very poor, it was immediately reacted with C_{60} in the presence of LHMDs. After quenching with TFA, C_{60} hexayne C_{60} dumbbell **261** was obtained in an overall yield of 5% based on the consumption of **288**. Like its hexayne precursors, compound **261** was not very stable either; therefore, only 1H NMR spectroscopic analysis was performed to characterize its molecular structure. It is also worth noting that in this synthetic route, all terminal alkyne intermediates, including **279**, **287**, and **289**, were neither purified by column flash chromatography nor characterized by spectroscopic analysis, due to their chemical instability. Especially, compound **289** was found to be only moderately stable in dilute solution. Once the solvent was evaporated off, compound **289** decomposed instantaneously into insoluble black solids, the formation of which likely involved a solid-state polymerization mechanism.



Scheme 3.14: Synthesis of C_{60} -hexayne- C_{60} dumbbell **261**. Reagents and conditions: (i) K_2CO_3 , CH_3OH , THF; (ii) CuCl/TMEDA , air, acetone, 90% over two steps; (iii) K_2CO_3 , CH_3OH , THF; (iv) CuCl/TMEDA , air, acetone, 39% over two steps; (v) TBAF, THF; (vi) C_{60} , LHMDS, THF then TFA, 5% over two steps.

3.2.1.5 Star-shaped tetrafullerene-oligoynes adducts

Our quest for C_{60} -oligoynes derivatives went beyond the linear dumbbell-shaped motif, and a series of star-shaped tetrafullerene-oligoynes adducts were investigated in order to expand the body of knowledge with respect to multiple C_{60} -oligoynes derivatives. Two compounds **290a** and **290b** (see Figure 3.3) were first targeted in the synthesis.

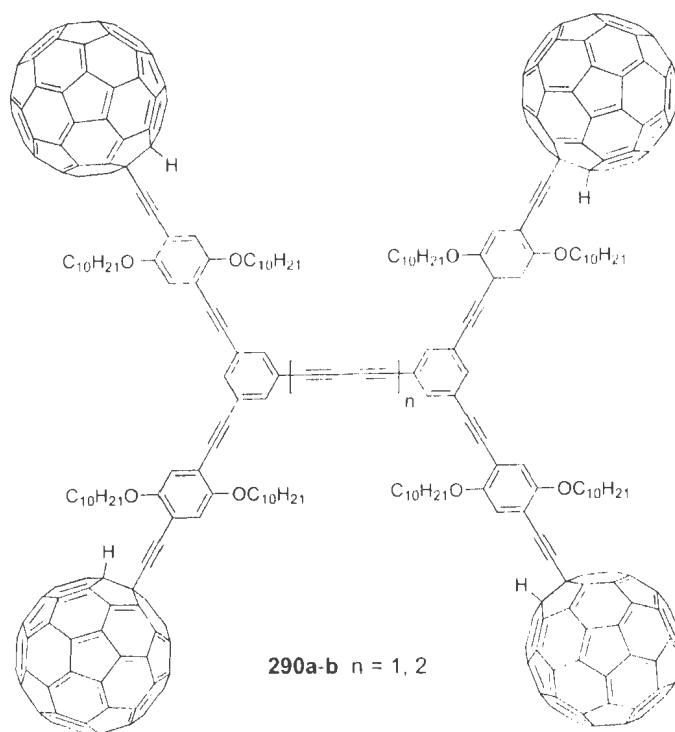
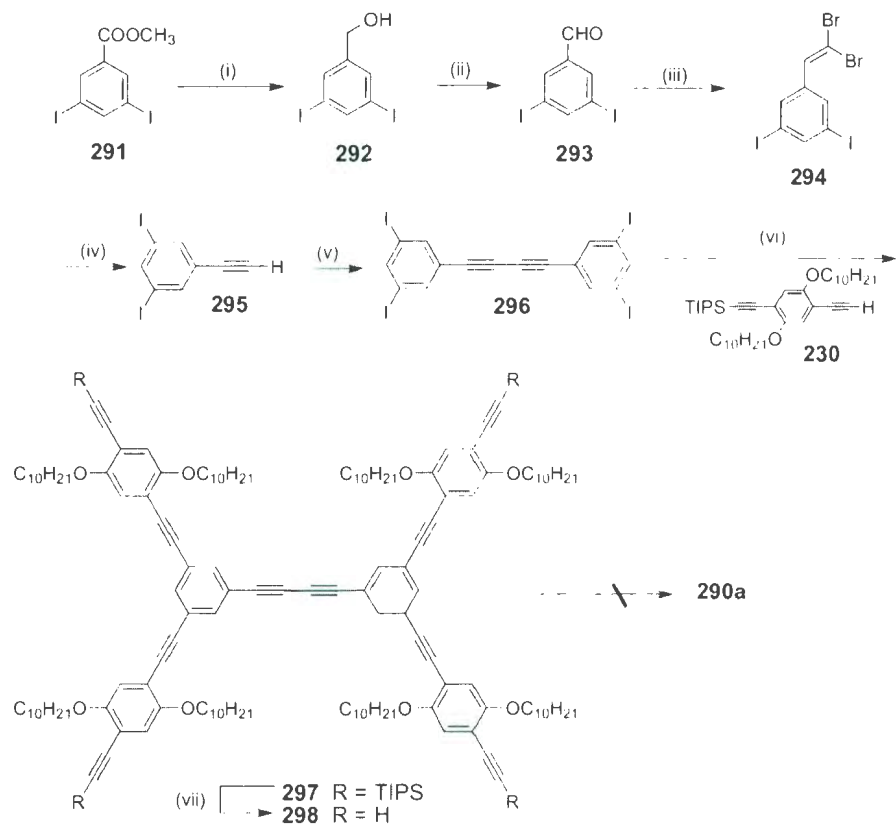


Figure 3.3: Structures of star-shaped bisfullerene-oligoynes adducts **290a-b**.

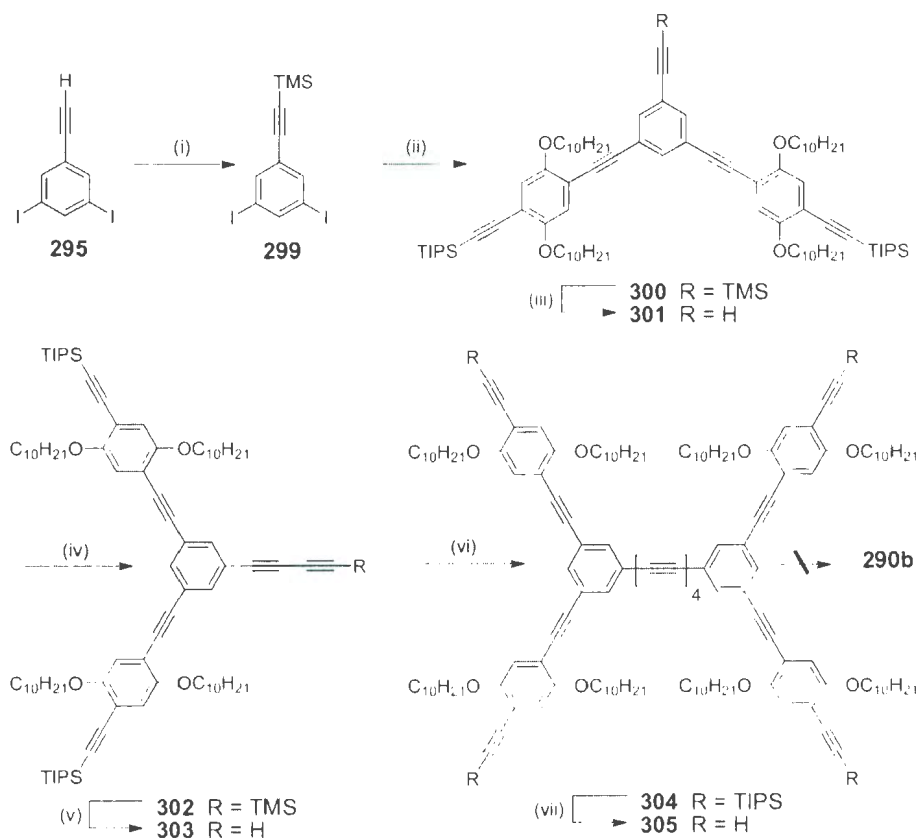
The effort to synthesize **290a** is outlined in Scheme 3.15. Starting from methyl 3,5-diiodobenzoate (**291**), benzaldehyde **293** was obtained through two steps of typical functional group interconversions. Compound **293** was then converted into terminal alkyne **295** in good yield via a Corey-Fuchs reaction. Hay coupling of **295** led

to diyne **296** as a pale white solid with limited stability. So compound **296** was immediately subjected to a Sonogashira coupling reaction with terminal alkyne **230** to yield star-shaped phenylacetylene oligomer **297**. Treating **297** with TBAF in THF gave compound **298**, the key precursor to target compound **290a**. However, an *in situ* ethynylation of C₆₀ with **298** did not afford the desired product **290a**, but rather insoluble substances, the molecular structures of which could not be characterized.

In parallel with the above synthetic effort for **290a**, a tetrayne-centered star-shaped tetrafullerene adduct **290b** was also targeted. As shown in Scheme 3.16, terminal alkyne **295** was first deprotonated with LDA and then silylated with TMSCl to give compound **299**. From compound **299**, phenylacetylene oligomer **300** was readily prepared in a high yield of 92% via a Sonogashira coupling reaction with **230**. Compound **300** was desilylated with K₂CO₃ to form terminal alkyne **301**, which was subjected to a Hay coupling with excess TMSA to produce oligomer **302**. Selective desilylation of **302** followed by another Hay coupling afforded tetrayne **304** in a very good yield. Compound **304** was then desilylated with TBAF to afford terminal alkyne **305**. At this point, the synthesis reached a dead end. Compound **290b** could not be obtained from terminal alkyne **305** via the *in situ* ethynylation reaction.



Scheme 3.15: Attempted synthesis of star-shaped tetrafullerene adduct **290a**.
 Reagents and conditions: (i) LiBH_4 , THF, EtOH, 74% or DIBAL, CH_2Cl_2 , 95%;
 (ii) PCC, CH_2Cl_2 , 95%; (iii) CBr_4 , PPh_3 , CH_2Cl_2 , 93%; (iv) LDA, THF, 87%; (v)
 CuCl/TMEDA , air, acetone, 66%; (vi) $\text{PdCl}_2(\text{PPh}_3)_2$, CuI, Et_3N , THF, 80%; (vii)
 K_2CO_3 , CH_3OH , THF, 73%.

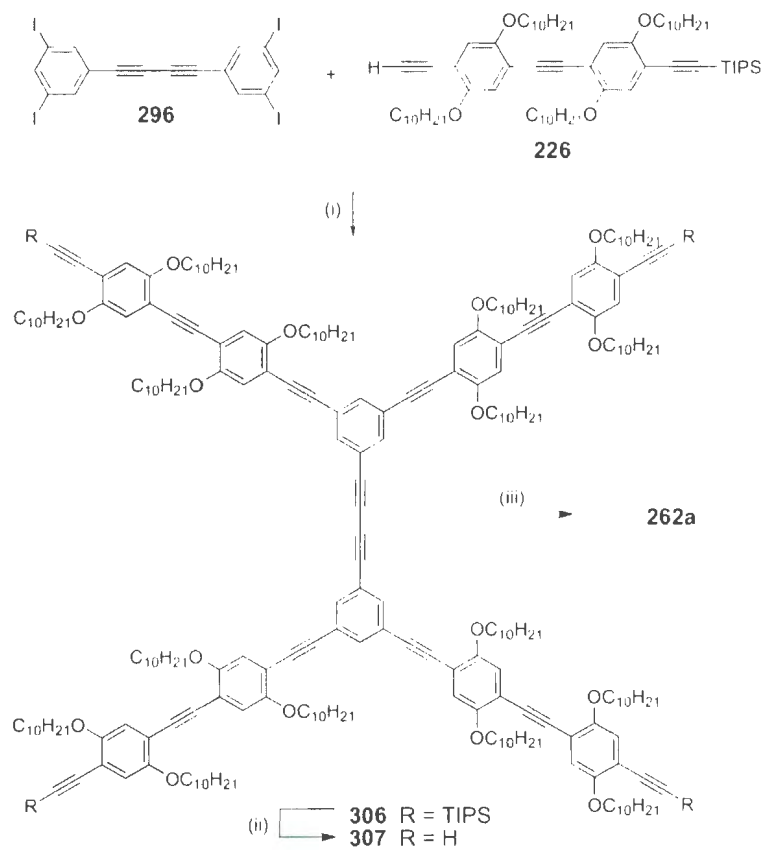


Scheme 3.16: Attempted synthesis of star-shaped tetrafullerene adduct **290b**.
 Reagents and conditions: (i) LDA, THF then TMSCl, 80%; (ii) **230**, PdCl₂(PPh₃)₂, CuI, Et₃N, THF, 92%; (iii) K₂CO₃, CH₃OH, THF, 100%; (iv) TMSA, CuCl·TMEDA, air, acetone, 89%; (v) K₂CO₃, CH₃OH, THF, 81%; (vi) CuCl·TMEDA, air, acetone, 86%; (vii) TBAF, THF, 97%.

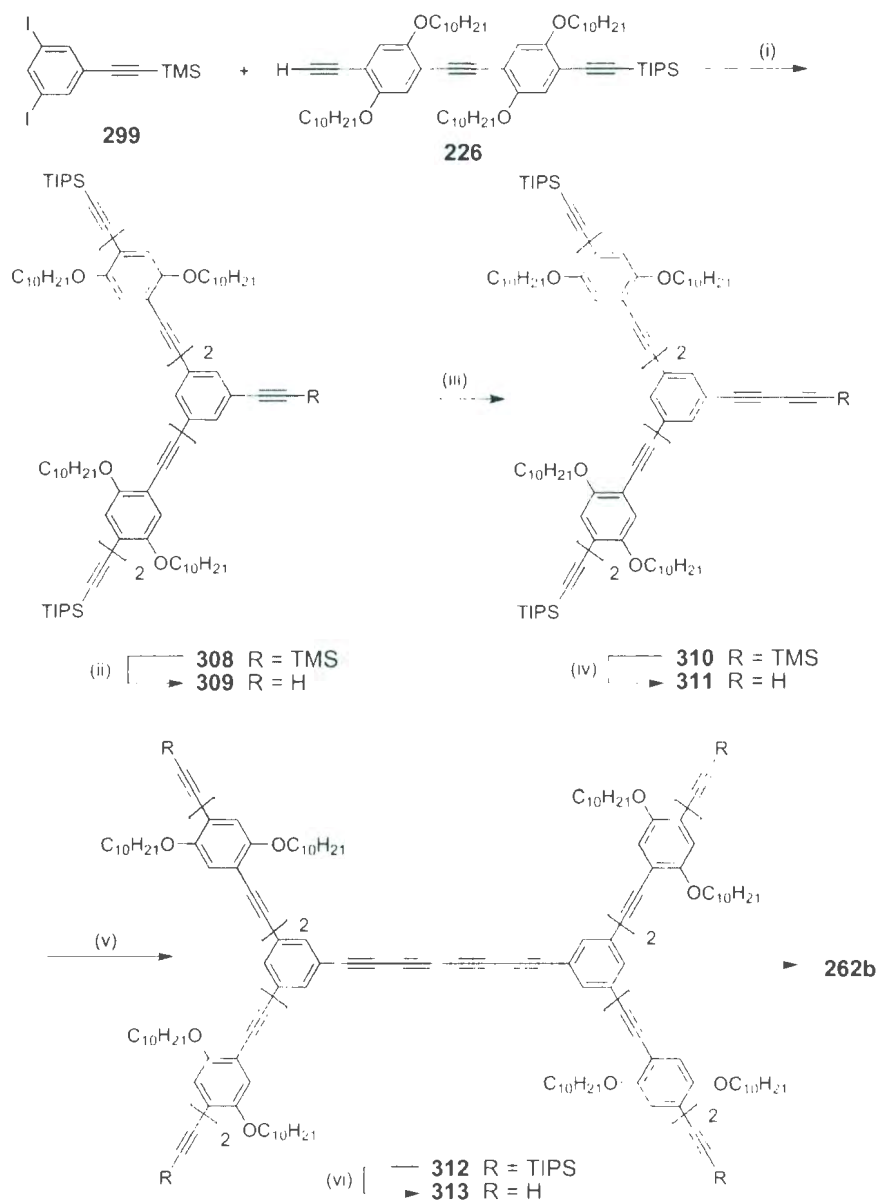
To circumvent the solubility problem, the structures of our target star-shaped tetrafullerene adducts were accordingly revised with more bis(alkoxyl) substituted phenylene units as in compounds **262a** and **262b** (see Figure 3.2).

The redesign of more soluble star-shaped phenylacetylene π skeletons has indeed brought success in making the diyne-bridged bisfullerene adduct **262a**. As illustrated in Scheme 3.17, a Sonogashira coupling reaction between **296** and **226** first gave TIPS protected star-shaped diyne precursor **306** in a yield of 86%. Removal of the TIPS groups in **306** afforded terminal alkyne **307**, which was subsequently converted into compound **262a** via an *in situ* ethynylation reaction with C_{60} . Although the yield of the ethynylation reaction was around 20%, it is still a remarkable achievement given the fact that *four* fullereryl groups have been incorporated in this single operational step.

In a similar manner, tetrayne-centered tetrafullerene adduct **262b** was anticipated to be readily prepared from oligomer precursor **313** as shown in Scheme 3.18. The synthesis of TIPS protected star-shaped oligomer **312** was done following the similar iterative strategies used in the synthesis of oligomers **305** and **307**. When oligomer **312** was subjected to a typical desilylation with TBAF, however, a new problem emerged: the resulting terminal alkyne **313** was too unstable to be isolated as a neat product. In fact, compound **313** was found to decompose so rapidly into a dark colored substance, presumably through solid-state polymerizations, that no opportunity was available to carry on any further reactions with it.



Scheme 3.17: Synthesis of star-shaped diyne-bridged tetrafullerene adduct **262a**.
 Reagents and conditions: (i) $\text{PdCl}_2(\text{PPh}_3)_2$, CuI , Et_3N , THF, 86%; (ii) TBAF, THF, 100%; (iii) LHMDS, C_{60} , THF then TFA, 20%.



Scheme 3.18: Attempted synthesis of star-shaped tetrayne-bridged tetrafullerene adduct **262b**. Reagents and conditions: (i) $\text{PdCl}_2(\text{PPh}_3)_2$, CuI , Et_3N , THF, 36%; (ii) K_2CO_3 , CH_3OH , THF, 83%; (iii) TMSA, $\text{PdCl}_2(\text{PPh}_3)_2$, CuI , Et_3N , THF, 84%; (iv) K_2CO_3 , CH_3OH , THF, 91%; (v) CuCl TMEDA, air, acetone, 83%; (vi) TBAF, THF, 0%.

3.2.2 Spectroscopic and microscopic characterizations of thermally induced solid-state polymerization

3.2.2.1 Differential scanning calorimetric analysis

As described in Section 3.1, conjugated oligoynes can be polymerized to form extended and higher ordered poly(enyne) networks in the solid state under conditions such as heat, irradiation, and pressure. To investigate the thermally induced solid-state reactivity of the oligoyne- C_{60} adducts synthesized in this chapter, differential scanning calorimetric (DSC) analysis was conducted on selected oligoyne precursors and C_{60} oligoyne C_{60} dumbbells under N_2 environments. Detailed DSC spectra are given in Figure 3.4.

Figure 3.4A shows the DSC profile of diyne precursor **265**, in which two distinct exothermic peaks are clearly observed at 151 and 254 °C, respectively. Given the broad lineshapes the two peaks display, they can be reasonably attributed to random solid-state polymerizations rather than ordered topochemical reactions such as 1,2- or 1,4-addition, for if otherwise the peaks would appear more intense and sharper.

The DSC spectrum of tetrayne precursor **280** in Figure 3.4B shows one sharp endothermic peak at 71 °C, which corresponds to a melting process, and a broad exothermic peak at 165 °C that appears typical of random solid-state polymerizations of conjugated tetrayne species.

Figure 3.4C depicts the DSC curve of short C_{60} diyne C_{60} dumbbell **259a**. There is a broad exothermic peak of moderate intensity centered at 145 °C and a noticeable hump (exothermic) around 198 °C. In comparison to its diyne precursor **265**, dumbbell **259a** is more thermally robust and solid-state reaction occurs to a

much lesser degree. Possibly, the bulky nature of C_{60} endcapping groups is the cause of reduced solid-state reactivity of the diyne moiety in this temperature range. At temperatures higher than 270 °C, the DSC curve drifts abruptly to the endothermic direction, which is likely due to the decomposition of phenylacetylene components.

The DSC profile of short C_{60} tetrayne C_{60} dumbbell **260a** (Figure 3.4D) shows only one relatively broad exothermic peak ranging from 156 to 240 °C with a maximum at 212 °C. The broad peak width suggests that the tetrayne moiety in **260a** undergoes polymerization in a random, rather than the regioselective (topochemical) manner. Unlike that of diyne dumbbell **259a**, the DSC trace of tetrayne dumbbell **260a** remains nearly flat from 240 to 350 °C, manifesting good thermal stability for the polymerized product in this temperature range. Moreover, the enthalpy for the exothermic process (ΔH) is determined to be 77.6 kJ · mol⁻¹. Since this value is considerably smaller than that of tetrayne precursor **280** (317.7 kJ · mol⁻¹), it is concluded that the degree of polymerization is rather low.

The DSC trace of long C_{60} diyne C_{60} dumbbell **259b** in Figure 3.4E shows a weak exothermic peak at 141 °C along with a barely noticeable hump at 196 °C. The features herein are clear indicative of appreciable thermal robustness and very low solid-state reactivity of **259b** in comparison to the other oligoyne species.

The DSC profile of long C_{60} tetrayne C_{60} dumbbell **260b** in Figure 3.4F features a strong, broad exothermic peak centered at 140 °C, together with a weak exothermic hump at 198 °C. Apparently, this tetrayne dumbbell also undergoes random solid-state polymerization at these temperatures. Furthermore, there is a pronounced decomposition profile starting from 270 °C, likely due to the degradation of phenylacetylene moieties.

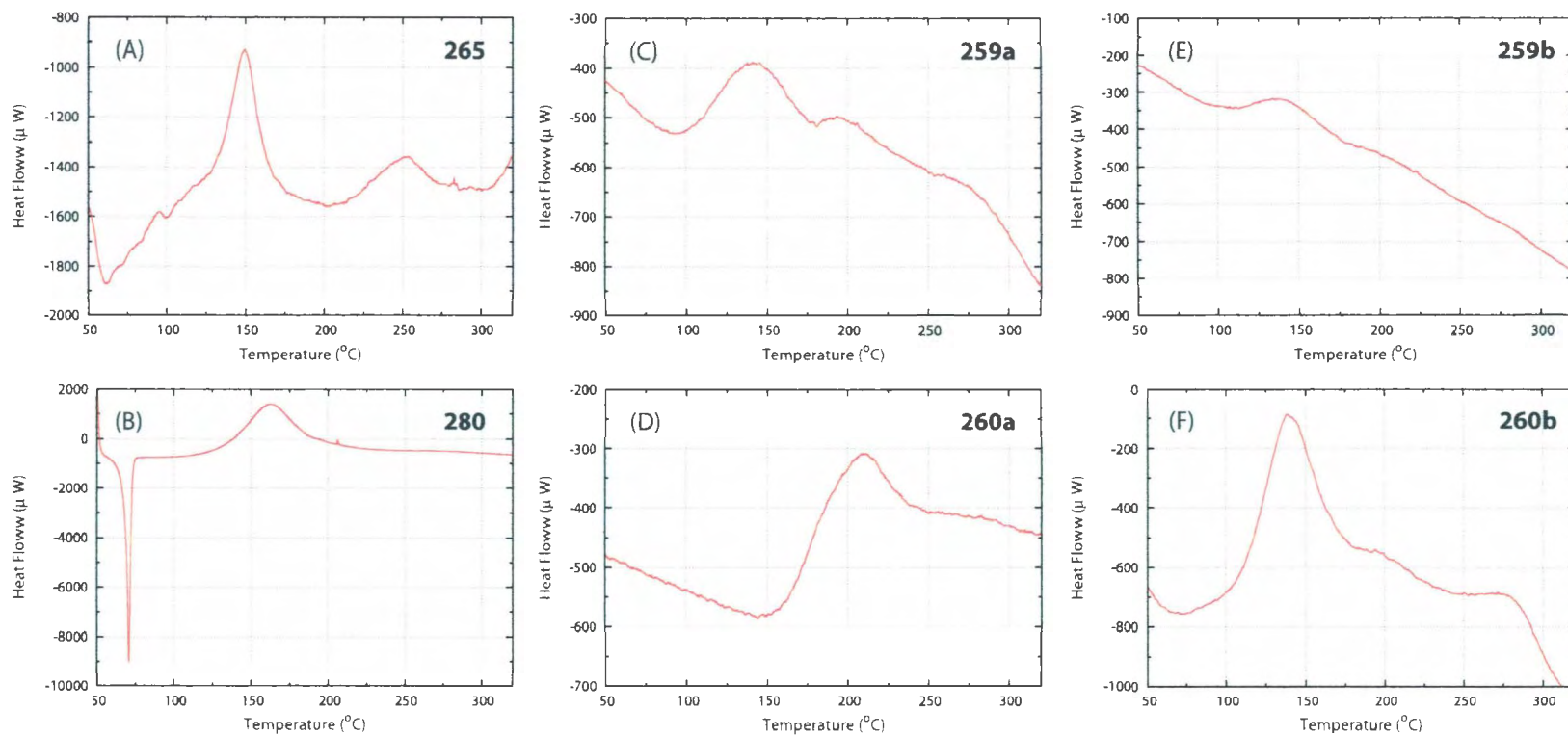


Figure 3.4: DSC profiles for (A) diyne precursor **265**, (B) tetrayne precursor **280**, (C) short C_{60} -diyne- C_{60} **259a**, (D) short C_{60} -tetrayne- C_{60} **260a**, (E) long C_{60} -diyne- C_{60} **259b**, and (F) long C_{60} -tetrayne- C_{60} **260b**.

3.2.2.2 UV-Vis spectroscopic analysis

To shed more light on the structure changes of the oligoyne units in response to heating, UV-Vis spectroscopic characterization was performed on the synthesized C_{60} oligoyne adducts. In these experiments, the UV-Vis absorption spectra for the compounds were measured in solution (toluene), solid-state thin film, and solid-state thin films after heating at 160 °C for *ca.* 1 h, respectively. Herein the heating temperature was chosen at 160 °C because it was a common temperature at which most of the oligoyne- C_{60} adducts underwent exothermic solid-state polymerization reactions as indicated by the DSC results (see Figure 3.4). Detailed UV-Vis spectral data and pertinent discussions are given as follows.

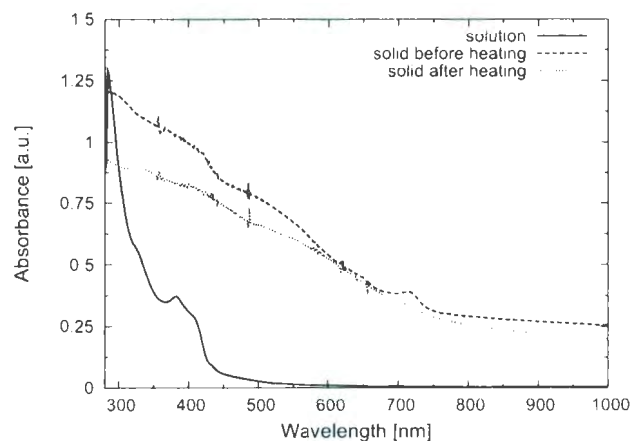


Figure 3.5: UV-Vis spectra of short C_{60} diyne C_{60} dumbbell **259a** measured in solution, solid-state film, and solid-state film after heating at 160 °C for *ca.* 1 h.

In Figure 3.5, the UV-Vis absorption bands of the solid-state film of short C_{60} diyne C_{60} dumbbell **259a**, which correspond to the electronic transitions of the diyne

moiety (*ca.* 350–450 nm), appears much broader than those measured in solution. The observation of band width broadening is likely due to significant aggregation effects in the solid state. In addition, an intense absorption tail extending from *ca.* 450 to 1000 nm in the spectrum of solid film can be observed and is assigned to the $\pi \rightarrow \pi^*$ transitions of C_{60} . After heating the film, the absorption features of C_{60} remains almost the same, while the diyne absorption region becomes monotonous and featureless. Such spectral changes suggest the diyne moieties have undergone solid-state polymerization reactions to a certain degree at 160 °C, which is in consistent with the DSC results aforementioned. Moreover, the nearly unchanged C_{60} absorption tail in the spectrum of heated solid film signifies that the C_{60} moieties retain good chemical stability at this temperature. This property is indeed beneficial for the preparation of C_{60} based carbon-rich polymers using respective oligyne- C_{60} adducts as precursors.

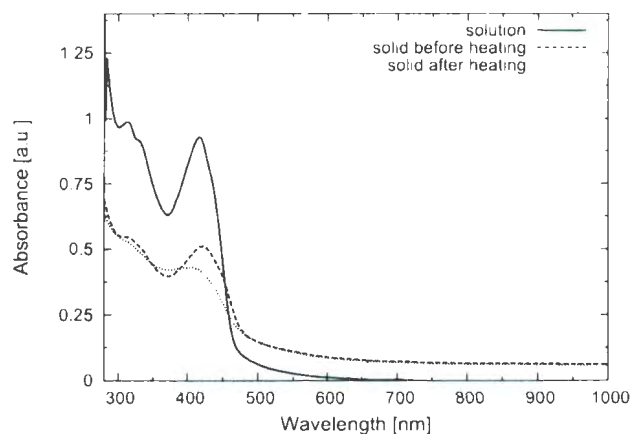


Figure 3.6: UV-Vis spectra of long C_{60} diyne C_{60} dumbbell **259b** measured in solution, solid film, and solid film after heating at 160 °C for *ca.* 1 h.

In Figure 3.6, the UV-Vis absorption curves of long C_{60} diyne C_{60} **259b** look much alike in both solution and the solid state. The incorporation of more decyloxy-substituted phenylacetylene segments must have not only improved the quality of thin film formation, but effectively reduced intramolecular aggregation in the solid state, since there is no dramatic lineshape broadening as observed in Figure 3.5. After heating the thin film at 160 °C for 1 h, the UV-Vis spectrum shows only slightly reduced absorption in the region of *ca.* 370 to 470 nm, while the rest of the spectrum remains virtually unaltered. Nevertheless, the fact that the characteristic absorption bands corresponding to the diyne moiety are still observable after heating is a strong indication that the long diyne dumbbell **259b** is relatively thermally robust at 160 °C. This conclusion is in agreement with the DSC data for **259b** as well.

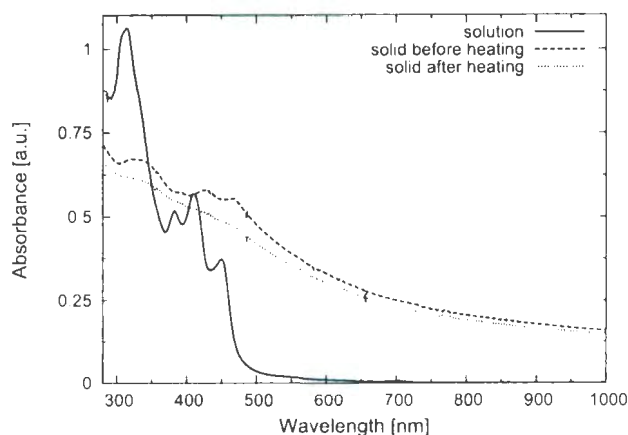


Figure 3.7: UV-Vis spectra of short C_{60} tetrayne C_{60} dumbbell **260a** measured in solution, solid film, and solid film after heating at 160 °C for *ca.* 1 h.

The UV-Vis spectrum of short C_{60} tetrayne C_{60} dumbbell **260a** measured in solution shows three distinctive absorption bands in the region of 380–460 nm, which

are characteristic of the vibronic modes of a conjugated tetrayne. In the spectrum of its solid thin film, the same set of bands is still discernible, but appear substantially broad in shape, likely as a result of strong solid-state aggregation. After heating the film at 160 °C for 1 h, markedly different UV-Vis absorption features can be observed: the three characteristic tetrayne bands disappear completely, while the higher-energy bands below 300 nm and the fullerene absorption tail (beyond *ca.* 550 nm) are hardly changed. These results indicate that solid-state polymerizations have taken place primarily among the tetrayne moieties.

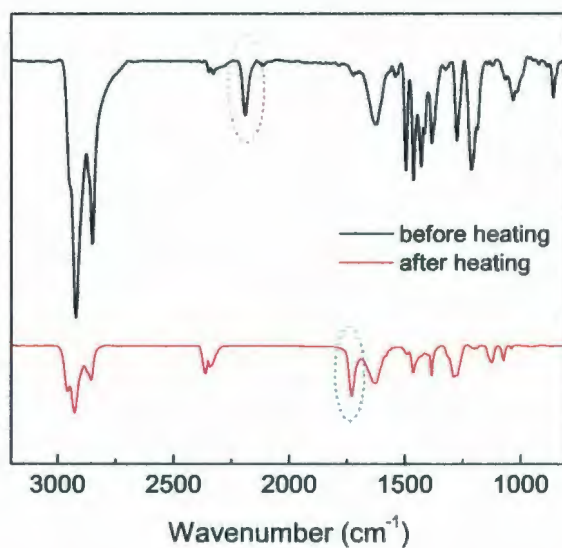


Figure 3.8: IR spectra for short C₆₀-tetrayne-C₆₀ dumbbell **260a** before and after heating at 160 °C for 1 h.

To gain deeper insight into the solid-state reactivity of tetrayne dumbbell **260a**, IR spectroscopic analysis was undertaken on its solid samples before and after heating at

160 °C for 1 h. From the IR data given in Figure 3.8, it is notable that the vibrational frequency at *ca.* 2100 cm⁻¹ characteristics of C≡C bond stretching is completely lost after heating the sample. A plausible rationalization for this is that the thermally induced polymerization occurs in an irregular cycloaromatization manner. In the meantime, the heated sample shows a new vibrational band at 1728 cm⁻¹, which is typical of C=O stretching. Given the fact that the heating of solid samples was conducted in an open air environment, it is very likely that oxygen has participated in the solid-state reaction to form carbonyl groups. To further investigate the solid-state structure of the polymers formed under these conditions, X-ray powder diffraction (XRD) analysis was also attempted. However, the results do not indicate any crystalline features but merely amorphous solids.

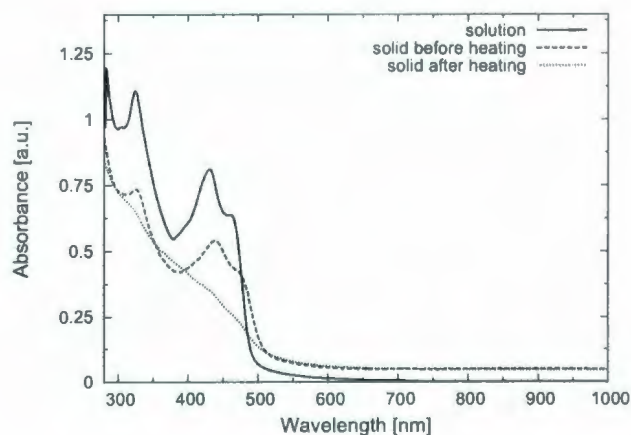


Figure 3.9: UV-Vis spectra of long C₆₀-tetrayne-C₆₀ dumbbell **260b** measured in solution, solid film, and solid film after heating at 160 °C for *ca.* 1 h.

In Figure 3.9, the UV-Vis spectrum of long C₆₀-tetrayne-C₆₀ dumbbell **260b** measured in solution shows two discernible vibronic bands in the region of 390 to

480 nm. The solid thin film shows a spectral envelope similar to that obtained in the solution phase, indicating relatively insignificant $\pi - \pi$ aggregation as a result of increased bulky solubilizing bis(decyloxy)phenylacetylene subunits in comparison to its short analogue **260a**. After heating the solid film of **260b** at 160 °C for 1 h, the UV-Vis absorption features corresponding to the tetrayne moiety are completely lost, presumably due to significant solid-state polymerization reactions.

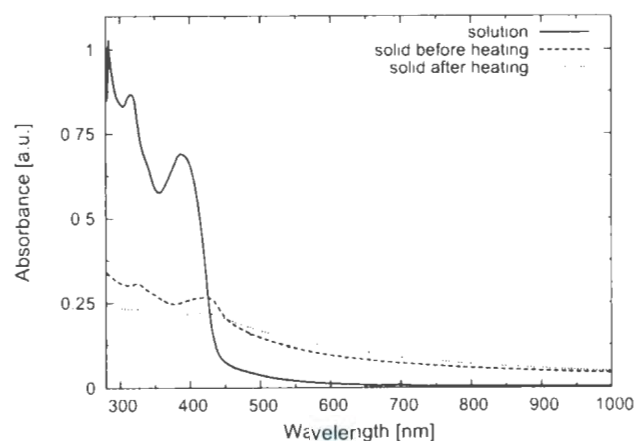


Figure 3.10: UV-Vis spectra of star-shaped tetrafullerene-diyne adduct **262a**, measured in solution, solid film, and solid film after heating at 160 °C for *ca.* 1 h.

Finally, UV-Vis spectral analysis on star-shaped tetrafullerene-diyne adduct **262a** was carried out in the same manner as the other oligyne- C_{60} adducts employed. Likewise, the solid-state UV-Vis absorption trace for **262a** shows relatively broader lineshapes than does the spectrum measured in solution. After heating at 160 °C for 1 h, the UV-Vis profile of the solid film shows decreased intensity in the high-energy absorption region (300–450 nm). Nonetheless, the $\pi \rightarrow \pi^*$ transition bands

corresponding to the diyne centered phenylacetylene framework as well as the C_{60} cages are still discernible, indicating a moderate to low level of reactivity in the solid state.

3.2.2.3 Study of morphological properties by atomic force microscopy

In order to disclose the morphological properties of the oligyne- C_{60} adducts on surface, atomic force microscopic (AFM) analysis in non-contact mode was performed. In the experiments, samples of oligyne- C_{60} adducts were first prepared in dilute solutions (*ca.* 10^{-6} to 10^{-7} M in toluene). The solutions were spin-cast on freshly cleaved mica surfaces at a spin rate of 2,000 rpm. Surface morphologies of the resulting thin films were examined by AFM both before and after being subjected to heating at 160 °C for 1 h. The acquired AFM images are summarized as follows.

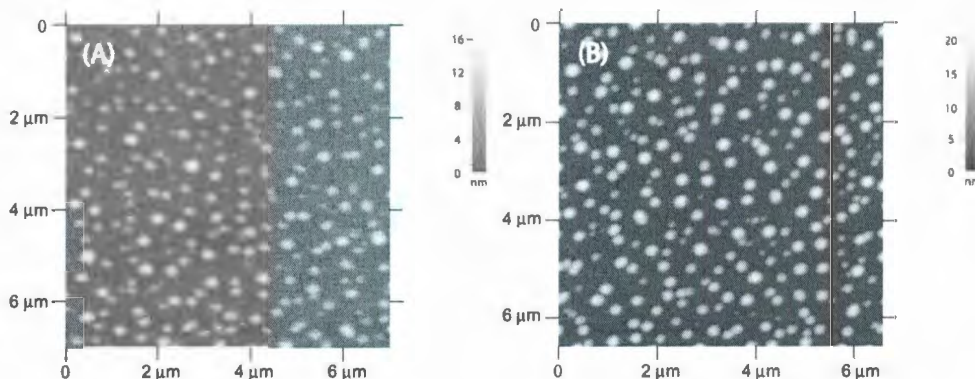


Figure 3.11: Surface morphology of short C_{60} -diyne- C_{60} dumbbell **259a** on mica measured by AFM: (A) before heating; (B) after heating at 160 °C for *ca.* 1 h.

According to the AFM studies, short diyne dumbbell **259a** is found to significantly aggregate into spherical nanoclusters on mica surface before heating. Since AFM

imaging only gives reliable and accurate distance measurements in the vertical (Z) direction, the sizes of these nanospheres are determined by their vertical diameters. From Figure 3.11A, the distribution of the nanospheres of **259a** is in a relatively narrow range of *ca.* 10 to 20 nm. After heating the sample at 160 °C for 1 h, there are no noticeable morphological changes observed for these nanospheres as shown in Figure 3.11B.

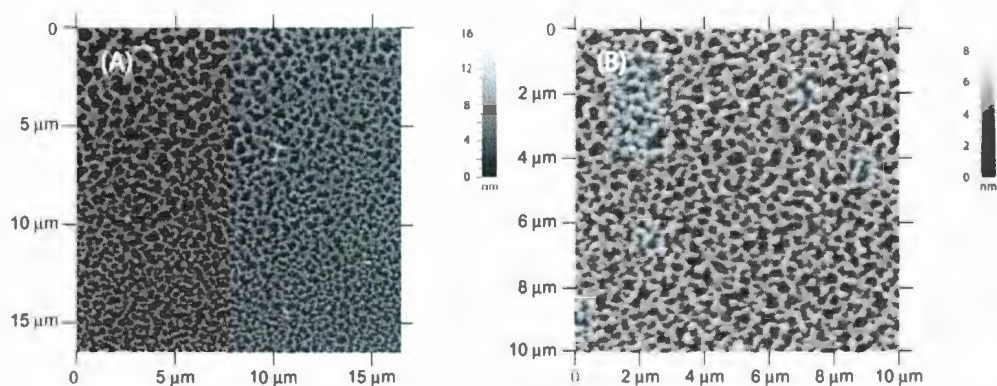


Figure 3.12: Surface morphology of long C_{60} diyne- C_{60} dumbbell **259b** on mica measured by AFM: (A) before heating; (B) after heating at 160 °C for *ca.* 1 h.

Long diyne dumbbell **259b** aggregates on mica in a pattern of cross-linked “worms” (Figure 3.12A). The vertical heights of these “worms” are rather uniform, ranging from *ca.* 4 to 6 nm. Like the short diyne dumbbell, these unique nanostructures show no changes in morphology after heating (see Figure 3.12B), which is consistent with the relatively high thermal stability of diyne species as revealed by previous DSC and UV-Vis analyses.

The most remarkable morphological transformation corresponding to solid-state polymerization is found in the case of short C_{60} -tetrayne- C_{60} dumbbell **260a**. As

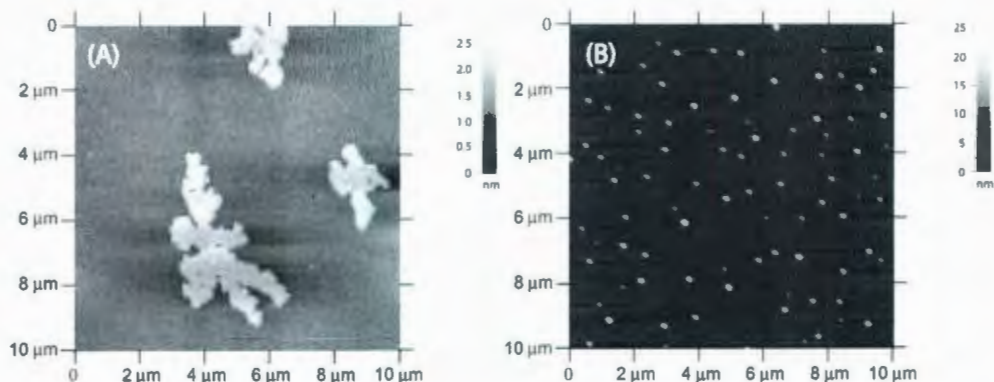


Figure 3.13: Surface morphology of short C_{60} tetrayne- C_{60} dumbbell **260a** on mica measured by AFM: (A) before heating; (B) after heating at 160 °C for *ca.* 1 h.

shown in Figure 3.13, compound **260a** forms discrete “flake-like islands” on the surface with vertical heights around 1–2 nm. The thickness of these aggregates fits well the depth of nanostructures composed of single or double molecular layer of compound **260a**, given that the diameter of C_{60} is approximately 1 nm. Upon heating at 160 °C for *ca.* 1 h, however, the random “flakes” agglomerate into an ordered array of spherical nanoparticles on the surface, with rather narrowly distributed vertical diameters. Cross-section analysis shows that the average vertical diameter of these nanospheres is around 20 nm. The transformation from random aggregates of **260a** into ordered, uniform nanospheres by means of thermal annealing can be thus related to the solid-state polymerization of the tetrayne moiety in **260a** as revealed by DSC, UV-Vis, and IR analyses.

Long C_{60} -tetrayne- C_{60} dumbbell **260b** displays better film forming properties than its short homologue **260a**. As can be seen from Figure 3.14A, the surface morphology for aggregates of **260b** appears as a random, continuous thin film with a height of *ca.* 2–4 nm. After heating at 160 °C for *ca.* 1 h, the quality of the thin

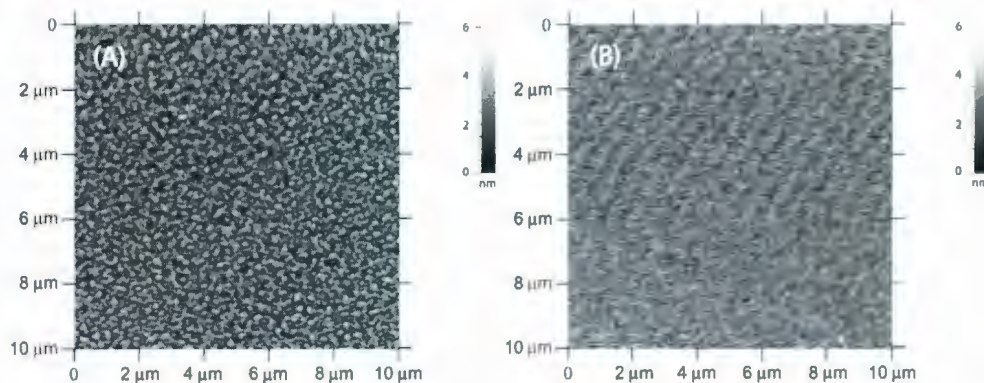


Figure 3.14: Surface morphology of long C_{60} -tetrayne- C_{60} dumbbell **260b** on mica measured by AFM: (A) before heating; (B) after heating at 160 °C for *ca.* 1 h.

film is further improved with a height less than 1 nm (Figure 3.14B). In contrast to the case of **260a**, there are no discrete nanostructures observed in the AFM image of thermally annealed tetrayne **260b**. Obviously, the additional two alkyoxy substituted phenylacetylene subunits have greatly altered the solid-state aggregation behavior of dumbbell-shaped bisfullerene adducts.

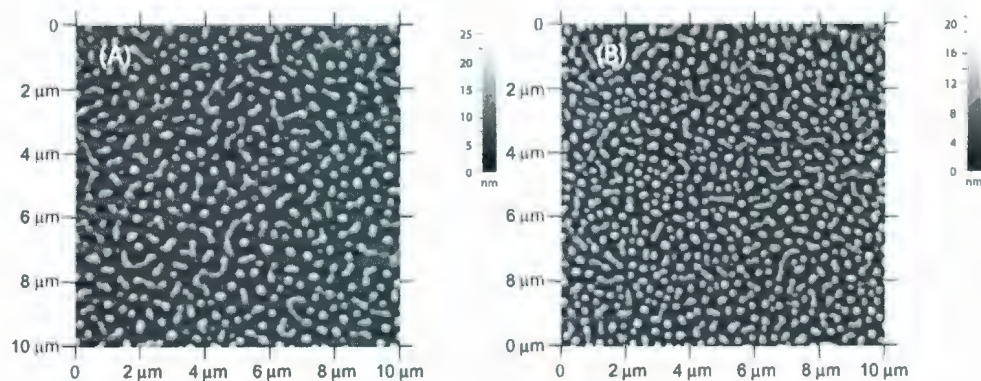


Figure 3.15: Surface morphology of star-shaped tetrafullerene-diyne adduct **262a** on mica measured by AFM: (A) before heating; (B) after heating at 160 °C for *ca.* 1 h.

Star-shaped tetrafullerene-diyne adduct **262a** forms a mixture of spherical, semi-spherical, and short “worm-like” nano-aggregates on the surface of mica as shown in Figure 3.15A. The height distribution of these nanostructures is narrow and measured to be about 1 nm, which corresponds well to single molecular layered aggregates. After thermal annealing at 160 °C for *ca.* 1 h, the morphological features are virtually unchanged (Figure 3.15B). This result hence testifies to the thermal stability of **262a** elicited from its previous UV-Vis data.

3.3 Conclusions

In this chapter, several dumbbell-shaped linear bisfullerene-encapped conjugated oligoynes as well as a star-shaped tetrafullerene-oligoyne were synthesized using an *in situ* ethynylation reaction. The solid-state polymerization of these compounds on mica surface at elevated temperatures have been investigated by UV-vis, FT-IR, differential scanning calorimetry (DSC), and X-ray diffraction techniques. Thermally induced polymerization processes of these C₆₀-oligoynes compounds are monitored by atomic force microscopy (AFM) and it has been found that the morphological properties of these compounds on the solid surface are dependent on chemical structures. Structure and solid-state reactivity morphology relationships for these C₆₀-oligoynes adducts have been established and the information obtained provides a useful guiding for designing C₆₀ based carbon-rich nanomaterials via solid-state aggregation and polymerization reactions. In a general sense, the more fullerene components present in the molecular structure, the stronger the tendency the molecules to self-assemble in spherical nanoscopic structures. On the other hand,

when more solubilizing alkyl groups are incorporated, the better thin film formation ability the molecules show. Thermally induced polymerization can significantly alter the morphological properties of the nanoassemblies.

3.4 Experimental

General procedures and methods

Chemicals and reagents were purchased from commercial suppliers and used without further purification. [60]Fullerene (purity 99.5 %) was purchased from MTR Ltd. Tetrabutylammonium fluoride (1 M in THF) and lithium hexamethyldisilazide (1 M in THF) were purchased from Aldrich. THF was distilled from sodium benzophenone. Et₃N and toluene were distilled from LiH. Catalysts, Pd(PPh₃)₄ and Pd(PPh₃)₂Cl₂, were prepared from PdCl₂ according to standard procedures. All reactions were performed in standard, dry glassware under an inert atmosphere of N₂ unless otherwise noted. Evaporations and concentrations were done at H₂O aspirator pressure. Flash column chromatography was carried out with silica gel 60 (230-400 mesh) from VWR International. Thin-layer chromatography (TLC) was carried out with silica gel 60 F254 covered on plastic sheets and visualized by UV light or KMnO₄ stain. Melting points (Mp) were measured with a Fisher-Johns melting point apparatus and are uncorrected. ¹H and ¹³C NMR spectra were measured on a Bruker Avance 500 MHz spectrometer. Chemical shifts are reported in ppm downfield from the signal of the internal reference SiMe₄. Coupling constants (*J*) are given in Hz. The coupling constants of some aryl proton signals are reported as pseudo first-order spin

systems, even though they are second-order spin systems. Infrared spectra (IR) were recorded on a Bruker Tensor 27 spectrometer. UV-Vis spectra were recorded on an Agilent 8453 UV-Vis or a Cary 6000i UV-Vis-NIR spectrophotometer. APCI mass spectra were measured on an Agilent 1100 series LCMSD spectrometer, and high-resolution MALDI-TOF mass spectra on an Applied Biosystems Voyager instrument with dithranol as the matrix. AFM imaging was conducted on a QScope 250 scanning probe microscope in non-contact (tapping) mode. Differential scanning calorimetry (DSC) experiments were performed on a Seiko I DSC 210 instrument. Thin films for morphological properties study were prepared using Laurell WS-400B-6NPP-LITE spin processor. XRD data were collected using Rigaku Ru-200 12kW Automated Powder Diffractometer.

Compound 259a. Compound **259a** (32 mg, 0.014 mmol, 21%) was obtained as a brownish solid by the same *in situ* ethynylation protocol as described in the synthesis of **196a**, using compound **266** (50 mg, 0.057 mmol), C_{60} (205 mg, 0.286 mmol), LHMDs (0.29 mL, 1 M, 0.29 mmol) and dry THF (240 mL). IR (KBr) 2921, 2852, 2200, 2087, 1654, 1602, 1496, 1464 cm^{-1} ; 1H NMR ($CDCl_3/CS_2$, 500 MHz) δ 7.22 (s, 2H), 7.15 (s, 2H), 7.08 (s, 2H), 4.13 (t, $J = 6.0$ Hz, 4H, $OC'H_2$), 4.10 (t, $J = 5.0$ Hz, 4H, $OC'H_2$), 1.96-1.89 (m, 8H), 1.68-1.62 (m, 4H), 1.60-1.51 (m, 4H), 1.40-1.20 (m, 48H), 0.88 (t, $J = 6.5$ Hz, 6H, CH_3), 0.83 (t, $J = 7.0$ Hz, 6H, CH_3); ^{13}C NMR ($CDCl_3/CS_2$, 125 MHz) δ 155.2, 154.4 (two C-O in the phenyl rings), 151.6, 151.4, 147.8, 147.5, 146.8, 146.58, 146.56, 146.4, 146.0, 145.8, 145.7, 145.6, 145.5, 144.9, 144.7, 143.4, 142.79, 142.76, 142.3, 142.2, 142.17, 142.1, 141.9, 141.8, 140.6, 140.5, 136.2, 135.3 (28 discernible sp^2 carbons of the 30 different sp^2 carbons in the C_60

symmetrical C₆₀ core), 117.5, 117.1, 114.2, 113.5 (four aromatic carbons in the phenyl rings), 98.4, 80.5, 80.1, 79.9 (four alkynyl carbons), 70.4, 69.9 (two C-O carbons in the alkyl chains), 62.1, 55.6 (two *sp*³ carbons on fullerene cages), 32.2, 30.4, 30.2, 30.1, 30.01, 29.96, 29.7, 29.6, 29.4, 26.8, 26.4, 23.1, 14.5, 14.4; MALDI-TOF MS *m/z* calcd for C₁₈₀H₉₀O₄ 2314.68, found 2316.26 [M + H]⁺.

Compound 259b. Compound **259b** (32 mg, 0.010 mmol, 33%) was obtained as a brownish solid by the same *in situ* ethynylation protocol as described in the synthesis of **196a**, using compound **268** (53 mg, 0.031 mmol), C₆₀ (112 mg, 0.156 mmol), and LHMDS (0.16 mL, 1 M, 0.16 mmol) dry THF (150 mL). IR (KBr) 2920, 2851, 2199, 2139, 2090, 1653, 1603, 1495, 1464, 1424 cm⁻¹; ¹H NMR (CDCl₃, CS₂, 500 MHz) δ 7.29 (s, 2H), 7.19 (s, 2H), 7.14 (s, 2H), 7.05 (s, 2H), 7.04 (s, 2H), 4.16-4.03 (m, 16H, OCH₂), 1.96-1.85 (m, 16H), 1.70-1.50 (m, 16H), 1.40-1.20 (m, 96H), 0.92-0.82 (m, 24H, CH₃); ¹³C NMR (CDCl₃, CS₂, 125 MHz) δ 155.3, 151.8, 154.0, 153.6 (four C-O in the phenyl rings), 151.9, 151.8, 147.9, 147.7, 147.0, 146.7, 146.5, 146.1, 146.0, 145.9, 145.75, 145.67, 145.0, 144.8, 143.5, 143.3, 142.91, 142.87, 142.4, 142.35, 142.30, 142.2, 141.99, 141.91, 140.7, 140.6, 136.4, 135.5 (28 discernible *sp*² carbons of the 30 different *sp*² carbons in the C_s symmetrical C₆₀ core), 118.2, 117.6, 117.4, 117.2, 115.6, 115.2, 113.3, 113.0 (eight aromatic carbons in the phenyl rings), 97.9, 92.3, 92.0, 80.5, 79.9, 79.7 (six alkynyl carbons), 70.1, 70.0, 69.8 (three signals of the four C-O carbons in the phenyl rings), 62.2, 55.8 (two *sp*³ carbons on fullerene cages), 32.2, 30.2, 30.1, 30.0, 29.96, 29.89, 29.8, 29.7, 29.62, 29.56, 29.4, 26.8, 26.3, 26.2, 22.9, 14.4 (CH₃); MALDI-TOF MS *m/z* calcd for C₂₃₆H₁₇₈O₈ 3139.35, found 3140.35 [M + H]⁺.

Compound 260a. Compound **260a** (32 mg, 0.016 mmol, 31%) was obtained as a brownish solid by the same *in situ* ethynylation protocol as described in the synthesis of **196a**, using compound **281** (48 mg, 0.052 mmol), C₆₀ (189 mg, 0.263 mmol), LHMDS (0.27 mL, 1 M, 0.27 mmol) and dry THF (240 mL). IR (KBr) 2920, 2850, 2190, 2115, 1628 cm⁻¹; ¹H NMR (CDCl₃/CS₂, 500 MHz) δ 7.19 (s, 2H), 7.12 (s, 2H), 7.04 (s, 2H), 4.10 (t, *J* = 6.5 Hz, 4H, OCH₂), 4.08 (t, *J* = 7.0 Hz, 4H, OCH₂), 1.90-1.84 (m, 8H), 1.64 (m, 4H), 1.54 (m, 4H), 1.46-1.15 (m, 48H), 0.90 (t, *J* = 6.5 Hz, 6H, CH₃), 0.83 (t, *J* = 6.0 Hz, 6H, CH₃); ¹³C NMR (CDCl₃/CS₂, 125 MHz) δ 156.7, 154.7 (two C-O in the phenyl rings), 151.9, 151.7, 148.2, 147.9, 147.1, 147.0, 146.9, 146.8, 146.3, 146.20, 146.16, 146.03, 145.99, 145.90, 145.2, 145.0, 143.8, 143.2, 143.1, 142.7, 142.6, 142.5, 142.4, 142.22, 142.16, 140.93, 140.89, 136.6, 135.7 (29 discernible *sp*² carbons of the 30 different *sp*² carbons in the *C_s* symmetrical C₆₀ core), 118.2, 117.3, 115.7, 112.3 (four aromatic carbons in the phenyl rings), 99.3, 80.6, 80.5, 75.4, 70.3, 70.0, 69.6, 65.4 (six alkynyl carbons and two C-O carbons in the alkyl chains), 62.4, 56.0 (two *sp*³ carbons in the fullerene cages), 32.6 (br), 30.5, 30.3 (br), 30.1 (br), 26.7 (br), 23.4 (br), 14.8 (br); MALDI-TOF MS *m/z* calcd for C₁₈₀H₉₀O₄ 2362.68, found 2365.25 [M + H]⁺.

Compound 260b. Compound **260b** (36 mg, 0.011 mmol, 35%) was obtained as a brownish solid by the same *in situ* ethynylation protocol as described in the synthesis of **196a**, using compound **285** (58 mg, 0.033 mmol), C₆₀ (130 mg, 0.181 mmol), LHMDS (0.18 mL, 1 M, 0.18 mmol) and dry THF (150 mL). IR (KBr) 2922, 2852, 2192, 2117, 2077, 1653, 1603, 1541, 1506, 1496 cm⁻¹; ¹H NMR (CDCl₃/CS₂, 500 MHz) δ 7.29 (s, 2H), 7.19 (s, 2H), 7.13 (s, 2H), 7.03 (s, 2H), 7.01 (s, 2H), 4.17-

4.01 (m, 16H, OCH₂), 1.97-1.82 (m, 16H), 1.70-1.49 (m, 16H), 1.40-1.20 (m, 96H), 0.95-0.82 (m, 24H); ¹³C NMR (CDCl₃, CS₂, 125 MHz) δ 156.5, 154.8, 153.9, 153.5 (four C-O in the phenyl rings), 151.9, 151.7, 147.9, 147.7, 147.0, 146.7, 146.5, 146.1, 146.0, 145.9, 145.8, 145.7, 145.0, 144.8, 143.5, 143.3, 142.90, 142.88, 142.4, 142.3, 142.29, 142.2, 141.98, 141.91, 140.7, 140.6, 136.4, 135.5 (28 discernible *sp*² carbons of the 30 different *sp*² carbons in the C_s symmetrical C₆₀ core), 118.3, 117.5, 117.2, 116.7, 115.0, 113.5, 111.3 (aromatic carbons in the phenyl rings), 98.0, 93.0, 91.8, 80.5, 79.8, 75.2, 70.1, 70.0, 69.9, 69.8, 69.1, 65.0 (eight alkynyl carbons and four C-O carbons in the alkyl chains), 62.2, 55.8 (two *sp*³ carbons in the fullerene cages), 32.2, 30.2, 30.1, 29.9, 29.89, 29.83, 29.7, 29.6, 29.5, 29.4, 26.8, 26.3, 26.2, 22.9, 14.39, 14.36; MALDI-TOF MS *m/z* calcd for C₂₄₀H₁₇₈O, 3187.35, found 3187.81 [M + H]⁺.

Compound 261. Compound **261** (6.00 mg, 0.0025 mmol, 5%) was obtained as a brownish unstable solid by the same *in situ* ethynylation protocol as described in the synthesis of **196a**, using compound **289** (50 mg, 0.052 mmol), C₆₀ (185 mg, 0.257 mmol), LHMDs (0.26 mL, 1 M, 0.26 mmol) and dry THF (180 mL). ¹H NMR (CDCl₃, CS₂, 500 MHz) δ 7.16 (s, 2H), 7.10 (s, 2H), 7.01 (s, 2H), 4.09-4.05 (m, 8H, OCH₂), 1.93-1.84 (m, 8H), 1.65-1.60 (m, 1H), 1.54-1.50 (m, 4H), 1.29-1.19 (m, 48H), 0.90-0.81 (m, 12H).

Compound 262a. Compound **262a** (11 mg, 0.0017 mmol, 20%) was obtained as a brownish solid by the same *in situ* ethynylation protocol as described in the synthesis of **196a**, using compound **307** (30 mg, 0.0083 mmol), C₆₀ (60 mg, 0.083 mmol), LHMDs (0.10 mL, 1 M, 0.10 mmol) and dry THF (120 mL). IR (KBr) 2922,

2851, 2211, 2150, 1632, 1576, 1504, 1464 cm^{-1} ; ^1H NMR ($\text{CDCl}_3/\text{CS}_2$, 500 MHz) δ 7.71 (s, 2H), 7.66 (s, 4H), 7.29 (s, 4H), 7.18 (s, 4H), 7.15 (s, 4H), 7.08 (s, 4H), 7.05 (s, 4H), 4.17-4.01 (m, 32H, OCH_2), 1.93-1.87 (m, 32H), 1.70-1.54 (m, 32H), 1.42-1.20 (m, 192H), 0.91-0.81 (m, 48H, CH_3); ^{13}C NMR ($\text{CDCl}_3/\text{CS}_2$, 125 MHz) δ 155.0, 154.3, 154.1, 154.0 (four C-O in the phenyl rings), 152.1, 152.0, 148.2, 147.9, 147.2, 146.9, 146.8, 146.4, 146.3, 146.25, 146.18, 146.0, 145.98, 145.91, 145.2, 145.1, 143.7, 143.2, 143.1, 142.7, 142.6, 142.54, 142.46, 142.23, 142.16, 140.93, 140.86, 136.6, 135.7 (29 discernible sp^2 carbons of the 30 different sp^2 carbons in the C₆₀ symmetrical C₆₀ core), 135.1, 124.8, 122.7, 117.48, 117.42, 117.3, 117.1, 115.3, 115.1, 113.7, 113.2 (aromatic carbons in the phenyl rings), 97.8, 93.1, 92.1, 92.0, 88.1, 80.6 (alkynyl carbons), 70.0, 69.9, 69.8, 69.7 (four C-O carbons in the alkyl chains), 62.2, 55.8 (2 sp^3 carbons in the fullerene cages), 32.2, 30.2, 30.1, 30.0, 29.96, 29.92, 29.8, 29.7, 26.8, 26.5, 26.3, 23.0, 14.4; MALDI-TOF MS m/z calcd for $\text{C}_{488}\text{H}_{362}\text{O}_{16}$ 6476.75, found 6477.11 $[\text{M} + \text{H}]^+$.

1,4-Bis(decyloxy)-2-ethynyl-5-iodobenzene (263). To a solution of compound **203** (472 mg, 0.760 mmol) in 1:1 MeOH : THF (20 mL) was added K_2CO_3 (50 mg, 0.36 mmol). After being stirred at rt for 2 h, the reaction solvent was evaporated *in vacuo*. To the residue was added hexane and 1 M HCl. The organic layer was isolated and then washed with brine, and dried over MgSO_4 . Filtration to remove MgSO_4 followed by evaporation under vacuum afforded deprotected terminal alkyne **263** (412 mg, 0.762 mmol, 99%). Mp 50-51 $^\circ\text{C}$; IR (KBr) 3289, 2955, 2921, 2850, 2107, 1588, 1495, 1467 cm^{-1} ; ^1H NMR (CDCl_3 , 500 MHz) δ 7.29 (s, 1H), 6.87 (s, 1H), 3.96 (t, J = 6.5 Hz, 2H, OCH_2), 3.93 (t, J = 6.5 Hz, 2H, OCH_2), 3.29 (s, 1H), 1.81-1.78 (m, 4H), 1.54-1.44 (m, 4H), 1.36-1.25 (m, 24 H), 0.90-0.87 (m, 6H, CH_3);

^{13}C NMR (CDCl_3 , 125 MHz) δ 155.3, 152.2 (two C-O in the phenyl rings), 124.3, 117.2, 112.7, 88.8, 82.2, 80.1 (four aromatic carbons and two alkynyl carbons), 70.6, 70.4 (two C-O carbons in the alkyl chains), 32.3, 30.0, 29.8, 29.58, 29.57, 26.6, 26.5, 26.3, 23.1, 14.5; APCI-MS m/z calcd For $\text{C}_{28}\text{H}_{15}\text{IO}_2$ 540.3, found 541.3 $[\text{M} + \text{H}]^+$.

1,4-Bis(2,5-bis(decyloxy)-4-iodophenyl)buta-1,3-diyne (264). Compound **263** (215 mg, 0.387 mmol) was dissolved in acetone (10 mL), then Hay catalyst³³⁰ (5 mL) was added. The mixture was stirred at rt under exposure to air for 36 h. When TLC analysis showed no starting material present, acetone was evaporated *in vacuo*, and CHCl_3 (10 mL) was added. The resulting content was washed with aq HCl (1 M), satd NaHCO_3 , and brine sequentially. The organic layer was dried over MgSO_4 and evaporated *in vacuo* to give the crude product. The crude product was purified by silica flash column chromatography (hexanes/ CH_2Cl_2 , 85:15) to yield compound **264** (160 mg, 0.146 mmol, 75%) as a pale yellow solid. Mp 104–105 °C; IR (KBr) 2918, 2847, 2149, 1494 cm^{-1} ; ^1H NMR (CDCl_3 , 500 MHz) δ 7.29 (s, 2H), 6.87 (s, 2H), 3.96 (t, J = 6.0 Hz, 4H, OCH_2), 3.93 (t, J = 6.5 Hz, 4H, OCH_2), 1.83–1.77 (m, 8H), 1.50–1.44 (m, 8H), 1.36–1.25 (m, 48 H), 0.88 (t, J = 6.5 Hz, 6H, CH_3), 0.86 (t, J = 6.5 Hz, 6H, CH_3); ^{13}C NMR (CDCl_3 , 125 MHz) δ 155.8, 152.0 (two C-O in the phenyl rings), 124.2, 116.8, 112.5, 89.4, 79.0, 78.8 (four aromatic carbons and two alkynyl carbons), 70.3, 70.2 (two C-O carbons in the alkyl chains), 32.1, 29.8 (br), 29.5 (br), 29.4, 29.3, 26.4, 26.1, 22.9, 14.3; MALDI-TOF MS m/z calcd For $\text{C}_{56}\text{H}_{88}\text{I}_2\text{O}_4$ 1078.48, found 1078.44 $[\text{M}]^+$.

1,4-Bis(2,5-bis(decyloxy)-4-((trimethylsilyl)ethynyl)phenyl)buta-1,3 - diyne (265). Compound **264** (481 mg, 0.446 mmol), trimethylsilylacetylene (0.32 mL, 1.37 mmol), PdCl₂(PPh₃)₂ (31 mg, 0.044 mmol), CuI (17 mg, 0.091 mmol) and Et₃N (15 mL) were added to THF (15 mL). The solution was bubbled by N₂ at rt for 5 min and then stirred at rt under N₂ protection for 4 h. After the reaction was complete as checked by TLC analysis, the solvent was removed by rotary evaporation. To the residue obtained was added chloroform. The mixture was filtered over MgSO₄ pad. Then it was sequentially washed with aq HCl (10%) and brine. The organic layer was dried over MgSO₄ and concentrated under vacuum. The crude product was then purified by silica flash column chromatography (hexanes/CH₂Cl₂, 10:1) to yield compound **265** (367 mg, 0.360 mmol, 86%) as a yellow solid. Mp 119–120 °C; IR (KBr) 2923, 2901, 2869, 2850, 2157, 1499, 1469 cm⁻¹; ¹H NMR (CDCl₃, 500 MHz) δ 6.92 (s, 2H), 6.91 (s, 2H), 3.97 (t, *J* = 7.0 Hz, 4H, OCH₂), 3.94 (t, *J* = 6.5 Hz, 4H, OCH₂), 1.82-1.77 (m, 8H), 1.51-1.45 (m, 8H), 1.34-1.28 (m, 48 H), 0.88 (t, *J* = 7.0 Hz, 6H, CH₃), 0.86 (t, *J* = 7.0 Hz, 6H, CH₃), 0.26 (s, 18H, Si(CH₃)₃); ¹³C NMR (CDCl₃, 125 MHz) δ 155.0, 154.2 (two C-O in the phenyl rings), 117.9, 117.5, 115.1, 113.0, 101.2, 101.0, 79.6, 79.5 (four aromatic carbons and four alkynyl carbons), 70.0, 69.7 (two C-O carbons in the alkyl chains), 32.1, 29.9, 29.8, 29.7, 29.6, 29.4, 26.2, 26.1, 22.9, 14.3, 0.15 (Si(CH₃)₃); MALDI-TOF MS *m/z* calcd. for C₆₆H₁₀₆O₄Si₂ 1018.76, found 1020.71 [M+H]⁺.

1,4-Bis(2,5-bis(decyloxy)-4-ethynylphenyl)buta-1,3-diyne (266). To a solution of compound **265** (367 mg, 0.360 mmol) in 1:1 MeOH/THF (20 mL) was added K₂CO₃ (50 mg, 0.036 mmol). After being stirred at rt for 1 h, the reaction

solvent was removed by rotary evaporation. The residue was dissolved in chloroform and sequentially washed with aq HCl (10%) and brine. The organic layer dried over MgSO₄. Filtration to remove MgSO₄ followed by evaporation under vacuum afforded **266** as a yellow solid (302 mg, 0.345 mmol, 96%). Mp 110–111 °C; IR (KBr) 3283, 2923, 2850, 2140, 2105, 1500, 1469 cm⁻¹; ¹H NMR (CDCl₃, 500 MHz) δ 6.96 (s, 2H), 6.95 (s, 2H), 3.971 (t, *J* = 6.5 Hz, 4H, OCH₂), 3.965 (t, *J* = 7.0 Hz, 4H, OCH₂), 3.35 (s, 2H), 1.84–1.77 (m, 8H), 1.50–1.41 (m, 8H), 1.36–1.25 (m, 18 H), 0.88 (t, *J* = 7.0 Hz, 6H, CH₃), 0.86 (t, *J* = 6.0 Hz, 6H, CH₃); ¹³C NMR (CDCl₃, 125 MHz) δ 155.0, 154.2 (two C-O in the phenyl rings), 118.1, 117.9, 113.9, 113.4, 83.1, 80.1, 79.4 (aromatic carbons and alkynyl carbons), 70.0, 69.9 (two C-O carbons in the alkyl chains), 32.1, 29.9, 29.8, 29.79, 29.76, 29.6, 29.3, 26.1, 22.9, 14.3; MALDI-TOF MS *m/z* calcd for C₆₀H₉₀O₄ 874.68, found 876.61 [M + H]⁺.

1,4-Bis(4-((2,5-bis(decyloxy)-4-((triisopropylsilyl)ethynyl)phenyl)ethynyl)-2,5-bis(decyloxy)phenyl)buta-1,3-diyne (267). To a solution of **226** (226 mg, 0.224 mmol) in acetone (30 mL) was added Hay catalyst (5 mL). The mixture was stirred at rt under exposure to air overnight. The reaction solvent was evaporated *in vacuo*. To the residue was added CHCl₃. The resulting content was washed with aq HCl (1 M), satd NaHCO₃, and brine sequentially. The organic layer was dried over MgSO₄ and evaporated *in vacuo* to give the crude product, which was further purified by silica flash column chromatography (hexanes/CH₂Cl₂, 3:1) to give compound **267** (96 mg, 0.48 mmol, 43%) as a yellow solid. Mp 72–73 °C; IR (KBr) 2924, 2852, 2146, 1622, 1497, 1470 cm⁻¹; ¹H NMR (CDCl₃, 500 MHz) δ 6.99 (s, 4H), d 6.94 (s, 4H), 4.03–3.94 (m, 16H, OCH₂), 1.86–1.77 (m, 16H), 1.50 (m, 16H), 1.36–1.25 (m, 96 H),

1.15 (s, 42H, Si(CH(CH₃)₂)₃), 0.89-0.85 (m, 24H, CH₃); ¹³C NMR (CDCl₃, 125 MHz) δ 155.2, 154.6, 153.5 (C-O in the phenyl rings), 118.2, 118.1, 117.3, 116.7, 115.7, 114.44, 114.41, 112.8, 103.3, 96.8, 92.5, 91.4, 79.8, 79.6 (eight aromatic carbons and six alkynyl carbons), 70.1, 70.0, 69.5 (C-O carbons in the alkyl chains), 32.1, 29.91, 29.85, 29.77, 29.74, 29.7, 29.6, 29.5, 29.4, 26.5, 26.2, 22.9, 18.9, 14.3, 11.6; MALDI-TOF MS *m/z* calcd For C₁₃₄H₂₁₈O₈Si₂ 2011.62, found 2012.77 [M + H]⁺.

1,4-Bis(4-((2,5-bis(decyloxy)-4-ethynylphenyl)ethynyl)-2,5-bis(decyloxy)-phenyl)buta-1,3-diyne (268). To a solution of compound **267** (303 mg, 0.154 mmol) in THF (20 mL) was added TBAF (0.1 mL, 1 M, 0.1 mmol). The mixture was stirred at rt for 12 h. The reaction solvent was evaporated *in vacuo*. To the residue was added CHCl₃. The resulting content was washed with aq HCl (1 M), satd NaHCO₃, and brine sequentially. The organic layer was dried over MgSO₄ and evaporated *in vacuo* to give the crude product, which was further purified by silica flash column chromatography (hexanes/CH₂Cl₂, 7:3) to yield compound **268** (211 mg, 0.124 mmol, 82%) as a yellow solid. Mp 93–94 °C; IR (KBr) 3315, 2925, 2850, 2195, 2136, 2106, 1639, 1618, 1497, 1469 cm⁻¹; ¹H NMR (CDCl₃, 500 MHz) δ 6.70 (s, 6H), 6.99 (s, 2H), 4.03-3.99 (m, 16H, OCH₂), 3.35 (s, 2H), 1.87-1.79 (m, 16H), 1.54-1.46 (m, 16H), 1.36-1.26 (m, 96H), 0.90-0.86 (m, 24H, CH₃); MALDI-TOF MS *m/z* calcd for C₁₁₆H₁₇₈O₈ 1699.35, found 1699.96 [M + H]⁺.

3-(2,5-Bis(decyloxy)-4-iodophenyl)prop-2-yn-1-ol (269). Compound **202** (6.40 g, 9.96 mmol), propargyl alcohol (0.42 mL, 7.11 mmol), PdCl₂(PPh₃)₂ (122 mg, 0.174 mmol), CuI (66.6 mg, 0.351 mmol) and Et₃N (30 mL) were added to THF (30

mL). The solution was bubbled by N₂ at rt for 5 min and then stirred at rt under N₂ protection for 12 h. After the reaction was complete as checked by TLC analysis, the solvent was removed by rotary evaporation. To the residue obtained was added chloroform. The mixture was filtered over MgSO₄ pad. Then it was sequentially washed with aq HCl (10%) and brine. The organic layer was dried over MgSO₄ and concentrated under vacuum. The crude product was then purified by silica flash column chromatography (EtOAc/CH₂Cl₂ 5:95) to yield compound **269** (3.20 g, 5.61 mmol, 56%) as a yellow solid. Mp 64–65 °C; ¹H NMR (CDCl₃, 500 MHz) δ 7.00 (s, 1H), 6.55 (s, 1H), 4.24 (s, 2H), 3.687 (t, *J* = 6.5 Hz, 2H), 3.64 (t, *J* = 6.5 Hz, 2H), 2.19 (s, 1H, OH), 1.54–1.49 (m, 4H), 1.25–1.15 (m, 4H), 1.06–1.01 (m, 24 H), 0.63 (t, *J* = 7.0 Hz, 6H, CH₃); ¹³C NMR (CDCl₃, 125 MHz) δ 154.3, 151.9 (two C-O in the phenyl ring), 124.0, 116.4, 113.0, 92.2, 87.9, 81.7 (four aromatic carbons and two alkynyl carbons), 70.16, 70.12 (two C-O carbons in the alkyl chains), 51.8 (CH₂OH), 32.0, 29.72, 29.66, 29.4, 29.28, 29.25, 26.2, 26.0, 22.8, 14.2; APCI-MS (positive) *m/z* calcd for C₂₉H₄₇O₃ 570.26, found 553.3 [M-OH]⁺.

3-(2,5-Bis(decyloxy)-4-((triisopropylsilyl)ethynyl)phenyl)prop-2-yn-1-ol (270). Compound **269** (475 mg, 0.832 mmol), triisopropylsilylacetylene (0.185 mL, 0.832 mmol), PdCl₂(PPh₃)₂ (14.4 mg, 0.0205 mmol), CuI (7.8 mg, 0.041 mmol) were added to Et₃N (20 mL). The solution was bubbled by N₂ at rt for 5 min and then stirred at rt under N₂ protection for 12 h. After the reaction was complete as checked by TLC analysis, the solvent was removed by rotary evaporation. To the residue obtained was added chloroform. The mixture was filtered over MgSO₄ pad. Then it was sequentially washed with aq HCl (10%) and brine. The organic layer was dried

over MgSO_4 and concentrated under vacuum. The crude product was then purified by silica flash column chromatography ($\text{EtOAc}:\text{CH}_2\text{Cl}_2$, 5:95) to yield compound **270** (519 mg, 0.833 mmol, 100%) as a yellow solid. Mp 52–53 °C; IR (KBr) 3374 (br), 2924, 2863, 2228, 2151, 1499, 1468, 1409, 1388 cm^{-1} ; ^1H NMR (CDCl_3 , 500 MHz) δ 6.91 (s, 1H), 6.88 (s, 1H), 4.52 (s, 2H), 3.97 (t, $J = 6.5$ Hz, 2H), 3.91 (t, $J = 6.5$ Hz, 2H), 2.26 (s, 1H, OH), 1.80–1.74 (m, 4H), 1.48–1.45 (m, 4H), 1.28 (br, 24 H), 0.889 (t, $J = 6.5$ Hz, 3H, CH_3), 0.887 (t, $J = 6.5$ Hz, 3H, CH_3); ^{13}C NMR (CDCl_3 , 125 MHz) δ 154.5, 153.4 (two C–O carbons in the phenyl ring), 117.9, 116.9, 114.4, 113.5, 103.0, 96.6, 92.7, 82.2 (four aromatic carbons and four alkynyl carbons), 70.0, 69.4 (two C–O carbons in the alkyl chains), 51.9 (CH_2OH), 32.1, 29.81, 29.75, 29.7, 29.6, 29.55, 29.54, 29.4, 26.4, 26.1, 22.9, 18.9, 14.3, 11.6; APCL-MS (positive) m/z calcd for $\text{C}_{40}\text{H}_{68}\text{O}_3\text{Si}$ 624.49, found 607.5 $[\text{M}-\text{OH}]^+$.

3-(2,5-Bis(decyloxy)-4-((triisopropylsilyl)ethynyl)phenyl)propiolaldehyde (271). To a solution of oxalyl chloride (0.74 mL, 8.5 mmol) in CH_2Cl_2 (15 mL) was added a solution of DMSO (0.81 mL, 11 mmol) in CH_2Cl_2 (15 mL) at -78 °C. The mixture was stirred under N_2 for 10 min. Then it was added dropwise to a solution of **270** (1.77 g, 2.84 mmol) in CH_2Cl_2 (30 mL) at -78 °C. The reaction was further stirred for 15 minutes. Then the reaction was treated with triethylamine (2.1 mL, 14 mmol) and allowed to warm to -10 °C over 1 h. The mixture was treated with water (20 mL) and allowed to warm to rt. The organic layer was separated, washed with brine, dried over MgSO_4 and concentrated under vacuum. The crude product was then purified by silica flash column chromatography (hexane CH_2Cl_2 , 3:1) to yield compound **271** (1.42 g, 2.28 mmol, 80%) as a yellow solid. Mp 36–37

°C. IR (neat) 2925, 2858, 2190, 2153, 1685, 1661, 1604, 1498, 1467, 1413, 1387 cm^{-1} ; ^1H NMR (CDCl_3 , 500 MHz) δ 9.44 (s, 1H, CHO), 6.97 (s, 1H), 6.95 (s, 1H), 4.01 (t, J = 6.5 Hz, 2H, OCH_2), 3.93 (t, J = 6.5 Hz, 2H, OCH_2), 1.84-1.76 (m, 4H), 1.49-1.46 (m, 4H), 1.37-1.28 (m, 24H), 1.15 (s, 21H, $\text{Si}(\text{CH}(\text{CH}_3)_2)_3$), 0.89 (t, J = 6.5 Hz, 6H, CH_3); ^{13}C NMR (CDCl_3 , 125 MHz) δ 176.7 (CHO), 155.4, 154.3 (two C-O carbons in the phenyl ring), 118.1, 117.65, 117.61, 109.6, 102.5, 99.2, 93.5, 92.6 (four aromatic carbons and four alkynyl carbons), 69.9, 69.6 (two C-O carbons in the alkyl chains), 32.1, 29.83, 29.80, 29.76, 29.7, 29.6, 29.5, 29.3, 26.4, 26.1, 22.9, 18.9, 14.3, 11.6; APCI-MS (positive) m/z calcd for $\text{C}_{40}\text{H}_{66}\text{O}_3\text{Si}$ 622.5, found 623.5 $[\text{M} + \text{H}]^+$.

((2,5-Bis(decyloxy)-4-iodophenyl)buta-1,3-diynyl)trimethylsilane (275).

To a flask containing compound **263** (849 mg, 1.57 mmol) trimethylsilylacetylene (0.70 mL, 4.9 mmol), acetone (20 mL) was added Hay catalyst (2 mL). The mixture was stirred at rt under exposure to air for 2 h. When TLC analysis showed no starting material present, hexanes (40 mL) was added. The resulting content was washed with aq HCl (1 M), satd NaHCO_3 , and brine sequentially. The organic layer was dried over MgSO_4 and evaporated *in vacuo* to give a dark yellow solid. The crude product was purified by silica flash column chromatography (hexanes CH_2Cl_2 , 5:1) to yield compound **275** (675 mg, 1.06 mmol, 68%) as a yellow solid. Mp 41-42 °C. IR (neat) 2922, 2851, 2208, 2104, 1496 cm^{-1} ; ^1H NMR (CDCl_3 , 500 MHz) δ 7.27 (s, 1H), 6.83 (s, 1H), 3.94 (t, J = 7.0 Hz, 2H, OCH_2), 3.90 (t, J = 6.5 Hz, 2H, OCH_2), 1.79 (m, 4H), 1.47 (m, 4H), 1.40-1.22 (m, 24 H), 0.88 (t, J = 6.0 Hz, 6H, CH_3), 0.22 (s, 9H); ^{13}C NMR (CDCl_3 , 125 MHz) δ 156.1, 152.0 (two C-O carbons in the phenyl ring), 124.2, 111.9, 91.8, 89.6, 88.2, 78.8, 73.3, 70.11, 70.12, 70.14 (four aromatic carbons,

four alkynyl carbons and two C-O carbons in the alkyl chains), 32.1, 29.8 (br), 29.5 (br), 29.3, 26.3, 26.1, 22.9, 14.4, -0.1; APCI-MS (positive) m/z calcd For $C_{33}H_{53}IO_2Si$ 636.7, found 636.3 $[M]^+$.

1,8-Bis(2,5-bis(decyloxy)-4-iodophenyl)octa-1,3,5,7-tetrayne (276). To a solution of compound **275** (277 mg, 0.401 mmol) in 1:1 MeOH THF (8 mL) was added K_2CO_3 (20 mg, 0.14 mmol). After being stirred at rt for 2 h, the reaction mixture was quenched with water (10 mL) and then extracted with hexanes (30 mL). The organic layer was isolated and washed with brine and dried over $MgSO_4$. Filtration to remove $MgSO_4$ followed by concentration under vacuum afforded a dark solid, which was immediately transferred into a flask containing acetone (6 mL) and Hay catalyst (2 mL). The mixture was stirred at rt under exposure to air overnight, and then was briefly worked up to afford the crude product, which was further purified by silica flash column chromatography (hexanes CH_2Cl_2 , 9:1) to give compound **276** (132 mg, 0.107 mmol, 53%) as a yellow solid. Mp 70–71 °C; IR (neat) 2916, 2849, 2198, 1494 cm^{-1} ; 1H NMR ($CDCl_3$, 500 MHz) δ 7.27 (s, 2H), 6.82 (s, 2H), 3.93 (t, J 6.5 Hz, 4H, OCH_2), 3.90 (t, J 6.5 Hz, 4H, OCH_2), 1.81–1.75 (m, 8H), 1.51–1.43 (m, 8H), 1.35–1.29 (m, 48 H), 0.89–0.87 (m, 12H, CH_3); ^{13}C NMR ($CDCl_3$, 125 MHz) δ 156.9, 151.9 (two C-O carbons in the phenyl rings), 120.0, 116.8, 110.8, 90.9, 79.0, 74.6, 70.3, 70.1 (four aromatic carbons and four alkynyl carbons), 68.6, 64.6 (two C-O carbons in the alkyl chains), 32.2, 32.1, 29.81, 29.78, 29.59, 29.54, 29.51, 29.38, 29.31, 29.3, 26.3, 26.1, 22.94, 22.91, 14.36, 14.33; MALDI-TOF MS m/z calcd For $C_{60}H_{88}I_2O_4$ 1126.48, found 1128.28 $[M+H]^+$.

((2,5-Bis(decyloxy)-4-((triisopropylsilyl)ethynyl)phenyl)buta-1,3-diynyl)-trimethylsilane (278). Method 1: Compound **275** (675 mg, 1.06 mmol), triisopropylsilylacetylene (0.28 mL, 1.2 mmol), PdCl₂(PPh₃)₂ (37 mg, 0.053 mmol), CuI (30 mg, 0.16 mmol) and Et₃N (3 mL) were added to THF (20 mL). The solution was bubbled by N₂ at rt for 5 min and then stirred at 45 °C under N₂ protection overnight. After the reaction was complete as checked by TLC analysis, the solvent was removed by rotary evaporation. To the residue was added CHCl₃ and 1M HCl. The organic layer was isolated and washed with brine and dried over MgSO₄. Filtration to remove MgSO₄ followed by evaporation under vacuum afforded the crude product which was then purified by silica flash column chromatography (hexanes/CH₂Cl₂ 10:1) to yield compound **278** (630 mg, 0.911 mmol, 86%) as a pale yellowish wax.

Method 2: To a flask containing acetone (10 mL) was added **230** (119 mg, 0.200 mmol), trimethylsilylacetylene (0.169 mL, 1.22 mmol) and Hay catalyst (5 mL). The mixture was stirred at rt under exposure to air for 20 h. When TLC analysis showed no starting material present, acetone was evaporated *in vacuo*. CHCl₃ (30 mL) was added. The resulting content was washed with aq HCl (1 M), satd NaHCO₃, and brine sequentially. The organic layer was dried over MgSO₄ and evaporated *in vacuo* to give the crude product, which was purified by silica flash column chromatography (hexanes/CH₂Cl₂, 10:1) to yield compound **278** (102 mg, 0.142 mmol, 71%) as a yellow wax. IR (neat) 2924, 2857, 2201, 2151, 2100, 1497 cm⁻¹; ¹H NMR (CDCl₃, 500 MHz) δ 6.90 (s, 1H), 6.89 (s, 1H), 3.97 (t, *J* = 6.5 Hz, 2H, OCH₂), 3.92 (t, *J* = 6.0 Hz, 2H, OCH₂), 1.82-1.72 (m, 4H), 1.50-1.42 (m, 4H), 1.40-1.24 (m, 24 H), 1.14 (s, 21H), 0.89 (t, *J* = 7.0 Hz, 6H, CH₃), 0.23 (s, 9H, Si(CH₃)₃); ¹³C NMR (CDCl₃, 125

MHz) δ 155.5, 154.5 (two C-O carbons in the phenyl ring), 118.1, 117.7, 115.7, 112.4, 103.1, 97.9, 92.2, 88.5, 79.4, 73.9 (four aromatic carbons and six alkynyl carbons), 70.3, 69.7 (two C-O carbons in the alkyl chains), 32.3, 32.2, 30.3, 30.1, 30.0, 29.9, 29.8, 29.6, 29.0, 26.6, 26.4, 26.2, 23.1, 19.4, 19.2, 19.0, 18.9, 18.6, 14.5, 11.8, -0.1; MALDI-TOF MS m/z calcd for $C_{44}H_{74}O_2Si_2$ 690.52, found 691.26 $[M+H]^+$.

1,8-Bis(2,5-bis(decyloxy)-4-((triisopropylsilyl)ethynyl)phenyl)octa-1,3,-5,7-tetrayne (280). To a solution of compound **278** (277 mg, 0.401 mmol) in 1:1 MeOH/THF (8 mL) was added K_2CO_3 (20 mg, 0.14 mmol). After being stirred at rt for 2 h, the reaction mixture was quenched with water (10 mL) and then extracted with hexanes (30 mL). The organic layer was isolated and washed with brine and dried over $MgSO_4$. Filtration to remove $MgSO_4$ followed by concentration under vacuum afforded a dark solid, which was immediately transferred into a flask containing acetone (6 mL) and Hay catalyst (2 mL). The mixture was stirred at rt under exposure to air overnight, and then was briefly worked up to afford the crude product. Silica flash column chromatography (hexanes/ CH_2Cl_2 , 9:1) gave compound **280** (132 mg, 0.107 mmol, 53%) as a brownish solid. Mp 58–59 °C; IR (neat) 2921, 2852, 2193, 2150, 1498 cm^{-1} ; 1H NMR ($CDCl_3$, 500 MHz) δ 6.89 (s, 4H), 3.97 (t, $J = 6.5$ Hz, 4H, OCH_2), 3.91 (t, $J = 6.5$ Hz, 4H, OCH_2), 1.83–1.74 (m, 8H), 1.51–1.44 (m, 8H), 1.40–1.24 (m, 48 H), 1.14 (s, 42H, $Si(CH(CH_3)_3)$), 0.89 (m, 12H, CH_3); ^{13}C NMR ($CDCl_3$, 125 MHz) δ 156.4, 154.5 (two C-O carbons in the phenyl rings), 117.9, 117.7, 116.6, 111.4 (four aromatic carbons), 103.1, 98.7, 79.7, 75.3, 70.2, 69.7, 69.1, 65.0 (six alkynyl carbons and two C-O carbons in the alkyl chains), 32.5, 32.4, 32.3, 30.4, 30.0, 29.9, 29.8, 29.6, 29.0, 26.4, 26.2, 23.2, 23.1, 19.4, 19.2, 19.1, 19.0, 18.9,

18.7, 14.5, 11.8; MALDI-TOF MS m/z calcd for $C_{32}H_{130}O_1Si_2$ 1234.95, found 1237.12 $[M+H]^+$.

1,8-Bis(2,5-bis(decyloxy)-4-ethynylphenyl)octa-1,3,5,7-tetrayne (281).

To a solution of compound **280** (190 mg, 0.154 mmol) in THF (4 mL) was added TBAF (0.09 mL, 1 M, 0.09 mmol). The mixture was stirred at rt for 10 min. The solvent was removed by rotary evaporation. To the residue was added $CHCl_3$ and 1M HCl. The organic layer was isolated and washed with brine and dried over $MgSO_4$. Filtration to remove $MgSO_4$ followed by evaporation under vacuum afforded the crude product, which was further purified by silica flash column chromatography (hexanes, CH_2Cl_2 1:9) to yield compound **281** (110 mg, 0.119 mmol, 77%) as a brownish waxy solid. IR (KBr) 3314, 3293, 2916, 2850, 2195, 1604, 1530 cm^{-1} ; 1H NMR ($CDCl_3$, 500 MHz) δ 6.94 (s, 2H), 6.93 (s, 2H), 3.96 (t, $J = 6.5$ Hz, 8H, OCH_2), 3.38 (s, 2H), 1.82- 1.76 (m, 8H), 1.50-1.42 (m, 8H), 1.40-1.22 (m, 48H), 0.88 (m, 12H, CH_3); ^{13}C NMR ($CDCl_3$, 125 MHz) δ 156.2, 154.1 (two C-O carbons in the phenyl rings), 118.1, 117.8, 115.0, 111.8 (four aromatic carbons), 83.7, 79.7, 79.6, 74.7, 70.0, 69.9, 68.9, 64.7 (four alkynyl carbons and two C-O in the alkyl chains), 32.14, 32.13, 29.9, 29.80, 29.77, 29.6, 29.5, 29.3, 29.1, 26.14, 26.09; 22.93, 22.89, 14.35, 14.33; MALDI-TOF MS m/z calcd for $C_{64}H_{90}O_1$ 922.68, found 923.57 $[M+H]^+$.

((4-((2,5-Bis(decyloxy)-4-((triisopropylsilyl)ethynyl)phenyl)ethynyl)-2,5-bis(decyloxy)phenyl)buta-1,3-diyne)trimethylsilane (282). To a solution of **226** (590 mg, 0.586 mmol) and trimethylsilylacetylene (1.02 mL, 3.52 mmol) in acetone (20 mL) was added Hay catalyst (5 mL). The mixture was stirred at rt under

exposure to air overnight. The reaction solvent was evaporated *in vacuo*. To the residue was added CHCl_3 . The resulting content was washed with aq HCl (1 M), satd NaHCO_3 , and brine sequentially. The organic layer was dried over MgSO_4 and evaporated *in vacuo* to give the crude product. Silica flash column chromatography (hexanes/ CH_2Cl_2 , 4:1) gave compound **282** (513 mg, 0.465 mmol, 79%) as a yellow solid. Mp 70–71 °C; IR (KBr) 2923, 2852, 2196, 2150, 2100, 1622, 1497, 1468, 1389 cm^{-1} ; ^1H NMR (CDCl_3 , 500 MHz) δ 6.96 (s, 1H), 6.93 (s, 3H), 4.02–3.93 (m, 8H, OCH_2), 1.83–1.77 (m, 8H), 1.50–1.47 (m, 8H), 1.34–1.24 (m, 48 H), 1.15 (s, 21H, $\text{Si}(\text{CH}(\text{CH}_3)_2)_3$), 0.90–0.86 (m, 12H), 0.23 (s, 9H, $\text{Si}(\text{CH}_3)_3$); ^{13}C NMR (CDCl_3 , 125 MHz) δ 155.5, 154.6, 153.5, 153.4 (four C–O carbons in the phenyl rings), 118.3, 118.2, 117.2, 116.7, 115.9, 114.4, 112.1, 103.2, 96.7, 92.5, 91.9, 91.2, 88.4, 79.4, 73.7 (aromatic carbons and alkynyl carbons), 70.0, 69.9, 69.4 (C–O carbons in the alkyl chains), 32.1, 29.8, 29.74, 29.65, 29.57, 29.47, 29.4, 26.4, 26.2, 22.9, 18.9, 14.3, 11.6, 0.19; APCI-MS (positive) m/z calcd for $\text{C}_{72}\text{H}_{118}\text{O}_4\text{Si}_2$ 1102.9, found 1103.7 $[\text{M} + \text{H}]^+$.

1,8-Bis(4-((2,5-bis(decyloxy)-4-((triisopropylsilyl)ethynyl)phenyl)ethynyl)-2,5-bis(decyloxy)phenyl)octa-1,3,5,7-tetrayne (284). To a solution of compound **282** (513 mg, 0.465 mmol) in 1:1 MeOH/THF (30 mL) was added K_2CO_3 (100 mg, 0.72 mmol). After being stirred at rt for 2 h, the reaction solvent was evaporated *in vacuo*. To the residue was added CHCl_3 and then 1 M HCl. The organic layer was isolated and washed with brine and dried over MgSO_4 . Filtration to remove MgSO_4 followed by concentration under vacuum afforded a dark solid, which was immediately transferred into a flask containing acetone (20 mL) and Hay catalyst (5 mL). The mixture was stirred at rt under exposure to for 12 h. The reaction solvent

was evaporated *in vacuo*. To the residue was added CHCl_3 . The resulting content was washed with aq HCl (1 M), satd NaHCO_3 , and brine sequentially. The organic layer was dried with MgSO_4 and evaporated *in vacuo* to give the crude product. Silica flash column chromatography (hexane/ CH_2Cl_2 4:1) gave compound **284** (405 mg, 0.196 mmol, 85%) as a brownish solid. Mp 71–72 °C; IR (KBr) 2923, 2853, 2194, 2149, 1623, 1499, 1468, 1423, 1388 cm^{-1} ; ^1H NMR (CDCl_3 , 500 MHz) δ 6.98 (s, 2H), 6.97 (s, 2H), 6.95 (s, 4H), 4.04–3.94 (m, 16H, OCH_2), 1.85–1.81 (m, 16H), 1.51–1.48 (m, 16H), 1.37–1.25 (m, 96 H), 1.16 (s, 42H, $\text{Si}(\text{CH}(\text{CH}_3)_2)_3$), 0.92–0.87 (m, 24H, OCH_2); ^{13}C NMR (CDCl_3 , 125 MHz) δ 156.4, 154.6, 153.6, 153.4 (four C–O carbons in the phenyl rings), 118.2, 118.1, 117.0, 116.8, 116.7, 114.6, 114.2, 111.0 (eight aromatic carbons), 103.2, 96.9, 93.2, 91.2, 79.7, 75.2, 70.0, 69.91, 69.85, 69.4, 69.0, 64.9 (eight alkynyl carbons and four C–O carbons in the alkyl chains), 32.2, 32.1, 29.9, 29.88 (br), 29.83, 29.80, 29.75, 29.71, 29.68, 29.66, 29.6 (br), 29.5, 29.3, 26.4, 26.21, 26.17, 22.94, 22.90, 18.9, 14.35, 14.31, 11.6; MALDI-TOF MS m/z calcd for $\text{C}_{138}\text{H}_{218}\text{O}_8\text{Si}_2$ 2059.62, found 2060.33 $[\text{M} + \text{H}]^+$.

1,8-Bis(4-((2,5-bis(decyloxy)-4-ethynylphenyl)ethynyl)-2,5-bis(decyloxy)-phenyl)octa-1,3,5,7-tetrayne (285). To a solution of compound **284** (405 mg, 0.196 mmol) in THF (25 mL) was added TBAF (0.1 mL, 1 M, 0.1 mmol). The mixture was stirred at rt for 3 h. The reaction solvent was evaporated *in vacuo*. To the residue was added CHCl_3 . The resulting content was washed with aq HCl (1 M), satd NaHCO_3 , and brine sequentially. The organic layer was dried over MgSO_4 and evaporated *in vacuo* to give the crude product, which was further purified by silica flash column chromatography (hexanes/ CH_2Cl_2 , 3:1) to yield compound **285** (287

mg, 0.164 mmol, 83%) as a brownish solid. Mp 92–93 °C; IR (KBr) 3314, 2924, 2851, 2194, 2106, 1627, 1499, 1468, 1422, 1386 cm^{-1} ; ^1H NMR (CDCl_3 , 500 MHz) δ 6.973 (s, 2H), 6.969 (s, 2H), 6.96 (s, 4H), 4.01–3.96 (m, 16H, OCH_2), 3.34 (s, 2H), 1.85–1.78 (m, 16H), 1.52–1.44 (m, 16H), 1.36–1.24 (m, 96H), 0.90–0.86 (m, 24H, CH_3); ^{13}C NMR (CDCl_3 , 125 MHz) δ 156.4, 154.4, 153.6, 153.5 (four C–O carbons in the phenyl rings), 118.3, 118.2, 117.2, 117.1, 116.7, 114.8, 113.1, 111.2 (eight aromatic carbons), 92.8, 91.4, 82.6, 80.2, 79.7, 75.1, 69.9, 69.89, 69.83, 69.0, 64.9 (alkynyl carbons and four C–O carbons in the alkyl chains), 32.15, 32.12, 29.9, 29.83, 29.80, 29.77, 29.6, 29.58, 29.50, 29.43, 29.41, 29.3, 26.2, 22.9, 14.3; MALDI-TOF MS m/z calcd for $\text{C}_{120}\text{H}_{178}\text{O}_8$ 1747.35, found 1749.25 $[\text{M} + \text{H}]^+$.

((2,5-Bis(decyloxy)-4-((triisopropylsilyl)ethynyl)phenyl)hexa-1,3,5-tri-ynyl)trimethylsilane (286). To a solution of compound **278** (1.00 g, 1.45 mmol) in 1:1 MeOH/THF (60 mL) was added K_2CO_3 (500 mg, 3.62 mmol). After being stirred at rt for 2 h, the reaction solvent was evaporated *in vacuo*. To the residue was added hexane and 1 M HCl. The organic layer was isolated and washed with brine and dried over MgSO_4 . Filtration to remove MgSO_4 followed by evaporation under vacuum afforded the deprotected terminal alkyne, which was immediately transferred into a flask containing trimethylsilylacetylene (15 mL, 0.11 mol), acetone (90 mL), and Hay catalyst (10 mL). The mixture was stirred at rt under exposure to air for 6 h. When TLC analysis showed no starting material present, the reaction solvent was evaporated *in vacuo*. To the residue was added CHCl_3 . The resulting mixture was washed with aq HCl (1 M), satd NaHCO_3 , and brine sequentially. The organic layer was dried over MgSO_4 and evaporated *in vacuo* to give a brown wax. The

crude product was purified by silica flash column chromatography (hexanes/CH₂Cl₂, 95:5) to yield compound **286** (930 mg, 1.30 mmol, 90% based on consumed **278**) as a brown wax. IR (KBr) 2924, 2854, 2170, 2152, 2077, 1450, 1469 cm⁻¹; ¹H NMR (CDCl₃, 500 MHz) δ 6.88 (s, 2H), 3.96 (t, *J* = 6.5 Hz, 2H, OCH₂), 3.90 (t, *J* = 6.50 Hz, 2H, OCH₂), 1.78-1.75 (m, 4H), 1.47-1.45 (m, 4H), 1.29-1.27 (m, 24 H), 1.13 (s, 21H, Si(CH(CH₃)₃)); 0.90-0.87 (m, 6H), 0.22 (s, 9H, Si(CH₃)₃); ¹³C NMR (CDCl₃, 125 MHz) δ 156.0, 154.3, 117.7, 117.5, 116.2, 111.4 (six aromatic carbons), 102.8, 98.2, 89.7, 88.5, 79.3, 73.9, 70.0, 69.5, 68.3, 62.0 (eight alkynyl carbons and two C-O carbons), 32.14, 32.13, 29.84, 29.81, 29.7, 29.60, 29.58, 29.55, 29.4, 26.4, 26.2, 22.94, 22.91, 18.9, 14.36, 14.33, 11.6, 0.27; MALDI-TOF MS *m/z* calcd for C₄₆H₇₄O₂Si₂ 714.52, found 716.49 [M+H]⁺.

1,12-Bis(2,5-bis(decyloxy)-4-((triisopropylsilyl)ethynyl)phenyl)dodeca-1,3,5,7,9,11-hexayne (288). To a solution of compound **286** (930 mg, 1.30 mmol) in 1:1 MeOH/THF (40 mL) was added K₂CO₃ (200 mg, 1.40 mmol). After being stirred at rt for 1.5 h, the reaction solvent was evaporated *in vacuo*. To the residue was added CHCl₃ and then 1 M HCl. The organic layer was isolated and washed with brine and dried over MgSO₄. Filtration to remove MgSO₄ followed by concentration under vacuum afforded a dark solid, which was immediately transferred into a flask containing acetone (80 mL) and Hay catalyst (10 mL). The mixture was stirred at rt under exposure to for 2 h. The reaction solvent was evaporated *in vacuo*. To the residue was added CHCl₃. The resulting mixture was washed with aq HCl (1 M), satd NaHCO₃, and brine sequentially. The organic layer was dried over MgSO₄ and evaporated *in vacuo* to give the crude product. The crude product was further purified

by silica flash column chromatography (hexane/CH₂Cl₂, 95:5) to give compound **288** (325 mg, 0.253 mmol, 39%) as a brownish wax. IR (KBr) 2925, 2859, 2153, 2046, 1499, 1466, 1416 cm⁻¹; ¹H NMR (CDCl₃, 500 MHz) δ 6.89 (s, 2H), 6.88 (s, 2H), 3.97 (t, *J* = 6.5 Hz, 4H, OCH₂), 3.92 (t, *J* = 6.5 Hz, 4H, OCH₂), 1.78-1.77 (m, 8H), 1.47-1.45 (m, 8H), 1.33-1.27 (m, 48 H), 1.13 (s, 42H, Si(CH₃)₃), 0.91-0.87 (m, 12H, OCH₂); ¹³C NMR (CDCl₃, 125 MHz) δ 156.7, 154.3, 117.7, 117.5, 116.9, 110.6 (six aromatic carbons), 102.8, 98.9, 79.3, 74.8, 70.0, 69.5, 68.9, 65.6, 64.3, 63.2 (eight alkynyl carbons and two C-O carbons in the alkyl chains), 32.2, 32.1, 30.1, 29.8, 29.7, 29.6, 29.3, 26.4, 26.2, 22.94, 22.91, 19.4, 19.3, 19.1, 19.0, 18.8, 14.35, 14.33, 11.6; MALDI-TOF MS *m/z* calcd for C₈₂H₁₃₀O₄Si₂ 1282.95, found 1284.96.

(3,5-Diiodophenyl)methanol (292). Method 1: To a solution of **291** (521 mg, 1.34 mmol) in 30 mL THF and EtOH (THF/EtOH = 1:1) was added LiBH₄ (175 mg, 8.04 mmol) in three portions over a period of 42 h at rt. Then the reaction was worked up by adding 1 M HCl (20 mL) at 0 °C and extracted with CH₂Cl₂ (3 × 30 mL). The extract was washed with brine, dried over MgSO₄, and the solvent was removed. The crude product was purified by silica flash column chromatography (hexane/CH₂Cl₂, 4:1) to give **292** (355 mg, 0.986 mmol, 74%) as a white solid.

Method 2: To a solution of **291** (1.00 g, 2.58 mmol) in dry CH₂Cl₂ (20 mL) was added DIBAL (8.67 mL, 1M in THF, 8.67 mmol) at 0 °C in two portions during a period of 4 h. The reaction treated with 1 M HCl slowly at 0 °C, and extracted with CH₂Cl₂. The organic layer was washed with brine, dried over MgSO₄. After removing CH₂Cl₂, the crude product yielded was purified by silica flash column chromatography (hexane/CH₂Cl₂, 4:1) to give **292** (880 mg, 2.45 mmol, 95%) as a white solid. Mp

147–148 °C; ^1H NMR (CDCl_3 , 500 MHz) δ 7.98 (s, 1H), 7.69 (s, 2H), 4.62 (d, J 6.5 Hz, 2H), 1.76 (t, J 6.0 Hz, 1H); ^{13}C NMR (CDCl_3 , 125 MHz) δ 145.0, 144.4, 135.2, 95.1, 63.7; GC-MS m/z (%) 360 ($[\text{M}]^+$, 100).

3,5-Diiodobenzaldehyde (293). To a stirred solution of PCC (1.37 g, 6.34 mmol) in 20 mL CH_2Cl_2 was added a solution of **292** (1.14 g, 3.17 mmol) in 10 mL of CH_2Cl_2 . The reaction was stirred for another 2 h. The solvent was removed under vacuum to give a crude product of **293**. The crude product was then purified by silica flash column chromatography (hexanes/EtOAc, 80:20) to give compound **293** (1.08 g, 3.02 mmol, 95%) as a white solid. Mp 133–134 °C; ^1H NMR (CDCl_3 , 500 MHz) δ 9.83 (s, 1H), 8.29 (t, J 1.5 Hz, 1H), 8.14 (d, J 1.5 Hz, 2H); ^{13}C NMR (CDCl_3 , 125 MHz) δ 189.5, 151.0, 139.4, 138.2, 195.7; GC-MS m/z (%) 358 ($[\text{M}]^+$, 100), 329 ($[\text{M}-\text{CHO}]^+$, 12).

1-(2,2-Dibromovinyl)-3,5-diiodobenzene (294). To a flask filled with 30 mL of dry CH_2Cl_2 were added CBr_4 (0.94 g, 2.8 mmol) and PPh_3 (1.19 g, 5.69 mmol). The mixture was stirred for 5 min to produce a red solution. Then a solution of **293** (0.68 g, 1.9 mmol) in 15 mL of CH_2Cl_2 was added dropwise. The reaction was stirred overnight. The solvent was removed by rotary evaporation. The crude product was then purified by silica flash column chromatography (hexanes/ CH_2Cl_2 , 95:5) to give compound **294** (0.91 g, 1.77 mmol, 93%) as a white solid. Mp 58–59 °C; ^1H NMR (CDCl_3 , 500 MHz) δ 7.99 (s, 1H), 7.78 (s, 2H), 7.27 (s, 1H); ^{13}C NMR (CDCl_3 , 125 MHz) δ 144.9, 138.7, 136.3, 133.8, 94.9, 93.1; APCL-MS (positive) m/z calcd for $\text{C}_8\text{H}_4\text{Br}_2\text{I}_2$ 513.7, found 513.8 ($[\text{M}]^+$).

1-Ethynyl-3,5-diiodobenzene (295). LDA (1.8 M in THF, 2.5 mL, 1.8 M in THF, 4.43 mmol) was slowly added to a solution of **294** (910 mg, 1.77 mmol) in THF (15 mL) at -78 °C. After stirring at this temperature for 1 h, the reaction was quenched by addition of a satd NH₄Cl solution (10 mL), and the mixture was diluted with hexane (100 mL). The organic phase was then washed with brine, dried over MgSO₄, and concentrated under vacuum. The crude product was purified by silica flash column chromatography (pure hexanes) to give compound **295** (544 mg, 1.54 mmol, 87%) as a white solid. Mp 128–129 °C; ¹H NMR (CDCl₃, 500 MHz,) δ 8.02 (s, 1H), 7.77 (s, 2H), 3.16 (s, 1H); ¹³C NMR (CDCl₃, 125 MHz) δ 145.7, 140.1, 125.8, 94.3, 80.5, 80.0; GC-MS *m/z* (%) 354 ([M]⁺, 100), 227 ([M - I]⁺, 23).

1,4-Bis(3,5-diiodophenyl)buta-1,3-diyne (296). To a solution of **295** (70 mg, 0.20 mmol) in 1:1 acetone-CH₂Cl₂ (20 mL) was added Hay catalyst (2 mL). The mixture was stirred at rt under exposure to air for 48 h. The solvent was removed by rotary evaporation. To the residue was added 1 M HCl (20 mL). The mixture was extracted by plenty of CHCl₃. The organic solution was washed with brine, and dried over MgSO₄. Then CHCl₃ was removed under vacuum to give the crude compound. The crude product was further purified by recrystallization from CHCl₃ to give pure **296** (46 mg, 0.065 mmol, 66%) as a white solid. mp 200 °C (dec); IR (KBr) 3075, 3027, 2911, 2198, 1760, 1735, 1618, 1566, 1523, 1399 cm⁻¹; ¹H NMR (CDCl₃, 500 MHz) δ 7.70 (t, *J* = 1.0 Hz, 1H), 7.42 (d, *J* = 1.0 Hz, 2H); ¹³C NMR was not obtained due to low solubility; APCI-MS (positive) *m/z* calcd for C₁₆H₆I₄ 705.7, found 705.7 [M]⁺.

1,4-Bis(3,5-bis((2,5-bis(decyloxy)-4-((triisopropylsilyl)ethynyl)phenyl)ethynyl)phenyl)buta-1,3-diyne (297). Compound **296** (44 mg, 0.063 mmol), **230** (150 mg, 0.252 mmol), PdCl₂(PPh₃)₂ (8.9 mg, 0.013 mmol), and CuI (1.8 mg, 0.0063 mmol) were added to Et₃N (10 mL). The solution was bubbled by N₂ at rt for 5 min and then stirred at rt under N₂ protection for 12 h. After the reaction was complete as checked by TLC analysis, the solvent was removed by rotary evaporation. To the residue obtained was added chloroform. The mixture was filtered over MgSO₄ pad. Then it was sequentially washed with aq HCl (10%) and brine. The organic layer was dried over MgSO₄ and concentrated under vacuum. The crude product was then purified by silica flash column chromatography (hexanes/CH₂Cl₂, 8:2) to yield compound **297** (123 mg, 0.0478 mmol, 80%) as a yellow solid. Mp 87–88 °C; IR (KBr) 2924, 2859, 2211, 2150, 1633, 1578, 1501, 1467, 1421, 1386 cm⁻¹; ¹H NMR (CDCl₃, 500 MHz) δ 7.67 (s, 2H), 7.61 (d, *J* = 1.5 Hz, 4H), 6.95 (s, 4H), 6.94 (s, 4H), 4.02 (t, *J* = 6.5 Hz, 4H, OCH₂), 3.97 (t, *J* = 6.5 Hz, 4H, OCH₂), 1.87–1.76 (m, 16H), 1.57–1.47 (m, 16H), 1.31–1.21 (m, 96 H), 1.53 (s, 42H, Si(CH(CH₃)₂)₃), 0.89 (t, *J* = 6.5 Hz, 12H, CH₃), 0.84 (t, *J* = 7.0 Hz, 12H, OCH₂); ¹³C NMR (CDCl₃, 125 MHz) δ 154.5, 153.8, 135.1, 134.9, 124.8, 122.6, 118.0, 116.7, 114.8, 113.6 (ten aromatic carbons), 103.1, 97.0, 92.8, 87.9, 80.6, 74.9 (six alkynyl carbons), 70.0, 69.5 (two C-O carbons in the alkyl chains), 32.16, 32.13, 29.9, 29.85, 29.83, 29.7, 29.69, 29.62, 29.6, 26.4, 26.38, 22.9, 18.9, 14.3, 11.6; MALDI-TOF MS *m/z* calcd for C₁₇₂H₂₆₆O₈Si₄ 2571.95, found 2573.57 [M + H]⁺.

1,4-Bis(3,5-bis((2,5-bis(decyloxy)-4-ethynylphenyl)ethynyl)phenyl)buta-1,3-diyne (298). To a solution of compound **297** (123 mg, 0.0478 mmol) in THF

(6 mL) was added TBAF (0.05 mL, 1 M, 0.05 mmol). The mixture was stirred at rt for 30 min. The solvent was removed by rotary evaporation. To the residue was added CHCl_3 and 1 M HCl. The organic layer was isolated and washed with brine and dried over MgSO_4 . Filtration to remove MgSO_4 followed by evaporation under vacuum afforded the crude product, which was further purified by silica flash column chromatography (hexanes/ CH_2Cl_2 , 7:3) to yield compound **298** (68 mg, 0.035 mmol, 73%) as a brownish wax. IR (KBr) 3283, 2923, 2852, 2210, 2104, 1604, 1578, 1533, 1501, 1469, 1420, 1389 cm^{-1} ; ^1H NMR (CDCl_3 , 500 MHz) δ 7.67 (s, 2H), 7.62 (d, $J = 1.5$ Hz, 4H), 6.99 (s, 4H), 6.98 (s, 4H), 4.01 (t, $J = 6.0$ Hz, 8H, OCH_2), 3.35 (s, 4H), 1.87-1.80 (m, 16H), 1.57-1.46 (m, 16H), 1.42-1.21 (m, 96 H), 0.88 (t, $J = 7.0$ Hz, 12H, CH_3), 0.84 (t, $J = 6.5$ Hz, 12H, CH_3); ^{13}C NMR (CDCl_3 , 125 MHz) δ 154.3, 153.9, 135.1, 130.0, 124.7, 122.6, 118.0, 117.2, 114.1, 113.4 (ten aromatic carbons), 93.0, 87.6, 82.7, 80.5, 80.1, 74.9 (six alkynyl carbons), 69.9 (C-O carbon in alkyl chains), 32.1, 29.9, 29.79, 29.76, 29.6, 29.56, 29.54, 29.5, 29.4, 26.3, 26.1, 22.9, 14.3; MALDI-TOF MS m/z calcd for $\text{C}_{136}\text{H}_{186}\text{O}_8$ 1947.41, found 1948.98 $[\text{M} + \text{H}]^+$.

((3,5-Diiodophenyl)ethynyl)trimethylsilane (299). To a solution of **295** (120 mg, 0.234 mmol) in THF (8 mL) was added LDA (0.39 mL, 1.8 M in THF, 0.702 mmol) dropwise at -78 °C. The reaction was maintained at -78 °C and stirred for 1 h. To the formed red solution was added TMSCl (0.12 mL, 0.94 mmol) dropwise and stirred for 1.5 h. To the light yellow solution was added 1 M HCl (5 mL) at -78 °C. The reaction was then warmed to rt and extracted with CH_2Cl_2 . The organic phase was washed with brine, dried over MgSO_4 , filtered, and the solvent was evaporated. The crude product was purified by silica flash column chromatography (hexanes/ CH_2Cl_2 ,

1:9) to give compound **299** (80 mg, 0.19 mmol, 80%) as a colorless oil. ^1H NMR (CDCl_3 , 500 MHz) δ 7.99 (t, J = 1.5 Hz, 1H), 7.77 (d, J = 1.0 Hz, 2H), 0.25 (s, 9H) GC-MS m/z (%) 426 ($[\text{M}]^+$, 40), 411 ($[\text{M} - \text{CH}_3]^+$, 100).

(4,4'-(5-((Trimethylsilyl)ethynyl)-1,3-phenylene)bis(ethyne-2,1-diyl)bis(2,5-bis(decyloxy)-4,1-phenylene))bis(ethyne-2,1-diyl)bis(triisopropylsilane) (300). Compound **299** (54 mg, 0.13 mmol), **230** (150 mg, 0.252 mmol), $\text{PdCl}_2(\text{PPh}_3)_2$ (9 mg, 0.01 mmol), CuI (8 mg, 0.03 mmol) were added to Et_3N (5 mL). The solution was bubbled by N_2 at rt for 5 min and then stirred at rt under N_2 protection for 12 h. After the reaction was complete as checked by TLC analysis, the solvent was removed by rotary evaporation. To the residue obtained was added chloroform. The mixture was filtered through a MgSO_4 pad. Then it was sequentially washed with aq HCl (10%) and brine. The organic layer was dried over MgSO_4 and concentrated under vacuum. The crude product was purified by silica flash column chromatography (hexanes/ CH_2Cl_2 , 85:15) to yield compound **300** (158 mg, 0.116 mmol, 92%) as a yellow wax. IR (KBr) 2925, 2862, 2152, 1579, 1500, 1467, 1422, 1386 cm^{-1} ; ^1H NMR (CDCl_3 , 500 MHz) δ 7.61 (s, 1H), 7.57 (d, J = 1.5 Hz, 2H), 6.95 (s, 2H), 6.93 (s, 2H), 4.02 (t, J = 6.5 Hz, 4H, OCH_2), 3.96 (t, J = 6.0 Hz, 4H, OCH_2), 1.87-1.76 (m, 8H), 1.57-1.46 (m, 8H), 1.42-1.22 (m, 48 H), 1.16 (s, 42H), 0.89 (t, J = 7.0 Hz, 6H), 0.86 (t, J = 7.5 Hz, 6H), 0.26 (s, 9H); ^{13}C NMR (CDCl_3 , 125 MHz) δ 154.6, 153.8, 134.5, 134.2, 124.4, 124.1, 118.0, 116.7, 114.7, 113.8 (ten aromatic carbons), 103.6, 103.2, 96.9, 95.7, 93.2, 87.4 (six alkynyl carbons), 70.1, 69.5 (two C-O carbons), 32.1, 29.9, 29.8, 29.73, 29.70, 29.63, 29.59, 29.56, 29.4, 26.4, 26.3, 22.9, 18.9, 18.8, 14.3, 11.6, 0.07; MALDI-TOF MS m/z calcd for $\text{C}_{89}\text{H}_{142}\text{O}_4\text{Si}_3$

1359.02, found 1359.28 [M]⁺.

(4,4'-(5-Ethynyl-1,3-phenylene)bis(ethyne-2,1-diyl)bis(2,5-bis(decyloxy)-4,1-phenylene))bis(ethyne-2,1-diyl)bis(triisopropylsilane) (301). To a solution of compound **300** (158 mg, 0.116 mmol) in 1:1 MeOH/THF (20 mL) was added K₂CO₃ (50 mg, 0.36 mmol). The mixture was stirred at rt for 2 h, then the reaction solvent was removed by rotary evaporation. The residue was diluted in CH₂Cl₂ and sequentially washed with aq HCl (10%) and brine. The organic layer was dried over MgSO₄ and concentrated under vacuum to afford the crude product of **301**, which was further purified by silica flash column chromatography (hexanes/CH₂Cl₂, 9:1) to yield compound **301** (150 mg, 0.116 mmol, 100%) as a yellow wax. IR (KBr) 3312, 2925, 2862, 2212, 2151, 1603, 1581, 1499, 1467, 1422, 1385 cm⁻¹; ¹H NMR (CDCl₃, 500 MHz) δ 7.65 (s, 1H), 7.59 (d, *J* = 1.5 Hz, 2H), 6.95 (s, 2H), 6.94 (s, 2H), 4.02 (t, *J* = 6.0 Hz, 4H, OCH₂), 3.97 (t, *J* = 6.0 Hz, 4H, OCH₂), 3.10 (s, 1H), 1.86-1.78 (m, 8H), 1.56-1.48 (m, 8H), 1.42-1.22 (m, 48 H), 1.16 (s, 42H), 0.90 (t, *J* = 6.5 Hz, 6H, CH₃), 0.86 (t, *J* = 7.0 Hz, 6H, CH₃); ¹³C NMR (CDCl₃, 125 MHz) δ 154.5, 153.8, 134.64, 134.61, 124.5, 123.1, 118.0, 116.6, 114.7, 113.7 (ten aromatic carbons), 103.2, 96.9, 93.0, 87.6, 82.3, 78.4 (six alkynyl carbons), 70.0, 69.5 (two C-O carbons in the alkyl chains), 32.1, 29.9, 29.85, 29.83, 29.74, 29.70, 29.6, 29.59, 29.56, 26.42, 26.38, 22.9, 18.9, 14.3, 11.6; MALDI-TOF MS *m/z* calcd for C₈₆H₁₃₄O₄Si₂ 1286.98, found 1286.94 [M]⁺.

(4,4'-(5-((Trimethylsilyl)buta-1,3-diynyl)-1,3-phenylene)bis(ethyne-2,1-diyl)bis(2,5-bis(decyloxy)-4,1-phenylene))bis(ethyne-2,1-diyl)bis(triisopro -

pylsilane) (302). To a flask containing acetone (8 mL) was added **301** (150 mL, 0.116 mmol), trimethylsilylacetylene (0.164 mL, 1.16 mmol) and Hay catalyst (2 mL). The mixture was stirred at rt under exposure to air for 40 h. When TLC analysis showed no starting material present, acetone was evaporated *in vacuo*. CHCl₃ (30 mL) was added. The resulting content was washed with aq HCl (1 M), satd NaHCO₃, and brine sequentially. The organic layer was dried over MgSO₄ and evaporated *in vacuo* to give the crude product. The crude product was purified by silica flash column chromatography (hexanes/CH₂Cl₂, 4:1) to yield compound **302** (143 mg, 0.103 mmol, 89%) as a yellow wax. IR (KBr) 2925, 2861, 2211, 2151, 2102, 1620, 1579, 1499, 1467, 1421, 1385 cm⁻¹; ¹H NMR (CDCl₃, 500 MHz) δ 7.65 (s, 1H), 7.56 (d, *J* = 1.5 Hz, 2H), 6.95 (s, 2H), 6.93 (s, 2H), 4.02 (t, *J* = 6.5 Hz, 1H, OCH₂), 3.97 (t, *J* = 6.5 Hz, 4H, OCH₂), 1.87-1.78 (m, 8H), 1.57-1.46 (m, 8H), 1.41-1.25 (m, 48 H), 1.16 (s, 42H, Si(CH(CH₃)₂)₃), 0.90 (t, *J* = 7.0 Hz, 6H, CH₃), 0.87 (t, *J* = 7.0 Hz, 6H, CH₃), 0.25 (s, 9H, Si(CH₃)₃); ¹³C NMR (CDCl₃, 125 MHz) δ 154.5, 153.8, 135.1, 135.0, 124.7, 122.4, 118.0, 116.7, 114.8, 113.6 (ten aromatic carbons), 103.1, 97.0, 92.8, 91.6, 97.9, 87.8, 75.3, 75.2 (eight alkynyl carbons), 70.0, 69.5 (two C-O carbons in the alkyl chains), 32.1, 29.92, 29.9, 29.8, 29.74, 29.70, 29.67, 29.59, 29.56, 26.41, 26.36, 22.9, 18.9, 18.8, 14.3, 11.6, 0.22; MALDI-TOF MS *m/z* calcd for C₉₁H₁₄₂O₄Si₃ 1383.02, found 1384.39 [M + H]⁺.

(4,4'-(5-(Buta-1,3-diyne)-1,3-phenylene)bis(ethyne-2,1-diyl)bis(2,5-bis-(decyloxy)-4,1-phenylene))bis(ethyne-2,1-diyl)bis(triisopropylsilane) (303). To a solution of compound **302** (143 mg, 0.103 mmol) in 1:1 MeOH THF (8 mL) was added K₂CO₃ (50 mg, 0.36 mmol). The mixture was stirred at rt for 2 h, then

the reaction solvent was removed by rotary evaporation. The residue was diluted in CH_2Cl_2 and sequentially washed with aq HCl (10%) and brine. The organic layer was dried over MgSO_4 and concentrated under vacuum to afford the crude product of **303**, which was further purified by silica flash column chromatography (hexanes/ CH_2Cl_2 , 85:15) to yield compound **303** (110 mg, 0.0838 mmol, 81%) as a yellow wax. IR (KBr) 3312, 2925, 2861, 2214, 2151, 1617, 1578, 1499, 1467, 1422, 1385 cm^{-1} ; ^1H NMR (CDCl_3 , 500 MHz) δ 7.67 (s, 1H), 7.60 (d, $J = 1.5$ Hz, 2H), 6.95 (s, 2H), 6.93 (s, 2H), 4.02 (t, $J = 6.5$ Hz, 4H, OCH_2), 3.97 (t, $J = 6.5$ Hz, 4H, OCH_2), 2.50 (s, 1H), 1.87-1.77 (m, 8H), 1.57-1.46 (m, 8H), 1.42-1.23 (m, 48 H), 1.16 (s, 42H $\text{Si}(\text{CH}(\text{CH}_3)_2)_3$), 0.90 (t, $J = 7.0$ Hz, 6H, CH_3), 0.86 (t, $J = 7.0$ Hz, 6H, CH_3); ^{13}C NMR (CDCl_3 , 125 MHz) δ 154.7, 154.0, 135.4, 135.3, 125.0, 122.2, 118.2, 116.8, 115.1, 113.7 (ten aromatic carbons), 103.3, 97.2, 92.9, 88.2, 74.8, 74.0, 72.2, 70.2, 69.7, 68.3 (eight alkynyl carbons and two C-O carbon in the alkyl chains), 32.3, 30.1, 30.07, 30.04, 29.95, 29.91, 29.83, 29.81, 29.8, 26.63, 26.6, 23.1, 19.2, 14.5, 11.8; MALDI-TOF MS m/z calcd for $\text{C}_{88}\text{H}_{133}\text{O}_4\text{Si}_2$ 1309.97, found 1311.90 $[\text{M}+\text{H}]^+$.

1,8-Bis(3,5-bis((2,5-bis(decyloxy)-4-((triisopropylsilyl)ethynyl)phenyl)-ethynyl)phenyl)octa-1,3,5,7-tetrayne (304). To a round bottom flask containing acetone (8 mL) was added **303** (110 mg, 0.0838 mmol), and then Hay catalyst (5 mL). The mixture was stirred at rt under exposure to air for 20 h. When TLC analysis showed no starting material present, acetone was evaporated *in vacuo*. To the residue was added CHCl_3 . The resulting content was washed with aq HCl (1 M), satd NaHCO_3 , and brine sequentially. The organic layer was dried over MgSO_4 and evaporated *in vacuo* to give the crude product. The crude product was purified

by silica flash column chromatography (hexanes CH_2Cl_2 , 85:15) to yield compound **304** (94 mg, 0.036 mmol, 86%) as a pale yellow solid. Mp 89–90 °C; IR (KBr) 2924, 2856, 2208, 2150, 1577, 1500, 1467, 1421, 1408, 1387 cm^{-1} ; ^1H NMR (CDCl_3 , 500 MHz) δ 7.69 (s, 2H), 7.61 (d, J = 1.5 Hz, 4H), 6.95 (s, 4H), 6.93 (s, 4H), 4.02 (t, J = 6.5 Hz, 8H, OCH_2), 3.97 (t, J = 6.5 Hz, 8H, OCH_2), 1.88–1.78 (m, 16H), 1.59–1.47 (m, 16H), 1.44–1.26 (m, 96 H), 1.16 (s, 84H, $\text{Si}(\text{CH}(\text{CH}_3)_3)$), 0.90 (t, J = 7.0 Hz, 12H OCH_2), 0.88 (t, J = 7.0 Hz, 12H, OCH_2); ^{13}C NMR (CDCl_3 , 125 MHz) δ 154.5, 153.9, 135.6, 135.4, 124.9, 121.5, 117.9, 116.6, 114.9, 113.4 (ten aromatic carbons), 103.1, 97.1, 92.6, 88.2, 76.3, 75.4, 70.0, 69.5, 67.8, 63.8 (eight alkynyl carbons and two C–O carbons), 32.2, 32.1, 30.0, 29.9, 29.7, 29.6, 26.4, 22.94, 22.92, 18.9, 18.8, 14.4, 14.3, 11.6; MALDI-TOF MS m/z calcd for $\text{C}_{176}\text{H}_{266}\text{O}_8\text{Si}_4$ 2619.95, found 2620.67 $[\text{M} + \text{H}]^+$.

1,8-bis(3,5-bis((2,5-bis(decyloxy)-4-ethynylphenyl)ethynyl)phenyl)octa-1,3,5,7-tetrayne (305). To a solution of compound **304** (90 mg, 0.0343 mmol) in THF (8 mL) was added TBAF (0.05 mL, 1 M, 0.05 mmol). The mixture was stirred at room temperature for 5 min. The solvent was removed by rota vapor. To the residue was added CHCl_3 and 1 M HCl. The organic layer was isolated and washed with brine and dried over MgSO_4 . Filtration to remove MgSO_4 followed by evaporation under vacuum afforded the crude product (66 mg, 0.033 mmol, 97%) as dark brown wax. Due to the poor stability of compound **305**, it was not characterized by spectroscopic analysis and used directly for next step.

1,4-Bis(3,5-bis((4-((2,5-bis(decyloxy)-4-((triisopropylsilyl)ethynyl)phenyl)ethynyl)-2,5-bis(decyloxy)phenyl)-ethynyl)phenyl)buta-1,3-diyne (306).

Compound **297** (30 mg, 0.043 mmol), compound **226** (173 mg, 0.172 mmol), PdCl₂(PPh₃)₂ (6.0 mg, 0.0086 mmol), and CuI (3.3 mg, 0.017 mmol) were added to Et₃N (10 mL). The solution was bubbled by N₂ at rt for 5 min and then stirred at rt under N₂ protection for 12 h. After the reaction was complete as checked by TLC analysis, the solvent was removed by rotary evaporation. To the obtained residue was added chloroform. The mixture was filtered over MgSO₄ pad. Then it was sequentially washed with aq HCl (10%) and brine. The organic layer was dried over MgSO₄ and concentrated under vacuum. The crude product was then purified by silica flash column chromatography (hexanes/CH₂Cl₂, 7:3) to yield compound **306** (156 mg, 0.0369 mmol, 86%) as a yellow wax. IR (KBr) 2924, 2855, 2213, 2149, 1624, 1579, 1507, 1467, 1425, 1385 cm⁻¹; ¹H NMR (CDCl₃, 500 MHz) δ 7.69 (s, 2H), 7.64 (d, *J* = 6.5 Hz, 4H), 7.03 (s, 4H), 7.01 (s, 4H), 6.97 (s, 4H), 6.95 (s, 4H), 4.07-4.02 (m, 24H, OCH₂), 3.97 (t, *J* = 6.5 Hz, 8H, OCH₂), 1.88-1.77 (m, 32H), 1.59-1.46 (m, 32H), 1.39-1.25 (m, 192 H), 1.16 (s, 84H, Si(CH₃)₂)₃), 0.91-0.84 (m, 48H, CH₃); ¹³C NMR (CDCl₃, 125 MHz) δ 154.6, 154.0, 153.6, 153.5 (four C-O carbons in the phenyl rings), 135.1, 134.9, 124.7, 122.6, 118.1, 117.3, 117.2, 116.7, 115.1, 114.5, 114.2, 113.4 (twelve aromatic carbons), 103.2, 96.8, 93.0, 92.1, 91.4, 87.9, 80.5, 74.9 (eight alkynyl carbons), 70.1, 70.0, 69.8, 69.4 (four C-O carbons in the alkyl chains), 32.2, 30.0, 29.91, 29.87, 29.8, 29.7, 29.6, 29.55, 26.5, 26.4, 26.2, 22.9, 19.0, 14.4, 11.6; MALDI-TOF MS *m/z* calcd for C₂₈₃H₄₄₀O₁₆Si₄ 4221.29, found 4222.90 [M + H]⁺.

1,4-Bis(3,5-bis((4-((2,5-bis(decyloxy)-4-ethynylphenyl)ethynyl)-2,5-bis-(decyloxy)phenyl)ethynyl)phenyl)buta-1,3-diyne (307). To a solution of compound **306** (156 mg, 0.0369 mmol) in THF (6 mL) was added TBAF (0.1 mL, 1

M, 0.1 mmol). The mixture was stirred at rt for 30 min. The solvent was removed by rotary evaporation. To the residue was added CHCl_3 and 1 M HCl. The organic layer was isolated and washed with brine and dried over MgSO_4 . Filtration to remove MgSO_4 followed by evaporation under vacuum afforded the crude product, which was further purified by silica flash column chromatography (hexanes/ CH_2Cl_2 , 7:3) to yield compound **307** (134 mg, 0.0372 mmol, 100%) as a brownish solid. mp 61-62 °C; IR (KBr) 3315, 3296, 2924, 2853, 2209, 2105, 1602, 1577, 1506, 1468, 1426, 1387 cm^{-1} ; ^1H NMR (CDCl_3 , 500 MHz) δ 7.68 (s, 2H), 7.63 (s, 4H), 7.02 (s, 4H), 7.003 (s, 4H), 6.99 (s, 4H), 6.98 (s, 4H), 4.06-3.99 (m, 32H, OCH_2), 3.35 (s, 4H), 1.88-1.79 (m, 32H), 1.58-1.41 (m, 32H), 1.38-1.23 (m, 192 H), 0.90-0.83 (m, 48H, CH_3); ^{13}C NMR (CDCl_3 , 125 MHz) δ 154.4, 154.1, 153.7, 153.6 (four C-O carbons in the phenyl rings), 135.1, 134.9, 124.8, 122.6, 118.3, 117.5, 117.4, 117.3, 115.1, 115.06, 113.6, 112.9 (twelve aromatic carbons), 93.0, 91.7, 91.6, 87.9, 82.5, 80.6, 80.3, 74.9 (eight alkynyl carbons), 70.0, 69.9 (two C-O carbons in the alkyl chains), 32.1, 30.0, 29.9, 29.85, 29.81, 29.80, 29.7, 29.58, 29.56, 29.4, 26.4, 26.2, 22.9, 14.4; MALDI-TOF MS m/z calcd for $\text{C}_{248}\text{H}_{362}\text{O}_{16}$ 3596.75, found 3597.75 $[\text{M}+\text{H}]^+$.

Compound 308. Compound **299** (70 mg, 0.163 mmol), **226** (329 mg, 0.326 mmol), $\text{PdCl}_2(\text{PPh}_3)_2$ (11.4 mg, 0.0163 mmol), CuI (6.2 mg, 0.033 mmol) were added to Et_3N (6 mL). The solution was bubbled by N_2 at rt for 5 min and then stirred for 8 h at rt. After the reaction was complete as checked by TLC analysis, the solvent was removed by rotary evaporation. The resulting residue was diluted with chloroform. The mixture was filtered through a MgSO_4 pad. The solution obtained was sequentially washed with aq HCl (10%) and brine. The organic layer was dried

over MgSO_4 and concentrated under vacuum to give the crude product of **308**, which was further purified by silica flash column chromatography (hexanes/ CH_2Cl_2 , 4:1) to yield compound **308** (330 mg, 0.151 mmol, 36%) as a yellow solid. Mp 42–43 °C; IR (KBr) 2925, 2855, 2210, 2148, 1624, 1579, 1508, 1469, 1426, 1386 cm^{-1} ; ^1H NMR (CDCl_3 , 500 MHz) δ 7.61 (s, 1H), 7.57 (d, $J = 1.5$, 2H), 7.02 (s, 2H), 6.98 (s, 2H), 6.95 (s, 2H), 6.94 (s, 2H), 4.04–4.01 (m, 12H, OCH_2), 3.95 (t, $J = 6.5$ Hz, 4H, OCH_2), 1.87–1.76 (m, 16H), 1.53–1.48 (m, 16H), 1.37–1.24 (m, 96 H), 1.15 (s, 42H, $\text{Si}(\text{CH}(\text{CH}_3)_2)_3$), 0.90–0.83 (m, 24H, CH_3), 0.26 (s, 9H, $\text{Si}(\text{CH}_3)_3$); ^{13}C NMR (CDCl_3 , 125 MHz) δ 154.5, 153.9, 153.6, 153.5, 134.6, 134.2, 124.3, 124.0, 118.1, 117.4, 117.3, 116.7, 114.9, 114.5, 114.2, 113.6 (sixteen aromatic carbons), 103.6, 103.2, 96.7, 95.7, 93.3, 92.0, 91.4, 87.4 (eight alkynyl carbons), 70.0, 69.9, 69.8, 69.4 (four C–O carbons in the alkyl chains), 32.1, 29.90, 29.86, 29.76, 29.7, 29.69, 29.6, 29.59, 29.4, 26.4, 26.3, 26.2, 22.9, 18.9, 14.3, 11.6, 0.07; MALDI-TOF MS m/z calcd for $\text{C}_{145}\text{H}_{230}\text{O}_8\text{Si}_3$ 2183.69, found 2183.03.

Compound 309. To a solution of compound **308** (336 mg, 0.154 mmol) in 1:1 MeOH/THF (6 mL) was added K_2CO_3 (50 mg, 0.36 mmol). The mixture was stirred at rt for 2 h, then the solvent was removed by rotary evaporation. The residue was diluted in CH_2Cl_2 and sequentially washed with aq HCl (10%) and brine. The organic layer was dried over MgSO_4 and concentrated under vacuum to afford the crude product of **309**, which was further purified by silica flash column chromatography (hexanes/ CH_2Cl_2 , 7:3) to yield compound **309** (268 mg, 0.127 mmol, 83%) as a yellow solid. Mp 65–66 °C; IR (KBr) 3262, 2955, 2924, 2855, 2209, 2149, 1670, 1626, 1580, 1508, 1467, 1426, 1385 cm^{-1} ; ^1H NMR (CDCl_3 , 500 MHz) δ 7.67 (s, 1H), 7.61

(d, $J = 1.0$, 2H), 7.03 (s, 2H), 7.01 (s, 2H), 6.97 (s, 2H), 6.96 (s, 2H), 4.06-4.02 (m, 12H, OCH₂), 3.97 (t, $J = 6.5$ Hz, 4H, OCH₂), 3.12 (s, 1H), 1.89-1.77 (m, 16H), 1.57-1.48 (m, 16H), 1.42-1.26 (m, 96 H), 1.17 (s, 42H, Si(CH(CH₃)₂)₃), 0.92-0.85 (m, 24H, CH₃); ¹³C NMR (CDCl₃, 125 MHz) δ 154.5, 154.0, 153.6, 153.5, 134.7, 134.6, 124.5, 118.1, 117.3, 117.2, 116.6, 115.0, 114.5, 114.2, 113.5 (fifteen aromatic carbons), 103.2, 96.7, 93.2, 92.0, 91.4, 87.6, 82.3, 78.4 (eight alkynyl carbons), 70.0, 69.9, 69.8, 69.4 (four C-O carbons in the alkyl chains), 32.1, 29.9, 29.86, 29.82, 29.8, 29.7, 29.6, 29.5, 26.5, 26.4, 26.2, 22.9, 18.9, 14.3, 11.6; MALDI-TOF MS m/z calcd for C₁₁₂H₂₂₂O₈Si₂ 2111.65, found 2112.62 [M + H]⁺.

Compound 310. To a flask containing acetone (10 mL) were added **309** (268 mg, 0.127 mmol), trimethylsilylacetylene (0.179 mL, 1.27 mmol) and Hay catalyst (5 mL). The mixture was stirred at rt under exposure to air for 45 h. When TLC analysis showed no starting material present, acetone was evaporated *in vacuo*. CHCl₃ (30 mL) was added. The resulting mixture was washed with aq HCl (1 M), satd NaHCO₃, and brine sequentially. The organic layer was dried over MgSO₄ and evaporated *in vacuo* to give the crude product. The crude product was purified by silica flash column chromatography (hexanes/CH₂Cl₂, 7:3) to yield compound **310** (235 mg, 0.106 mmol, 84%) as a yellow solid. Mp 57–58 °C; IR (KBr) 2958, 2924, 2854, 2209, 2150, 2101, 1624, 1579, 1557, 1539, 1507, 1467, 1427, 1386 cm⁻¹; ¹H NMR (CDCl₃, 500 MHz) δ 7.67 (s, 1H), 7.58 (d, $J = 1.5$, 2H), 7.03 (s, 2H), 7.00 (s, 2H), 6.97 (s, 2H), 6.96 (s, 2H), 4.06-4.02 (m, 12H, OCH₂), 3.97 (t, $J = 6.0$ Hz, 4H, OCH₂), 1.88-1.80 (m, 16H), 1.55-1.50 (m, 16H), 1.41-1.26 (m, 96 H), 1.17 (s, 42H, Si(CH(CH₃)₂)₃), 0.92-0.86 (m, 24H, CH₃), 0.26 (s, 9H, Si(CH₃)₃); ¹³C NMR (CDCl₃, 125 MHz) δ 154.6, 154.1, 153.7,

153.5, 135.0, 135.0, 124.7, 122.5, 118.2, 117.4, 117.3, 116.7, 115.2, 114.6, 114.3, 113.4 (sixteen aromatic carbons), 103.3, 96.7, 93.0, 92.1, 91.6, 91.4, 87.9, 87.8, 75.3, 75.2 (ten alkynyl carbons), 70.1, 70.0, 69.8, 69.5 (four C-O carbons in the alkyl chains), 32.1, 29.9, 29.85, 29.80, 29.75, 29.72, 29.7, 29.6, 26.45, 26.38, 26.2, 22.9, 18.9, 14.3, 11.6; MALDI-TOF MS m/z calcd for $C_{147}H_{230}O_8Si_3$ 2207.69, found 2208.18 $[M + H]^+$.

Compound 311. To a solution of compound **310** (230 mg, 0.104 mmol) in 1:1 MeOH/THF (20 mL) was added K_2CO_3 (50 mg, 0.36 mmol). The mixture was stirred at rt for 1 h, then the solvent was removed by rotary evaporation. The residue was diluted in $CHCl_3$ and sequentially washed with aq HCl (10%) and brine. The organic layer was dried over $MgSO_4$ and concentrated under vacuum to afford the crude product of **311**, which was further purified by silica flash column chromatography (hexanes/ CH_2Cl_2 , 7:3) to yield compound **311** (201 mg, 0.094 mmol, 91%) as a yellow solid. Mp 57–58 °C; IR (KBr) 3314, 2924, 2855, 2212, 2149, 1670, 1636, 1578, 1560, 1542, 1508, 1468, 1426, 1386 cm^{-1} ; 1H NMR ($CDCl_3$, 500 MHz) δ 7.67 (s, 1H), 7.60 (d, $J = 1.5$, 2H), 7.02 (s, 2H), 6.99 (s, 2H), 6.96 (s, 2H), 6.95 (s, 2H), 4.05–4.01 (m, 12H, OCH_2), 3.95 (t, $J = 6.5$ Hz, 4H, OCH_2), 2.50 (s, 1H), 1.87–1.77 (m, 16H), 1.56–1.49 (m, 16H), 1.40–1.25 (m, 96 H), 1.15 (s, 42H, $Si(CH(CH_3)_2)_3$), 0.90–0.84 (m, 24H, CH_3); ^{13}C NMR ($CDCl_3$, 125 MHz) δ 154.6, 154.1, 153.7, 153.5, 135.2, 135.1, 124.8, 122.0, 118.2, 117.4, 117.3, 116.7, 115.2, 114.5, 114.3, 113.4 (sixteen aromatic carbons), 103.3, 96.7, 92.9, 92.1, 91.4, 88.0, 74.6, 73.8, 72.0, 70.1 (ten alkynyl carbons), 70.0, 69.8, 69.4, 68.1 (four C-O carbons in the alkyl chains), 32.1, 29.93, 29.89, 29.84, 29.81, 29.75, 29.72, 29.7, 29.6, 26.43, 26.40, 26.2, 22.9, 18.9, 14.3, 11.6; MALDI-TOF MS m/z calcd for $C_{144}H_{222}O_8Si_2$ 2135.65, found 2136.59 $[M + H]^+$.

Compound 312. To a flask containing 1:1 acetone CH_2Cl_2 (10 mL) was added **311** (200 mg, 0.0940 mmol) and Hay catalyst (5 mL). The mixture was stirred at rt under exposure to air for 2 h. When TLC analysis showed no starting material present, acetone was evaporated *in vacuo*. CHCl_3 (30 mL) was added. The resulting content was washed with aq HCl (1 M), satd NaHCO_3 , and brine sequentially. The organic layer was dried over MgSO_4 and evaporated *in vacuo* to give the crude product. The crude product was purified by silica flash column chromatography (hexanes CH_2Cl_2 , 7:3) to yield compound **312** (166 mg, 0.0389 mmol, 83%) as a yellow wax. IR (KBr) 2923, 2854, 2207, 2149, 1578, 1507, 1467, 1426, 1388 cm^{-1} ; ^1H NMR (CDCl_3 , 500 MHz) δ 7.68 (s, 2H), 7.62 (d, $J = 1.5$, 4H), 7.02 (s, 4H), 6.998 (s, 4H), 6.95 (s, 4H), 6.94 (s, 4H), 4.05-4.01 (m, 24H, OCH_2), 3.95 (t, $J = 6.5$ Hz, 8H, OCH_2), 1.88-1.76 (m, 32H), 1.55-1.48 (m, 32H), 1.37-1.25 (m, 192H), 1.15 (s, 84H, $\text{Si}(\text{CH}(\text{CH}_3)_2)_3$), 0.90-0.85 (m, 48H); ^{13}C NMR (CDCl_3 , 125 MHz) δ 154.6, 154.1, 153.7, 153.5, 135.4, 125.0, 121.5, 118.2, 117.4, 117.3, 116.8, 115.3, 114.5, 114.4, 113.3 (fifteen aromatic carbons), 103.3, 96.8, 92.8, 92.1, 91.4, 88.2, 75.4, 70.1, 70.0, 69.8, 69.5, 67.8, 63.8 (thirteen alkynyl carbons and C-O carbons in the alkyl chains), 32.1, 30.0, 29.9, 29.85, 29.78, 29.7, 29.6, 26.5, 26.2, 22.9, 18.9, 14.4, 14.3, 11.6; MALDI-TOF MS m/z calcd for $\text{C}_{288}\text{H}_{442}\text{O}_{16}\text{Si}_1$ 4269.28, found 4269.52.

Chapter 4

Study of 2D Conjugated H-Shaped OPE/OPV Fluorophores

4.1 Introduction

One-dimensionally (1D) π -conjugated oligomers have been the mainstay of advanced molecular materials for new electronic and optoelectronic devices over the past few decades. Higher order, multidimensional π -conjugated systems, particularly 2D π -conjugated arylene-based oligomers,³³¹⁻³³⁴ have been gaining increasing attention to a substantial degree within the past few years. The rationale for aiming at complex 2D conjugated molecular architectures is largely based on the ample opportunities to attain greatly enhanced or even unprecedented electronic and optoelectronic functions resulting from the versatile electronic couplings among the multiple constituent linearly π -conjugated branches in the 2D conjugated systems. In addition, the relatively high solubility of 2D conjugated oligomers compared to their corresponding

linear counterparts can also be considered as an advantage in device applications.

There are a large number of 2D conjugated oligomers with novel structures and functionalities emerging in the recent literature on conjugated molecular systems. Recent representative contributions to this field include cross-shaped oligo(phenyleneethynylene)s (OPEs),³³⁵⁻³³⁸ oligo(phenylenevinylene)s (OPVs),³³⁹⁻³⁴¹ oligo(thiophene)s (OTs),³⁴² swivel cruciform OTs,^{343,344} and cruciform OPE-OPV co-oligomers,³⁴⁵⁻³⁴⁹ to name a few. The development of these new conjugated materials has greatly widened the scope of π -oligomer candidates applicable in advanced molecular devices such as sensors,^{335,345-349} switches,³⁵⁰ nonlinear optics (NLO),^{351,352} organic field effect transistors (OFETs),³⁴² and organic photoluminescence.³³⁵

In 2003, Meier and co-workers prepared a series of star-shaped conjugated OPV oligomers **314a-c** with a 1,3,5-triazine as the pivotal core (Figure 4.1). Intramolecular charge transfer has been observed on these molecules due to the push-pull effect among the alkoxy-substituted OPV branches and the central triazine ring, which act as electron donors and acceptor respectively. In neutral solution, the long-wavelength absorption of **314a-c** converges to $\lambda_{\infty} = 427$ nm, and the effective conjugation length is determined to be $n_{\text{ECL}} = 7$. These 2D conjugated oligomers are predicted to be potential NLO materials.³⁵³

In 2006, Scherf and co-workers synthesized a pentathiophene-based swivel cruciform **315** (Figure 4.2). Besides possessing similar electronic properties to those of normal linear oligo(thiophenes), this structurally novel 2D oligothiophene has greatly increased solubility that allows for the fluidic preparation of homogeneous microcrystalline films. The output performance of the OFETs fabricated based on as-prepared **315** is characterized with high field-effect mobility up to $0.012 \text{ cm}^2 \cdot \text{V}^{-1}$

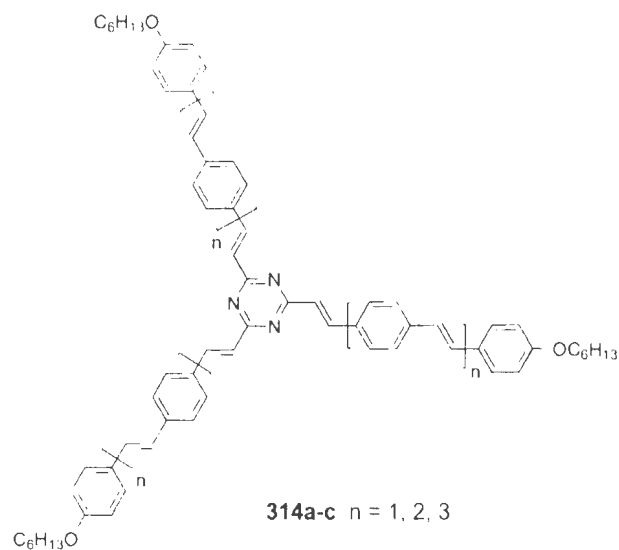


Figure 4.1: Star-shaped 1,3,5-triazene centered OPV oligomers **314a-c** by Meier *et al.*

cm^{-1} , high on/off ratio ($> 10^5$), and very low turn-on voltages ($V_{\text{on}} = 0 \text{ V}$). The low turn-on voltage is a highly desirable OFET characteristic for constructing low power consuming FETs. Also, the exhibited field-effect mobility is one of the highest values reported to date for wet-processed devices using oligo(thiophenes).³⁴⁴

Crystallinity of conjugated oligomers caused by $\pi-\pi$ stacking is believed to be the reason that fluorescence in the solid state tends to diminish. To be practically useful in solid-state luminescent devices, materials ought to have a weak penchant for crystallization.^{354,355} In 2007, Ma and co-workers designed and synthesized a 2D diphenylamino-substituted OPV **316** (Figure 4.3).³³⁹ Both quantum chemical calculations and ^1H NMR studies confirmed that the molecule took a swivel cruciform geometry because of the steric crowding around the central biphenyl core. The unique molecular shape has efficiently suppressed crystalline and intermolecular $\pi-\pi$

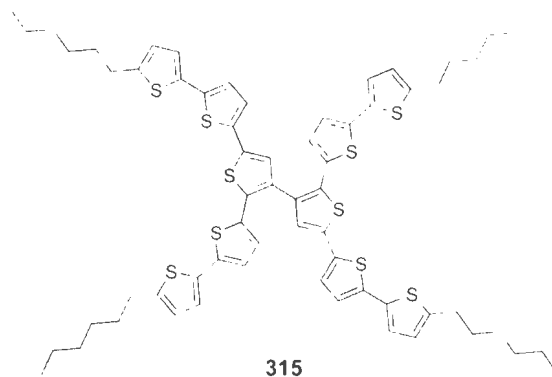


Figure 4.2: Swivel cruciform oligothiophene **315** by Scherf and co-workers.

interactions. Morphology and thermal properties studied by AFM, X-ray diffraction, and DSC analysis clearly show that compound **316** is resistant to crystallization and can form high-quality amorphous thin films. Experimentally, the neat solid of **316** is observed to strongly emit green-blue fluorescent light due to steady-state absorption and two-photon absorption. The photoluminescence (PL) efficiency (η_{solid}) of **316** in the solid state is measured as 29%, which is far greater than that of a corresponding linear model compound, **317** ($\eta_{\text{solid}} = 16\%$). Because of its high PL efficiency, good film-forming ability, and strong two-photon absorption, compound **316** is currently viewed as a good candidate for applications in solid-state optoelectronic devices.³³⁹

Most recently, Haley and co-workers developed a series of donor-acceptor (D/A) substituted tetrakis(arylethynyl)benzenes (TAEBS) **318-326** (Figure 4.4).³⁵⁶ Emission from charge recombination between radical cations $\text{TAEB}^{\bullet+}$ and radical anions $\text{TAEB}^{\bullet-}$ evolved from these compounds during the process of pulse radiolysis in benzene was monitored. It was found that the charge recombination between $\text{TAEB}^{\bullet+}$ and $\text{TAEB}^{\bullet-}$ gave $^1\text{TAEB}^*$ as the emissive species due to the large repulsion

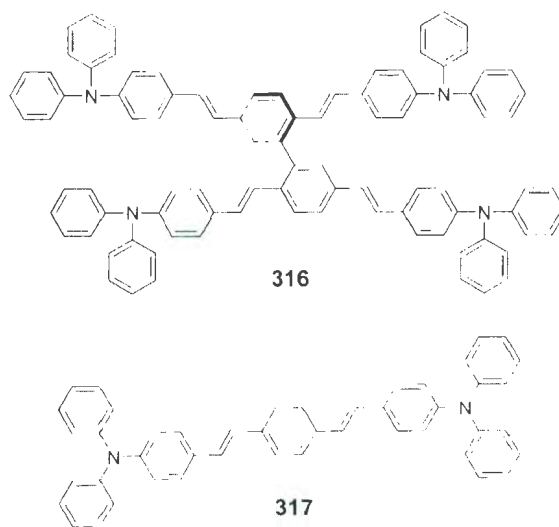


Figure 4.3: Swivel cruciform OPV **316** and linear OPV **317**.

between substituents caused by the rotation of C-C single bonds. Furthermore, because of the multifold types of charge-transfer pathways, the emission spectra of $^1\text{TAEB}^*$ with intramolecular charge transfer (ICT) characteristics become dependent on the substitution pattern and the types of donor and acceptor groups during pulse radiolysis. In this light, by controlling the substitution pattern (types of acceptors, relative positions between donors and acceptors), fine-tuning of radiolysis-induced emission color with peak ranges 498-545 nm was realized by the authors. The specific emission properties of D-A substituted TAEBs suggest a new way to manipulate the optical band gaps of conjugated materials.³⁵⁶

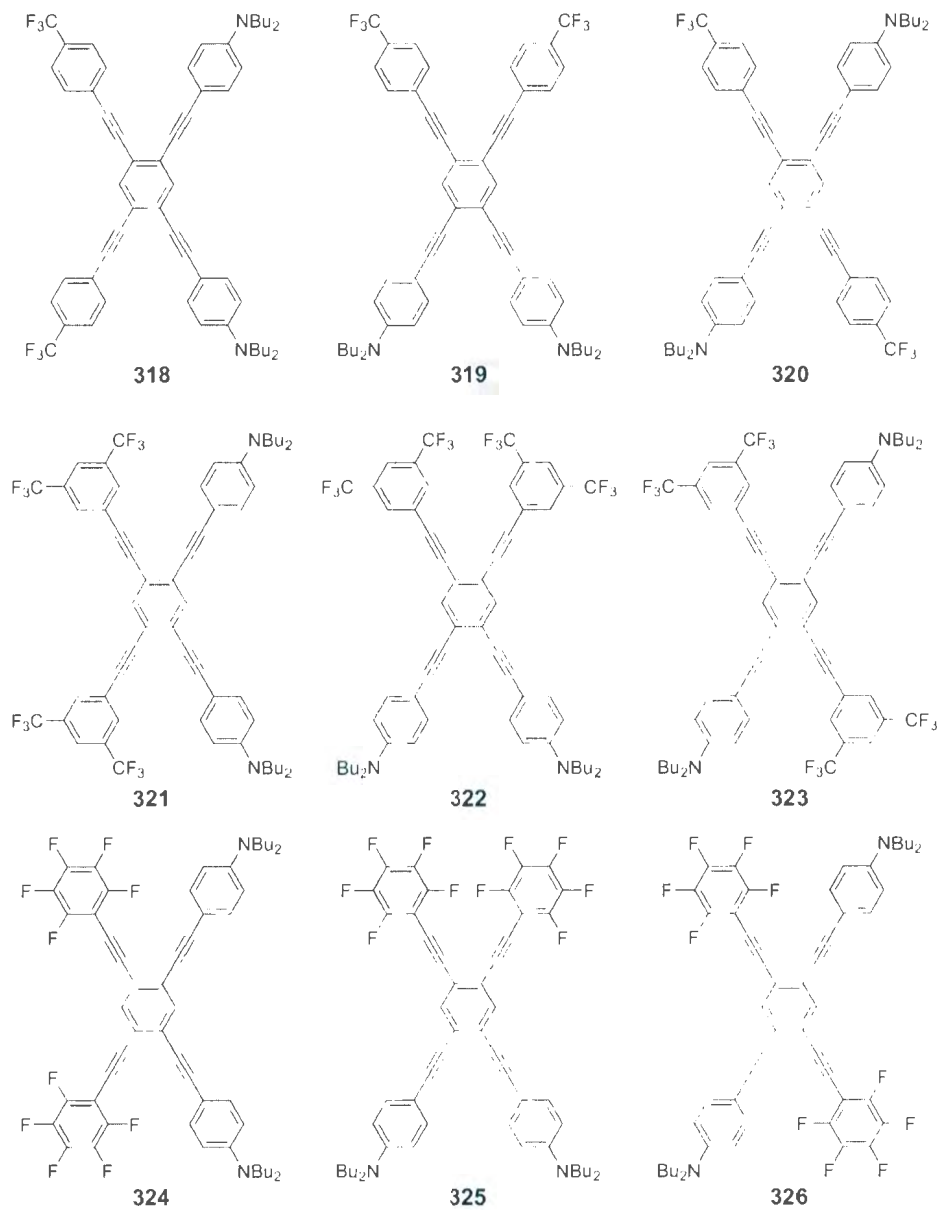


Figure 4.4: D/A substituted OPE cruciforms developed by Haley *et al.*

The Bunz group, which has continually explored a type of OPE OPV cruciform systems since 2002, should probably receive the credit of making the most significant contribution to the recent research on 2D π -oligomers. In 2005, for example, this group successfully synthesized a series of 2D D⁺A substituted conjugated co-oligomers **327-330** (Figure 4.5) and discovered that dramatic blue and/or red shifts of emission and absorption took place upon coordination of metal cations, such as Zn²⁺, with oligomers **328-330**. Detailed photophysical data are given in Table 4.1. Such photophysical properties of these functional cruciform oligomers have rendered them valuable uses in molecular sensory applications.³⁴⁹

Bunz further rationalized the observed spectral changes shown in Table 4.1 on the basis of frontier molecular orbital (FMO) perturbations. In a general sense, the spatial locations of the HOMO and LUMO in each of the cruciform oligomers **327-330** are calculated to be “orthogonal” (*i.e.* non-superimposable in orientation), which is in sharp contrast to the scenarios of most simple 1D linear conjugated oligomers where HOMO and LUMO are usually spatially overlapped. In the OPE OPV cruciform oligomers, the HOMO is located on the distyrylbenzene branch, while the LUMO is located on the bisarylethynyl axis of the molecule. The blue shift in **328** and the red shift in **329** upon addition of zinc ions can be explained as follows. In **328**, addition of the zinc ions will lead to lowered HOMO energy due to the electron-withdrawing effect of the positive charge caused by zinc coordination to the dibutylamino groups. The LUMO will not be significantly affected, since it is located at the noncoordinating OPE branch of the cruciform. The reverse is true for **329**. Upon coordination of the pyridine nitrogen to the metal cation, the energy level of LUMO in **329** should drop, while the HOMO remains kind of unaffected. As for compound **330**, although

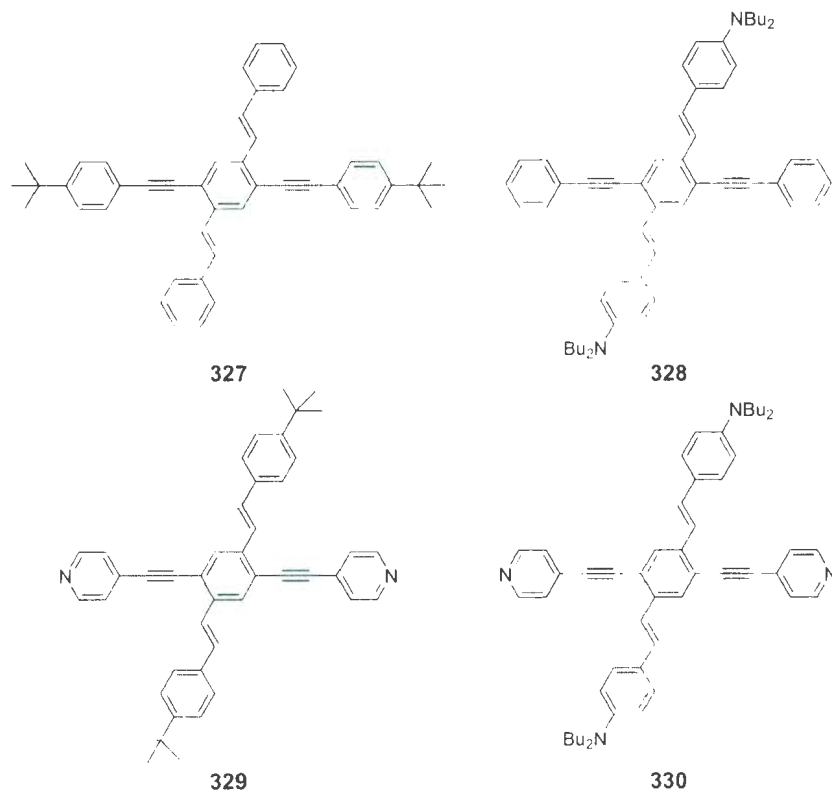


Figure 4.5: Cruciform OPE/OPV fluorophores developed by Bunz *et al.* as molecular sensors.

Bunz did not provide any detailed explanations for the observed optical data, a likely rationalization may be made as follows. Upon addition of Zn^{2+} ions, the cations will first coordinate with the dibutylamino groups, which will give rise to a hypsochromic shift. As the addition of cation continues, the excess cations will begin to coordinate with the pyridine nitrogen, which in turn induces backward bathochromic shifts.³⁴⁹

The main theme of this chapter is to systematically study two groups of 2D conjugated OPE/OPV based co-oligomers **331-335** and **336-339**, the structures of which are shown in Figure 4.6. The top row of Figure 4.6 lists a group of 2D

Table 4.1: Photophysical data for cruciform OPE/OPV **327-330**.

Compound	327	328	329	330
λ_{abs}	330	340, 446	328, 373(sh)	335, 440
$\lambda_{abs} (+ Zn^{2+})$	N/A	331	353, 456(sh)	350
$\epsilon (M^{-1} cm^{-1})$	92,000	48,000	83,700	53,800
λ_{em}	421, 442	530	456	571
$\lambda_{em} (+ Zn^{2+})$	N/A	430	564	418 (1 equiv)
Φ_f	0.83	0.31	0.49	0.08
$\Phi_f (+ Zn^{2+})$	N/A	0.66	0.01	0.10 (1 equiv), 0.10 (4 equiv)

OPE/OPV co-oligomers with relatively longer OPE branches and more solubilizing groups, while the bottom row shows a group of OPE/OPV co-oligomers with relatively shorter OPE branches and without solubilizing side chains. The 2D π oligomers designed herein are termed “H-mers” due to their unique H-shaped π -topology. Compared to the 2D oligomers briefly reviewed in the previous context, these H-mers feature relatively more complex conjugation dimensionality and electronic interactions. Examination of the π -electron delocalization patterns on one of the short H-mers (*e.g.* **339**) reveals three linear conjugation paths a, b, and c, while path c (highlighted bold in Figure 4.6) represents the longest linear π conjugation route among the others. Paths d, e, and f are cross-conjugated, along which weak electronic communications may be induced as well.^{147,154} The design of these H-mers is aimed to create a class of new 2D conjugated fluorophore cores whose electronic and photonic behavior can be flexibly manipulated or fine-tuned via chemical functionalization with

various electroactive and chromophoric groups. Furthermore, with the properties of these H-mers thoroughly characterized, it is anticipated that comprehensive structure-property relationships can be disclosed, based on which rational molecular tailoring for practical device applications would be eventually enabled. The following sections outline the detailed synthesis and photophysical investigations of these target H-mers.

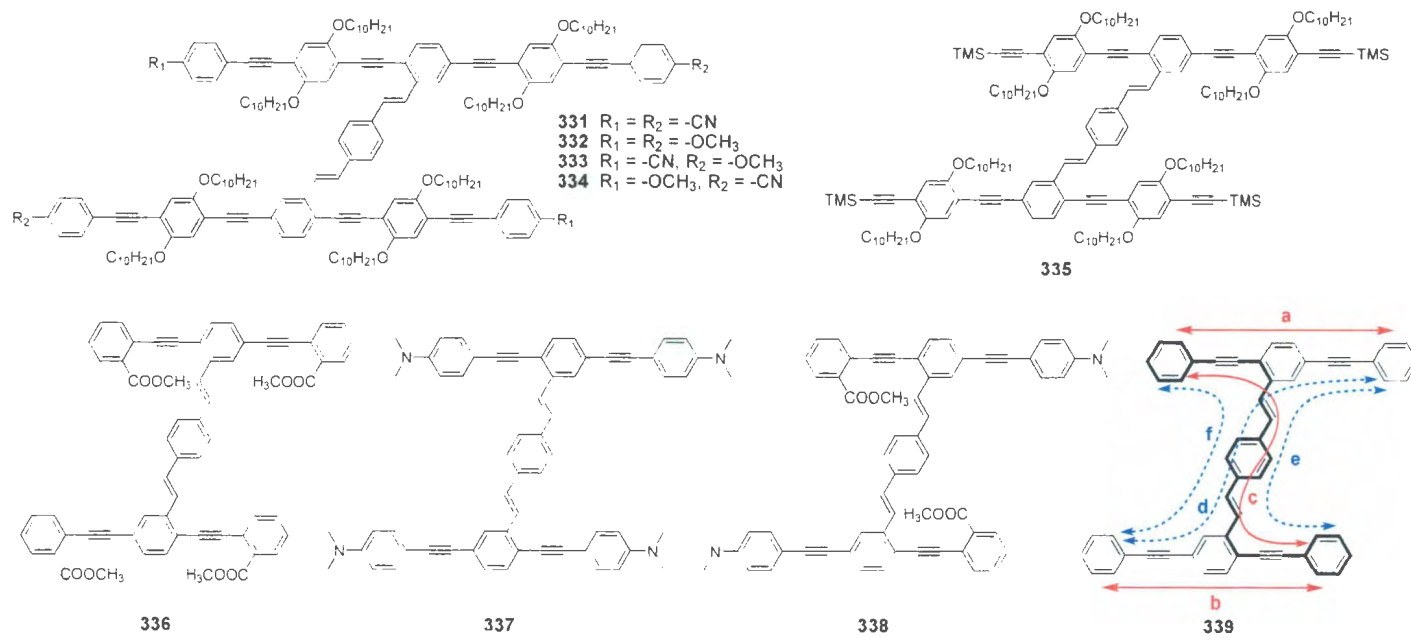


Figure 4.6: Target 2D conjugated OPE/OPV H-mers **331-339** in this chapter.

4.2 Results and discussion

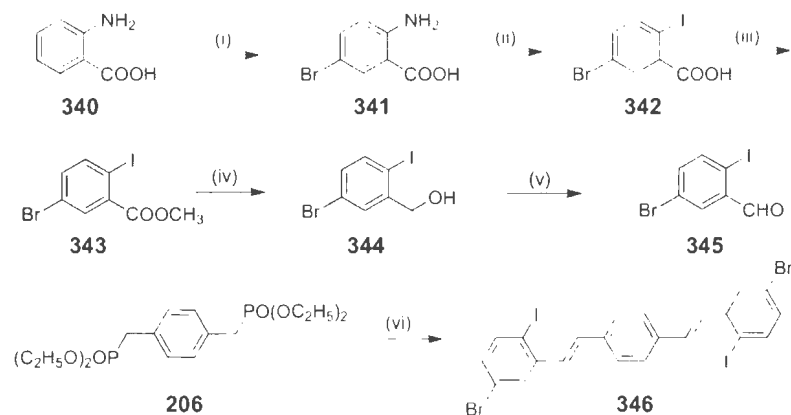
4.2.1 Synthesis of OPE/OPV based H-mers

4.2.1.1 Synthesis of long H-mer series

In the structure of the designed H-mers, there are four terminal phenyl groups which can be further functionalized with electroactive groups, such as D and/or A substituents. Due to the relatively low synthetic demand, two symmetrically D/A-functionalized long H-mers, **331** and **332**, were first prepared in this work.

The synthesis began with the preparation of a key building block, **346**, as shown in Scheme 4.1. First, 2-aminobenzoic acid (**340**) was brominated with Br₂ to give 2-amino-5-bromobenzoic acid (**341**). Compound **341** underwent a diazotization reaction followed by treatment with KI to afford 5-bromo-2-iodobenzoic acid (**342**), which was then subjected to a Fischer esterification with MeOH in the presence of H₂SO₄ to yield methyl ester **343**. Compound **343** was reduced into benzyl alcohol **344** by diisobutylaluminum hydride (DIBAL). Oxidation of **344** with pyridinium dichromate (PDC) resulted in the formation of 5-bromo-2-iodobenzaldehyde (**345**) in a quantitative yield. Compound **345** was subjected to a Wittig-Horner reaction with the phosphonate ylide that was generated by treating **206** with NaH, affording dibromodiiodo-OPV precursor **346** in a reasonable yield.

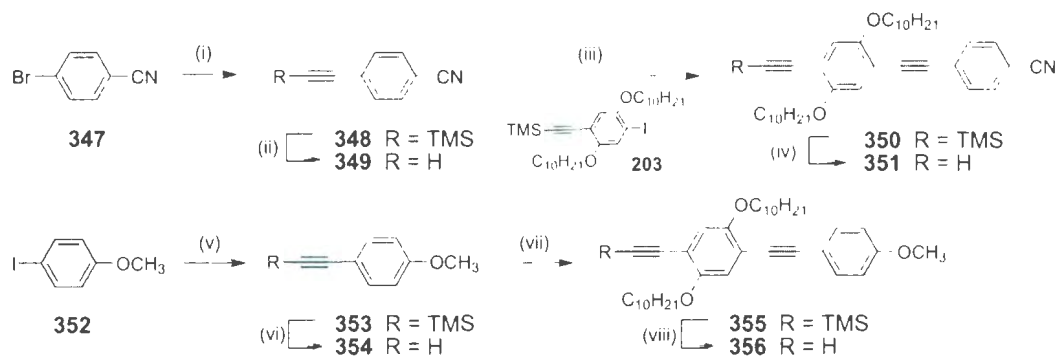
Besides **346**, two other important precursors, phenylene ethynylene dimers **351** and **356**, were prepared as outlined in Scheme 4.2. For the synthesis of **351**, a commercially available benzene derivative, **347**, was first converted into **348** via the Sonogoshira coupling. Treating **348** with K₂CO₃ resulted in the formation of terminal



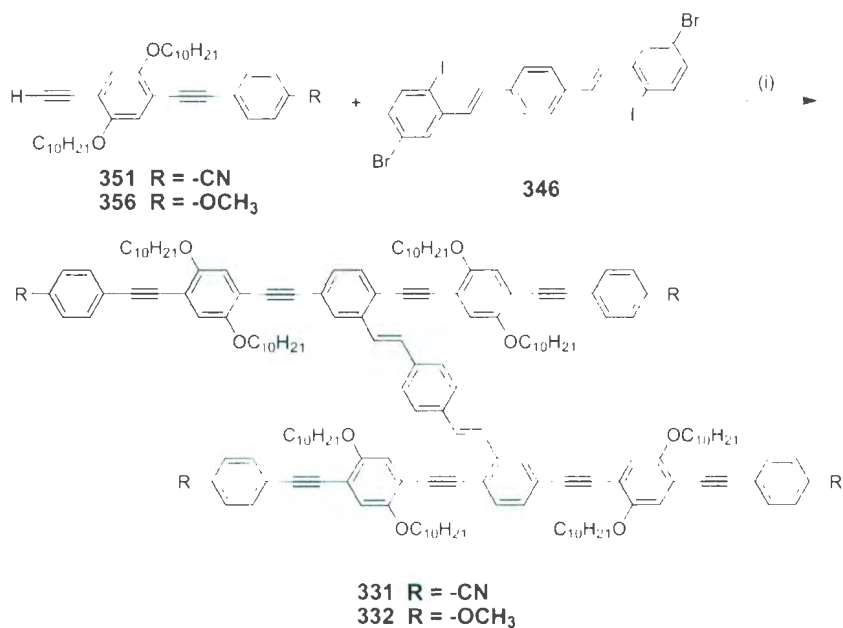
Scheme 4.1: Synthesis of OPV precursor **346**. Reagents and conditions: (i) Br_2 , CH_3COOH , 53%; (ii) NaNO_2 , H_2SO_4 then KI , 60%; (iii) H_2SO_4 , CH_3OH , 98%; (iv) DIBAL, CH_2Cl_2 , 100%; (v) PDC, CH_2Cl_2 , 98%; (vi) NaH , THF then **345**, 45%.

alkyne **349** in a yield of 91%. After this, one more Sonogashira coupling of **349** with iodoarene **203** was implemented under the catalysis of Pd-Cu to give compound **350**, which was desilylated with K_2CO_3 to afford phenylene ethynylene dimer **351** in a yield of 88%. Following a similar multi-step coupling route, another desired precursor, **356**, was obtained from 4-iodoanisole (**352**) in a very high overall yield.

With precursors **346**, **351** and **356** in hand, two functionalized H-mers, **331** and **332**, were readily synthesized by a Sonogashira coupling reaction in decent yields, using $\text{Pd}(\text{PPh}_3)_4$ as the catalyst (Scheme 4.3). Note that the two H-mers feature symmetrical substitutions with either electron withdrawing $-\text{CN}$ groups (in **331**) or electron donating $-\text{OCH}_3$ groups (in **332**) on the four termini of the H-mer backbone.

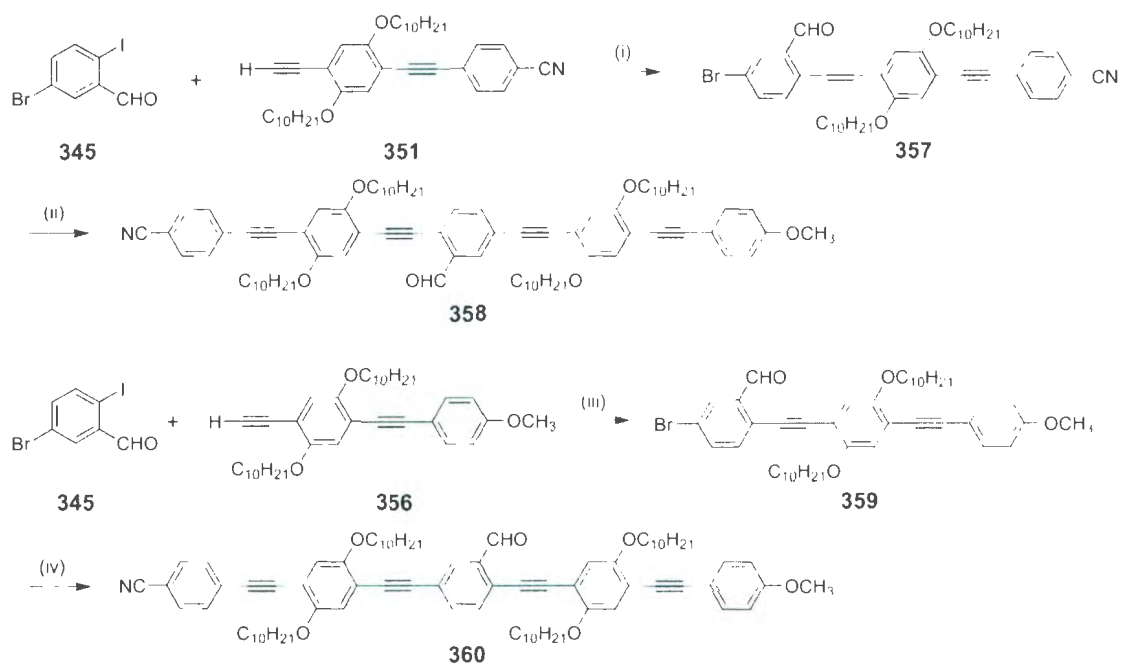


Scheme 4.2: Synthesis of phenylene ethynylene dimers **351** and **356**. Reagents and conditions: (i) TMSA, Pd(PPh₃)₂Cl₂, CuI, Et₃N, 95%; (ii) K₂CO₃, THF, CH₃OH, 91%; (iii) **203**, Pd(PPh₃)₂Cl₂, CuI, Et₃N, 100%; (iv) K₂CO₃, THF, CH₃OH, 88%; (v) TMSA, Pd(PPh₃)₂Cl₂, CuI, Et₃N, 100%; (vi) K₂CO₃, THF, CH₃OH, 100%; (vii) **203**, Pd(PPh₃)₂Cl₂, CuI, Et₃N, 92%; (viii) K₂CO₃, THF, CH₃OH, 96%.

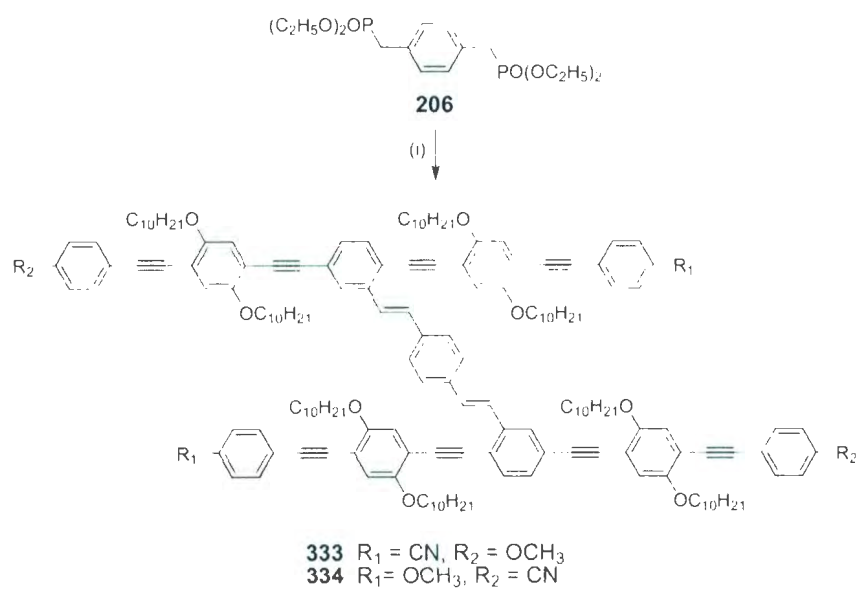


Scheme 4.3: Synthesis of D A-substituted H-mers **331** and **332**. Reagents and conditions: (i) Pd(PPh₃)₄, CuI, Et₃N, 59% for **331** and 57% for **332**.

Since the D-A substituted long H-mers, **333** and **334**, consist of unsymmetrically functionalized OPE branches, bearing a donor (OCH₃) on one end and an acceptor group (CN) on the other, their synthesis was undertaken through a different route than that for D:A substituted H-mers **331** and **332** (Note that D-A herein refers to "donor and acceptor", while D:A denotes "donor or acceptor"). The two D-A substituted H-mers **333** and **334** are regio-isomers to one another. As shown in Scheme 4.4, D-A substituted OPE branches **358** and **360** were prepared first by using 5-bromo-2-iodobenzaldehyde (**345**) as the starting material. Because iodoarene is more reactive than bromoarene in metal-catalyzed cross coupling reaction, OPEs **358** and **360** can be synthesized through different coupling sequences, and the molar ratios of starting materials in the carbon-carbon bond forming coupling reaction must be carefully controlled. Once **358** and **360** were obtained, H-mer **333** and **334** were prepared by a Wittig-Horner reaction between the phosphonate ylide resulting from **206** and respective OPE precursors (see Scheme 4.5).



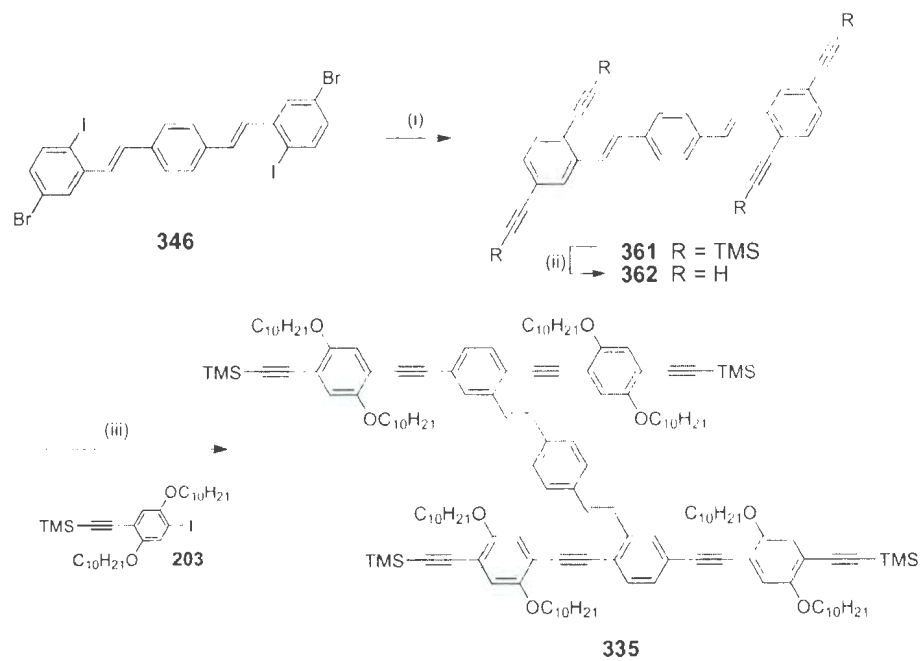
Scheme 4.4: Synthesis of symmetrically D-A substituted OPEs **358** and **360**. Reagents and conditions: (i) $\text{Pd}(\text{PPh}_3)_2\text{Cl}_2$, CuI , Et_3N , 81%; (ii) **356**, $\text{Pd}(\text{PPh}_3)_4$, CuI , Et_3N , 80%; (iii) $\text{Pd}(\text{PPh}_3)_2\text{Cl}_2$, CuI , Et_3N , 28%; (iv) **351**, $\text{Pd}(\text{PPh}_3)_2\text{Cl}_2$, CuI , Et_3N , 71%.



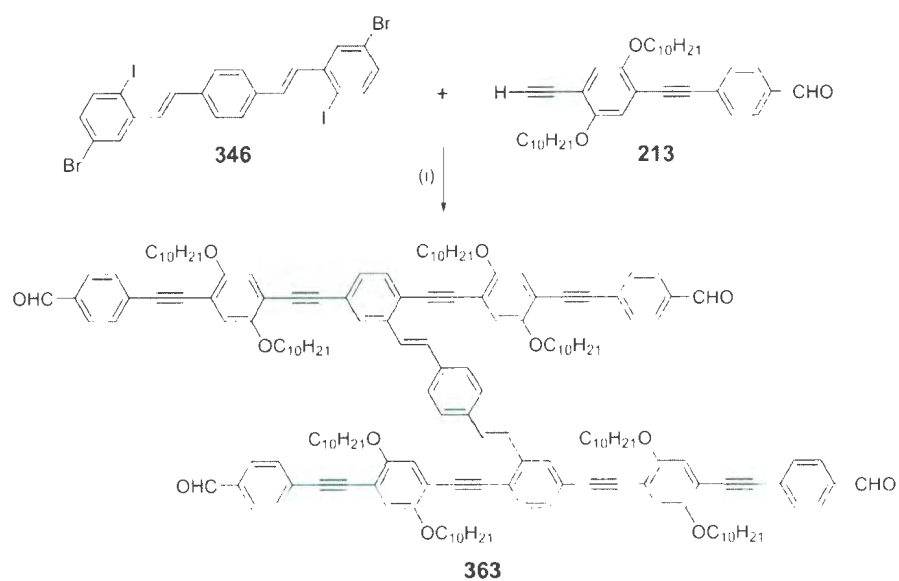
Scheme 4.5: Synthesis of D-A substituted long H-mers **333** and **334**. Reagents and conditions: (i) NaH, THF then **358** or **360**, 21% for **333** and 59% for **334**.

In addition to the aforementioned D-A and D-A substituted H-mers, another H-mer **335** with the same molecular π -framework as the previous ones, but without any D/A substituents was also prepared. This molecule was intended to serve as a standard to be compared with other functionalized H-mers, so as to better probe the electronic effects imposed by the D/A groups attached to the phenyl termini of the H-mer backbone. As shown in Scheme 4.6, treating OPV **346** with excess TMSA under Sonogashira coupling conditions resulted in **361** in 82% yield. Desilylation of **361** with K_2CO_3 afforded the desired terminal alkyne **362** as a brownish solid. Using compound **362** as a precursor, H-mer **335** was then prepared via a Sonogashira cross-coupling reaction with iodoarene **203**.

Following a similar synthetic strategy to the preparation of D-A H-mers **331-335**, another series of substituted H-mers **363** and **365** were prepared as shown in Schemes 4.7 and 4.8. In these H-mers, aldehyde groups were utilized as the acceptors in place of the -CN groups in the previous H-mers. Besides from probing the electronic substitution effects, the use of aldehyde groups was also intended to explore their potential of enabling further extension of π -conjugation via such reactions as Wittig-Horner or Schiff base condensation.

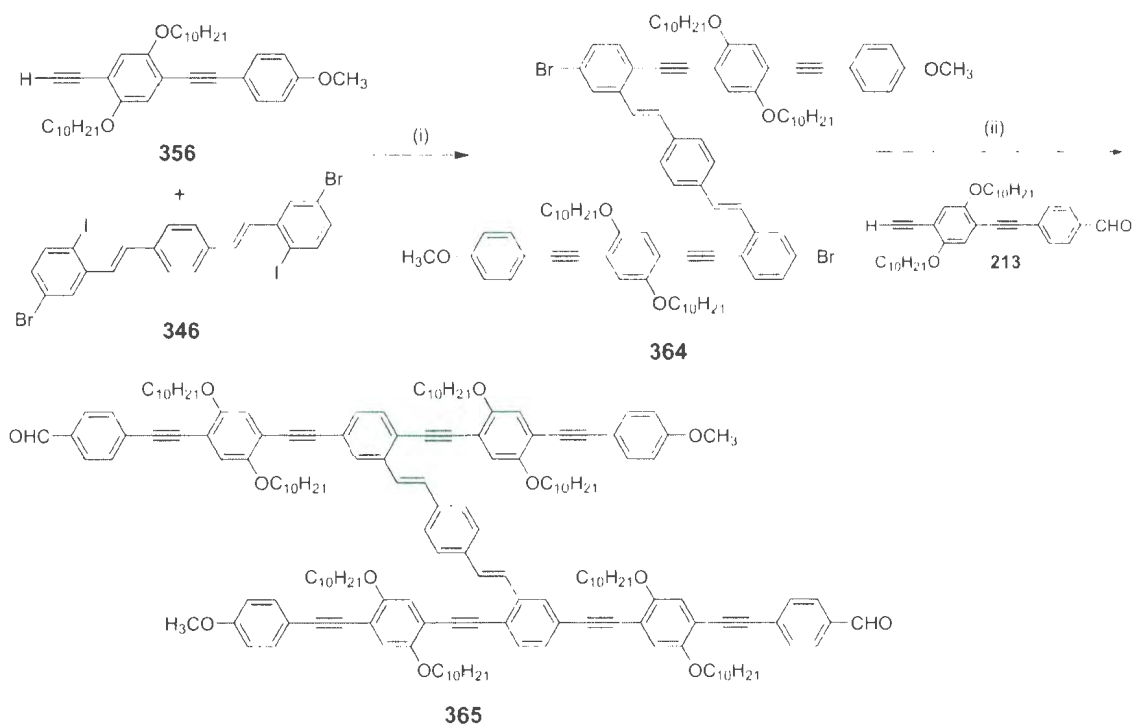


Scheme 4.6: Synthesis of unsubstituted long H-mers **335**. Reagents and conditions: (i) TMSA, Pd(PPh₃)₂Cl₂, CuI, Et₃N, 82%; (ii) K₂CO₃, THF, CH₃OH, 100%; (iii) **203**, Pd(PPh₃)₂Cl₂, CuI, Et₃N, 36%.



Scheme 4.7: Synthesis of aldehyde-substituted H-mer **363**. Reagents and conditions:

(i) Pd(PPh₃)₄, CuI, Et₃N, 68%.



Scheme 4.8: Synthesis of D-A substituted H-mer **365**. Reagents and conditions: (i) $\text{Pd}(\text{PPh}_3)_4$, CuI , Et_3N , 48%; (ii) **213**, $\text{Pd}(\text{PPh}_3)_4$, CuI , Et_3N , 61%.

4.2.1.2 Synthesis of short H-mer series

In this subsection, the synthesis of another series of functionalized conjugated H-mers **336-339** is discussed. Compared with the previous long D-A H-mer series, the D group used for the short H-mers herein is changed from OCH₃ group to a much stronger D group, NMe₂, in order to both enhance electronic substitution effects and to incorporate new binding sites for complexation of the H-mers with acidic or metallic species (*i.e.* potential as chemical sensors). The OPE chain length on the short H-mers is shortened to trimer, so that electronic communications among the electroactive groups can be further enhanced.

Outlined in Scheme 4.9 is the initial synthetic approach attempted for an A-functionalized H-mer, **336**. First, using **345** as the starting material, aldehyde **367** was obtained through a cross-coupling reaction followed by a desilylation step. In parallel to the preparation of **367**, iodoarene **370** was synthesized through a sequence of Sandmeyer and Fischer esterification reactions on commercially available 2-aminobenzoic acid (**340**). Next, Sonogashira coupling of terminal alkyne **367** and iodoarene **370** was performed to afford OPE **371** in a yield of 63%. From **371**, one more step of Wittig-Horner reaction was envisioned to furnish the desired H-mer **336**. However, this reaction was unsuccessful despite numerous attempts.

The unsuccessful outcome in the above synthesis shifted our focus to an alternative route as illustrated in Scheme 4.10. In this approach, terminal alkyne **362** was used as one of the substrates for cross-coupling reaction. The desired H-mer **336** was obtained in high purity through recrystallization of the crude product from CH₂Cl₂ and hexanes. The yield after purification was 70% and the avoidance of column

chromatographic separation is particularly beneficial for large-scale preparation. It is worth noting that COOCH₃ group was chosen as the acceptor to functionalize **336** not only because of its electron withdrawing ability (albeit COOCH₃ is a moderate A group) suited for probing substitution effects, but also its versatility to be readily transformed into carboxylic acids via simple hydrolysis. As the -COOH functionality is a commonly used linkage group binding to various bioactive molecules (*e.g.* through ester or amide bond), novel H-mer based bioconjugates can be potentially prepared in our future work, which may further lead us to some appealing applications in the fields of biosensing and bioimaging.

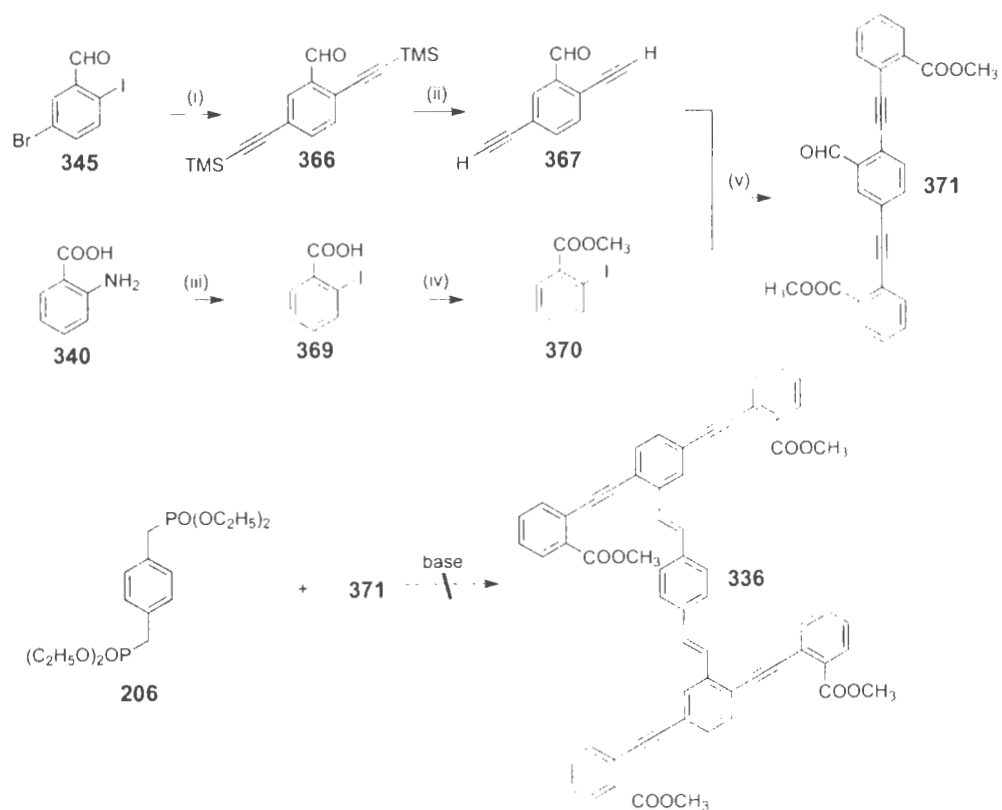
The synthesis of D-substituted (NMe₂) short H-mer **337** is outlined in Scheme 4.11. The first step was iodination of *N,N*-dimethylaniline (**372**) in dioxane in the presence of pyridine, yielding iodoarene **373**. Next, compound **373** was cross-coupled with terminal alkyne **362** under Sonogashira conditions to afford H-mer **337**. Herein piperidine was found to result in much better yields as both base and solvent for this coupling reaction in comparison to the commonly used triethylamine.

The attempt to synthesize D-A substituted H-mer **338** initially adopted the same strategy as outlined in Scheme 4.9. Although this route previously failed in obtaining H-mer **336**, it was still explored for the preparation of **338** with the hope that the alteration from ester to amino substituents would lead to an optimistic outcome. In this approach (see Scheme 4.12), compound **345** was first cross-coupled with TIPSA to give **374** in 89% yield. Another Sonogashira coupling between **374** and TMSA afforded **375** in a very high yield. Selective desilylation of **375** with K₂CO₃ led to **376**, which was then cross-coupled with iodoarene **370** to yield compound **377**. Desilylation of **377** with TBAF provided terminal alkyne **378**, which was

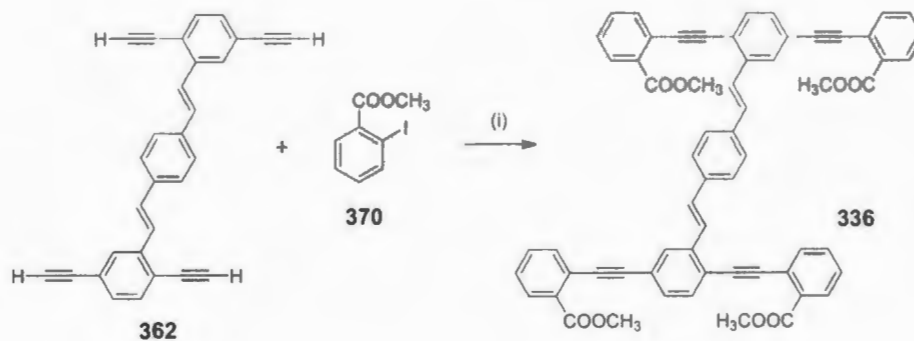
subsequently coupled with iodoarene **373** to form OPE precursor **379**. At this point, it would require one more step of Wittig-Horner reaction to finalize the synthesis; however, this very step again encountered tremendous difficulties, hence forcing us to abandon this synthetic approach.

An alternative approach as shown in Scheme 4.13 turned out to be very successful in preparing H-mer **338**. In this approach, the central OPV moiety was first constructed by a Wittig-Horner reaction between **206** and **374**, leading to one of the key building blocks, **380**. Cross coupling **380** with TMSA then generated **381**. Compound **381** was desilylated and then subjected to another Sonogashira coupling with iodoarene **370** to give compound **383**. Repetition of the desilylation-Sonogashira coupling sequence eventually afforded H-mer **338** in a reasonable yield.

Apart from the D/A functionalized H-mers, two π -conjugated oligomers **339** and **389** were also prepared as shown in Scheme 4.14. Compound **339** can be viewed as a short H-mer backbone without any substituents, while compound **389** is a one-dimensional linear π -framework endcapped with two electron-donating groups (NMe_2). The two molecules provide valuable references in the subsequent electronic spectroscopic characterizations in term of probing various effects arising from electronic substitution and conjugation dimensionality on the H-mer π framework.

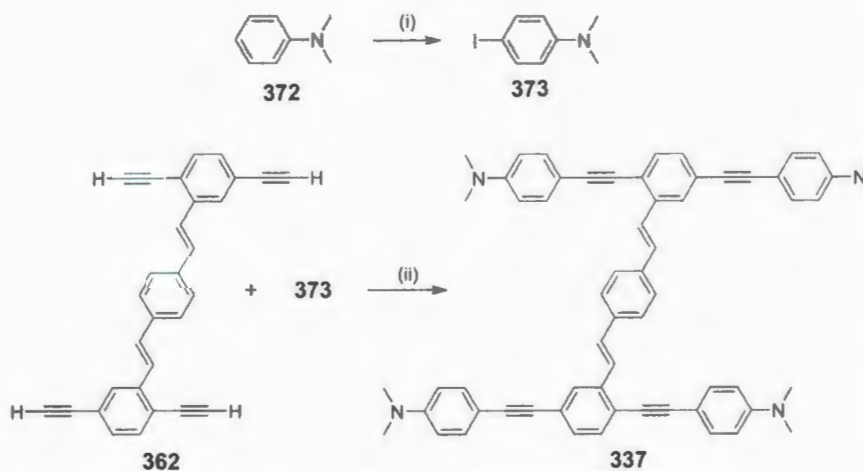


Scheme 4.9: Attempted synthesis of A-substituted short H-mer **336**. Reagents and conditions: (i) TMSA, Pd(PPh₃)₂Cl₂, CuI, Et₃N, 100%; (ii) K₂CO₃, THF, CH₃OH, 90%; (iii) NaNO₂, H₂SO₄ then KI, 64%; (iv) H₂SO₄, CH₃OH, 96%; (v) Pd(PPh₃)₂Cl₂, CuI, Et₃N, 63%.



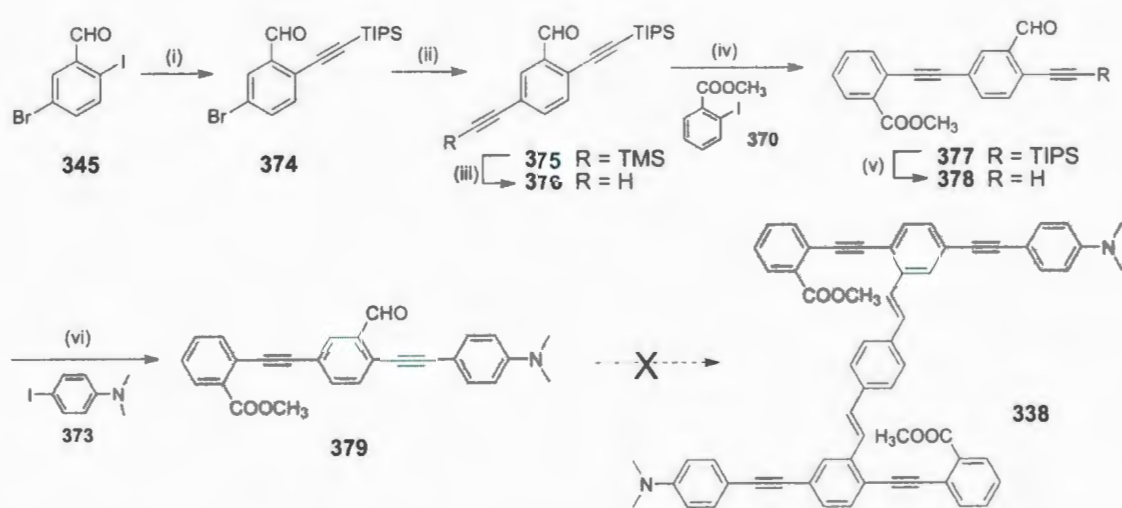
Scheme 4.10: Synthesis of A-substituted short H-mer **336**. Reagents and conditions:

(i) $\text{Pd}(\text{PPh}_3)_2\text{Cl}_2$, CuI , Et_3N , 70%.

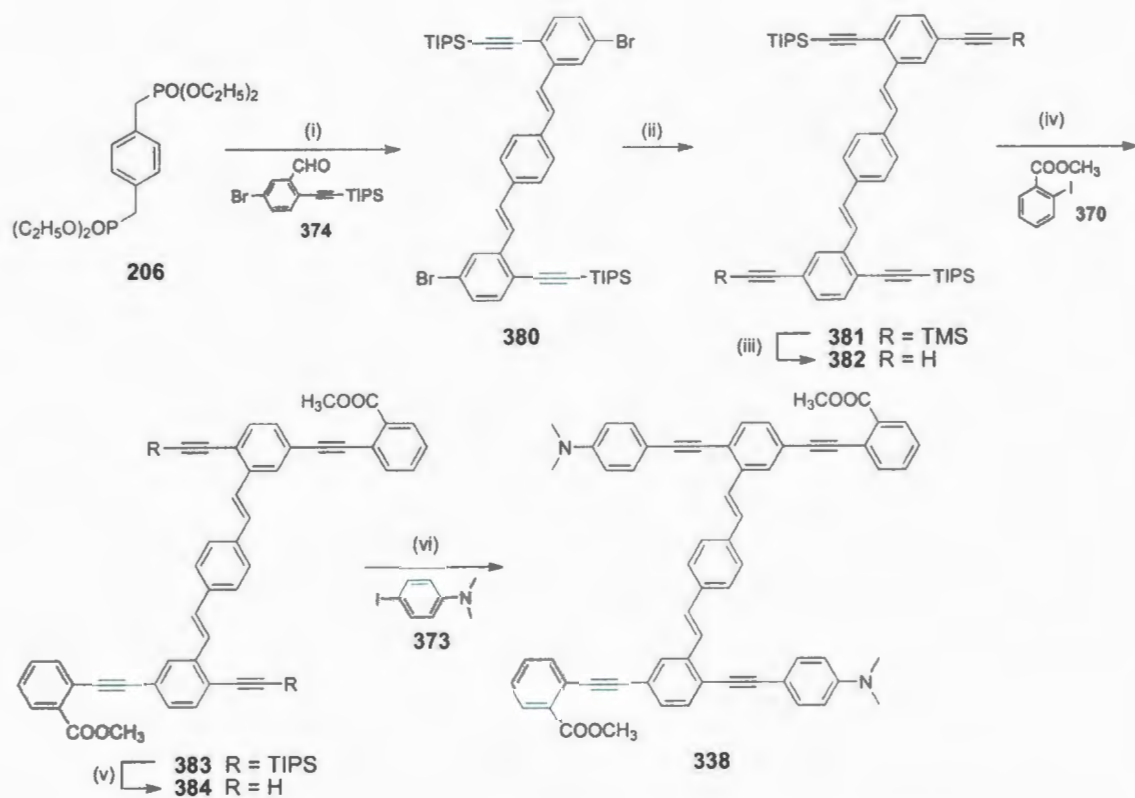


Scheme 4.11: Synthesis of D-substituted short H-mer **337**. Reagents and conditions:

(i) I_2 , pyridine, dioxane, 61%; (ii) $\text{Pd}(\text{PPh}_3)_2\text{Cl}_2$, CuI , piperidine, 79%.



Scheme 4.12: Attempted synthesis of D-A substituted short H-mer **338**. Reagents and conditions: (i) TIPSA, Pd(PPh₃)₂Cl₂, CuI, Et₃N, 94%; (ii) TMSA, Pd(PPh₃)₂Cl₂, CuI, Et₃N, 99%; (iii) K₂CO₃, THF, CH₃OH, 100%; (iv) **370**, Pd(PPh₃)₂Cl₂, CuI, Et₃N, 76%; (v) TBAF, THF, 78%; (vi) **373**, Pd(PPh₃)₂Cl₂, CuI, Et₃N, 47%.



Scheme 4.13: Synthesis of D-A substituted short H-mer **338**. Reagents and conditions: (i) NaH , THF then **374**, 45%; (ii) TMSA, $\text{Pd}(\text{PPh}_3)_2\text{Cl}_2$, CuI, Et_3N , 93%; (iii) K_2CO_3 , THF, CH_3OH , 79%; (iv) **370**, $\text{Pd}(\text{PPh}_3)_2\text{Cl}_2$, CuI, Et_3N , 76%; (v) TBAF, THF, 91%; (vi) **373**, $\text{Pd}(\text{PPh}_3)_2\text{Cl}_2$, CuI, piperidine, THF, 47%.

4.2.2 Electronic spectroscopic properties

4.2.2.1 Electronic spectroscopic properties of long H-mers

The UV-Vis absorption spectra of long H-mers **331**–**335** were measured in CHCl_3 at room temperature and are shown in Figure 4.7. Detailed maximum absorption wavelengths (λ_{max}) and extinction coefficients (ϵ) are enumerated in Table 4.2.

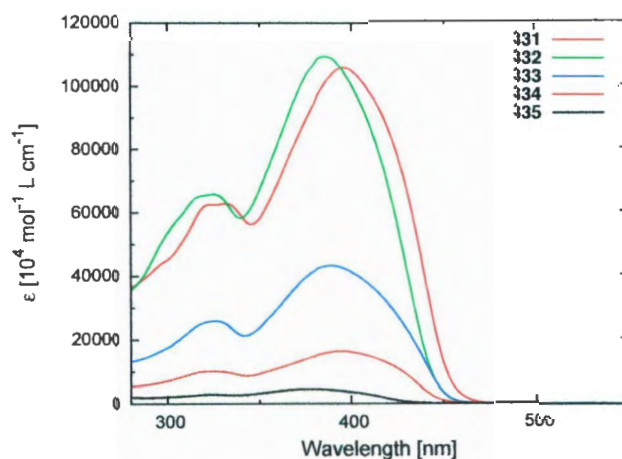


Figure 4.7: UV-Vis absorption spectra of long H-mers **331**–**335** measured in CHCl_3 .

From Figure 4.7, it can be clearly observed that the three long H-mers that are substituted with strong electron-withdrawing CN groups, **331**, **333**, and **334**, show maximum absorption (λ_{max}) at relatively long wavelengths (393–397 nm). Tetramethoxy-substituted long H-mer **332** shows blueshifted λ_{max} at 386 nm, while non-substituted long H-mer **335** has the lowest λ_{max} value at 376 nm. It is also notable that symmetrical D- or A-substituted H-mers **331** and **332** exhibit extinction coefficients greater than those of D-A substituted H-mers **333** and **334** by more than two-fold. The difference in molar absorptivity can be generally related to different

transition moments and molecular symmetry. Using the unsubstituted H-mer **335** as a standard, the redshifts of λ_{max} for the long H-mers arising from D/A substitution effects are rather small, less than 21 nm (*ca.* 1407 cm^{-1}), in comparison to the cases for D/A substituted linear phenylacetylene oligomers. The weakened electronic substitution effects are likely due to the non-planar long H-mer backbone as a result of the bulky decyloxy chains appended.

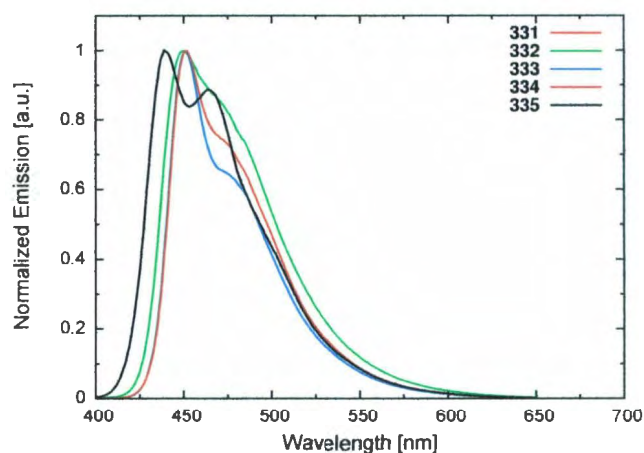


Figure 4.8: Fluorescence spectra of long H-mers **331–335** measured in degassed CHCl_3 .

Electronic emission spectra for long H-mers **331–335** are shown in Figure 4.8. All the long H-mers are very emissive upon electronic excitation and give fluorescence quantum yields in the range of 0.52–0.72 as measured in diluted CHCl_3 solutions. The substituted H-mers **331–334** show a very similar maximum emission peak (λ_{em}) at *ca.* 450 nm (see Table 4.2), while the unsubstituted H-mer **335** shows a λ_{em} value at 439 nm, which is merely blueshifted by about 11 nm (*ca.* 557 cm^{-1}). In line with the UV-Vis data, the rather small spectral shifts observed in Figure 4.8 corroborate that

the electronic substitution effects on the long H-mer backbone are small. In addition to the maximum emission peak, an emission shoulder peak is also clearly discernible in each spectrum, the origin of which can be attributed to vibronic progressions.

4.2.2.2 Electronic spectroscopic properties of short H-mers

Figure 4.9 shows the UV-Vis absorption spectra of short H-mers **336-339** measured in CHCl_3 at room temperature. In contrast to the long H-mer series, the spectral behavior of short H-mers is subject to different electronic substitution effects to a dramatic extent. Tetrakis(*N,N*-dimethylamino)-substituted short H-mer **337** exhibits the most redshifted λ_{max} relative to that of unsubstituted short H-mer **339** (see Table 4.2). The spectral shift as a result of tetra-donor substitutions is about 40 nm (*ca.* 3.333 cm^{-1}), which is considerably larger than the shifts observed in its long H-mer analogues. D-A and A- substituted short H-mers **338** and **336** also show significantly redshift λ_{max} values at 358 and 345 nm respectively versus that of **339**. The substantial spectral shifts signify strong electronic interactions between the short H-mer backbone and the substituent groups, and the enhanced electronic substitution effects can be reasoned by the more planar π -framework of the short H-mers than that of the long H-mers.

The first excited-state (S_1) properties of short H-mers **336-339** were investigated by steady-state fluorescence spectroscopy, and the spectral profiles are given in Figure 4.10. The spectrum of unfunctionalized H-mer **339** shows a distinctive vibronic progression with three bands at 425, 450, and 480(sh) nm respectively. The vibronic spacing is 1.348 cm^{-1} , which can be attributed to an averaged vibrational mode with the largest contribution from the C-C stretch in the central vinylene moiety

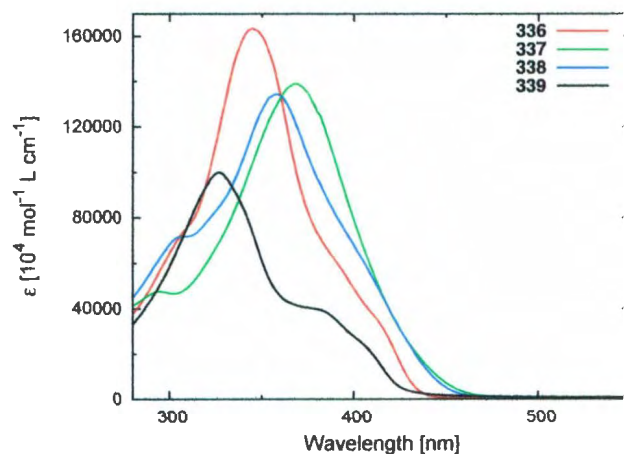


Figure 4.9: UV-Vis absorption spectra of short H-mers **336** -**339** measured in CHCl_3 .

of **339**.³⁵⁷ The emissions of A-substituted (COOMe) H-mer **336** are observed at 442, 462, 491(sh) nm, which are only slightly redshifted relative to that of **339**. For D-A substituted (NMe_2 and COOMe) H-mer **338** and D-substituted (NMe_2) H-mer **337**, broad peaks centered at 500 (**338**) and 506 nm (**337**) instead of distinctive vibronic bands are observed in the spectra. Unlike H-mer **336**, the maximum emission wavelengths (λ_{em}) of **337** and **338** are substantially redshifted relative to unsubstituted H-mer **339** (see Table 4.2). In addition, the fluorescence quantum yields of short H-mers **336**–**339** are determined in the range of 0.36–0.56, which are slightly lower than those of the long H-mers, likely due to stronger π - π stacking in solution.

4.2.3 Molecular sensing properties of functional H-mers

The observation of spectral changes of the H-mers in response to various electronic substitution has suggested a potential to utilize the H-mers as effective sensing

Table 4.2: Summary of photophysical data for H-mers **331-339** and OPE **389**.

Entry	Absorption		Emission			Entry	Absorption		Emission		
	λ (nm)	ϵ ($10^4 \text{ M}^{-1} \text{ cm}^{-1}$)	λ (nm)	Φ	τ (ns)		λ (nm)	ϵ ($10^4 \text{ M}^{-1} \text{ cm}^{-1}$)	λ (nm)	Φ	τ (ns)
331	322	6.7	450	0.72	1.3	337	295	0.48	506	0.43	6.4
	397	1.1	480 (sh)		1.3		367	1.4			
332	325	6.5	450	0.52	1.6	338	305 (sh)	7.4	500	0.56	5.3
	368	1.1	479 (sh)		1.8		358	14			
333	326	1.9	450	0.7	1.3	339	327	9.9	425	0.49	1.2
	391	3.2	480 (sh)		1.4		386	3.8	450		1.2
334	323	1.0	451	0.62	1.5			480 (sh)		1.3	
	393	1.6	488 (sh)		1.6	389	289	2.0	419	0.5	0.62
335	324	0.29	439	0.54	2.0		368	6.0	455		0.66
	376	0.46	465		2.2		388 (sh)	4.8			
336	245	7.6	442	0.36	2.0						
	303 (sh)	7.6	462		2.0						
	345	17									
	415 (sh)	3.3									

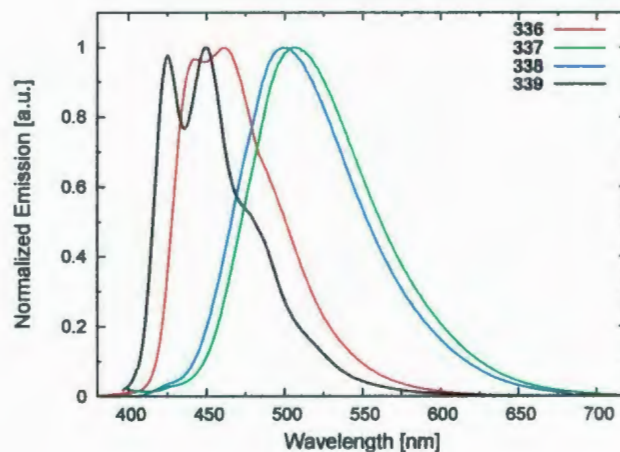


Figure 4.10: Fluorescence spectra of short H-mers **336–339** measured in degassed CHCl_3 .

chromophores and fluorophores in the detection of different molecular species, if the binding of H-mers to other substrates could induce significantly altered electronic interactions on the H-mer backbone.^{345–349} To explore their sensing functions, the long and short H-mers **331–339** were subjected to UV-Vis and fluorescence titrations with a variety of metal ions and a strong Brønsted acid, TFA. Table 4.3 summarizes the outcomes of spectral (UV-Vis and fluorescence) responses observed in different titration experiments.

For the long H-mers, only unsubstituted **335** was found to show pronounced spectral changes upon titration with AgOTf . The UV-Vis and fluorescence titration curves are shown in Figure 4.11.

From Figure 4.11A, the two $\pi \rightarrow \pi^*$ transition bands at 376 and 324 nm are observed to decrease steadily in intensity, together with an increasing absorption tail from 450 to 550 nm, as AgOTf is progressively added into the solution of **335**. The origins of such spectral responses are not clarified yet; however, the binding of Ag^+

Table 4.3: Summary of sensing effectiveness of H-mers **331-339** towards various species. Note that “+” denotes significant spectral changes observed upon titration, “-” denotes no spectral changes upon titration.

Entry	TFA	AgOTf	Cu(OTf) ₂	Zn(OTf) ₂	Mg(OTf) ₂
331					
332					
333					
334					
335		+			
336					
337	+	+	+		
338	+	+	+		
339					

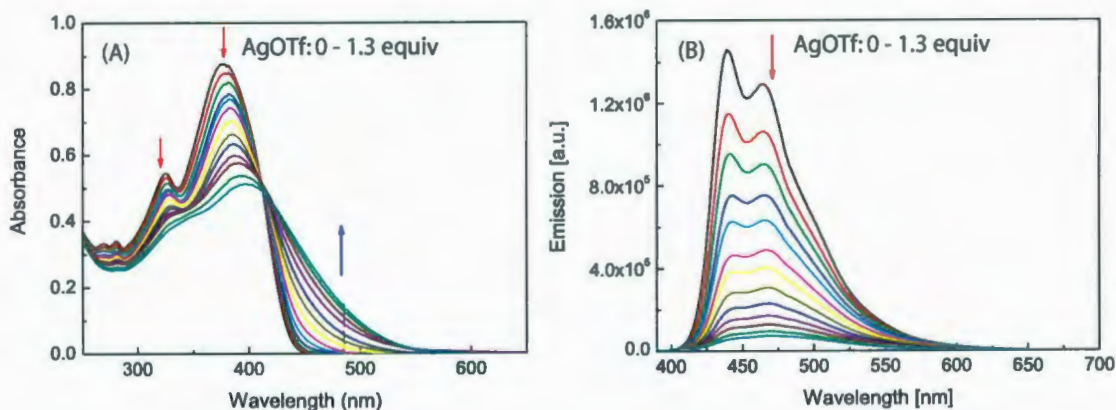


Figure 4.11: Titration results of H-mer **335** with AgOTf (0–1.3 equiv) in CHCl_3 : (A) UV-Vis profiles; (B) fluorescence profiles.

to acetylene bonds that further planarizes the H-mer backbone of **335** could offer a plausible explanation. From the fluorescence titration profiles shown in Figure 4.11B, the emission intensity of **335** decreases substantially with increasing addition of AgOTf. Upon titration with *ca.* 1.0 equiv of AgOTf, the fluorescence intensity appears to be suppressed by nearly ten-fold. The quenching effect is indicative of strong complexation of **335** with Ag^+ ion.

For short H-mers **337** and **338**, the UV-Vis and fluorescence titration curves obtained under the conditions of TFA, AgOTf, and $\text{Cu}(\text{OTf})_2$ additions are given in Figures 4.12 and 4.13. To better understand the spectral responses these H-mers display, similar titration experiments were conducted on model compound **389**, which consists of a trimeric phenylacetylene oligomer backbone endcapped with two NMe_2 groups. From the titration results depicted in Figures 4.12 to 4.14, it can be concluded that the complexation between the NMe_2 groups and H^+ or metal ions has significantly reduced the electron-donating properties of NMe_2 ; as a result,

its electronic nature is reversed from electron-releasing to electron-withdrawing. The change of electronic substitution effect hence alters the electronic characteristics of the H-mer backbone through π conjugation. As such, the amino-functionalized H-mers are bestowed with effective absorption and fluorescence sensing functions towards Brønsted acids or selected transition metal ions that can strongly bind to the NMe₂ groups.

4.3 Conclusions

In this chapter, a series of structurally distinctive two-dimensional conjugated, H-shaped cooligomers based on OPE-OPV building blocks were prepared mainly via Sonogashira coupling and Wittig-Horner reactions. Electronic and spectroscopic properties of the H-mers are investigated by UV-vis absorption and fluorescence spectroscopic characterizations. It is discovered that electronic and photonic behavior of the H-mers can be flexibly manipulated or tuned by chemical functionalization with various electroactive and chromophoric groups at the terminal positions of the oligomers. Furthermore, both experimental and theoretical analysis demonstrate that H-mers functionalized with suitable groups (*e.g.* amino) show fluorescence sensing function to Brønsted acids and transition metal ions. The results of this project verify that the π -conjugated scaffold of H-mers can be utilized as a versatile fluorophore platform for various fluorescence applications.

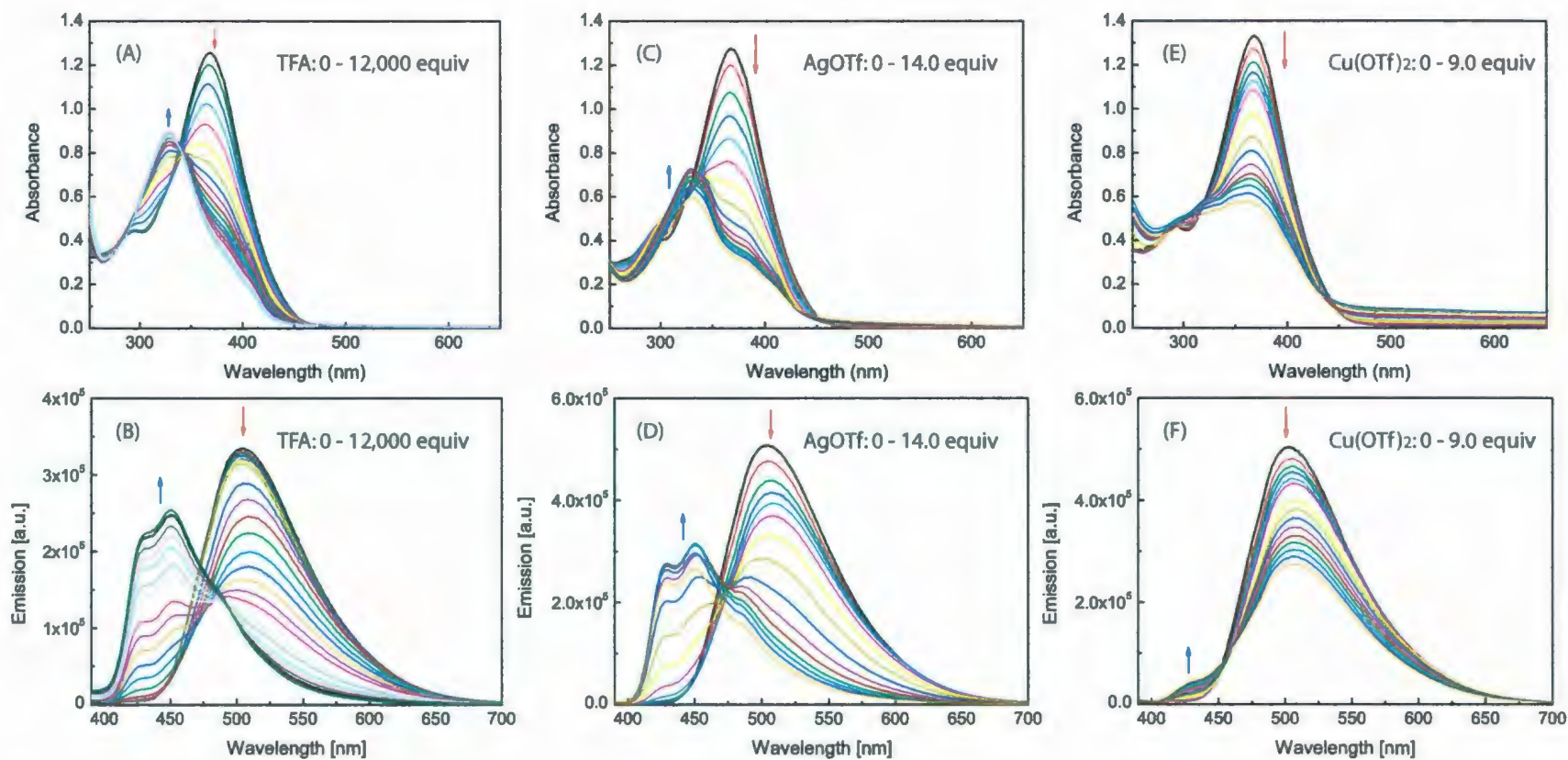


Figure 4.12: Titration results of H-mer **337** in CHCl_3 : (A) UV-Vis profiles with TFA (0–12,000 equiv); (B) fluorescence profiles with TFA (0–12,000 equiv); (C) UV-Vis profiles with AgOTf (0–14.0 equiv); (D) fluorescence profiles with AgOTf (0–14.0 equiv); (E) UV-Vis profiles with $\text{Cu}(\text{OTf})_2$ (0–9.0 equiv); (F) fluorescence profiles with $\text{Cu}(\text{OTf})_2$ (0–9.0 equiv).

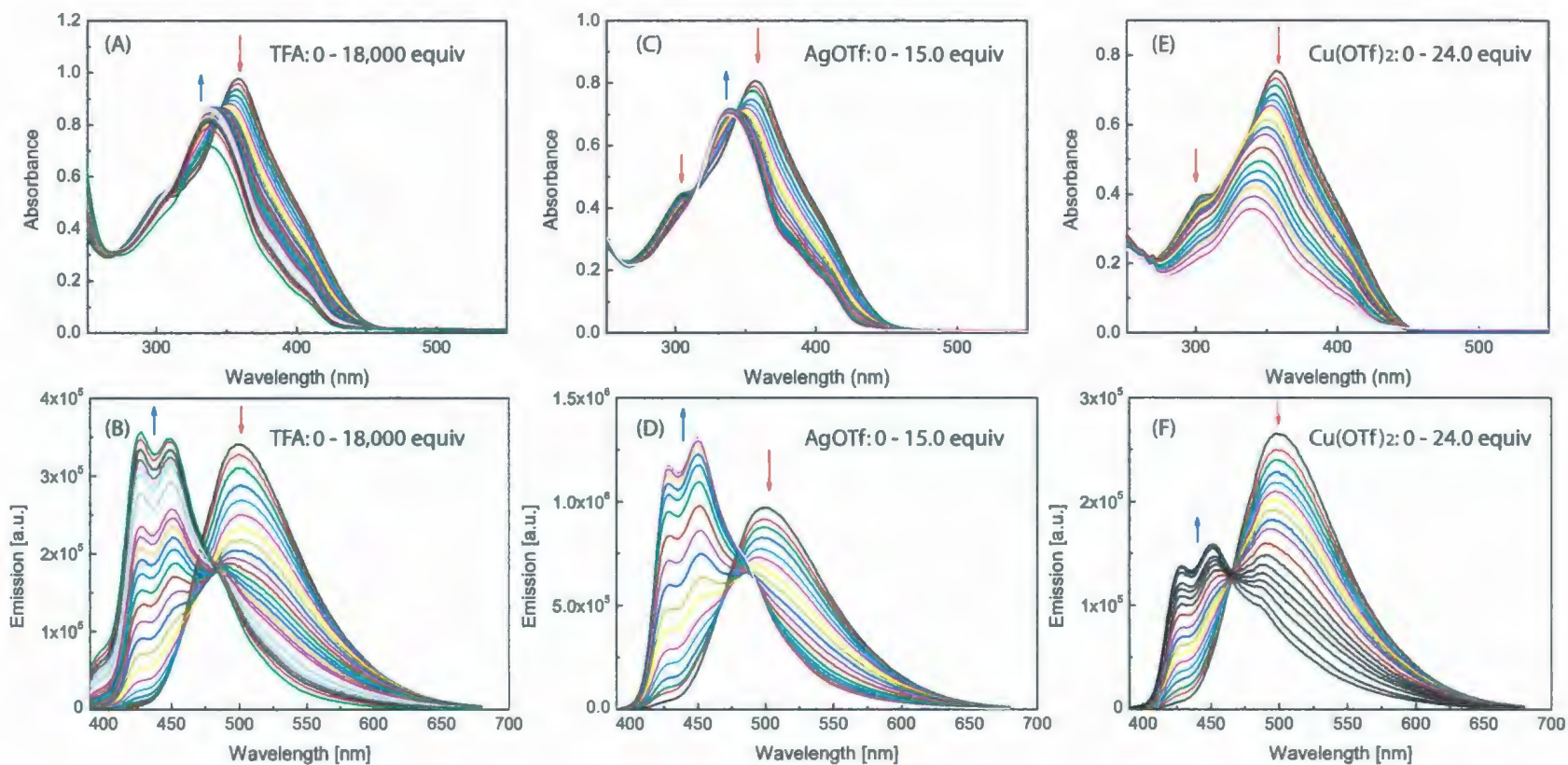


Figure 4.13: Titration results of H-mer **338** in CHCl_3 : (A) UV-Vis profiles with TFA (0-18,000 equiv); (B) fluorescence profiles with TFA (0-18,000 equiv); (C) UV-Vis profiles with AgOTf (0-15.0 equiv); (D) fluorescence profiles with AgOTf (0-15.0 equiv); (E) UV-Vis profiles with $\text{Cu}(\text{OTf})_2$ (0-24.0 equiv); (F) fluorescence profiles with $\text{Cu}(\text{OTf})_2$ (0-24.0 equiv).

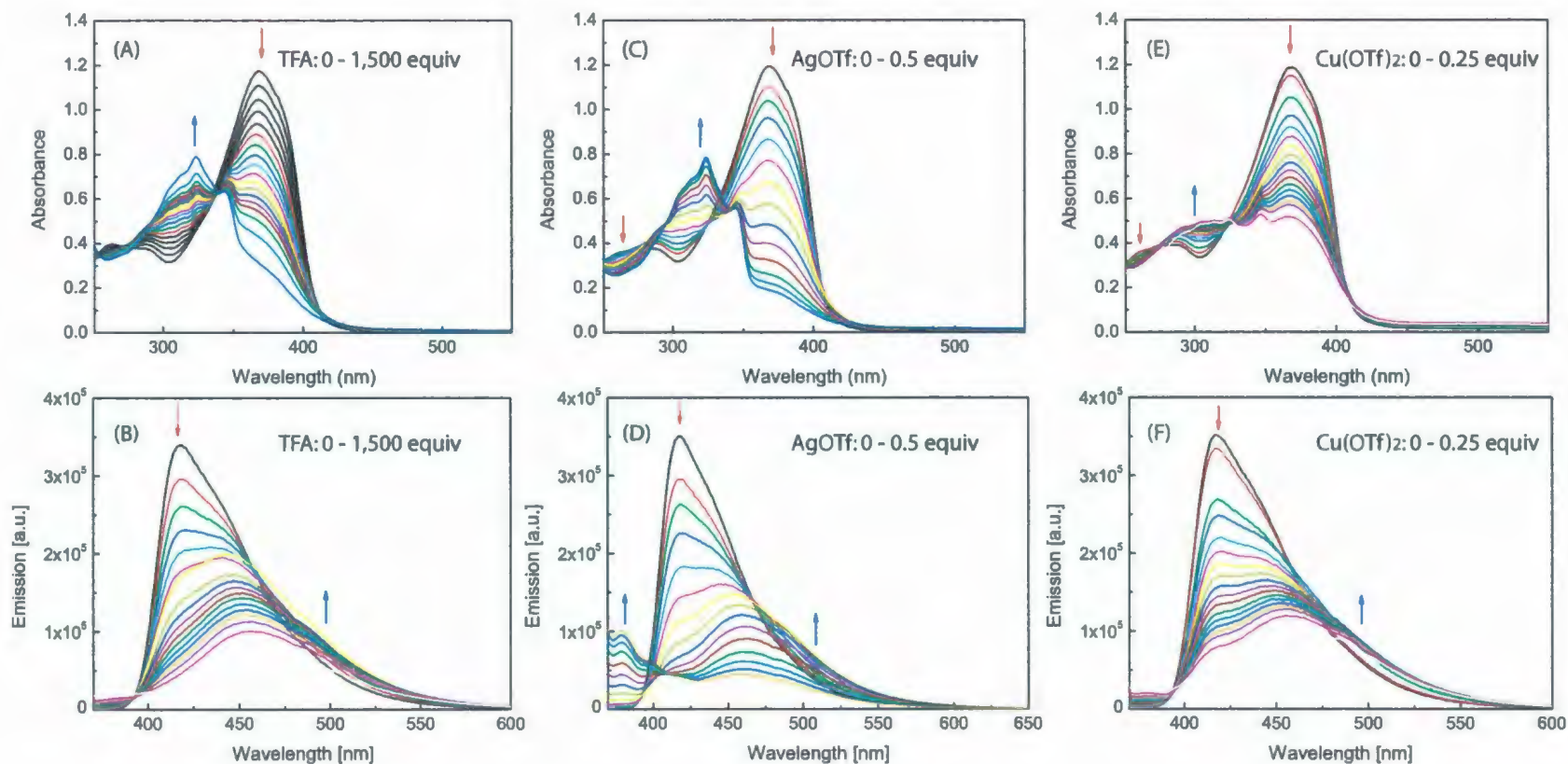


Figure 4.14: Titration results of OPE **389** in CHCl_3 : (A) UV-Vis profiles with TFA (0–15,00 equiv); (B) fluorescence profiles with TFA (0–15,00 equiv); (C) UV-Vis profiles with AgOTf (0–0.5 equiv); (D) fluorescence profiles with AgOTf (0–0.5 equiv); (E) UV-Vis profiles with $\text{Cu}(\text{OTf})_2$ (0–0.25 equiv); (F) fluorescence profiles with $\text{Cu}(\text{OTf})_2$ (0–0.25 equiv).

4.4 Experimental

General procedures and methods

Chemicals and reagents were purchased from commercial suppliers and used without further purification. Tetrabutylammonium fluoride (1 M in THF) and lithium hexamethyldisilazide (1 M in THF) were purchased from Aldrich. THF was distilled from sodium/benzophenone. Et₃N and toluene were distilled from LiH. Catalysts, Pd(PPh₃)₄ and Pd(PPh₃)₂Cl₂, were prepared from PdCl₂ according to standard procedures. All reactions were performed in standard, dry glassware under an inert atmosphere of N₂ unless otherwise noted. Evaporations and concentrations were done at H₂O aspirator pressure. Flash column chromatography was carried out with silica gel 60 (230-400 mesh) from VWR International. Thin-layer chromatography (TLC) was carried out with silica gel 60 F254 covered on plastic sheets and visualized by UV light or KMnO₄ stain. Melting points (Mp) were measured with a Fisher-Johns melting point apparatus and are uncorrected. ¹H and ¹³C NMR spectra were measured on a Bruker Avance 500 MHz spectrometer. Chemical shifts are reported in ppm downfield from the signal of the internal reference SiMe₄. Coupling constants (*J*) are given in Hz. The coupling constants of some aryl proton signals are reported as pseudo first-order spin systems, even though they are second-order spin systems. Infrared spectra (IR) were recorded on a Bruker Tensor 27 spectrometer. UV-Vis spectra were recorded on an Agilent 8453 UV-Vis or a Cary 6000i UV-Vis-NIR spectrophotometer. Fluorescence spectra were measured in CHCl₃ at ambient temperature using a Quantamaster 10000 fluorometer. APCI mass spectra were measured on an Agilent 1100 series LCMSD spectrometer, and high-

resolution MALDI-TOF mass spectra on an Applied Biosystems Voyager instrument with dithranol as the matrix.

Compound 331. Compound **351** (112 mg, 0.207 mmol), **346** (19 mg, 0.033 mmol), Pd(PPh₃)₄ (24 mg, 0.021 mmol), CuI (7.8 mg, 0.041 mmol) were added to Et₃N (6 mL). The solution was bubbled by N₂ at rt for 5 min and then heated to 50 °C under stirring and N₂ protection for 17 h. After the reaction was complete as checked by TLC analysis, the solvent was removed by rotary evaporation. The resulting residue was diluted with chloroform. The mixture was filtered through a MgSO₄ pad. The solution obtained was sequentially washed with aq HCl (10%) and brine. The organic layer was dried over MgSO₄ and concentrated under vacuum to give crude **331**, which was further purified by silica flash column chromatography (hexanes/CH₂Cl₂, 1:1) to yield compound **331** (47 mg, 0.019 mmol, 59%) as a yellow solid. Mp 134–135 °C; IR (KBr) 2924, 2853, 2226, 2207, 1693, 1663, 1552, 1533, 1514, 1467, 1417, 1385 cm⁻¹; ¹H NMR (CDCl₃, 500 MHz) δ 7.92 (s, 2H), 7.81 (d, *J* = 15.5 Hz, 2H, alkenyl H), 7.67–7.59 (m, 20H), 7.57 (d, *J* = 8.5 Hz, 2H), 7.42 (dd, *J* = 1.5 Hz, *J* = 8.5 Hz, 2H), 7.29 (d, *J* = 15.5 Hz, 2H, alkenyl H), 7.07 (s, 4H), 7.06 (s, 2H), 7.05 (s, 2H), 4.09–4.03 (m, 16H), 1.93–1.82 (m, 12H), 1.77–1.72 (m, 4H), 1.62–1.49 (m, 12H), 1.45–1.18 (m, 100H), 0.90–0.83 (m, 24H, CH₃); ¹³C NMR (CDCl₃, 125 MHz) δ 154.20, 154.17, 153.9, 153.8 (four Ar-O carbons), 139.0, 137.3, 132.8, 132.3, 132.20, 132.18, 132.1, 130.7, 130.4, 128.61, 128.56, 128.0, 127.5, 126.6, 123.8, 122.5, 118.73, 118.69, 117.3, 117.2, 117.0, 116.9, 115.3, 115.0, 113.31, 113.28, 111.7, 111.6 (two C=N, 24 Ar carbons and two alkenyl carbons), 95.3, 94.0, 93.5, 93.4, 93.1, 90.8, 90.7, 87.9 (eight alkynyl carbons), 70.1, 69.9, 69.8 (OCH₂ carbons), 32.1, 29.9, 29.8, 29.64, 29.61.

29.5, 29.4, 26.3, 26.1, 22.9, 14.3; APCI-MS (positive) m/z calcd for $C_{170}H_{206}N_4O_8$ 2431.58, found 2432.81 $[M + H]^+$.

1,4-Bis(2,5-bis((2,5-bis(decyloxy)-4-((4-methoxyphenyl)ethynyl)phenyl)-ethynyl)styryl)benzene (332). Compound **356** (113 mg, 0.207 mmol), **346** (19 mg, 0.32 mmol), $Pd(PPh_3)_4$ (25 mg, 0.022 mmol), CuI (12 mg, 0.063 mmol) were added to Et_3N (8 mL). The solution was degassed by bubbling N_2 at rt for 5 min and then heated to 60 °C under stirring and N_2 protection for 18 h. After the reaction was complete as checked by TLC analysis, the solvent was removed by rotary evaporation. The resulting residue was diluted with chloroform. The mixture was filtered through a $MgSO_4$ pad. The solution obtained was sequentially washed with aq HCl (10%) and brine. The organic layer was dried over $MgSO_4$ and concentrated under vacuum to give the crude product of **332**, which was further purified by silica flash column chromatography (hexanes/ CH_2Cl_2 , 1:1) to yield compound **332** (45 mg, 0.018 mmol, 57%) as a yellow solid. Mp 98–99 °C; IR (KBr) 2953, 2923, 2853, 2204, 1608, 1515, 1498, 1466, 1417, 1383 cm^{-1} ; 1H NMR ($CDCl_3$, 500 MHz) δ 7.91 (s, 2H), 7.81 (d, $J = 17.0$ Hz, 2H, alkenyl H), 7.60 (s, 4H, central Ar-H), 7.55 (d, $J = 8.0$ Hz, 2H), 7.50 (d, $J = 8.5$ Hz, 4H), 7.48 (d, $J = 8.5$ Hz, 4H), 7.40 (d, $J = 8.5$ Hz, 2H), 7.28 (d, $J = 17.0$ Hz, 2H, alkenyl H), 7.06 (s, 2H), 7.05 (s, 4H), 7.03 (s, 2H), 6.89 (d, $J = 8.5$ Hz, 4H), 6.86 (d, $J = 8.5$ Hz, 4H), 4.08–4.02 (m, 16H, OCH_2), 3.84 (s, 1H, OCH_3), 3.82 (s, 1H, OCH_3), 1.91–1.82 (m, 12H), 1.77–1.71 (m, 4H), 1.61–1.51 (m, 12H), 1.43–1.17 (m, 100H), 0.90–0.82 (m, 24H, CH_3); ^{13}C NMR ($CDCl_3$, 125 MHz) δ 159.91, 159.87 (two aromatic carbons connected to OCH_3 group), 154.02, 153.97, 153.7 (aromatic carbons connected to the $OC_{10}H_{21}$ groups), 138.9, 137.3, 133.3, 132.7, 130.7, 130.2,

128.0, 127.5, 126.6, 123.8, 122.5, 117.24, 117.20, 117.1, 115.8, 115.2, 115.0, 114.20, 114.18, 113.7, 113.5 (aromatic carbons and alkenyl carbons), 95.5, 95.4, 94.7, 93.3, 88.0, 84.92, 84.89 (alkynyl carbons), 70.04, 69.95, 69.92, 69.9 (four OCH₂ carbons), 55.5, 55.47 (two OCH₃ carbons), 32.1, 29.9, 29.8, 29.7, 29.68, 29.65, 29.63, 29.58, 29.4, 22.9, 14.3; APCI-MS (positive) *m/z* calcd for C₁₇₀H₂₁₈O₁₂ 2451.64, found 2453.68 [M + H]⁺.

Compound 333. To an oven-dried flask protected under N₂ atmosphere were added compound **206** (12.8 mg, 0.337 mmol), NaH (2.02 mg, 0.0843 mmol), and dry THF (8 mL). Upon gentle heating at *ca.* 50 °C, the solution gradually turned into a pink color. Aldehyde **358** (80 mg, 0.067 mmol) dissolved in THF (5 mL) was added in small portions over a period of 1 h through a syringe. The reaction was kept under stirring and heating for another 2 h before work-up. The small excess NaH was carefully quenched with water and the mixture was extracted three times with chloroform. The chloroform layer was washed with brine, dried over MgSO₄, and concentrated to form a yellow solid. The yellow solid was purified by silica flash column chromatography (hexanes/CH₂Cl₂, 1:1) to give compound **333** (35 mg, 0.014 mmol, 21%) as a yellow solid. Mp 126–127 °C; IR (KBr) 2923, 2853, 2227, 2206, 1634, 1605, 1557, 1514, 1496, 1468, 1417, 1393 cm⁻¹; ¹H NMR (CDCl₃, 500 MHz) δ 7.91 (s, 2H), 7.80 (d, *J* = 16.5 Hz, 2H, alkenyl H), 7.62 (d, *J* = 8.0 Hz, 4H), 7.60 (s, 4H, central Ar-H), 7.58 (d, *J* = 8.0 Hz, 4H), 7.55 (d, *J* = 7.0 Hz, 2H), 7.50 (d, *J* = 8.5 Hz, 4H), 7.43 (d, *J* = 7.0 Hz, 2H), 7.28 (d, *J* = 16.5 Hz, 2H, alkenyl H), 7.06 (s, 2H), 7.05 (s, 2H), 7.041 (s, 2H), 7.036 (s, 2H), 6.90 (d, *J* = 8.5 Hz, 4H), 4.08–4.02 (m, 16H, OCH₂), 3.85 (s, 6H, OCH₃), 1.90–1.82 (m, 12H), 1.77–1.71 (m, 4H), 1.61–1.49 (m,

12H), 1.42-1.17 (m, 100H), 0.90-0.82 (m, 24H, CH₃); ¹³C NMR (CDCl₃, 125 MHz) δ 159.9 (one aromatic carbon attached to OCH₃ group), 154.2, 154.0, 153.8, 153.7 (four aromatic carbons connected to OC₁₀H₂₁ group), 139.0, 137.3, 133.3, 132.8, 132.22, 132.16, 130.8, 130.3, 128.6, 128.0, 127.5, 126.6, 124.1, 122.2, 118.7, 117.4, 117.3, 117.1, 116.9, 115.8, 115.4, 115.1, 114.2, 113.4, 113.2, 111.6, (one CN carbon, 25 aromatic carbons and two alkenyl carbons) 95.5, 94.6, 94.1, 93.5, 92.9, 90.8, 88.3, 84.8 (eight alkynyl carbons), 70.2, 70.0, 69.9, 69.8 (four OCH₂ carbons), 55.5 (one OCH₃), 32.1, 29.9, 29.8, 29.69, 29.66, 29.64, 29.58, 29.4, 26.3, 26.1, 22.9, 14.3; MALDI-TOF MS *m/z* calcd for C₁₇₀H₂₁₂N₂O₁₀ 2441.61, found 2442.97 [M + H]⁺.

Compound 334. To an oven-dried flask protected under a N₂ atmosphere were added compound **206** (2.88 mg, 0.00761 mmol), NaH (0.36 mg, 0.0152 mmol), and dry THF (6 mL). Upon gentle heating at *ca.* 50 °C, the solution gradually turned into a pink color. Aldehyde **360** (18 mg, 0.015 mmol) dissolved in THF (5 mL) was added in small portions over a period of 1 h through a syringe. The reaction was kept under stirring and heating for another 1 h before work-up. The small excess NaH was carefully quenched with water and the mixture was extracted three times with chloroform. The chloroform layer was washed with brine, dried over MgSO₄, and concentrated to form a yellow solid. The yellow solid was purified by silica flash column chromatography (hexanes/CH₂Cl₂, 1:1) to give compound **334** (11 mg, 0.0045 mmol, 59%) as a yellow solid. Mp 121–122 °C; IR (KBr) 2924, 2854, 2226, 2202, 1649, 1635, 1558, 1540, 1514, 1469, 1418, 1385 cm⁻¹; ¹H NMR (CDCl₃, 500 MHz) δ 7.91 (s, 2H), 7.80 (d, *J* = 15.5 Hz, 2H, alkenyl H), 7.66 (d, *J* = 8.5 Hz, 4H), 7.62 (d, *J* = 8.5 Hz, 4H), 7.60 (s, 4H, central H), 7.55 (d, *J* = 8.0 Hz, 2H), 7.48 (d, *J* = 8.5 Hz,

4H), 7.41 (d, $J = 8.0$ Hz, 2H), 7.28 (d, $J = 15.5$ Hz, 2H, alkenyl H), 7.07 (s, 2H), 7.06 (s, 2H), 7.04 (s, 4H), 6.87 (d, $J = 8.5$ Hz, 4H), 4.09-4.02 (m, 16H, OCH₂), 3.83 (s, 6H, OCH₃), 1.91-1.83 (m, 12H), 1.76-1.71 (m, 4H), 1.61-1.51 (m, 12H), 1.44-1.17 (m, 100H), 0.90-0.82 (m, 24H, CH₃); ¹³C NMR (CDCl₃, 125 MHz) δ 159.9 (one aromatic carbon attached to OCH₃ group), 154.2, 154.0, 153.8, 153.7 (four aromatic carbons connected to OC₁₀H₂₁ group), 139.0, 137.3, 133.3, 132.8, 132.3, 132.2, 130.7, 130.3, 128.7, 128.1, 127.5, 126.6, 123.5, 122.8, 118.8, 117.22, 117.19, 117.0, 115.8, 115.24, 115.17, 114.2, 113.6, 113.2, 111.6 (CN, alkenyl and aromatic carbons), 95.55, 95.47, 93.5, 93.4, 93.2, 90.8, 87.7, 84.9 (eight alkynyl carbons), 70.0, 69.96, 69.8 (OCH₂ carbons), 55.5 (one OCH₃), 32.1, 29.9, 29.8, 29.79, 29.71, 29.66, 29.63, 29.58, 29.4, 26.3, 26.2, 22.9, 14.3; MALDI-TOF MS m/z calcd for C₁₇₀H₂₁₂N₂O₁₀ 2441.61, found 2442.96 [M + H]⁺.

1,4-Bis(2,5-bis((2,5-bis(decyloxy)-4-((trimethylsilyl)ethynyl)phenyl)ethynyl)styryl)benzene (335). Compound **362** (16 mg, 0.044 mmol), **203** (106 mg, 0.174 mmol), PdCl₂(PPh₃)₂ (6.11 mg, 0.00870 mmol), CuI (3.31 mg, 0.0174 mmol) were added to Et₃N (8 mL). The solution was degassed by bubbling N₂ at rt for 5 min and then stirred for 4 h at rt, then heated to 50 °C under stirring and N₂ protection for 20 h. After the reaction was complete as checked by TLC analysis, the solvent was removed by rotary evaporation. The resulting residue was diluted with chloroform. The mixture was filtered through a MgSO₄ pad. The solution obtained was sequentially washed with aq HCl (10%) and brine. The organic layer was dried over MgSO₄ and concentrated under vacuum to give the crude product of **335**, which was further purified by silica flash column chromatography (hexanes, CH₂Cl₂, 7:3) to

yield compound **335** (36 mg, 0.016 mmol, 36%) as a colorless oil. IR (KBr) 2956, 2925, 2854, 2153, 1698, 1683, 1650, 1635, 1558, 1539, 1504, 1470, 1415 cm^{-1} ; ^1H NMR (CDCl_3 , 500 MHz) δ 7.90 (s, 2H), 7.78 (d, $J = 16.0$ Hz, 2H, alkenyl H), 7.58 (s, 4H, central Ar H), 7.54 (d, $J = 8.5$ Hz, 2H), 7.40 (d, $J = 8.5$ Hz, 2H), 7.27 (d, $J = 16.0$ Hz, 2H, alkenyl H), 7.01 (s, 1H), 7.00 (s, 2H), 6.99 (s, 1H), 4.06-3.99 (m, 16H, OCH_2), 1.90-1.18 (m, 128H), 0.92-0.83 (m, 24H, CH_3), 0.30 (s, 18H, $\text{Si}(\text{CH}_3)_3$), 0.29 (s, 18H, $\text{Si}(\text{CH}_3)_3$); ^{13}C NMR (CDCl_3 , 125 MHz) δ 154.4, 153.81, 153.8, 139.0, 137.3, 132.8, 130.7, 130.3, 128.1, 127.5, 126.5, 123.7, 122.5, 117.7, 117.6, 117.11, 117.06, 114.4, 114.2, 101.3, 100.6, 100.5, 94.9, 93.5, 93.1, 87.9, 70.0, 69.9, 69.8, 32.1, 29.9, 29.83, 29.77, 29.7, 29.64, 29.29.62, 29.6, 29.4, 26.3, 26.1, 22.9, 14.3, 0.19; MODI-TOF MS m/z calcd for $\text{C}_{154}\text{H}_{226}\text{O}_8\text{Si}_4$ 2315.64, found 2316.99 $[\text{M} + \text{H}]^+$.

Compound 336. To an oven-dried flask protected under a N_2 atmosphere were charged compound **362** (26 mg, 0.069 mmol), **370** (108 mg, 0.412 mmol), $\text{PdCl}_2(\text{PPh}_3)_2$ (9.69 mg, 0.0138 mmol), CuI (5.24 mg, 0.0276 mmol), and Et_3N (3 mL). The solution was degassed by bubbling N_2 at rt for 5 min and then stirred at rt under N_2 protection for 18 h. After the reaction was complete as checked by TLC analysis, the solvent was removed by rotary evaporation. The resulting residue was diluted with chloroform. The mixture was filtered through a MgSO_4 pad. The solution obtained was sequentially washed with aq HCl (10%) and brine. The organic layer was dried over MgSO_4 and concentrated under vacuum to give the crude product of **336**, which was further purified by recrystallization from CH_2Cl_2 and hexanes to yield compound **336** (44 mg, 0.048 mmol, 70%) as a yellow solid. Mp 175–176 $^\circ\text{C}$; IR (KBr) 3060, 2948, 2840, 2208, 1728, 1595, 1532 cm^{-1} ; ^1H NMR (CDCl_3 , 500 MHz)

δ 8.06-7.96 (m, 8H), 7.75 (s, 4H, central Ar-H), 7.74-7.70 (m, 4H), 7.61 (d, $J = 8.5$ Hz, 2H), 7.57-7.53 (m, 4H), 7.47-7.42 (m, 6H), 7.31 (d, $J = 16.5$ Hz, 2H, alkenyl H); ^{13}C NMR (CDCl_3 , 125 MHz) δ 166.8, 166.5 (two C=O carbons), 139.7, 137.3, 134.5, 134.4, 133.3, 132.10, 132.07, 132.0, 131.5, 131.2, 130.8, 130.4, 128.4, 128.3, 128.0, 127.8, 126.4, 124.2, 123.9, 123.8, 122.6 (one coincidental aromatic carbon not observed), 95.0, 94.4, 93.3, 90.2 (4 alkynyl carbons), 52.49, 52.47 (two OCH_3 carbons); MALDI-TOF MS m/z calcd for $\text{C}_{62}\text{H}_{42}\text{O}_8$ 914.29, found 915.55 $[\text{M} + \text{H}]^+$.

Compound 337. To an oven-dried flask protected under a N_2 atmosphere were charged compound **362** (25 mg, 0.066 mmol), **373** (140 mg, 0.568 mmol), $\text{PdCl}_2(\text{PPh}_3)_2$ (9.27 mg, 0.0132 mmol), CuI (5.0 mg, 0.026 mmol), and piperidine (3 mL). The solution was degassed by bubbling N_2 at rt for 5 min and then stirred at rt under N_2 protection for 24 h. After the reaction was complete as checked by TLC analysis, the solvent was removed by rotary evaporation. The resulting residue was diluted with chloroform. The mixture was filtered through a MgSO_4 pad. The solution obtained was sequentially washed with aq HCl (10%) and brine. The organic layer was dried over MgSO_4 and concentrated under vacuum to give the crude product of **337**, which was further purified by recrystallization from CH_2Cl_2 and hexanes to yield compound **337** (44 mg, 0.052 mmol, 79%) as a yellow solid. Mp > 300 °C; IR (KBr) 3034, 2891, 2856, 2798, 2202, 1607, 1523, 1443 cm^{-1} ; ^1H NMR (CDCl_3 , 500 MHz) δ 7.84 (s, br, 2H), 7.75 (d, $J = 16.0$ Hz, 2H, alkenyl H), 7.60 (s, 4H, central Ar-H), 7.48-7.43 (m, 10 H), 7.34 (d, $J = 8.0$ Hz, 2H), 7.26 (d, $J = 16.5$ Hz, 2H, alkenyl H), 6.70-6.67 (m, 8H), 3.10 (s, 12H, $\text{N}(\text{CH}_3)_3$), 2.99 (s, 12H, $\text{N}(\text{CH}_3)_3$); a meaningful ^{13}C NMR spectrum could not be obtained due to poor solubility; MALDI-TOF MS

m/z calcd for $C_{62}H_{54}N_4$ 854.43, found 855.23 $[M + H]^+$.

Dimethyl 2,2'-(3,3'-(1*E*,1'*E*)-2,2'-(1,4-phenylene)bis(ethene-2,1-diyl)bis(4-((4-(dimethylamino)phenyl)ethynyl)-3,1-phenylene))bis(ethyne-2,1-diyl)-dibenzoate (338). To an oven-dried flask protected under a N_2 atmosphere were charged compound **384** (47 mg, 0.073 mmol), **373** (36 mg, 0.15 mmol), $PdCl_2(PPh_3)_2$ (5.1 mg, 0.0072 mmol), CuI (2.8 mg, 0.015 mmol), piperidine (2.5 mL), and dry THF (2.5 mL). The solution was degassed by bubbling N_2 at rt for 5 min and then stirred at 30 °C under N_2 protection for 12 h. After the reaction was complete as checked by TLC analysis, the solvent was removed by rotary evaporation. The resulting residue was diluted with chloroform. The mixture was filtered through a $MgSO_4$ pad. The solution obtained was sequentially washed with aq HCl (10%) and brine. The organic layer was dried over $MgSO_4$ and concentrated under vacuum to give the crude product of **338**, which was purified by silica flash column chromatography (CH_2Cl_2) to yield compound **338** as yellow solid (30 mg, 0.034 mmol, 47%). Mp 225–226 °C; IR (KBr) 2960, 2930, 2860, 2195, 1728, 1609, 1524, 1488, 1464 cm^{-1} ; 1H NMR ($CDCl_3$, 500 MHz) δ 8.01 (d, $J = 7.5$ Hz, 2H), 7.91 (s, 2H), 7.76 (d, $J = 16.5$ Hz, 2H, alkenyl H), 7.69 (d, $J = 8.5$ Hz, 2H), 7.61 (s, 4H, central Ar-H), 7.54–7.47 (m, 8H), 7.43–7.39 (m, 4H), 7.28 (d, $J = 16.5$ Hz, 2H, alkenyl H), 6.70 (d, $J = 9.0$ Hz, 4H), 4.00 (s, 6H, OCH_3), 3.00 (s, 12H, $N(CH_3)_2$); ^{13}C NMR ($CDCl_3$, 125 MHz) δ 166.9 (C=O), 150.5, 138.5, 137.3, 134.3, 132.9, 132.4, 131.98, 131.95, 130.8, 130.48, 130.43, 128.2, 127.4, 126.6, 123.9, 123.6, 122.6, 112.1, 109.9 (of 20 aromatic and alkenyl carbons, one coincidental peak not observed), 98.2, 94.6, 89.7, 86.3 (4 alkynyl carbons), 52.5 (OCH_3), 40.4 ($N(CH_3)_2$); APCI-MS (positive) m/z calcd for $C_{62}H_{14}N_2O_4$ 884.4, found

885.5 [M + H]⁺.

1,4-Bis(2,5-bis(phenylethynyl)styryl)benzene (339). To an oven-dried flask protected under a N₂ atmosphere were charged compound **362** (30 mg, 0.079 mmol), iodobenzene (129 mg, 0.635 mmol), PdCl₂(PPh₃)₂ (11.2 mg, 0.0159 mmol), CuI (6.0 mg, 0.032 mmol), and piperidine (3 mL). The solution was degassed by bubbling N₂ at rt for 5 min and then heated to 50 °C under stirring and N₂ protection overnight. After the reaction was complete as checked by TLC analysis, the solvent was removed by rotary evaporation. The resulting residue was diluted with chloroform. The mixture was filtered through a MgSO₄ pad. The solution obtained was sequentially washed with aq HCl (10%) and brine. The organic layer was dried over MgSO₄ and concentrated under vacuum to give the crude product **339**, which was further purified by recrystallization from CH₂Cl₂ and hexanes to yield compound **339** (36 mg, 0.053 mmol, 67%) as a yellow solid. Mp > 300 °C; IR (KBr) 3262, 3052, 2208, 1631, 1597, 1499 cm⁻¹; ¹H NMR (CDCl₃, 500 MHz) δ 7.91 (s, br, 2H), 7.73 (d, *J* = 17.0 Hz, 2H, alkenyl H), 7.61 (s, 4H, central Ar-H), 7.60-7.57 (m, 8H), 7.55 (d, *J* = 8.5 Hz, 2H), 7.41-7.37 (m, 14H), 7.28 (d, *J* = 14.5 Hz, 2H, alkenyl H); Meaningful ¹³C NMR could not be obtained due to poor solubility; MALDI-TOF MS *m/z* calcd for C₅₄H₃₄ 682.27, found 683.26 [M + H]⁺.

2-Amino-5-bromobenzoic acid (341). Anthranilic acid (15.0 g, 0.11 mol) was dissolved in 250 mL of glacial acetic acid and cooled below 16 °C. Then 7.1 mL of bromine (22.1 g, 0.138 mol) was added dropwise. The product was filtered off and then boiled up with 500 mL of water containing 25 mL of concentrated hydrochloric

acid. The content was filtered hot with suction. The insoluble residue was extracted twice with 500 mL of boiling water. The filtrates upon cooling yielded compound **341** (12.5 g, 0.058 mol, 53%) as a white solid. Mp 215–126 °C; ^1H NMR (CDCl_3 , 500 MHz) δ 8.03 (d, $J = 2.0$ Hz, 1H), 7.38 (dd, $J = 9.0, 3.0$ Hz, 1H), 6.59 (d, $J = 9.0$ Hz, 1H) (protons of NH_2 and COOH were not observed due to rapid proton exchange); ^{13}C NMR (CDCl_3 , 125 MHz) δ 171.0, 150.2, 138.0, 134.3, 118.7, 110.8, 107.7.

5-Bromo-2-iodobenzoic acid (342). A solution of **341** (3.9 g, 0.018 mol), NaNO_2 (1.5 g, 0.022 mol) and NaOH (0.90 g, 0.023 mmol) in 55 mL of water was added dropwise to a stirred and cooled solution of 6.4 mL of HCl in 9 mL of water at 0 °C over a period of 1.5 h. The stirring was continued for 30 min at 0 °C and the formed suspension of diazonium salt was added to a stirred solution of KI (4.5 g, 0.027 mol) and 1.1 mL of H_2SO_4 in 7.5 mL of water at 35–40 °C over 20 min. The mixture was then heated to 90 °C and stirred for 30 min. Unreacted iodine was removed by steam distillation. The mixture was stirred and cooled. The crude product was filtered and washed with water, and then dissolved in 40% NaOH . The polymeric components were separated by decantation and the clear solution was acidified with concentrated HCl . The product was extracted by diethyl ether. The extract was dried with MgSO_4 and concentrated under vacuum. The residue was crystallized from 50% aqueous ethanol to give compound **342** (3.56 g, 0.0109 mol, 60%) as a pale yellow solid. Mp 160–161 °C; ^1H NMR (CDCl_3 , 500 MHz) δ 8.13 (d, $J = 1.5$ Hz, 1H), 7.90 (d, $J = 9.0$ Hz, 1H), 7.34 (dd, $J = 8.5, 2.0$ Hz, 1H) (proton on COOH was not observed due to rapid proton exchange); ^{13}C NMR (CDCl_3 , 125 MHz) δ 170.2, 143.5, 136.9, 135.2, 134.8, 122.6, 93.0; GC-MS m/z (%) 328 ($[\text{M}]^+$, ^{81}Br , 80), 326 ($[\text{M}]^+$,

^{79}Br , 80), 311 ($[\text{M} - \text{OH}]^+$, ^{81}Br , 50), 309 ($[\text{M} - \text{OH}]^+$, ^{79}Br , 50), 202 ($[\text{M} - \text{I}]^+$, ^{81}Br , 30), 200 ($[\text{M} - \text{I}]^+$, ^{79}Br , 30).

Methyl 5-bromo-2-iodobenzoate (343). To 50 mL of methanol was added compound **342** (5.1 g, 0.016 mol) and 2.0 mL of H_2SO_4 . The solution was refluxed overnight. The reaction was cooled down to rt. Methanol was removed by rotary evaporation. The residue was dissolved in EtOAc. The solution was washed by brine, and dried over MgSO_4 . After removal of EtOAc under vacuum, the resulted crude product was purified by silica column flash chromatography (hexanes CH_2Cl_2 , 1:1) to yield compound **343** (5.2 g, 0.015 mol, 98%) as a pale yellow solid. Mp 18–19 °C; ^1H NMR (CDCl_3 , 500 MHz) δ 7.94 (d, $J = 2.0$ Hz, 1H), 7.84 (d, $J = 8.0$ Hz, 1H), 7.28 (dd, $J = 8.0, 2.5$ Hz, 1H), 3.94 (s, 3H, CH_3); ^{13}C NMR (CDCl_3 , 125 MHz) δ 165.5, 142.7, 136.5, 135.7, 133.9, 122.3, 92.3, 52.8; GC-MS m/z (%) 342 ($[\text{M}]^+$, ^{81}Br , 60), 340 ($[\text{M}]^+$, ^{79}Br , 60), 311 ($[\text{M} - \text{OCH}_3]^+$, ^{81}Br , 65), 309 ($[\text{M} - \text{OCH}_3]^+$, ^{79}Br , 65), 283 ($[\text{M} - \text{COOCH}_3]^+$, ^{81}Br , 25), 281 ($[\text{M} - \text{COOCH}_3]^+$, ^{79}Br , 25).

(5-Bromo-2-iodophenyl)methanol (344). To a solution of compound **343** (5.2 g, 0.015 mol) in dry CH_2Cl_2 (30 mL) was added DIBAL (30.5 mL, 1 M in THF, 30.5 mmol) at 0 °C; The reaction was slowly warmed up to rt and stirred overnight. The mixture was cooled to 0 °C, treated with 15% aqueous citric acid slowly, and extracted with CH_2Cl_2 . The organic layer was washed with brine, and dried with MgSO_4 . After removal of CH_2Cl_2 under vacuum, the resulting crude product was purified by silica column flash chromatography (hexanes: CH_2Cl_2 , 1:1) to give compound **344** as a white solid (4.79 g, 0.0153 mol, 100%). Mp 111–155 °C;

^1H NMR (CDCl_3 , 500 MHz) δ 7.65 (d, J = 8.5 Hz, 1H), 7.62 (d, J = 2.5 Hz, 1H), 7.13 (dd, J = 9.0, 2.0 Hz, 1H), 4.63 (d, J = 6.0 Hz, 2H, CH_2), 2.13 (t, J = 6.0 Hz, 1H, OH); ^{13}C NMR (CDCl_3 , 125 MHz) δ 144.8, 140.5, 132.4, 131.3, 123.2, 94.8, 68.9; GC-MS m/z (%) 314 ($[\text{M}]^+$, ^{81}Br , 99), 312 ($[\text{M}]^+$, ^{79}Br , 100), 233 ($[\text{M} - \text{Br}]^+$, 45).

5-Bromo-2-iodobenzaldehyde (345). To a stirred solution of PDC (11.0 g, 0.0288 mol) in 60 mL of CH_2Cl_2 was added a solution of **344** (4.50 g, 0.0141 mol) in 20 mL of CH_2Cl_2 . The reaction was stirred for another 4 h. The solvent was removed under vacuum to give the crude product of **345**. The crude product was purified by silica flash column chromatography (hexanes CH_2Cl_2 , 70:30) to give compound **345** (4.40 g, 0.0142 mol, 98%) as a white solid. Mp 89–90 °C; ^1H NMR (CDCl_3 , 500 MHz) δ 10.02 (s, 1H, CHO), 8.02 (d, J = 2.5 Hz, 1H), 7.84 (d, J = 8.5 Hz, 1H), 7.44 (dd, J = 8.5, 2.0 Hz, 1H); ^{13}C NMR (CDCl_3 , 125 MHz) δ 194.5 ($\text{C}=\text{O}$), 142.0, 138.4, 136.6, 133.3, 123.7, 98.4; GC-MS m/z (%) 312 ($[\text{M}]^+$, ^{81}Br , 99), 310 ($[\text{M}]^+$, ^{79}Br , 100), 283 ($[\text{M} - \text{CHO}]^+$, ^{81}Br , 20), 281 ($[\text{M} - \text{CHO}]^+$, ^{79}Br , 22), 186 ($[\text{M} - \text{I}]^+$, ^{81}Br , 46), 184 ($[\text{M} - \text{I}]^+$, ^{79}Br , 45).

1,4-Bis(5-bromo-2-iodostyryl)benzene (346). To an oven-dried flask protected under a N_2 atmosphere were charged compound **206** (472 mg, 1.25 mmol), NaH (75 mg, 3.1 mmol), and dry THF (10 mL). Upon gentle heating at *ca.* 50 °C, the solution gradually turned into a light yellow color. Aldehyde **345** (775 mg, 2.49 mmol) dissolved in THF (5 mL) was added in small portions over a period of 1 h through a syringe. The reaction was kept under stirring and heating for another 2 h before work-up. The small excess NaH was carefully quenched with aq HCl (10%)

and the mixture was extracted with chloroform three times. The chloroform layer was washed with brine, dried over MgSO_4 , and concentrated to form a yellow solid. The yellow solid was recrystallized from CHCl_3 and CH_3OH to give **346** (380 mg, 0.549 mmol, 45%) as a yellow solid. Mp 254-255 °C; IR (KBr) 3047, 1880, 1628, 1565, 1533 cm^{-1} ; ^1H NMR (CDCl_3 , 500 MHz) δ 7.76 (d, J = 1.5 Hz, 2H), 7.72 (d, J = 8.0 Hz, 2H), 7.58 (s, 4H, central Ar-H), 7.26 (d, J = 16.0 Hz, 2H, alkenyl H), 7.10 (dd, J = 8.5, 3.0 Hz, 2H), 6.98 (d, J = 16.0 Hz, 2H, alkenyl H); Meaningful ^{13}C NMR spectrum could not be obtained due to poor solubility. APCI-MS (positive) m/z calcd for $\text{C}_{22}\text{H}_{14}\text{Br}_2\text{I}_2$ 691.8, found 692.8 $[\text{M} + \text{H}]^+$.

4-((Trimethylsilyl)ethynyl)benzotrile (348). 4-Bromobenzotrile (1.0 g, 5.5 mmol), trimethylsilylacetylene (1.6 mL, 11 mmol), $\text{PdCl}_2(\text{PPh}_3)_2$ (94 mg, 0.14 mmol), CuI (52 mg, 0.27 mmol) were added to Et_3N (15 mL). The solution was bubbled by N_2 at rt for 5 min and then heated to 50 °C under stirring and N_2 protection overnight. After the reaction was complete as checked by TLC analysis, the solvent was removed by rotary evaporation. The resulting residue was diluted with chloroform. The mixture was filtered through a MgSO_4 pad. The solution obtained was sequentially washed with aq HCl (10%) and brine. The organic layer was dried over MgSO_4 and concentrated under vacuum to give the crude product of **348**, which was further purified by silica flash column chromatography (hexanes/EtOAc, 9:1) to yield compound **348** (1.05 g, 5.3 mmol, 95%) as a white solid. Mp 98-99 °C; ^1H NMR (CDCl_3 , 500 MHz) δ 7.59 (d, J = 8.5 Hz, 2H), 7.53 (d, J = 8.5 Hz, 2H), 0.28 (s, 9H); ^{13}C NMR (CDCl_3 , 125 MHz) δ 132.4, 131.9, 127.9, 118.3, 111.8, 103.0, 99.5, 0.25; GC-MS m/z (%) 199 ($[\text{M}]^+$, 20), 184 ($[\text{M} - \text{CH}_3]^+$, 100).

4-Ethynylbenzonitrile (349). To a solution of compound **348** (1.1 g, 5.3 mmol) in 1:1 MeOH/THF (16 mL) was added K_2CO_3 (50 mg, 0.36 mmol). The mixture was stirred at rt for 30 min, then the reaction solvent was removed by rotary evaporation. The residue was diluted in EtOAc and sequentially washed with aq HCl (10%) and brine. The organic layer was dried with $MgSO_4$ and concentrated under vacuum to afford the compound **349** as a white solid (0.61 g, 4.80 mmol, 91%), which was pure enough for next step. Mp 154-155 °C; IR (neat) 3297, 3055, 2987, 2231, 2105, 1604, 1499, 1422 cm^{-1} ; 1H NMR ($CDCl_3$, 500 MHz) δ 7.62 (d, $J = 8.5$ Hz, 2H), 7.57, (d, $J = 8.5$ Hz, 2H), 3.32 (s, 1H); ^{13}C NMR ($CDCl_3$, 125 MHz) δ 132.8, 132.2, 127.2, 118.4, 112.5, 82.0, 81.7; GC-MS m/z (%) 127 ($[M]^+$, 100), 100 ($[M - CN]^+$, 20).

4-((2,5-Bis(decyloxy)-4-((trimethylsilyl)ethynyl)phenyl)ethynyl)benzonitrile (350). Compound **349** (100 mg, 0.787 mmol), **203** (484 mg, 0.787 mmol), $PdCl_2(PPh_3)_2$ (27 mg, 0.039 mmol), CuI (15 mg, 0.079 mmol) were added to Et_3N (20 mL). The solution was bubbled by N_2 at rt for 5 min and then stirred at rt for 4 h under N_2 protection. After the reaction was complete as checked by TLC analysis, the solvent was removed by rotary evaporation. The resulting residue was diluted with chloroform. The mixture was filtered through a $MgSO_4$ pad. The solution obtained was sequentially washed with aq HCl (10%) and brine. The organic layer was dried over $MgSO_4$ and concentrated under vacuum to give the crude product of **350**, which was further purified by silica flash column chromatography (hexanes/ CH_2Cl_2 , 8:2) to yield compound **350** (482 mg, 0.787 mmol, 100%) as a colorless oil. IR (KBr) 2925, 2854, 2228, 2212, 2153, 1604, 1508, 1493, 1468, 1412, 1384 cm^{-1} ; 1H NMR ($CDCl_3$,

500 MHz) δ 7.63, 7.59 (AB system, $J = 8.0$ Hz, 4H), 6.96 (s, 2H), 4.01-3.97 (m, 4H, OCH₂), 1.84-1.80 (m, 4H), 1.55-1.49 (m, 4H), 1.37-1.28 (m, 24H), 0.90-0.87 (m, 6H, CH₃); ¹³C NMR (CDCl₃, 125 MHz) δ 154.3, 154.0, 132.2, 132.1, 128.6, 118.7, 117.3, 117.1, 115.1, 113.1, 111.6 (one CN carbon and ten aromatic carbons), 101.1, 101.0, 93.2, 90.7 (four alkynyl carbons), 69.8, 69.7 (two C-O carbons in the alkyl chains), 32.1, 29.9, 29.8, 29.6, 29.58, 29.54, 29.5, 26.2, 22.9, 14.3, 0.14; APCI-MS (positive) m/z calcd for C₄₀H₅₇NO₂Si 611.42, found 612.4 [M + H]⁺.

4-((2,5-Bis(decyloxy)-4-ethynylphenyl)ethynyl)benzotrile (351). To a solution of compound **350** (428 mg, 0.699 mmol) in 1:1 MeOH THF (10 mL) was added K₂CO₃ (100 mg, 0.724 mmol). The mixture was stirred at rt for 30 min, then the reaction solvent was removed by rotary evaporation. The residue was diluted in EtOAc and sequentially washed with aq HCl (10%) and brine. The organic layer was dried over MgSO₄ and concentrated under vacuum to afford the crude product of **351**, which was further purified by silica flash column chromatography (hexanes/CH₂Cl₂, 8:2) to yield compound **351** (333 mg, 0.617 mmol, 88%) as a colorless oil. IR (KBr) 3290, 3256, 2925, 2852, 2226, 2155, 2102, 1639, 1605, 1508, 1494, 1466, 1409, 1387 cm⁻¹; ¹H NMR (CDCl₃, 500 MHz) δ 7.64, 7.60 (AB system, $J = 8.5$ Hz, 4H), 7.00 (s, 1H), 6.99 (s, 1H), 4.03-3.99 (m, 4H, OCH₂), 3.37 (s, 1H), 1.86-1.80 (m, 4H), 1.55-1.46 (m, 4H), 1.38-1.26 (m, 24H), 0.90-0.87 (m, 6H, CH₃). ¹³C NMR (CDCl₃, 125 MHz) δ 154.3, 153.9, 132.21, 132.17, 128.5, 118.7, 117.8, 117.1, 113.9, 113.5, 111.7 (one CN carbon and ten aromatic carbons), 93.2, 90.5, 83.0, 80.0 (four alkynyl carbons), 69.9, 69.7 (two C-O carbons in the alkyl chains), 32.10, 32.09, 29.9, 29.8, 29.6, 29.53, 29.46, 29.3, 26.2, 26.1, 22.9, 14.3; APCI-MS (positive) m/z calcd for C₃₇H₄₉NO₂

539.38, found 540.4 [M + H]⁺.

((4-Methoxyphenyl)ethynyl)trimethylsilane (353). 4-Iodoanisole (1.00 g, 4.27 mmol), trimethylsilylacetylene (0.9 mL, 6.41 mmol), PdCl₂(PPh₃)₂ (37 mg, 0.053 mmol), CuI (20 mg, 0.106 mmol) were added to Et₃N (15 mL). The solution was bubbled by N₂ at rt for 5 min and stirred for 4 h under N₂ protection. After the reaction was complete as checked by TLC analysis, the solvent was removed by rotary evaporation. The resulting residue was diluted with chloroform. The mixture was filtered through a MgSO₄ pad. The solution obtained was sequentially washed with aq HCl (10%) and brine. The organic layer was dried over MgSO₄ and concentrated under vacuum to give the crude product of **353**, which was further purified by silica flash column chromatography (hexanes/CH₂Cl₂, 8:2) to yield compound **353** (0.92 g, 4.5 mmol, 100%) as a colorless oil. ¹H NMR (CDCl₃, 500 MHz) δ 7.40 (d, *J* = 9.5 Hz, 2H), 6.80, (d, *J* = 9.5 Hz, 2H), 3.76 (s, 3H), 0.24 (s, 9H); ¹³C NMR (CDCl₃, 125 MHz) δ 159.9, 133.6, 115.5, 114.0, 105.4, 92.5, 55.4, 0.26; GC-MS *m/z* (%) 204 ([M]⁺, 30), 189 ([M - CH₃]⁺, 100).

1-Ethynyl-4-methoxybenzene (354). To a solution of compound **353** (870 mg, 4.27 mmol) in 1:1 MeOH/CHCl₃ (16 mL) was added K₂CO₃ (200 mg, 1.45 mmol). The mixture was stirred at rt for 1 h, then the reaction solvent was removed by rotary evaporation. The residue was diluted in EtOAc and sequentially washed with aq HCl (10%) and brine. The organic layer was dried over MgSO₄ and concentrated under vacuum to afford compound **354** as a colorless oil (573 mg, 0.23 mmol, 100%), which was pure enough for next step. IR (neat) 3287, 3039, 3005, 2960, 2839, 2106, 1681,

1606, 1572, 1507, 1465, 1442, 1417, cm^{-1} ; ^1H NMR (CDCl_3 , 500 MHz) δ 7.41 (dd, $J = 12, 2.5$ Hz, 2H), 6.80 (dd, $J = 12, 2.5$ Hz, 2H), 3.74 (s, 3H), 3.01 (s, 1H); ^{13}C NMR (CDCl_3 , 125 MHz) δ 160.0, 133.6, 114.3, 114.0, 83.8, 76.0, 55.3; GC-MS m/z (%) 132 ($[\text{M}]^+$, 100), 117 ($[\text{M} - \text{CH}_3]^+$, 45).

((2,5-Bis(decyloxy)-4-((4-methoxyphenyl)ethynyl)phenyl)ethynyl)trimethylsilane (355). Compound **354** (108 mg, 0.818 mmol), **203** (500 mg, 0.818 mmol), $\text{PdCl}_2(\text{PPh}_3)_2$ (14 mg, 0.020 mmol), CuI (7.8 mg, 0.041 mmol) were added to Et_3N (15 mL). The solution was bubbled by N_2 at rt for 5 min and then stirred under N_2 protection overnight. After the reaction was complete as checked by TLC analysis, the solvent was removed by rotary evaporation. The resulting residue was diluted with chloroform. The mixture was filtered through a MgSO_4 pad. The solution obtained was sequentially washed with aq HCl (10%) and brine. The organic layer was dried over MgSO_4 and concentrated under vacuum to give crude **355**, which was further purified by silica flash column chromatography (hexanes/ CH_2Cl_2 , 85:15) to yield compound **355** (463 mg, 0.750 mmol, 92%) as a colorless oil. IR (KBr) 2955, 2923, 2854, 2209, 2153, 1607, 1570, 1514, 1497, 1468, 1442, 1410, 1388 cm^{-1} ; ^1H NMR (CDCl_3 , 500 MHz) δ 7.46 (d, $J = 9.5$, 2H), 6.94 (s, 1H), 6.93 (s, 1H), 6.86 (d, $J = 9.5$, 2H), 3.40-3.96 (m, 4H, OCH_2), 3.82 (s, 3H, OCH_3), 1.83-1.78 (m, 4H), 1.53-1.50 (m, 4H), 1.36-1.25 (m, 24H), 0.90-0.86 (m, 6H, CH_3), 0.26 (s, 9H, $\text{Si}(\text{CH}_3)_3$); ^{13}C NMR (CDCl_3 , 125 MHz) δ 159.8, 154.4, 153.5, 133.2, 117.5, 116.9, 115.8, 115.0, 114.3, 114.1, 113.5 (ten aromatic carbons), 101.5, 99.9, 95.2, 84.8 (four alkynyl carbons), 69.8, 69.6 (two C-O carbons in the alkyl chains), 55.3 (OCH_3 , 34.8, 32.1, 29.85, 29.80, 29.77, 29.63, 29.56, 29.53, 26.3, 26.2, 22.9, 14.3, 0.16; APCI-MS (positive) m/z calcd

for $C_{40}H_{60}O_3Si$ 616.43, found 617.4 $[M + H]^+$.

1,4-Bis(decyloxy)-2-ethynyl-5-((4-methoxyphenyl)ethynyl)benzene (356).

To a solution of compound **355** (463 mg, 0.750 mmol) in 1:1 MeOH $CHCl_3$ (16 mL) was added K_2CO_3 (200 mg, 1.44 mmol). The mixture was stirred at rt for 2 h, then the reaction solvent was removed by rotary evaporation. The residue was diluted in CH_2Cl_2 and sequentially washed with aq HCl (10%) and brine. The organic layer was dried over $MgSO_4$ and concentrated under vacuum to afford the crude product of **356**, which was further purified by silica flash column chromatography (hexanes/ CH_2Cl_2 , 85:15) to yield compound **356** (392 mg, 0.72 mmol, 96%) as a white solid. Mp 40–41 °C; IR (KBr) 3293, 2959, 2920, 2851, 2215, 2152, 1610, 1569, 1516, 1499, 1471, 1410, 1392 cm^{-1} ; 1H NMR ($CDCl_3$, 500 MHz) δ 7.42 (d, $J = 11$ Hz, 2H), 6.98 (s, 1H), 6.97 (s, 1H), 6.88 (d, $J = 11$ Hz, 2H), 4.01–3.97 (m, 4H, OCH_2), 3.82 (s, 3H, OCH_3), 3.33 (s, 1H), 1.85–1.79 (m, 4H, OCH_2), 1.54–1.45 (m, 4H), 1.36–1.26 (m, 24H), 0.90–0.87 (m, 6H, CH_3); ^{13}C NMR ($CDCl_3$, 125 MHz) δ 160.1, 154.6, 153.7, 133.5, 118.3, 117.2, 116.0, 115.6, 114.4, 112.6 (ten aromatic carbons), 95.5, 84.9, 82.5, 80.5 (four alkynyl carbons), 70.10, 70.05 (two C–O carbons in the alkyl chains), 55.7 (OCH_3), 32.35, 32.34, 30.1, 30.02, 30.0, 29.9, 29.8, 29.6, 26.5, 26.4, 23.1, 14.5; APCI-MS (positive) m/z calcd for $C_{37}H_{52}O_3$ 544.39, found 545.5 $[M + H]^+$.

4-((4-((4-Bromo-2-formylphenyl)ethynyl)-2,5-bis(decyloxy)phenyl)ethynyl)benzotrile (357). Compound **345** (32 mg, 0.10 mmol), **351** (55.6 mg, 0.103 mmol), $PdCl_2(PPh_3)_2$ (3.6 mg, 0.0051 mmol), CuI (1.96 mg, 0.0103 mmol) were added to Et_3N (6 mL). The solution was bubbled by N_2 at rt for 5 min and then

stirred at rt under N₂ protection for 3 h. After the reaction was complete as checked by TLC analysis, the solvent was removed by rotary evaporation. The resulting residue was diluted with chloroform. The mixture was filtered through a MgSO₄ pad. The solution obtained was sequentially washed with aq HCl (10%) and brine. The organic layer was dried over MgSO₄ and concentrated under vacuum to give the crude product of **357**, which was further purified by silica flash column chromatography (hexanes/CH₂Cl₂, 7:3) to yield compound **357** (60 mg, 0.083 mmol, 81%) as a white solid. Mp 82–83 °C; IR (KBr) 2918, 2851, 2207, 1690, 1631, 1603, 1583, 1552, 1533, 1513, 1497, 1469, 1420 cm⁻¹; ¹H NMR (CDCl₃, 500 MHz) δ 10.66 (s, 1H), 8.07 (d, *J* = 1.5 Hz, 1H), 7.69 (dd, *J* = 8.0, 1.5 Hz, 1H), 7.64, 7.60 (AB, *J* = 8.5 Hz, 4H), 7.49 (d, *J* = 8.0 Hz, 1H), 7.02 (s, 1H), 7.01 (s, 1H), 4.05–4.01 (m, 4H, OCH₂), 1.89–1.83 (m, 4H), 1.60–1.46 (m, 4H), 1.30–1.26 (m, 24H), 0.89–0.86 (m, 6H, CH₃); ¹³C NMR (CDCl₃, 125 MHz) δ 190.9 (CHO), 154.3, 154.0 (two C–O carbons in the phenyl rings), 137.2, 136.8, 134.3, 132.24, 132.20, 130.3, 128.5, 125.9, 123.4, 118.7, 116.7, 116.4, 114.1, 113.5, 111.8 (one CN carbon and 14 aromatic carbons), 94.3, 93.8, 90.5, 90.2 (four alkynyl carbons), 69.8, 69.6 (two C–O carbons in the alkyl chains), 32.1, 29.9, 29.82, 29.76, 29.6, 29.5, 29.4, 26.3, 22.9, 14.3; MALDI-TOF MS *m/z* calcd for C₄₄H₅₂BrNO₃ 721.3, 723.3 found 722.4 ([M + H]⁺, ⁷⁹Br), 724.4 (⁸¹Br, [M + H]⁺).

4-((4-((4-((2,5-Bis(decyloxy)-4-((4-methoxyphenyl)ethynyl)phenyl)ethynyl)-2-formylphenyl)ethynyl)-2,5-bis(decyloxy)phenyl)ethynyl)benzotrile (358**).** Compound **357** (61 mg, 0.084 mmol), **356** (142 mg, 0.261 mmol), Pd(PPh₃)₄ (15 mg, 0.13 mmol), CuI (5.0 mg, 0.026 mmol) were added to Et₃N (10 mL). The solution was bubbled by N₂ at rt for 5 min, stirred at rt for 3 h, and then heated

to 60 °C under stirring and N₂ protection for 4 h. After the reaction was complete as checked by TLC analysis, the solvent was removed by rotary evaporation. The resulting residue was diluted with chloroform. The mixture was filtered through a MgSO₄ pad. The solution obtained was sequentially washed with aq HCl (10%) and brine. The organic layer was dried over MgSO₄ and concentrated under vacuum to give the crude product of **358**, which was further purified by silica flash column chromatography (hexanes/CH₂Cl₂, 6:4) to yield compound **358** (80 mg, 0.067 mmol, 80%) as a yellow solid. Mp 128–129 °C; IR (KBr) 2922, 2851, 2224, 2208, 1696, 1649, 1604, 1557, 1515, 1486, 1467, 1417, 1387 cm⁻¹; ¹H NMR (CDCl₃, 500 MHz) δ 10.73 (s, 1H, CHO), 8.11 (d, *J* = 2.0 Hz, 1H), 7.70 (dd, *J* = 8.5, 2.0 Hz, 1H), 7.66, 7.62 (AB system, *J* = 8.5 Hz, 4H), 7.61 (d, *J* = 8.5 Hz, 1H), 7.49 (d, *J* = 8.5 Hz, 2H), 7.05 (s, 1H), 7.03 (s, 1H), 7.022 (s, 1H), 7.016 (s, 1H), 6.70 (d, *J* = 8.5 Hz, 2H), 4.07–4.04 (m, 4H), 4.07–4.04 (m, 8H, OCH₂), 3.85 (s, 3H, OCH₃), 1.91–1.84 (m, 8H), 1.56–1.48 (m, 8H), 1.40–1.27 (m, 48H), 0.91–0.86 (m, 12H, CH₃); ¹³C NMR (CDCl₃, 125 MHz) δ 191.5 (CHO), 159.9, 154.3, 154.1, 154.0, 153.6 (five C–O in the phenyl rings), 136.2, 136.1, 133.3, 133.0, 132.22, 132.19, 130.3, 128.5, 126.2, 124.5, 118.7, 117.2, 116.9, 116.7, 116.4, 115.7, 115.5, 114.2, 114.0, 113.8, 112.9, 111.7 (twenty-two aromatic carbons), 95.6, 94.8, 93.7, 93.4, 91.2, 90.7, 89.7, 84.8 (eight alkynyl carbons), 69.9, 69.8, 69.6 (C–O carbons in the alkyl chains), 55.5 (OCH₃), 32.1, 29.9, 29.83, 29.78, 29.7, 29.6, 29.56, 29.53, 29.5, 26.3, 22.9, 14.3; MALDI-TOF MS *m/z* calcd for C₈₁H₁₀₃NO₆ 1185.78, found 1186.12 [M + H]⁺.

2-((2,5-Bis(decyloxy)-4-((4-methoxyphenyl)ethynyl)phenyl)ethynyl)-5-bromobenzaldehyde (359). Compound **345** (32.0 mg, 0.103 mmol), **356** (55.6

mg, 0.103 mmol), PdCl₂(PPh₃)₂ (3.6 mg, 0.0051 mmol), CuI (1.96 mg, 0.0103 mmol) were added to Et₃N (8 mL). The solution was bubbled by N₂ at rt for 5 min and then stirred at rt under N₂ protection for 8 h. After the reaction was complete as checked by TLC analysis, the solvent was removed by rotary evaporation. The resulting residue was diluted with chloroform. The mixture was filtered through a MgSO₄ pad. The solution obtained was sequentially washed with aq HCl (10%) and brine. The organic layer was dried over MgSO₄ and concentrated under vacuum to give crude **359**, which was further purified by silica flash column chromatography (hexanes:CH₂Cl₂, 7:3) to yield compound **359** (21 mg, 0.029 mmol, 28%) as a white solid. Mp 75–76 °C; IR (KBr) 2920, 2872, 2852–2203, 1692, 1600, 1581, 1568, 1514, 1499, 1466, 1418 cm⁻¹; ¹H NMR (CDCl₃, 500 MHz) δ 10.68 (s, 1H), 8.08 (d, *J* = 1.5 Hz, 1H), 7.70 (dd, *J* = 8.5, 1.5 Hz, 1H), 7.50, 7.49 (AB system, *J* = 8.5 Hz, 4H), 7.02 (s, 1H), 7.01 (s, 1H), 6.90 (d, *J* = 8.5 Hz, 1H), 4.06–4.02 (m, 4H, OCH₂), 3.85 (s, 3H, OCH₃), 1.90–1.84 (m, 4H), 1.59–1.47 (m, 4H), 1.42–1.27 (m, 24H), 0.90–0.87 (m, 6H, CH₃); ¹³C NMR (CDCl₃, 125 MHz) δ 191.3 (CHO), 160.2, 154.7, 153.8 (C–O carbons in the phenyl rings), 137.4, 137.0, 134.5, 133.5, 130.5, 126.4, 123.3, 117.1, 116.5, 116.3, 115.8, 114.4, 112.1 (thirteen aromatic carbons), 96.2, 95.0, 89.7, 85.0 (four alkynyl carbons), 70.2, 69.7 (two C–O carbons in the alkyl chains), 55.7(CH₃), 32.3, 30.1, 30.05, 30.01, 30.0, 29.9, 29.8, 29.76, 29.70, 26.5, 23.1, 14.5; APCI-MS (positive) *m/z* calcd for C₄₄H₅₅BrO₄ 726.33, found 727.4 [M + H]⁺.

4-((4-((4-((2,5-Bis(decyloxy)-4-((4-methoxyphenyl)ethynyl)phenyl)ethynyl)-3-formylphenyl)ethynyl)-2,5-bis(decyloxy)phenyl)ethynyl)benzotrile (360**)**. Compound **359** (21 mg, 0.029 mmol), **351** (31.2 mg, 0.0578 mmol),

PdCl₂(PPh₃)₂ (2.0 mg, 0.0029 mmol), CuI (1.1 mg, 0.0058 mmol) were added to Et₃N (6 mL). The solution was bubbled by N₂ at rt for 5 min and then stirred for 3 h at rt and then heated to 60 °C under stirring and N₂ protection for 5 h. After the reaction was complete as checked by TLC analysis, the solvent was removed by rotary evaporation. The resulting residue was diluted with chloroform. The mixture was filtered through a MgSO₄ pad. The solution obtained was sequentially washed with aq HCl (10%) and brine. The organic layer was dried over MgSO₄ and concentrated under vacuum to give crude **360**, which was further purified by silica flash column chromatography (hexanes/CH₂Cl₂, 65:35) to yield compound **360** (24 mg, 0.020 mmol, 71%) as a yellow solid. Mp 98–99 °C; IR (KBr) 2954, 2924, 2852, 2204, 1694, 1632, 1553, 1535, 1516, 1484, 1468, 1453, 1416 cm⁻¹; ¹H NMR (CDCl₃, 500 MHz) δ 10.73 (s, 1H), 8.09 (d, *J* = 1.0 Hz, 1H), 7.68 (dd, *J* = 8.0, 1.0 Hz, 1H), 7.64, 7.60 (AB system, *J* = 8.0 Hz, 4H), 7.60 (d, *J* = 8.0 Hz, 1H), 7.48 (d, *J* = 8.5 Hz, 2H), 7.02 (s, 1H), 7.01 (br, 3H), 6.89 (d, *J* = 8.5 Hz, 2H), 4.05–4.03 (m, 4H, OCH₂), 3.83 (s, 3H, OCH₃), 1.90–1.82 (m, 8H), 1.58–1.47 (m, 8H), 1.39–1.25 (m, 48H), 0.89–0.85 (m, 12H, CH₃); ¹³C NMR (CDCl₃, 125 MHz) δ 191.7 (CHO), 160.0 (OCH₃), 154.5, 154.1, 153.9, 153.6 (four C–O carbons in the phenyl rings), 136.2, 136.0, 133.3, 133.0, 132.3, 132.2, 130.4, 128.6, 126.8, 123.9, 118.8, 117.1, 117.06, 117.0, 116.3, 116.0, 115.7, 114.6, 114.2, 113.5, 112.1, 111.7 (one CN carbon and twenty-one aromatic carbons), 96.0, 95.4, 94.2, 93.5, 90.7, 90.4, 89.0, 84.8 (eight alkynyl carbons), 70.00, 69.95, 69.8, 69.6 (four C–O carbons in the alkyl chains), 55.5 (OCH₃), 32.1, 29.9, 29.8, 29.79, 29.7, 29.6, 29.5, 26.3, 22.9, 14.3; MALDI-TOF MS *m/z* calcd for C₈₁H₁₀₃NO₆ 1185.78, found 1186.68 [M + H]⁺.

1,4-Bis(2,5-bis(trimethylsilyl)ethynyl)styryl)benzene (361). To an oven-dried flask protected under a N₂ atmosphere were charged compound **346** (171 mg, 0.247 mmol), trimethylsilylacetylene (0.21 mL, 0.30 g, 3.1 mmol), PdCl₂(PPh₃)₂ (25.5 mg, 0.0363 mmol), CuI (13.8 mg, 0.0726 mmol) and Et₃N (10 mL). The solution was bubbled by N₂ at rt for 5 min and then heated to 50 °C under stirring and N₂ protection overnight. After the reaction was complete as checked by TLC analysis, the solvent was removed by rotary evaporation. The resulting residue was diluted with chloroform. The mixture was filtered through a MgSO₄ pad. The solution obtained was sequentially washed with aq HCl (10%) and brine. The organic layer was dried over MgSO₄ and concentrated under vacuum to give crude **361**, which was further purified by silica flash column chromatography (hexanes/CH₂Cl₂, 8:2) to yield compound **361** (135 mg, 0.202 mmol, 82.3%) as a yellow solid. Mp 262–263 °C; IR (KBr) 3031, 2959, 2898, 2155, 1633, 1478 cm⁻¹; ¹H NMR (CDCl₃, 500 MHz) δ 7.81 (s, br, 2H), 7.68 (d, *J* = 16.5 Hz, 2H, alkenyl H), 7.57 (s, 4H, central Ar-H), 7.44 (d, *J* = 8.5 Hz, 2H), 7.30 (dd, *J* = 8.0, 1.5 Hz, 2H), 7.22 (d, *J* = 16.0 Hz, 2H, alkenyl H), 0.34 (s, 18H, Si(CH₃)₃), 0.30 (s, 18H, Si(CH₃)₃); ¹³C NMR (CDCl₃, 125 MHz) δ 139.3, 137.2, 132.8, 130.6, 130.5, 128.2, 127.3, 126.3, 123.6, 122.3 (8 aromatic and 2 alkenyl carbons), 104.8, 103.3, 101.9, 96.4 (4 alkynyl carbons), 0.19, 0.15 (Si(CH₃)₃); APCI-MS (positive) *m/z* calcd for C₄₂H₅₀Si₄ 666.3, found 667.4 [M + H]⁺.

1,4-Bis(2,5-diethynylstyryl)benzene (362). To a solution of compound **361** (135 mg, 0.202 mmol) in 1:1 MeOH/THF (10 mL) was added K₂CO₃ (50 mg, 0.36 mmol). The mixture was stirred at rt for 1 h, then the reaction solvent was removed by rotary evaporation. The residue was diluted in EtOAc and sequentially washed with

aq HCl (10%) and brine. The organic layer was dried over MgSO_4 and concentrated under vacuum to afford the crude product of **362**, which was further purified by silica flash column chromatography (hexanes/ CH_2Cl_2 , 8:2) to yield compound **362** (77 mg, 0.20 mmol, 100%) as a yellow solid. Mp > 300 °C; IR (KBr) 3275, 3030, 2155, 2099, 1635, 1538, 1478 cm^{-1} ; ^1H NMR (CDCl_3 , 500 MHz) δ 7.84 (d, $J = 1.5$ Hz, 2H), 7.62 (d, $J = 16.5$ Hz, 2H, alkenyl H), 7.56 (s, 4H, central Ar-H), 7.48 (d, $J = 8.5$ Hz, 2H), 7.33 (dd, $J = 8.0, 2.5$ Hz, 2H), 7.19 (d, $J = 16.5$ Hz, 2H, alkenyl H), 3.49 (s, 2H, alkynyl H), 3.20 (s, 2H, alkynyl H); ^{13}C NMR (CDCl_3 , 125 MHz) δ 139.8, 137.3, 133.7, 131.4, 130.9, 128.7, 127.7, 126.0, 123.2, 121.9 (8 aromatic and 2 alkenyl carbons), 84.3, 83.5, 82.0, 79.3 (4 alkynyl carbons); APCI-MS (positive) m/z calcd for $\text{C}_{30}\text{H}_{18}$ 378.1, found 379.2 $[\text{M} + \text{H}]^+$.

Compound 363. Compound **213** (125 mg, 0.230 mmol), **346** (25 mg, 0.036 mmol), $\text{Pd}(\text{PPh}_3)_4$ (15 mg, 0.013 mmol), CuI (8.0 mg, 0.042 mmol) were added to Et_3N (8 mL). The solution was bubbled by N_2 at rt for 5 min and then stirred at rt under N_2 protection for 1 h. Afterwards, the reaction was heated to 60 °C and stirred for 18 h under N_2 protection. After the reaction was complete as checked by TLC analysis, the solvent was removed by rotary evaporation. The resulting residue was diluted with chloroform. The mixture was filtered through a MgSO_4 pad. The solution obtained was sequentially washed with aq HCl (10%) and brine. The organic layer was dried over MgSO_4 and concentrated under vacuum to give the crude product of **363**, which was further purified by silica flash column chromatography (hexanes/ EtOAc , 7:3) to yield compound **363** (60 mg, 0.025 mmol, 68%) as a yellow solid. Mp 103–104 °C; IR (KBr) 2924, 2853, 2727, 2207, 1703, 1600, 1560, 1513, 1496,

1467, 1417, 1386 cm^{-1} ; ^1H NMR (CDCl_3 , 500 MHz) δ 10.03 (s, 2H, CHO), 10.00 (s, 2H, CHO), 7.91 (s, 2H), 7.88 (d, $J = 8.5$ Hz, 4H), 7.83 (d, $J = 8.5$ Hz, 4H), 7.81 (d, $J = 17.5$ Hz, 2H, alkenyl H), 7.68 (d, $J = 9.0$ Hz, 4H), 7.65 (d, $J = 8.5$ Hz, 4H), 7.60 (s, 4H), 7.56 (d, $J = 8.5$ Hz, 2H), 7.41 (d, $J = 8.0$ Hz, 2H), 7.28 (d, $J = 18$ Hz, 2H), 7.03 (s, 2H, central Ar-H), 7.06 (s, 4H), 7.05 (s, 2H), 4.09-4.03 (m, 16H, OCH_2), 1.92-1.17 (m, 128H), 0.88-0.79 (m, 24H, CH_3); ^{13}C NMR (CDCl_3 , 125 MHz) δ 191.53, 191.47 (two CHO), 154.19, 154.16, 153.93, 153.86 (four Ar-O), 139.0, 137.3, 135.61, 135.57, 132.8, 132.23, 132.20, 130.7, 130.3, 130.0, 129.9, 129.8, 129.7, 128.0, 127.5, 126.6, 123.8, 122.5, 117.4, 117.2, 117.1, 117.0, 115.1, 114.8, 113.7, 113.6 (two alkenyl carbons and twenty-four aromatic carbons), 95.3, 94.4, 94.3, 93.9, 93.1, 90.41, 90.39, 87.9 (eight alkynyl carbons), 70.1, 69.9, 69.8 (C-O carbons in the alkyl chains), 32.1, 29.9, 29.8, 29.78, 29.7, 29.6, 29.4, 26.35, 26.31, 26.1, 22.9, 14.3; MALDI-TOF MS m/z calcd for $\text{C}_{170}\text{H}_{210}\text{O}_{12}$ 2443.58, found 2444.97 $[\text{M} + \text{H}]^+$.

1,4-Bis(2-((2,5-bis(decyloxy)-4-((4-methoxyphenyl)ethynyl)phenyl)ethynyl)-5-bromostyryl)benzene (364). Compound **346** (35.5 mg, 0.0652 mmol), **356** (22.5 mg, 0.0326 mmol), $\text{PdCl}_2(\text{PPh}_3)_2$ (2.3 mg, 0.0033 mmol), CuI (1.2 mg, 0.0065 mmol) were added to Et_3N (8 mL). The solution was bubbled by N_2 at rt for 5 min and then was stirred at rt under N_2 protection for 7 h. After the reaction was complete as checked by TLC analysis, the solvent was removed by rotary evaporation. The resulting residue was diluted with chloroform. The mixture was filtered through a MgSO_4 pad. The solution obtained was sequentially washed with aq HCl (10%) and brine. The organic layer was dried over MgSO_4 and concentrated under vacuum to give the crude product of **364**, which was further purified by silica flash column

chromatography (hexanes/CH₂Cl₂, 7:3) to yield compound **364** (24 mg, 0.016 mmol, 48%) as a yellow solid. Mp 138–139 °C; IR (KBr) 2959, 2924, 2853, 2206, 1636, 1620, 1576, 1559, 1540, 1514, 1459, 1417, 1384 cm⁻¹; ¹H NMR (CDCl₃, 500 MHz) δ 7.86 (d, *J* = 2.0 Hz, 2H), 7.74 (d, *J* = 16 Hz, 2H, alkenyl H), 7.58 (s, 4H, central Ar-H), 7.48 (d, *J* = 8.5 Hz, 4H), 7.42 (d, *J* = 8.5 Hz, 2H), 7.36 (dd, *J* = 16.0, 2 Hz, 2H), 7.21 (d, *J* = 16.0 Hz, 2H), 7.05 (s, 2H), 7.02 (s, 2H), 6.87 (d, *J* = 8.5 Hz, 4H), 4.02 (t, *J* = 6.5 Hz, 8H, OCH₂), 3.83 (s, 6H, OCH₃), 1.87–1.81 (m, 4H), 1.74–1.69 (m, 4H), 1.56–1.50 (m, 4H), 1.38–1.16 (m, 52H), 0.87 (t, *J* = 6.0 Hz, 6H, CH₃), 0.85 (t, *J* = 6.0 Hz, 6H, CH₃); ¹³C NMR (CDCl₃, 125 MHz) δ 160.1, 154.2, 153.9 (three C-O carbons in the phenyl rings), 140.9, 137.4, 134.2, 133.5, 131.3, 130.6, 128.1, 127.8, 126.3, 123.1, 121.9, 117.37, 117.35, 116.0, 115.5, 114.4, 113.7 (two alkenyl carbons and fifteen aromatic carbons), 95.7, 92.9, 92.7, 85.1 (four alkynyl carbons), 70.23, 70.18 (two C-O carbons in the alkyl chains), 55.7 (OCH₃), 32.33, 32.31, 30.1, 30.05, 30.03, 30.0, 29.91, 29.85, 29.8, 29.6, 26.6, 26.4, 23.1, 14.5; MALDI-TOF MS *m/z* calcd for C₉₆H₁₁₆Br₂O₆ 1522.71, found 1523.79 [M + H]⁺.

Compound 365. Compound **364** (24 mg, 0.016 mmol), **213** (34 mg, 0.063 mmol), PdCl₂(PPh₃)₂ (1.1 mg, 0.0016 mmol), CuI (0.59 mg, 0.0031 mmol) were added to Et₃N (6 mL). The solution was bubbled by N₂ at rt for 5 min and then stirred at 65 °C under N₂ protection for 12 h. After the reaction was complete as checked by TLC analysis, the solvent was removed by rotary evaporation. The resulting residue was diluted with chloroform. The mixture was filtered through a MgSO₄ pad. The solution obtained was sequentially washed with aq HCl (10%) and brine. The organic layer was dried over MgSO₄ and concentrated under vacuum

to give the crude product of **365**, which was further purified by silica flash column chromatography (hexanes/CH₂Cl₂, 2:8) to yield compound **365** (23 mg, 0.0094 mmol, 61%) as a yellow solid. Mp 98-99 °C; ¹H NMR (CDCl₃, 500 MHz) δ 10.04 (s, 2H), 7.91 (s, 2H), 7.88 (d, *J* = 8.5 Hz, 4H), 7.81 (d, *J* = 15.0 Hz, 2H, alkenyl H), 7.69 (d, *J* = 8.5 Hz, 4H), 7.60 (s, 4H, central Ar-H), 7.55 (d, *J* = 8.0 Hz, 2H), 7.48 (d, *J* = 8.0 Hz, 4H), 7.41 (d, *J* = 8 Hz, 2H), 7.28 (d, *J* = 16.0 Hz, 2H), 7.07 (s, 2H), 7.06 (s, 4H), 7.04 (s, 2H), 6.87 (d, *J* = 15.0 Hz, 2H, alkenyl H), 4.09-4.02 (m, 16H, OCH₂), 3.83 (s, 6H, OCH₃), 1.92-1.17 (m, 128H), 0.89-0.82 (m, 24H, CH₃); MALDI-TOF MS *m/z* calcd for C₁₇₀H₂₁₄O₁₂ 2447.61, found 2449.32 [M + H]⁺.

2,5-Bis((trimethylsilyl)ethynyl)benzaldehyde (366). To an oven-dried flask protected under a N₂ atmosphere were charged compound **345** (540 mg, 1.74 mmol), trimethylsilylacetylene (0.98 mL, 0.68 g, 6.9 mmol), PdCl₂(PPh₃)₂ (60 mg, 0.085 mmol), CuI (30 mg, 0.16 mmol) and Et₃N (10 mL). The solution was bubbled by N₂ at rt for 5 min and then heated to 60 °C under stirring and N₂ protection overnight. After the reaction was complete as checked by TLC analysis, the solvent was removed by rotary evaporation. The resulting residue was diluted with chloroform. The mixture was filtered through a MgSO₄ pad. The solution obtained was sequentially washed with aq HCl (10%) and brine. The organic layer was dried over MgSO₄ and concentrated under vacuum to give crude **366**, which was further purified by silica flash column chromatography (hexanes/CH₂Cl₂, 8:2) to yield compound **366** (518 mg, 1.74 mmol, 100%) as a colorless oil. IR (KBr) 2960, 2922, 2158, 1700, 1597, 1481, 1410 cm⁻¹; ¹H NMR (CDCl₃, 500 MHz) δ 7.89 (d, *J* = 1.0 Hz, 1H), 7.50 (dd, *J* = 8.5, 1.0 Hz, 1H), 7.40 (d, *J* = 8.5 Hz, 1H), 0.20 (s, 9H), 0.17 (s, 9H) (signal from

CHO was missed due to the mistake of selecting 0-10 ppm range when running NMR); ^{13}C NMR (CDCl_3 , 125 MHz) δ 190.6 (CHO), 136.8, 136.7, 134.1, 131.1, 125.5, 123.6 (six aromatic carbons), 86.1, 82.0, 80.6, 79.0 (four alkynyl carbons); GC-MS m/z (%) 154 (100, $[\text{M}]^+$), 126 (98, $[\text{M}-\text{CHO}]$).

2,5-Diethynylbenzaldehyde (367). To a solution of compound **366** (518 mg, 1.74 mmol) in 1:1 MeOH:THF (12 mL) was added K_2CO_3 (50 mg, 0.36 mmol). The mixture was stirred at rt for 5 min, then the reaction solvent was removed by rotary evaporation. The residue was diluted in CHCl_3 and sequentially washed with aq HCl (10%) and brine. The organic layer was dried over MgSO_4 and concentrated under vacuum to afford pure compound **367** (240 mg, 1.56 mmol, 90%) as a yellow solid. Mp 142–143 °C; IR (KBr) 3283, 3259, 2866, 2104, 1682, 1599, 1481 cm^{-1} ; ^1H NMR (CDCl_3 , 500 MHz) δ 10.49 (s, 1H, CHO), 8.02 (d, $J = 1.0$ Hz, 1H), 7.64 (dd, $J = 8.5$, 1.0 Hz, 1H), 7.57 (d, $J = 8.5$ Hz, 1H), 3.56 (s, 1H), 3.24 (s, 1H); ^{13}C NMR (CDCl_3 , 125 MHz) δ 191.0 (CHO), 136.5, 136.2, 133.6, 130.7, 126.3, 124.2 (six aromatic carbons), 104.6, 103.4, 100.0, 98.1 (four alkynyl carbons); GC-MS m/z (%) 298 ($[\text{M}]^+$, 13), 283 ($[\text{M}-\text{CH}_3]^+$, 100), 268 ($[\text{M}-2\text{CH}_3]^+$, 8).

2-Iodobenzoic acid (359). A 250-mL round-bottomed flask containing anthranilic acid (4.60 g, 0.0335 mol), 30 mL of water, and 8 mL of concentrated hydrochloric acid was heated until the solid was dissolved. The mixture was then cooled in ice. When the temperature reached 0 to 5 °C, a solution of NaNO_2 (2.5 g, 0.036 mol) in 15 mL of water was added slowly. After 5 min, a solution of KI (6 g, 0.036 mol) in 8 mL of water was added. The mixture was let stand without cooling

for 5 min and then carefully warmed to around 45 °C with occasional swirling. When the reaction reached about 40 °C, a vigorous reaction ensued, characterized by gas evolution and separation of a tan solid. After reacting for 10 min, the mixture was heated to 90 °C for 10 min and then cooled in ice. A pinch of sodium bisulfite was added to destroy any iodine present, and the granular dark tan to brown product was collected and washed with water. The still-moist product was recrystallized from ethanol and water to give **369** (5.3 g, 0.021 mol, 64%) as a slightly yellow solid. Mp 159–160 °C; ¹H NMR (CDCl₃, 500 MHz) δ 8.08 (d, *J* = 8.0 Hz, 1H), 8.04 (d, *J* = 8.5 Hz, 1H), 7.46 (t, *J* = 8.0 Hz, 1H), 7.22 (t, *J* = 8.0 Hz, 1H) (proton on COOH was not observed due to rapid proton exchange); ¹³C NMR (CDCl₃, 125 MHz) δ 171.8 (C=O), 142.4, 134.0, 133.6, 132.6, 128.5, 95.2 (C-I); APCI-MS (negative) *m/z* calcd for C₇H₅IO₂ 247.9, found 246.8 [M – H] .

Methyl 2-iodobenzoate (370). To 40 mL of methanol was added 2-iodobenzoic acid (5.3 g, 0.021 mol) and 2.0 mL of H₂SO₄. The solution was refluxed overnight. The reaction was cooled down to rt. Methanol was removed by rotary evaporation. The residue was dissolved in EtOAc. The solution was washed by brine, and dried over MgSO₄. After removal of EtOAc under vacuum, the yielded crude product was purified by chromatography (hexanes/CH₂Cl₂, 1:4) to yield **370** (5.4 g, 0.02 mmol, 96%) as a colorless oil. ¹H NMR (CDCl₃, 500 MHz) δ 7.99 (d, *J* = 8.5 Hz, 1H), 7.80 (dd, *J* = 7.5, 1.0 Hz, 1H), 7.40 (t, *J* = 7.5 Hz, 1H), 7.15 (dd, *J* = 7.5, 1.5 Hz, 1H), 3.93 (CH₃); ¹³C NMR (CDCl₃, 125 MHz) δ 167.1 (C=O), 141.5, 135.2, 132.8, 131.1, 128.0, 94.2, 52.7 (CH₃); GC-MS *m/z* (%) 262 ([M]⁺, 95), 231 ([M – OCH₃]⁺, 100), 203 ([M – COOCH₃]⁺, 40).

Dimethyl 2,2'-(2-formyl-1,4-phenylene)bis(ethyne-2,1-diyl)dibenzoate (371). Compound **367** (80 mg, 0.52 mmol), **370** (273 mg, 1.04 mmol), PdCl₂(PPh₃)₂ (36 mg, 0.052 mmol), CuI (20 mg, 0.104 mmol) were added to Et₃N (10 mL). The solution was bubbled by N₂ at rt for 5 min and then stirred for 3 h at rt. After the reaction was complete as checked by TLC analysis, the solvent was removed by rotary evaporation. The resulting residue was diluted with chloroform. The mixture was filtered through a MgSO₄ pad. The solution obtained was sequentially washed with aq HCl (10%) and brine. The organic layer was dried over MgSO₄ and concentrated under vacuum to give the crude product of **371**, which was further purified by silica flash column chromatography (hexanes/CH₂Cl₂, 1:1) to yield compound **371** (139 mg, 0.329 mmol, 63%) as a yellow solid. Mp 144–145 °C; IR (KBr) 2999, 2950, 2215, 1719, 1687, 1597, 1564, 1500, 1446 cm⁻¹; ¹H NMR (CDCl₃, 500 MHz) δ 10.74 (s, 1H, CHO), 8.14 (s, 1H), 8.04 (d, *J* = 8.5 Hz, 1H), 8.01 (d, *J* = 8.0 Hz, 1H), 7.77 (d, *J* = 7.0 Hz, 1H), 7.71–7.69 (m, 2H), 7.66 (d, *J* = 8.0, 1H), 7.57–7.51 (m, 2H), 7.47–7.41 (m, 2H), 3.99 (s, 3H), 3.97 (s, 3H); ¹³C NMR (CDCl₃, 125 MHz) δ 191.8 (CHO), 166.5, 166.2 (two COOCH₃), 136.41, 136.39, 134.4, 134.3, 133.6, 132.08, 132.04, 131.95, 131.82, 130.9, 130.7, 130.4, 129.0, 128.6, 126.5, 124.4, 123.2, 122.9 (eighteen aromatic carbons), 96.7, 92.9, 91.5, 89.9 (four alkynyl carbons), 52.5, 52.4 (two OCH₃); APCI-MS (positive) *m/z* calcd for C₂₇H₁₈O₅ 422.1, found 423.2 [*M* + H]⁺.

4-Iodo-N,N-dimethylaniline (373). N,N-Dimethylaniline (1.21 g, 10 mmol) was dissolved in dioxane (50 mL) and pyridine (50 mL), and the solution was cooled to 0 °C. Iodine (3.8 g, 15 mmol) was added in one portion. The solution progressively

took a dark brown colour. After 1 h, the ice bath was removed. The solution was further stirred at rt for 1 h. A saturated solution of sodium thiosulfate was then added until the brown colour disappeared. The mixture was extracted with dichloromethane (200 mL) and washed with water (200 mL). After evaporation, the crude product was purified by silica flash column chromatography (hexanes/CH₂Cl₂, 1:1) to yield compound **373** (1.5 g, 6.1 mmol, 61%) as a white solid. Mp 80–81 °C; ¹H NMR (CDCl₃, 500 MHz) δ 7.47 (d, *J* = 9.0 Hz, 2H), 6.50 (d, *J* = 9.0 Hz, 2H), 2.93 (s, 6H, N(CH₃)₂); ¹³C NMR (CDCl₃, 125 MHz) δ 150.2, 137.7, 114.9, 77.6, 40.4 (N(CH₃)₂). GC-MS *m/z* (%) 247 ([M]⁺, 100).

5-Bromo-2-((triisopropylsilyl)ethynyl)benzaldehyde (374). Compound **345** (1.62 g, 5.20 mmol), triisopropylsilylacetylene (1.15 mL, 0.950 g, 5.20 mmol), PdCl₂(PPh₃)₂ (46 mg, 0.065 mmol), CuI (25 mg, 0.13 mmol) were added to Et₃N (20 mL). The solution was bubbled by N₂ at rt for 5 min and then stirred at rt and under N₂ protection for 24 h. After the reaction was complete as checked by TLC analysis, the solvent was removed by rotary evaporation. The resulting residue was diluted with chloroform. The mixture was filtered through a MgSO₄ pad. The solution obtained was sequentially washed with aq HCl (10%) and brine. The organic layer was dried over MgSO₄ and concentrated under vacuum to give the crude product of **374**, which was further purified by silica flash column chromatography (hexanes/CH₂Cl₂, 8:2) to yield compound **374** (1.78 g, 4.87 mmol, 94%) as a colorless oil. IR (KBr) 2944, 2891, 2866, 2736, 2156, 1695, 1582, 1469, 1383 cm⁻¹; ¹H NMR (CDCl₃, 500 MHz) δ 10.53 (s, 1H, CH=O), 8.05 (d, *J* = 2.0 Hz, 1H), 7.67 (dd, *J* = 8.5, 1.5 Hz, 1H), 7.47 (d, *J* = 8.0 Hz, 1H), 1.15 (s, 21H, *i*-Pr₃); ¹³C NMR (CDCl₃, 125 MHz) δ 190.4

(CH O), 137.5, 136.7, 135.4, 130.1, 125.9, 123.4 (6 aromatic carbons), 101.1, 100.9 (2 alkynyl carbons), 18.8, 11.4 (2 *i*-Pr₃ carbons); APCI-MS (positive) *m/z* calcd for C₁₈H₂₅⁸¹BrOSi 366.1 and C₁₈H₂₅⁷⁹BrOSi 364.1, found 367.1 and 365.1 [M + H]⁺.

2-((Triisopropylsilyl)ethynyl)-5-((trimethylsilyl)ethynyl)benzaldehyde (375). Compound **374** (417 mg, 1.14 mmol), trimethylsilylacetylene (0.322 mL, 2.28 mmol, mmol), PdCl₂(PPh₃)₂ (20 mg, 0.029 mmol), CuI (11 mg, 0.057 mmol) were added to Et₃N (10 mL). The solution was bubbled by N₂ at rt for 5 min and then stirred at 60 °C under N₂ protection for 12 h. After the reaction was complete as checked by TLC analysis, the solvent was removed by rotary evaporation. The resulting residue was diluted with chloroform. The mixture was filtered through a MgSO₄ pad. The solution obtained was sequentially washed with aq HCl (10%) and brine. The organic layer was dried over MgSO₄ and concentrated under vacuum to give the crude product of **375**, which was further purified by silica flash column chromatography (hexanes CH₂Cl₂, 85:15) to yield compound **375** (431 mg, 1.13 mmol, 99%) as a colorless oil. ¹H NMR (CDCl₃, 500 MHz) δ 10.58 (s, 1H, CH O), 8.01 (d, *J* = 1.5 Hz, 1H), 7.61 (dd, *J* = 8.0, 1.5 Hz, 1H), 7.54 (d, *J* = 8.0 Hz, 1H), 1.16 (s, 21H, *i*-Pr₃), 0.28 (s, 9H, CH₃); ¹³C NMR (CDCl₃, 125 MHz) δ 190.9 (CH O), 136.5, 136.3, 133.9, 130.7, 126.6, 124.1 (6 aromatic carbons), 103.4, 101.9, 101.3, 98.0 (4 alkynyl carbons), 18.8, 11.4 (2 *i*-Pr₃ carbons), 0.03 (CH₃); APCI-MS (positive) *m/z* calcd for C₂₃H₃₄OSi₂ 382.2, found 383.3 [M + H]⁺.

5-Ethynyl-2-((triisopropylsilyl)ethynyl)benzaldehyde (376). To a solution of compound **375** (431 mg, 1.13 mmol) in 1:1 MeOH/THF (12 mL) was added

K_2CO_3 (50 mg, 0.36 mmol). The mixture was stirred at rt for 1 h, then the reaction solvent was removed by rotary evaporation. The residue was diluted in CH_2Cl_2 and sequentially washed with aq HCl (10%) and brine. The organic layer was dried over MgSO_4 and concentrated under vacuum to afford the crude product of **376**, which was further purified by silica flash column chromatography (hexanes/ CH_2Cl_2 , 8:2) to yield compound **376** (371 mg, 1.2 mmol, 100%) as a colorless oil. ^1H NMR (CDCl_3 , 500 MHz) δ 10.57 (s, 1H, CH=O), 8.02 (d, J = 2.0 Hz, 1H), 7.63 (dd, J = 7.5, 2.0 Hz, 1H), 7.55 (d, J = 7.5 Hz, 1H), 3.23 (s, 1H, alkynyl proton), 1.15 (s, 21H, *t*-Pr₃); ^{13}C NMR (CDCl_3 , 125 MHz) δ 190.8 (CH=O), 136.8, 136.3, 134.0, 130.8, 127.1, 123.0 (6 aromatic carbons), 101.69, 101.63, 82.2, 80.3 (4 alkynyl carbons), 18.8, 11.4 (2 *t*-Pr₃ carbons); APCI-MS (positive) m/z calcd for $\text{C}_{20}\text{H}_{26}\text{OSi}$ 310.2, found 311.2 [$\text{M} + \text{H}$]⁺.

Methyl 2-((3-formyl-4-((triisopropylsilyl)ethynyl)phenyl)ethynyl)benzoate (377). Compound **376** (181 mg, 0.583 mmol), **370** (153 mg, 0.583 mmol), $\text{PdCl}_2(\text{PPh}_3)_2$ (21 mg, 0.0293 mmol), CuI (11.1 mg, 0.0586 mmol) were added to Et_3N (8 mL). The solution was bubbled by N_2 at rt for 5 min and then stirred at rt and under N_2 protection for 5 h. After the reaction was complete as checked by TLC analysis, the solvent was removed by rotary evaporation. The resulting residue was diluted with chloroform. The mixture was filtered through a MgSO_4 pad. The solution obtained was sequentially washed with aq HCl (10%) and brine. The organic layer was dried over MgSO_4 and concentrated under vacuum to give the crude product of **377**, which was further purified by silica flash column chromatography (hexanes/ CH_2Cl_2 , 6:4) to yield compound **377** (196 mg, 0.441 mmol, 76%) as a white

solid. Mp 82–83 °C; IR (KBr) 2942, 2890, 2865, 2153, 1710, 1694, 1600, 1493, 1463, 1450, 1384 cm^{-1} ; ^1H NMR (CDCl_3 , 500 MHz) δ 10.60 (s, 1H, CH–O), 8.09 (d, $J = 1.0$ Hz, 1H), 7.99 (d, $J = 8.5$ Hz, 1H), 7.72 (dd, $J = 8.5, 1.0$ Hz, 1H), 7.64 (d, $J = 8.0$ Hz, 1H), 7.58 (d, $J = 8.5$ Hz, 1H), 7.51 (t, $J = 8.5$ Hz, 1H), 7.41 (t, $J = 8.0$ Hz, 1H), 3.97 (s, 3H), 1.16 (s, 21H, $i\text{-Pr}_3$); ^{13}C NMR (CDCl_3 , 125 MHz) δ 191.0 (CH–O), 166.5 (carbonyl carbon on ester group), 136.38, 136.35, 134.3, 134.0, 132.1, 132.0, 130.8, 130.3, 128.6, 126.6, 124.3, 123.2 (12 aromatic carbons), 102.0, 101.4, 92.8, 91.4 (4 alkynyl carbons), 52.4 (OCH_3), 18.8, 11.4 (2 $i\text{-Pr}_3$ carbons); APCI-MS (positive) m/z calcd for $\text{C}_{28}\text{H}_{32}\text{O}_4\text{Si}$ 444.2, found 445.3 [$\text{M} + \text{H}$] $^+$.

Methyl 2-((4-ethynyl-3-formylphenyl)ethynyl)benzoate (378). To a solution of compound **377** (195 mg, 0.439 mmol) in THF (8 mL) was added TBAF (0.05 mL, 1 M, 0.05 mmol). The mixture was stirred at rt for 10 min. The reaction solvent was removed by rotary evaporation. The residue was dissolved in chloroform and sequentially washed with aq HCl (10%) and brine. The organic layer dried over MgSO_4 . Filtration to remove MgSO_4 followed by evaporation under vacuum afforded the crude product which was purified with silica flash column chromatography (hexanes/ CH_2Cl_2 , 7:3) to yield compound **378** as a yellow solid (99 mg, 0.34 mmol, 78%). Mp 120–121 °C; IR (KBr) 3251, 2960, 2855, 2152, 2101, 1724, 1692, 1600, 1566, 1492, 1433, 1389 cm^{-1} ; ^1H NMR (CDCl_3 , 500 MHz) δ 10.52 (s, 1H, CH–O), 8.10 (d, $J = 1.5$ Hz, 1H), 8.01 (d, $J = 8.0$ Hz, 1H), 7.75 (dd, $J = 8.0, 1.5$ Hz, 1H), 7.66 (d, $J = 8.0$ Hz, 1H), 7.61 (d, $J = 8.5$ Hz, 1H), 7.53 (t, $J = 8.5$ Hz, 1H), 7.43 (t, $J = 8.0$ Hz, 1H), 3.98 (s, 3H), 3.58 (s, 1H); ^{13}C NMR (CDCl_3 , 125 MHz) δ 190.8 (CH–O), 166.5 (carbonyl carbon on ester group), 136.7, 136.5, 134.4, 134.1, 132.2,

132.0, 130.8, 130.7, 128.7, 125.0, 124.9, 123.1 (12 aromatic carbons), 92.6, 91.6, 86.0, 79.3 (4 alkynyl carbons), 52.5 (OCH₃); APCI-MS (positive) *m/z* calcd for C₁₉H₁₂O₃ 288.1, found 289.1 [M + H]⁺.

Methyl 2-((4-((4-(*N,N*-dimethylamino)phenyl)ethynyl)-3-formylphenyl)ethynyl)benzoate (379). Compound **378** (99 mg, 0.34 mmol), **373** (85 mg, 0.34 mmol), PdCl₂(PPh₃)₂ (12 mg, 0.017 mmol), CuI (6.5 mg, 0.034 mmol) were added to Et₃N (6 mL). The solution was bubbled by N₂ at rt for 5 min and then stirred at 40 °C under N₂ protection for 7 h. After the reaction was complete as checked by TLC analysis, the solvent was removed by rotary evaporation. The resulting residue was diluted with chloroform. The mixture was filtered through a MgSO₄ pad. The solution obtained was sequentially washed with aq HCl (10%) and brine. The organic layer was dried over MgSO₄ and concentrated under vacuum to give crude **379**, which was further purified by silica flash column chromatography (hexanes/CH₂Cl₂, 1:1) to yield compound **379** (65 mg, 0.16 mmol, 47%) as a white solid. Mp 151–152 °C. IR (KBr) 2925, 2198, 1730, 1688, 1610, 1526, 1492, 1446, 1432, 1384 cm⁻¹; ¹H NMR (CDCl₃, 500 MHz) δ 10.64 (s, 1H, CH=O), 8.10 (d, *J* = 1.0 Hz, 1H), 8.01 (d, *J* = 8.0 Hz, 1H), 7.72 (dd, *J* = 8.5, 1.0 Hz, 1H), 7.66 (d, *J* = 8.5 Hz, 1H), 7.58 (d, *J* = 8.5 Hz, 1H), 7.52 (t, *J* = 8.5 Hz, 1H), 7.45 (d, *J* = 9.0 Hz, 1H), 7.42 (t, *J* = 8.0 Hz, 1H), 6.68 (d, *J* = 9.0 Hz, 1H), 3.99 (s, 3H), 3.02 (s, 6H); ¹³C NMR (CDCl₃, 125 MHz) δ 191.5 (CH=O), 166.6 (carbonyl carbon on ester group), 150.9, 136.5, 135.4, 134.3, 133.2, 132.9, 132.1, 132.0, 130.8, 130.7, 128.5, 127.9, 123.4, 123.0, 111.9, 108.7 (16 aromatic carbons), 100.6, 93.2, 90.9, 83.7 (4 alkynyl carbons), 52.5 (OCH₃), 40.3 (NCH₃); APCI-MS (positive) *m/z* calcd for C₂₇H₂₁NO₃ 407.2, found 408.2 [M + H]⁺.

1,4-Bis(5-bromo-2-((triisopropylsilyl)ethynyl)styryl)benzene (380). To an oven-dried flask protected under a N₂ atmosphere were charged compound **206** (51.8 mg, 0.137 mmol), NaH (9.9 mg, 0.41 mmol), and dry THF (4 mL). Upon gentle heating at *ca.* 40 °C, the solution gradually turned into a light yellow color. Aldehyde **374** (100 mg, 0.274 mmol) dissolved in THF (4 mL) was added in small portions over a period of 1 h through a syringe. The reaction was kept under stirring and heating for another 0.5 h before work-up. The small excess NaH was carefully quenched with aq HCl (10%) and the mixture was extracted with chloroform three times. The organic layer was dried over MgSO₄ and concentrated under vacuum to give crude **380**, which was further purified by silica flash column chromatography (hexanes/CH₂Cl₂, 9:1) to yield compound **380** (50 mg, 0.062 mmol, 45%) as a yellow solid. Mp 174–175 °C; IR (KBr) 2941, 2890, 2864, 2152, 1631, 1579, 1560, 1541, 1510, 1467 cm⁻¹; ¹H NMR (CDCl₃, 500 MHz) δ 7.83 (d, *J* = 1.5 Hz, 2H), 7.67 (d, *J* = 16.0 Hz, 2H, alkenyl H), 7.52 (s, 4H, central Ar-H), 7.36 (d, *J* = 8.5 Hz, 2H), 7.31 (dd, *J* = 7.5, 1.5 Hz, 2H), 7.14 (d, *J* = 16.5 Hz, 2H, alkenyl H), 1.18 (s, 42H, *t*-Pr₃); ¹³C NMR (CDCl₃, 125 MHz) δ 141.0, 137.0, 134.7, 131.0, 130.3, 127.53, 127.46, 125.8, 123.1, 121.6 (10 aromatic and alkenyl carbons), 104.6, 97.6 (2 alkynyl carbons), 19.0, 11.6 (2 *t*-Pr₃ carbons); APCI-MS (positive) *m/z* calcd for C₄₁H₅₆Br₂Si₂ 800.2, found 801.3 [M + H]⁺.

1,4-Bis(2-((triisopropylsilyl)ethynyl)-5-((trimethylsilyl)ethynyl)styryl)benzene (381). Compound **380** (305 mg, 0.381 mmol), trimethylsilylacetylene (0.2 mL, 0.14 g, 1.4 mmol), PdCl₂(PPh₃)₂ (26.8 mg, 0.0381 mmol), CuI (14.5 mg, 0.0762 mmol) were added to Et₃N (10 mL). The solution was bubbled by N₂ at rt for 5

min and then stirred at 60 °C under N₂ protection for 12 h. After the reaction was complete as checked by TLC analysis, the solvent was removed by rotary evaporation. The resulting residue was diluted with chloroform. The mixture was filtered through a MgSO₄ pad. The solution obtained was sequentially washed with aq HCl (10%) and brine. The organic layer was dried over MgSO₄ and concentrated under vacuum to give crude **381**, which was further purified by silica flash column chromatography (hexanes/CH₂Cl₂, 95:5) to yield compound **381** (297 mg, 0.356 mmol, 93%) as a yellow solid. Mp 211–212 °C; IR (KBr) 2943, 2893, 2865, 2154, 1632, 1595, 1534, 1511, 1477 cm⁻¹; ¹H NMR (CDCl₃, 500 MHz) δ 7.82 (s, br, 2H), 7.71 (d, *J* = 16.5 Hz, 2H, alkenyl H), 7.53 (s, 4H, central Ar-H), 7.44 (d, *J* = 7.0 Hz, 2H), 7.28 (dd, *J* = 8.0, 1.0 Hz, 2H), 7.19 (d, *J* = 16.5 Hz, 2H, alkenyl H), 1.19 (s, 42H, *i*-Pr₃), 0.29 (s, 18H, Si(CH₃)₃); ¹³C NMR (CDCl₃, 125 MHz) δ 139.2, 137.1, 133.3, 130.6, 130.5, 128.1, 127.7, 126.2, 123.5, 122.7 (10 aromatic and alkenyl carbons), 105.2, 104.9, 98.2, 96.2 (4 alkynyl carbons), 19.0, 11.6 (2 *i*-Pr₃ carbons), 0.14 (Si(CH₃)₃); APCI-MS (positive) *m/z* calcd C₅₄H₇₄Si₄ 834.5, found 835.6 [M + H]⁺.

1,4-Bis(5-ethynyl-2-((triisopropylsilyl)ethynyl)styryl)benzene (382). To a solution of compound **381** (335 mg, 0.401 mmol) in 1:1 MeOH:THF (12 mL) was added K₂CO₃ (50 mg, 0.36 mmol). The mixture was stirred at rt for 15 min, then the reaction solvent was removed by rotary evaporation. The residue was diluted in EtOAc and sequentially washed with aq HCl (10%) and brine. The organic layer was dried over MgSO₄ and concentrated under vacuum to afford crude **382**, which was further purified by silica flash column chromatography (hexanes/CH₂Cl₂, 95:5) to yield compound **382** (220 mg, 0.318 mmol, 79%) as a yellow solid. Mp 143–144

°C; IR (KBr) 3300, 3033, 2942, 2891, 2864, 2149, 1632, 1596, 1536, 1511, 1464 cm^{-1} ; ^1H NMR (CDCl_3 , 500 MHz) δ 7.87 (d, J = 1.0 Hz, 2H), 7.74 (d, J = 16.0 Hz, 2H, alkenyl H), 7.55 (s, 4H, central Ar-H), 7.34 (dd, J = 8.5, 1.0 Hz, 2H), 7.21 (d, J = 16.5 Hz, 2H, alkenyl H), 3.21 (s, 2H, alkynyl H), 1.22 (s, 42H, $i\text{-Pr}_3$); ^{13}C NMR (CDCl_3 , 125 MHz) δ 139.3, 137.1, 133.4, 130.7, 130.6, 128.3, 127.1, 126.1, 123.1, 122.4 (10 aromatic and alkenyl carbons), 105.0, 98.4, 83.5, 78.9 (4 alkynyl carbons), 19.0, 11.6 (2 $i\text{-Pr}_3$ carbons); APCI-MS (positive) m/z calcd for $\text{C}_{48}\text{H}_{58}\text{Si}_2$ 690.4, found 691.5 $[\text{M} + \text{H}]^+$.

Dimethyl 2,2'-(3,3'-(1*E*,1'*E*)-2,2'-(1,4-phenylene)bis(ethene-2,1-diyl)bis(4-((triisopropylsilyl)ethynyl)-3,1-phenylene))bis(ethyne-2,1-diyl)dibenzoate (383). To an oven-dried flask protected under a N_2 atmosphere were charged compound **382** (220 mg, 0.318 mmol), **370** (168 mg, 0.637 mmol), $\text{PdCl}_2(\text{PPh}_3)_2$ (22 mg, 0.032 mmol), CuI (12 mg, 0.064 mmol) and Et_3N (10 mL). The solution was bubbled by N_2 at rt for 5 min and then stirred at 40 °C under N_2 protection for 12 h. After the reaction was complete as checked by TLC analysis, the solvent was removed by rotary evaporation. The resulting residue was diluted with chloroform. The mixture was filtered through a MgSO_4 pad. The solution obtained was sequentially washed with aq HCl (10%) and brine. The organic layer was dried over MgSO_4 and concentrated under vacuum to give crude **383**, which was further purified by silica flash column chromatography (hexanes/ CH_2Cl_2 , 20:80) to yield compound **383** (233 mg, 0.243 mmol, 76%) as a yellow solid. Mp 185–186 °C; IR (KBr) 3032, 2943, 2891, 2864, 2210, 2148, 1731, 1631, 1597, 1567, 1489 cm^{-1} ; ^1H NMR (CDCl_3 , 500 MHz) δ 8.02 (dd, J = 8.0, 1.0 Hz, 2H), 7.92 (s, br, 2H), 7.75 (d, J = 16.5 Hz, 2H, alkenyl H),

7.70 (d, $J = 7.0$ Hz, 2H), 7.56 (s, 4H, central Ar-H), 7.54-7.51 (m, 4H), 7.44-7.42 (m, 4H), 7.24 (d, $J = 16.5$ Hz, 2H, alkenyl H), 4.00 (s, 6H, OCH₃), 1.21 (s, 42H, *i*-Pr₃); ¹³C NMR (CDCl₃, 125 MHz) δ 166.8 (C=O), 139.4, 137.1, 134.3, 133.4, 132.1, 132.0, 130.79, 130.68, 130.4, 128.4, 128.7, 127.4, 126.3, 123.74, 123.70, 122.8 (16 aromatic and alkenyl carbons), 105.3, 98.3, 94.3, 90.1 (4 alkynyl carbons), 52.5 (OCH₃), 19.0, 11.6 (2 *i*-Pr₃ carbons); APCI-MS (positive) m/z calcd for C₆₄H₇₀O₄Si₂ 958.5, found 959.6 [M + H]⁺.

Dimethyl 2,2'-(3,3'-(1*E*,1'*E*)-2,2'-(1,4-phenylene)bis(ethene-2,1-diyl)bis(4-ethynyl-3,1-phenylene))bis(ethyne-2,1-diyl)dibenzoate (384). To a solution of compound **383** (233 mg, 0.243 mmol) in THF (8 mL) was added TBAF (0.1 mL, 1 M, 0.1 mmol). The mixture was stirred at rt for 5 min, then the solvent was removed by rotary evaporation. The residue was dissolved in chloroform and sequentially washed with aq HCl (10%) and brine. The organic layer dried over MgSO₄. Filtration to remove MgSO₄ followed by evaporation under vacuum afforded the crude product which was purified with silica flash column chromatography (hexanes/CH₂Cl₂, 90:10) to yield compound **384** as a yellow solid (143 mg, 0.221 mmol, 91%). Mp > 300 °C; IR (KBr) 3290, 3029, 2953, 2920, 2850, 2212, 2099, 1724, 1667, 1646, 1598, 1565, 1489 cm⁻¹; ¹H NMR (CDCl₃, 500 MHz) δ 8.02 (d, $J = 8.5$ Hz, 2H), 7.92 (d, $J = 1.5$ Hz, 2H), 7.69 (d, $J = 8.5$ Hz, 2H), 7.65 (d, $J = 16.0$ Hz, 2H, alkenyl H), 7.59 (s, 4H, central Ar-H), 7.55-7.52 (m, 4H), 7.44-7.41 (m, 4H), 7.24 (d, $J = 17.0$ Hz, 2H, alkenyl H), 3.40 (s, 6H, OCH₃), 3.51 (s, 2H, alkynyl H); ¹³C NMR (CDCl₃, 125 MHz) δ 166.8 (C=O), 139.7, 137.1, 134.4, 133.5, 132.0, 131.1, 130.8, 130.4, 128.4, 128.0, 127.5, 126.0, 124.2, 123.6, 121.3 (of the 16 aromatic

and alkenyl carbons, one coincidental peak not observed), 94.0, 90.2, 84.0, 82.0 (4 alkynyl carbons), 52.5 (OCH₃); APCI-MS (positive) *m/z* calcd for C₁₆H₃₀O₄ 646.2 found 647.3 [M + H]⁺.

1,4-Bis((trimethylsilyl)ethynyl)benzene (387). To an oven-dried flask protected under a N₂ atmosphere were charged with compound **386** (329 mg, 1.00 mmol), trimethylsilylacetylene (0.566 mL, 393 mg, 4.00 mmol), PdCl₂(PPh₃)₂ (35 mg, 0.050 mmol), CuI (19 mg, 0.10 mmol) and Et₃N (15 mL). The solution was bubbled by N₂ at rt for 5 min and then stirred under N₂ protection for 2 h. After the reaction was complete as checked by TLC analysis, the solvent was removed by rotary evaporation. The resulting residue was diluted with chloroform. The mixture was filtered through a MgSO₄ pad. The solution obtained was sequentially washed with aq HCl (10%) and brine. The organic layer was dried over MgSO₄ and concentrated under vacuum to give the crude product of **387**, which was further purified by silica flash column chromatography (hexanes, CH₂Cl₂, 99:1) to yield compound **387** (273 mg, 1.00 mmol, 100%) as a yellow solid. Mp 121–122 °C; IR (KBr) 2956, 2898, 2155, 1618, 1504, 1492, 1413, 1327 cm⁻¹; ¹H NMR (CDCl₃, 500 MHz) δ 7.39 (s, 4H, central Ar-H), 0.26 (s, 18H, Si(CH₃)₃); ¹³C NMR (CDCl₃, 125 MHz) δ 132.0, 123.4 (two aromatic carbons), 104.8, 96.5 (two alkynyl carbons), 0.14 (Si(CH₃)₃); APCI-MS (positive) *m/z* calcd for C₁₆H₂₂Si₂ 270.1, found 272.0 [M + 2H]⁺.

1,4-Diethynylbenzene (388). To a solution of compound **387** (270 mg, 0.100 mmol) in 1:1 MeOH/CH₃Cl (16 mL) was added KOH (50 mg, 0.89 mmol). The mixture was stirred at rt for 1h, then the reaction solvent was removed by rotary

evaporation. The residue was diluted in CH_2Cl_2 and sequentially washed with aq HCl (10%) and brine. The organic layer was dried over MgSO_4 and concentrated under vacuum to afford pure **388** (113 mg, 0.900 mmol, 90%) as a yellow solid. Mp 98–99 °C; IR (KBr) 3263, 2925, 2854, 2103, 1617, 1538, 1507, 1494, 1465, 1403, 1383 cm^{-1} ; ^1H NMR (CDCl_3 , 500 MHz) δ 7.44 (s, 4H, central Ar-H), 3.17 (s, 2H); ^{13}C NMR (CDCl_3 , 125 MHz) δ 132.2, 122.8 (two aromatic carbons), 83.2, 79.3 (two alkynyl carbons); GC-MS m/z (%) 126 ($[\text{M}]^+$, 100).

4,4'-(1,4-Phenylenebis(ethyne-2,1-diyl))bis(N,N-dimethylaniline) (389).

To an oven-dried flask protected under a N_2 atmosphere were charged compound **388** (48 mg, 0.38 mmol), **385** (282 mg, 1.14 mmol), $\text{PdCl}_2(\text{PPh}_3)_2$ (27 mg, 0.038 mmol), CuI (14 mg, 0.076 mmol) were added to triethylamine (15 mL). The solution was bubbled by N_2 at rt for 5 min and then stirred at rt under N_2 protection for 2 h. After the reaction was complete as checked by TLC analysis, the solvent was removed by rotary evaporation. The resulting residue was diluted with chloroform. The mixture was filtered through a MgSO_4 pad. The solution obtained was sequentially washed with aq HCl (10%) and brine. The organic layer was dried over MgSO_4 and concentrated under vacuum to give crude **389**, which was further purified by silica flash column chromatography (hexanes CH_2Cl_2 , 7:3) to yield compound **389** (93.4 mg, 0.256 mmol, 67%) as a yellow solid. Mp 98–99 °C; IR (KBr) 2893, 2800, 2207, 1606, 1526, 1478, 1442, 1406, 1359 cm^{-1} ; ^1H NMR (CDCl_3 , 500 MHz) δ 7.44 (s, 4H, central Ar-H), 7.41 (d, $J = 9.0$ Hz, 4H), 6.67 (d, $J = 9.0$ Hz, 4H), 3.00 (s, 12H); ^{13}C NMR (CDCl_3 , 125 MHz) δ 150.4, 133.0, 131.3, 123.4, 112.1, 110.2 (six aromatic carbons), 92.5, 87.7 (two alkynyl carbons), 40.4 (CH_3); APCI-MS (positive) m/z

calcd for $C_{26}H_{24}N_2$ 364.2, found 365.3 $[M + H]^+$.

Chapter 5

Conclusions and Future Work

5.1 Concluding remarks

The main theme running throughout the research of this thesis resides at the interface between “organic synthesis” and “physical organic chemistry”; in other words, design and preparation of unprecedented molecular systems based on modern synthetic methodologies, followed by investigations on the interrelationships between molecular structure and property/reactivity using various state-of-the-art instrumental analytical techniques.

Major synthetic efforts in this thesis have been focused on the construction of three classes of carbon-rich conjugated oligomeric systems, namely C₆₀-OPE-OPV-C₆₀ triads, C₆₀-oligoyn-C₆₀ dumbbells, and H-shaped two-dimensional conjugated OPE/OPV co-oligomers. The combination of Pd-catalyzed Sonogashira coupling and Horner-Wittig olefination reactions turns out to be a potent strategy in preparing phenylene ethynylene and phenylene vinylene based co-oligomers with various 1D and

2D π -frameworks, as mainly demonstrated by the synthetic works in Chapters 2 and 4. Also, the synthesis of various C_{60} -oligomer adducts in Chapters 2 and 3 evince the effectiveness and reliability of the *in situ* alkylation reaction of C_{60} in terms of generating novel C_{60} -oligomer hybrids directly from conjugated oligomer precursors that bear terminal alkyne moieties. From a methodological viewpoint, the synthetic routes reported in this thesis work should be applicable to the synthesis of a wide range of π -conjugated oligomers, polymers, and related C_{60} derivatives that are structurally analogous to the compounds studied in this thesis.

In the investigations of structure-property relationships, the linear OPE OPV co-oligomers prepared in Chapter 2 show better electron-donating ability than their cruciform-shaped isomers, presumably due to a greater degree of π electron delocalization and relatively higher-lying HOMO energies. It is also found that the HOMO energies of cruciform OPE OPV co-oligomers can be considerably increased by incorporating electron donating groups to the molecular backbone. In the corresponding C_{60} -OPE OPV- C_{60} triad systems, there are no significant electronic interactions between the central oligomer units and the endcapping C_{60} groups based on the results of electronic absorption spectroscopic and cyclic voltammetric analyses. However, a substantial quenching of the radiative decay of the OPE OPV moieties is observed in the fluorescence spectra of both the linear and cruciform shaped C_{60} -OPE OPV- C_{60} ensembles, suggesting rapid intramolecular electron transfer from the oligomer to the C_{60} group.

The C_{60} -oligoyne- C_{60} dumbbells prepared in Chapter 3 are found to undergo random solid-state polymerizations at elevated temperatures. The solid-state reactivity as revealed by UV-Vis, IR, and DSC analyses stems from the central

oligoynes units, and longer oligoynes (*e.g.* tetraynes) appear to polymerize to a relatively higher degree than shorter oligoynes (*e.g.* diynes). AFM investigations show that the C₆₀-oligoynes-C₆₀ dumbbells can self-assemble into distinctive nanoscopic structures on surfaces, including nanospheres, nanoflakes, and nanorods. The morphological features are dependent on the structure of the molecule. As a general trend, if the C₆₀ contents in the molecular composition increase, the self-assemblies would favor a spherical shape, while if the phenylacetylene contents increase, the formation of continuous layers (lamellae) would be more favored. Moreover, upon thermally induced solid-state polymerization, the assembly of C₆₀-tetrayne-C₆₀ **260a** undergoes a dramatic transformation from a discontinuous flake-like morphology to an ordered array of nanospheres with an average diameter of 18-20 nm. This result suggests a potentially useful approach to produce nanoscale C₆₀-based materials by using solid-state polymerization reactions.

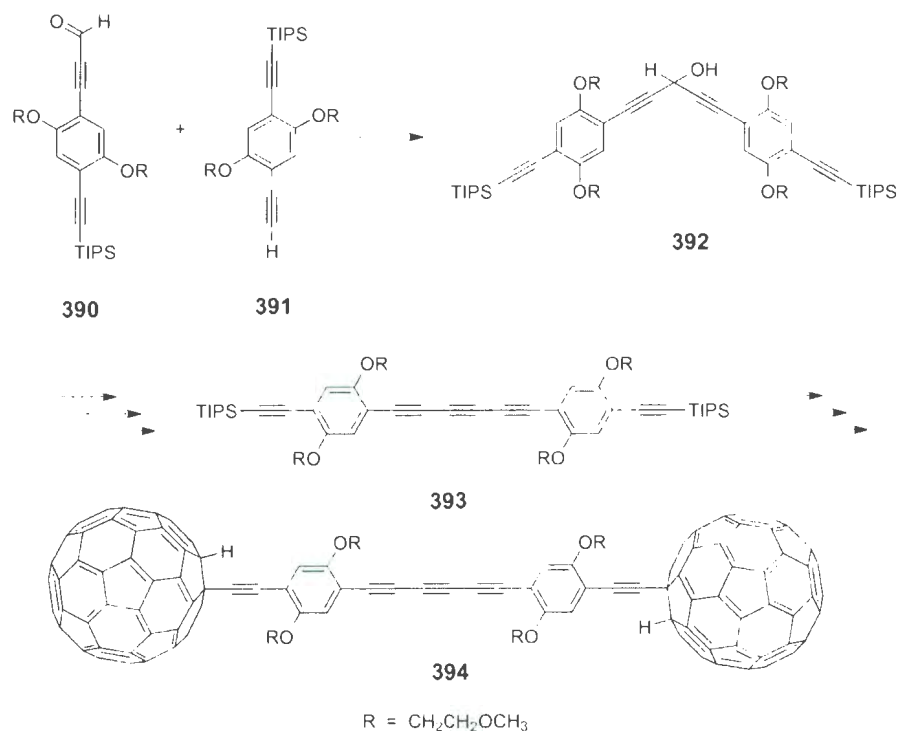
The 2D H-shaped OPE/OPV co-oligomers (H-mers) described in Chapter 4 show complex electron delocalization patterns. The π -electronic characteristics of the H-mers bearing long OPE branches are found to be almost immune to various electronic substitutions on the OPE termini, as a result of poor π -conjugation on the twisted OPE backbone. The short H-mers, on the contrary, show pronounced electronic substitution effects due to enhanced molecular planarity and electronic communications between the terminal groups and the H-mer core. Dramatic absorption and emission spectral shifts are observed when substituents of different electronic natures are attached to the OPE termini of the short H-mers. Furthermore, the spectral envelopes of two amino-substituted short H-mers **337** and **338** are found to be highly sensible to addition of a strong Brønsted acid TFA or selected transition

metal ions, Ag^+ and Cu^{2+} . These properties demonstrate the usefulness of these short H-mers as versatile chromophores fluorophores in functional chemical sensors.

5.2 Future work

Most of the target molecules have been successfully synthesized and their properties are systemically characterized in this thesis. However, there are still a number of problematic syntheses that need to be addressed in the future work. A major synthetic challenge lies in the synthesis of C_{60} oligoyne C_{60} compounds in Chapter 3, wherein the central oligoyne moiety consists of odd-numbered acetylenic bonds. Our preliminary efforts to prepare triyne **274** all ended with unsuccessful results. As discussed previously, the difficulty could be the steric crowding imposed by the long alkyl chains adjacent to the aldehyde group in precursor **271**, which prevents the occurrence of nucleophilic addition to the carbonyl group. If this is the case, alternative precursors such as **390** and **391** as proposed below should make it easier to obtain the desired triyne **394**, since the shorter alkyl chains present less steric hinderance and still maintain sufficient solubility for **394** (see Scheme 5.1).

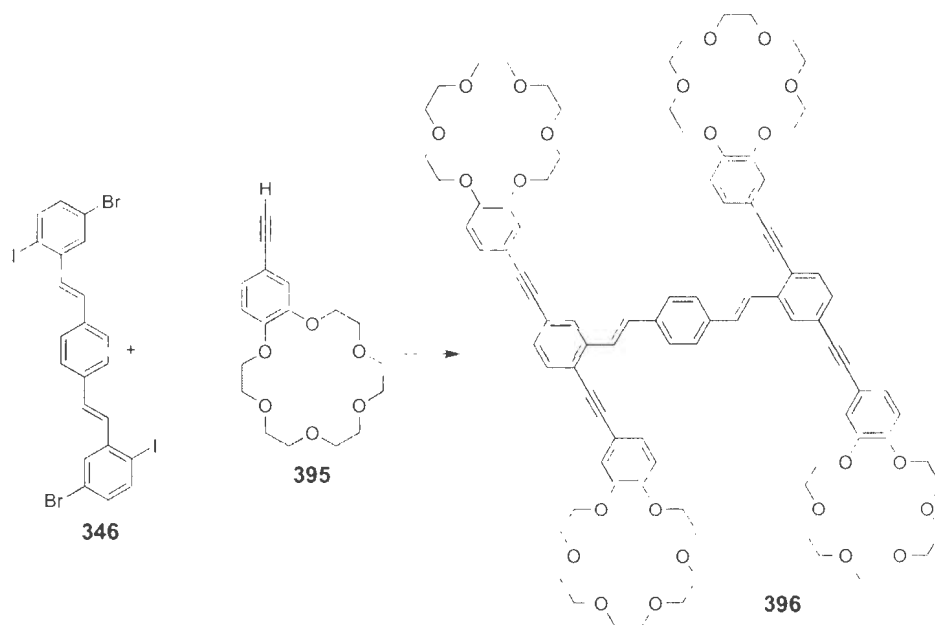
In Chapter 4, it has been verified that the electronic and photonic behavior of the H-mers can be flexibly manipulated or fine-tuned via chemical functionalization with various electroactive and chromophoric groups. This may offer opportunities for the H-mers to be further exploited as advanced optoelectronic materials. For instance, with compounds such as **346** described in Chapter 4, compound **396** should be readily obtained (see Scheme 5.2). The cyclic polyether moieties in **396** may enhance the binding of **396** with various alkali metal ions, hence rendering the new H-mer sensing



Scheme 5.1: Modified method to synthesis of bifullerene endcapped triyne **294**.

functions toward alkali metal ions.

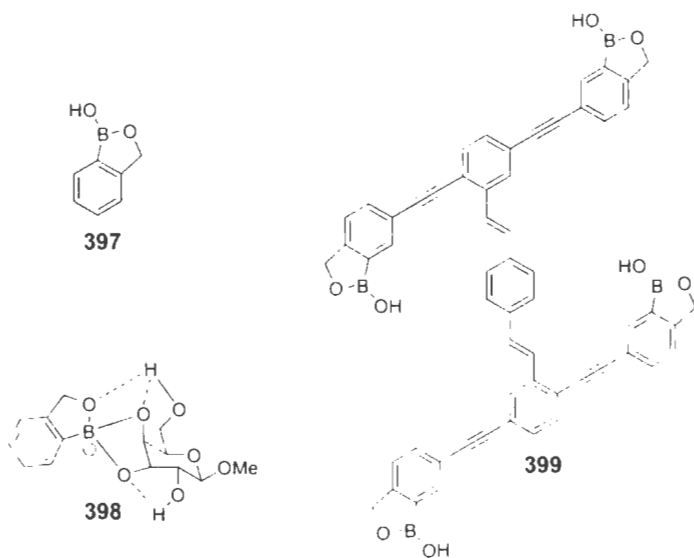
Of equal importance to metal sensing is the detection of carbohydrates using the H-mers. This can be possibly developed by attaching boronic acid groups to the H-mer backbone. Selective recognition of natural biopolymers such as polypeptides, oligonucleic acids and oligosaccharides by small molecules has fascinated organic chemists for several decades. Among them, the use of boronic acid derivatives is regarded as one of the most promising approaches for recognition of carbohydrate derivatives.³⁵⁸⁻³⁶¹ Most recently, Hall and co-workers reported benzoboroxoles such as **397** could be used as efficient glycopyranoside-binding agents to form complex **398** under physiological conditions.³⁶² In a similar vein, if compound **397** could be



Scheme 5.2: Compound **396** as potential metal ion sensor

integrated into the H-mer backbone to give such functional H-mers as **399** (Scheme 5.3), novel fluorescence sugar sensors would be possibly achieved.

Finally, it should be noted that our understanding of the photophysical properties of C_{60} -OPE 'OPV'- C_{60} triads prepared in Chapter 2 is still premature and awaits further investigations using sophisticated spectroscopic techniques, although photoinduced electron transfer has been identified as the major deactivation pathway according to present experimental evidence. We are currently collaborating with Dr. D. W. Thompson's group at Memorial University to unravel the exact photophysical mechanisms by means of nanosecond laser flash photolysis experiments. In addition, the binding constants for the amino-substituted short H-mers with various metal ions will be calculated using a global spectral fitting method. These results will be



Scheme 5.3: Compound **399** as potential fluorescence probes for carbohydrates

reported in the PhD dissertation of my colleague, Li Wang, as well as our collaborative publications in the future.

References

1. IUPAC, *Pure Appl. Chem.* **1996**, *68*, 2287-2311.
2. Orchin, M.; Macomber, R. S.; Pinhas, A. R.; Wilson, R. M. *The Vocabulary and Concepts of Organic Chemistry*; John Wiley: New Jersey, 2005; p 295.
3. Morawetz, H. *Polymers: The Origin and Growth of a Science*; John Wiley: New York, 1985; pp 3-7.
4. Hosler, D.; Burkett, S. L.; Tarkanian, M. J. *Science* **1999**, *284*, 1988-1991.
5. Braconnot, H. *Ann. Chim.(Paris)* **1811**, *79*, 265-304.
6. Lunn, R. W. *Ind. Eng. Chem.* **1939**, *31*, 1190-1192.
7. Baekeland, L. H. *Ind. Eng. Chem.* **1911**, *3*, 932-938.
8. Staudinger, H. *Ber. Dtsch. Chem. Ges.* **1920**, *53*, 1073-1085.
9. Moulay, S. *L'actualité Chimique* **1999**, *12*, 31-43.
10. Seymour, R. B. *J. Chem. Educ.* **1988**, *65*, 327-334.
11. Shirakawa, H.; Louis, E. J.; MacDiarmid, A. G.; Chiang, C. K.; Heeger, A. J. *J. Chem. Soc., Chem. Commun.* **1977**, 578-580.

12. News, *Current Science* **2000**, *79*, 1632-1635.
13. Burroughes, J. H.; Bradley, D. D. C.; Brown, A. R.; Marks, R. N.; Mackay, K.; Friend, R. H.; Burn, P. L.; Holmes, A. B. *Nature* **1990**, *347*, 539-541.
14. Kraft, A.; Grimsdale, A. C.; Holmes, A. B. *Angew. Chem. Int. Ed.* **1998**, *37*, 403-428.
15. Bleier, H. *Organic Materials for Photonics*; Elsevier, Amsterdam, 1993; pp 77-101.
16. Meier, H. *Angew. Chem., Int. Ed. Engl.* **1992**, *31*, 1399-1420.
17. Martin, P. J. *Introduction to Molecular Electronics*; Edward Arnold, London, 1995; pp 112-141.
18. Heeger, A. J.; Long, J., Jr. *Optics and Photonics News* **1996**, *7*, 24-30.
19. Nalwa, H. S. *Nonlinear Optics of Organic Molecules and Polymers*; CRC, New York, 1997; pp 611-797.
20. Feringa, L.; Jager, W. F.; de Lange, B. *Tetrahedron* **1993**, *49*, 8267-8310.
21. Martin, R. E.; Diederich, F. *Angew. Chem. Int. Ed.* **1999**, *38*, 1350-1377.
22. Friend, R. H.; Gymer, R. W.; Holmes, A. B.; Burroughes, J. H.; Marks, R. N.; Taliani, C.; Bradley, D. D. C.; Dos Santos, D. A.; Bredas, J. L.; Logdlund, M.; Salaneck, W. R. *Nature* **1999**, *397*, 121-128.
23. Tykwinski, R. R.; Gubler, U.; Martin, R. E.; Diederich, F.; Bosshard, C.; Gunter, P. *J. Phys. Chem. B* **1998**, *102*, 4451-4465.

24. Katz, H. E.; Bao, Z. J. *J. Phys. Chem. B* **2000**, *104*, 671–678.
25. Hoppe, H.; Sariciftci, N. S. *J. Mater. Res.* **2004**, *19*, 1924–1945.
26. Oakley, K. M.; McGehee, M. D. *Chem. Mater.* **2004**, *16*, 4533–4542.
27. Kline, R. J.; McGehee, M. D. *Poly. Rev.* **2006**, *46*, 27–45.
28. Zade, S. S.; Bendikov, M. *Org. Lett.* **2006**, *8*, 5243–5246.
29. Meier, H.; Stalmach, U.; Kolshorn, H. *Acta Polym.* **1997**, *48*, 379–384.
30. Stalmach, U.; Kolshorn, H.; Brehm, I.; Meier, H. *Liebigs Ann.* **1996**, 1449–1456.
31. Oelkrug, D.; Gierschner, J.; Egelhaaf, H.-J.; Lürer, L.; Tompert, A.; Müllen, K.; Stalmach, U.; Meier, H. *Synth. Met.* **2001**, *121*, 1693–1694.
32. Bäuerle, P.; Fischer, T.; Bidlingmeier, B.; Stabel, A.; Rabe, J. *Angew. Chem., Int. Ed. Engl.* **1995**, *34*, 303–307.
33. Grimme, J.; Martin, K.; Uckert, F.; Müllen, K.; Scherf, U. *Adv. Mater.* **1995**, *7*, 292–295.
34. Tour, J. M. *Chem. Rev.* **1996**, *96*, 537–553.
35. Elandalousi, E. H.; Frère, P.; Richomme, P.; Orduna, J.; Garin, J.; Roncali, J. *J. Am. Chem. Soc.* **1997**, *119*, 10774–10784.
36. Roncali, J. *Macromol. Rapid Commun.* **2007**, *28*, 1761–1775.
37. Meier, H. *Angew. Chem. Int. Ed.* **2005**, *44*, 2482–2506.

38. *Nanoscience and Nanotechnologies: Opportunities and Uncertainties*; Technical Report, 2004.
39. Tour, J. M. *Acc. Chem. Res.* **2000**, *33*, 791–804.
40. MacDonald, S. A.; Willson, C. G.; Frechet, J. M. J. *Acc. Chem. Res.* **1994**, *27*, 151–158.
41. Müllen, K. *Pure Appl. Chem.* **1993**, *65*, 89–96.
42. Era, M.; Tsutsui, T.; Saito, S. *Appl. Phys. Lett.* **1995**, *67*, 2436–2438.
43. Wang, Y. Z.; Sun, R. G.; Meghdadi, F.; Leising, G.; Epstein, A. J. *Appl. Phys. Lett.* **1999**, *74*, 3613–3615.
44. Grundlach, D. J.; Lin, Y. Y.; Jackson, T. N.; Schlom, D. G. *Appl. Phys. Lett.* **1997**, *71*, 3853–3855.
45. Deeg, O.; Kirsch, P.; Pauluth, D.; Bäuerle, P. *Chem. Commun.* **2002**, 2762–2763.
46. Baumeister, B.; Matile, S. *Chem. Commun.* **2000**, 913–914.
47. Baumeister, B.; Sakai, N.; Matile, S. *Angew. Chem. Int. Ed.* **2000**, *39*, 1955–1958.
48. Winum, J. Y.; Matile, S. *J. Am. Chem. Soc.* **1999**, *121*, 7961–7961.
49. Gattermann, L.; Ehrhardt, R. *Ber. Dtsch. Chem. Ges.* **1890**, *23*, 1226–1228.
50. Bush, M.; Weber, W. *J. Prakt. Chem.* **1936**, *1*, 146.

51. Kern, W.; Ebersbach, H. W.; Ziegler, I. *Makromol. Chem.* **1963**, *63*, 53-69.
52. Meier, H.; Stalmach, U.; Kolshorn, H. *Acta Polym.* **1997**, *48*, 379-384.
53. Marcy, H. O.; Rosker, M. J.; Warren, L. F.; Reinhardt, B. A.; Sinclair, M.; Seager, C. H. *J. Chem. Phys.* **1994**, *100*, 3325-3333.
54. Tour, J. M. *Adv. Mater.* **1994**, *6*, 190-198.
55. Kern, W.; Seibel, M.; Wirth, H.-O. *Makromol. Chem.* **1959**, *29*, 164-189.
56. Heitz, W.; Ullrich, R. *Makromol. Chem.* **1966**, *98*, 29-41.
57. Liess, P.; Hensel, V.; Schlüter, A. *Liebigs Ann.* **1996**, 1037-1040.
58. Scherf, U.; Müllen, K. *Makromol. Chem., Rapid Commun.* **1991**, *12*, 489-497.
59. Stampfl, J.; Graupner, W.; Leising, G.; Scherf, U. *J. Lumin.* **1995**, *63*, 117-123.
60. Grümme, J.; Scherf, F. *Macromol. Chem. Phys.* **1996**, *197*, 2297-2304.
61. Heidenhain, S. B.; Sakamoto, Y.; Suzuki, T.; Miura, A.; Fujikawa, H.; Mori, T.; Tokito, S.; Taga, Y. *J. Am. Chem. Soc.* **2000**, *122*, 10240-10241.
62. Frere, P.; Raimundo, J.-M.; Blanchard, P.; Delaunay, J.; Richomme, P.; Sauvajol, J.-L.; Orduna, J.; Garin, J.; Roncali, J. *J. Org. Chem.* **2003**, *68*, 5357-5360.
63. Afzali, A.; Breen, T.; Kagan, C. *Chem. Mater.* **2002**, *14*, 1742-1746.
64. Meng, H.; Zheng, J.; Lovinger, A.; Wang, B.-C.; Patten, P. V.; Bao, Z. *Chem. Mater.* **2003**, *15*, 1778-1787.

65. Horowitz, G.; Hajlaoui, M. *Adv. Mater.* **2000**, *12*, 1046-1050.
66. Suzuki, M.; Fukuyama, M.; Hori, Y.; Hotta, S. *J. Appl. Phys.* **2002**, *91*, 5706-5711.
67. Pisignano, D.; Anni, M.; Gigli, G.; Cingolani, R.; Zavelani-Rossi, M.; Lanzani, G.; Barbarella, G.; Favaretto, L. *Appl. Phys. Lett.* **2002**, *81*, 3534-3536.
68. Torsi, L.; Lovinger, A.; Crone, B.; Someya, T.; Dodabalapur, A.; Katz, H.; Gelperin, A. *J. Phys. Chem. B* **2002**, *106*, 12563-12568.
69. Noma, N.; Tsuzuki, T.; Shirota, Y. *Adv. Mater.* **1995**, *7*, 674-678.
70. Videlot, C.; Kassmi, A. E.; Fichou, D. *Solar Energy Mater. Solar Cells* **2000**, *63*, 69-82.
71. Steinkopf, W.; Kohler, W. *Liebigs Ann. Chem.* **1936**, *522*, 17-31.
72. Steinkopf, W.; Petersdorf, H.-J.; Gording, R. *Liebigs Ann. Chem.* **1937**, *527*, 272-274.
73. Steinkopf, W.; Leitsmann, R.; Hofmann, K.-H. *Liebigs Ann. Chem.* **1941**, *546*, 180-184.
74. Stetter, H. *Angew. Chem., Int. Ed. Engl.* **1976**, *15*, 639-647.
75. Hoeve, W. T.; Wynberg, H.; Havinga, E. E.; Meijer, E. W. *J. Am. Chem. Soc.* **1991**, *113*, 5887-5889.
76. Endou, M.; Ie, Y.; Kaneda, T.; Aso, Y. *J. Org. Chem.* **2007**, *72*, 2659-2661.

77. Krömer, J.; Carreras, I. R.; Führmann, G.; Munsch, C.; Wunderlin, M.; Debaerdemaeker, T.; Mena-Osteritz, E.; Bäuerle, P. *Angew. Chem. Int. Ed.* **2000**, *39*, 3481-3486.
78. Burroughes, J. H.; Bradley, D. D. C.; Brown, A. R.; Marks, R. N.; Mackay, K.; Friend, R. H.; Burn, P. L.; Holmes, A. B. *Nature* **1990**, *347*, 539-541.
79. Hide, F.; Díaz-García, M. A.; Schwartz, B. J.; Heeger, A. J. *Acc. Chem. Res.* **1997**, *30*, 430-436.
80. Kraft, A.; Grimsdale, A. C.; Holmes, A. B. *Angew. Chem. Int. Ed.* **1998**, *37*, 403-428.
81. Birgerson, J.; Kaeriyama, K.; Barta, P.; Bröms, P.; Fahlman, M.; Granlund, T.; Salaneck, W. R. *Adv. Mater.* **1996**, *8*, 982-985.
82. Friend, R. H. In *Conjugated Polymers and Related Materials*; Salaneck, W. R., Lundström, I., Rånby, B., Eds.; Oxford University Press, Oxford, 1993; pp 285-323.
83. Burn, P. L.; Holmes, A. B.; Kraft, A.; Bradley, D. D. C.; Brown, A. R.; Friend, R. H.; Gymer, R. W. *Nature* **1992**, *356*, 47-49.
84. Greenham, N. C.; Moratti, S. C.; Bradley, D. D. C.; Friend, R. H.; Holmes, A. B. *Nature* **1993**, *365*, 628-630.
85. Yu, G.; Cao, Y.; Andersson, M.; Gao, J.; Heeger, A. J. *Adv. Mater.* **1998**, *10*, 385-388.

86. Garten, F.; Hilberer, A.; Cacialli, F.; Esselink, E.; van Dam, Y.; Schlatmann, B.; Friend, R. H.; Klapwijk, T. M.; Hadziioannou, G. *Adv. Mater.* **1997**, *9*, 127-131.
87. Drefahl, G.; Plötner, G. *Chem. Ber.* **1961**, *94*, 907-914.
88. Drefahl, G.; Kühmstedt, R.; Oswald, H.; Hörhold, H. H. *Makromol. Chem.* **1970**, *131*, 89-103.
89. Schenk, R.; Gregorius, H.; Meerholz, K.; Heinze, J.; Müllen, K. *J. Am. Chem. Soc.* **1991**, *113*, 2634-2636.
90. Maddux, T.; Li, W. J.; Yu, L. P. *J. Am. Chem. Soc.* **1997**, *119*, 844-845.
91. Katayama, H.; Nagao, M.; Ozawa, F.; Ikegami, M.; Arai, T. *J. Org. Chem.* **2006**, *71*, 2699-2705.
92. Kunzleman, J.; Kinami, M.; Crenshaw, B. R.; Protasiewicz, J. D.; Weder, C. *Adv. Mater.* **2008**, *20*, 119-122.
93. Montali, A.; Bastiaansen, C.; Smith, P.; Weder, C. *Nature* **1998**, *392*, 261-264.
94. Zhou, Q.; Swager, T. M. *J. Am. Chem. Soc.* **1995**, *117*, 12593-12602.
95. Galda, P.; Rehahn, M. *Synthesis* **1996**, 614-620.
96. Weder, C.; Wrighton, M. S.; Spreiter, R.; Bosshard, C.; Günter, P. *J. Phys. Chem.* **1996**, *100*, 18931-18936.
97. Weder, C.; Wrighton, M. S. *Macromolecules* **1996**, *29*, 5157-5165.
98. Ziener, U.; Godt, A. *J. Org. Chem.* **1997**, *62*, 6137-6143.

99. Schumm, J. S.; Pearson, D. L.; II, L. J.; Hara, R.; Tour, J. M. *Nanotechnology* **1996**, *7*, 430-433.
100. Yang, J. S.; Swager, T. M. *J. Am. Chem. Soc.* **1998**, *120*, 5321-5322.
101. Weder, C.; Wrighton, M. S. *Macromolecules* **1996**, *29*, 5157-5165.
102. Lavastre, O.; Ollivier, L.; Dixneuf, P. H.; Sibandhit, S. *Tetrahedron* **1996**, *52*, 5495-5504.
103. Grubbs, R. H.; Kratz, D. *Chem. Ber.* **1993**, *126*, 147-157.
104. Schumm, J. S.; Pearson, D. L.; Tour, J. M. *Angew. Chem., Int. Ed. Engl.* **1994**, *33*, 1360-1363.
105. Nelson, J. C.; Saven, J. G.; Moore, J. S.; Wolynes, P. G. *Science* **1997**, *277*, 1793-1796.
106. Shirai, Y.; Osgood, A. J.; Zhao, Y.; Kelly, K. F.; Tour, J. M. *Nano Lett.* **2005**, *5*, 2330-2334.
107. Natta, G.; Mazzanti, G.; Corradini, P. *Atti. Accad. Naz. Lincei, Rend. Cl. Sci. Fis., Mat. Nat.* **1958**, *25*, 3-12.
108. Chiang, C. K.; Druy, M. A.; Gau, S. C.; Heeger, A. J.; Louis, E. J.; MacDiarmid, A. G.; Park, Y. W.; Shirakawa, H. *J. Am. Chem. Soc.* **1978**, *100*, 1013-1015.
109. *Handbook of Organic Conductive Molecules and Polymers*; Nalwa, H. S., Ed.; John Wiley & Sons: New York, 1997; Vol. 2, pp 61-95.

110. Kiehl, A.; Eberhardt, A.; Adam, M.; Enkelmann, V.; Müllen, K. *Angew. Chem., Int. Ed. Engl.* **1992**, *31*, 1588 1591.
111. Kitamura, T.; Ikeda, M.; Shigaki, K.; Inoue, T.; Anderson, N. A.; Ai, X.; Lian, T.; Yanagida, S. *Chem. Mater.* **2004**, *16*, 1806 1812.
112. Spangler, C. W.; McCoy, R. K.; Dembek, A. A.; Sapochak, L. S.; Gates, B. D. *J. Chem. Soc., Perkin Trans. 1* **1989**, 151 154.
113. Blanchard-Desce, M.; Alain, V.; Bedworth, P. V.; Marder, S. R.; Fort, A.; Runser, C.; Barzoukas, M.; Lebus, S.; Wortmann, R. *Chem. Eur. J.* **1997**, *3*, 1091 1104.
114. Lahti, P.; J. Obrzut, F. E.; Karasz, F. E. *Macromolecules* **1987**, *20*, 2023 2026.
115. Baughman, S. L.; Hsu, S.; Anderson, L. R.; Pez, G. P.; Signorelli, A. J. *Molecular Metals*; Plenum, New York, 1979; pp 187 201.
116. Czekelius, C.; Hafer, J.; Tonzetich, Z. J.; Schrock, R. R.; Christensen, R. L.; Müller, P. *J. Am. Chem. Soc.* **2006**, *128*, 16664 16675.
117. Fox, H. H.; Wolf, M. O.; O'Dell, R.; Lin, B. L.; Schrock, R. R.; Wrighton, M. S. *J. Am. Chem. Soc.* **1994**, *116*, 2827 2843.
118. Trost, B. M.; Rudd, M. T. *J. Am. Chem. Soc.* **2005**, *127*, 4763 4776.
119. Curl, R. F. *Angew. Chem. Int. Ed.* **1997**, *36*, 1567 1576.
120. Kroto, H. W. *Angew. Chem. Int. Ed.* **1997**, *36*, 1579 1593.
121. Smalley, R. E. *Angew. Chem. Int. Ed.* **1997**, *36*, 1595 1601.

122. Diederich, F.; Rubin, Y. *Angew. Chem., Int. Ed. Engl.* **1992**, *31*, 1101–1123.
123. Diederich, F. *Nature* **1994**, *369*, 199–207.
124. Faust, R. *Angew. Chem. Int. Ed.* **1998**, *37*, 2825–2828.
125. Bunz, U. H.; Rubin, Y.; Tobe, Y. *Chem. Soc. Rev.* **1999**, *28*, 107–119.
126. Hunter, J. M.; Fye, J. L.; Roskamp, E. J.; Jarrold, M. F. *J. Phys. Chem.* **1994**, *98*, 1810–1818.
127. Lagow, R. J.; Kampa, J. J.; Wei, H.-C.; Battle, S. L.; Genge, J. W.; Laude, D. A.; Harper, C. J.; Bau, R.; Stevens, R. C.; Haw, J. F.; Munson, E. *Science* **1995**, *267*, 362–367.
128. Homman, K. H. *Angew. Chem. Int. Ed.* **1998**, *37*, 2434–2451.
129. Grosser, T.; Hirsch, A. *Angew. Chem., Int. Ed. Engl.* **1993**, *32*, 1340–1342.
130. Schermann, G.; Grsser, T.; Hampel, F.; Hirsch, A. *Chem. Eur. J.* **1997**, *3*, 1105–1112.
131. Smith, P. P. K.; Buseck, P. R. *Science* **1982**, *216*, 984–986.
132. Glaser, G. *Ber. Dtsch. Chem. Ges.* **1869**, *2*, 422–424.
133. Bohlmann, F. *Angew. Chem.* **1955**, *67*, 389–394.
134. Armitage, J. B.; Jones, E. R. H.; Whiting, M. C. *J. Chem. Soc.* **1957**, 2012–2017.
135. Jones, E. R. H.; Lee, H. H.; Whiting, M. C. *J. Chem. Soc.* **1960**, 3483–3489.
136. Bohlmann, F. *Chem. Ber.* **1953**, *86*, 657–667.

137. Armitage, J. B.; Entwistle, N.; Jones, E. R. H.; Whiting, M. C. *J. Chem. Soc.* **1954**, 147-154.
138. Eastmond, R.; Johnson, T. R.; Walton, D. R. M. *Tetrahedron* **1972**, *28*, 4601-4616.
139. Johnson, T. R.; Walton, D. R. M. *Tetrahedron* **1972**, *28*, 4601-4616.
140. Mohr, W.; Stahl, J.; Hampel, F.; Gladysz, J. A. *Chem. Eur. J.* **2003**, *9*, 3324-3340.
141. Eisler, S.; Tykwinski, R. R. *J. Am. Chem. Soc.* **2000**, *122*, 10736-10737.
142. Morisaki, Y.; Luu, T.; Tykwinski, R. R. *Org. Lett.* **2006**, *8*, 689-692.
143. Luu, T.; Morisaki, Y.; Cunningham, N.; Tykwinski, R. R. *J. Org. Chem.* **2007**, *72*, 9622-9629.
144. Eisler, S.; Slepko, A. D.; Elliott, E.; Luu, T.; McDonald, R.; Hegmann, F. A.; Tykwinski, R. R. *J. Am. Chem. Soc.* **2005**, *127*, 2666-2676.
145. Metay, E.; Hu, Q.; Negishi, E.-I. *Org. Lett.* **2006**, *8*, 5773-5776.
146. Tykwinski, R. R.; Zhao, Y. *Synlett* **2002**, 1939-1953.
147. Gholami, M.; Tykwinski, R. R. *Chem. Rev.* **2006**, *106*, 4997-5027.
148. Nielsen, M. B.; Diederich, F. *Chem. Rev.* **2005**, *105*, 1837-1867.
149. Martin, R. E.; Diederich, F. *Angew. Chem. Int. Ed.* **1999**, *38*, 1350-1377.
150. Wudl, F.; Bitler, P. *J. Am. Chem. Soc.* **1986**, *108*, 4685-4687.

151. Anthony, J.; Boudon, C.; Diederich, F.; Gisselbrecht, J.-P.; Gramlich, V.; Gross, M.; Hobi, M.; Seiler, P. *Angew. Chem., Int. Ed. Engl.* **1994**, *33*, 763-766.
152. Martin, R. E.; Mäder, T.; Diederich, F. *Angew. Chem. Int. Ed.* **1999**, *38*, 817-821.
153. Phelan, N. F.; Orchin, M. *J. Chem. Ed.* **1968**, *45*, 633-637.
154. Zhao, Y.; Tykwinski, R. R. *J. Am. Chem. Soc.* **1999**, *121*, 458-459.
155. Zhao, Y.; Campbell, K.; Tykwinski, R. R. *J. Org. Chem.* **2002**, *67*, 336-344.
156. Boldi, A. M.; Anthony, J.; Gramlich, V.; Knobler, C. B.; Boudon, C.; Gisselbrecht, J.-P.; Gross, M.; Diederich, F. *Helv. Chim. Acta* **1995**, *78*, 779-788.
157. Zhao, Y.; McDonald, R.; Tykwinski, R. R. *Chem. Commun.* **2000**, 77-78.
158. Zhao, Y.; McDonald, R.; Tykwinski, R. R. *J. Org. Chem.* **2002**, *67*, 2805-2812.
159. *Organic Light-Emitting Devices: A Survey*; Shinar, J., Ed.; New York: Springer-Verlag, 2004.
160. *Organic Light Emitting Devices: Synthesis, Properties and Applications*; Müllen, K., Scherf, U., Eds.; Weinheim, Germany, Wiley-VCH, 2006.
161. Tang, C. W.; VanSlyke, S. A. *Appl. Phys. Lett.* **1987**, *51*, 913-915.
162. Burroughes, J. H.; Bradley, D. D. C.; Brown, A. R.; Marks, R. N.; MacKay, K.; Friend, R. H.; Burn, P. L.; Holmes, A. B. *Nature* **1990**, *347*, 539-541.

163. Geffroy, B.; le Roy, P.; Prat, C. *Polym. Int.* **2006**, *55*, 572–582.
164. Pardo, D. A.; Jabbour, G. E.; Peyghambarian, N. *Adv. Mater.* **2000**, *12*, 1249–1252.
165. Gustafsson, G.; Cao, Y.; Treacy, G. M.; Klavetter, F.; Colaneri, N.; Heeger, A. J. *Nature* **1992**, *357*, 477–479.
166. *Highly Efficient OLEDs with Phosphorescent Materials*; Yersin, H., Ed.; Weinheim, Germany, Wiley-VCH, 2007.
167. Geng, Y.; Culligan, S. W.; Trajkovska, A.; Wallace, J. U.; Chen, S. H. *Chem. Mater.* **2003**, *15*, 542–549.
168. Culligan, S. W.; Geng, Y.; Chen, S. H.; Klubek, K.; Vaeth, K. M.; Tang, C. W. *Adv. Mater.* **2003**, *15*, 1176–1180.
169. Geng, Y.; Chen, A. C. A.; Ou, J. J.; Chen, S. H.; Klubek, K.; Vaeth, K. M.; Tang, C. W. *Chem. Mater.* **2003**, *15*, 4352–4360.
170. Chen, A. C. A.; Culligan, S. W.; Geng, Y.; Chen, S. H.; Klubek, K.; Vaeth, K. M.; Tang, C. W. *Adv. Mater.* **2004**, *16*, 783–788.
171. Matsushima, T.; Adachi, C. *Chem. Mater.* **2008**, *20*, 2881–2883.
172. Chen, A. C.-A.; Wallace, J. U.; Wei, S. K.-H.; Zeng, L.; Chen, S. H.; Blanton, T. N. *Chem. Mater.* **2006**, *18*, 204–213.
173. Brunner, K.; van Dijken, A.; Borner, H.; Bastiaansen, J. J. A. M.; Kigger, N. M. M.; Langeveld, B. M. W. *J. Am. Chem. Soc.* **2004**, *126*, 6035–6042.

174. Tonzola, C. J.; Kulkarni, A. P.; Gifford, A. P.; Kaminsky, W.; Jenekhe, S. A. *Adv. Funct. Mater.* **2007**, *17*, 863-874.
175. Li, H.; Lin, Y.; Chou, P.; Cheng, Y.; Liu, R. *Adv. Funct. Mater.* **2007**, *17*, 520-530.
176. Katz, H. E. *Mater. Chem.* **1997**, *7*, 369-376.
177. Barbe, D. F.; Westgate, C. R. *J. Phys. Chem. Solids* **1970**, *31*, 2679-2687.
178. Koezuka, H.; Tsumura, A.; Ando, T. *Synth. Met.* **1987**, *18*, 699-704.
179. Bao, Z.; Rogers, J. A.; Katz, H. E. *J. Mater. Chem.* **1999**, *9*, 1895-1904.
180. Forrest, S. R. *Nature* **2004**, *428*, 911-918.
181. Sirringhaus, H. *Adv. Mater.* **2005**, *17*, 2411-2425.
182. Baude, P. F.; Ender, D. A.; Haase, M. A.; Kelley, T. W.; Muires, D. V.; Theiss, S. D. *Appl. Phys. Lett.* **2003**, *82*, 3964-3966.
183. Rogers, J. A.; Bao, Z.; Baldwin, K.; Dodabalapur, A.; Crone, B.; Raju, V. R.; Kuck, V.; Katz, H.; Amundson, K.; Ewing, J.; Drzaic, P. P. *Proc. Natl. Acad. Sci. U.S.A.* **2001**, *98*, 4835-4840.
184. Zhou, L. S.; Wang, A.; Wu, S. C.; Sun, J.; Park, S.; Jackson, T. N. *Appl. Phys. Lett.* **2006**, *88*, 083524.
185. Lee, S.; Koo, B.; Park, J. G.; Moon, H.; Hahn, J.; Kim, J. M. *MRS Bull.* **2006**, *31*, 455-458.

186. Huitema, H. E. A.; Gelinck, G. H.; van der Putten, J. B. P. H.; Kuijk, K. E.; Hart, C. M.; Cantatore, E.; Herwig, P. T.; van Breemen, A. J. J.; de Leeuw, D. M. *Nature* **2001**, *414*, 599-599.
187. Crone, B.; Dodabalapur, A.; Lin, Y.-Y.; Filas, R.; Bao, Z.; LaDuca, A.; Sarpeshkar, R.; Katz, H. E.; Li, W. *Nature* **2000**, *403*, 521-523.
188. Sirringhaus, H.; Tessler, N.; Friend, R. H. *Science* **1998**, *280*, 1741-1744.
189. Burns, S. E. et al. *J. Soc. Inf. Disp.* **2005**, *13*, 583-586.
190. Gelinck, G. H.; Huitema, H. E. A.; van Mil, M.; van Veenendaal, E.; van Lieshout, P. J. G.; Touwslager, F.; Patry, S. F.; Sohn, S.; Whitesides, T.; McCreary, M. D. *J. Soc. Inf. Disp.* **2006**, *14*, 113-118.
191. Horowitz, G. *Adv. Mater.* **1998**, *10*, 365-377.
192. Allard, S.; Forster, M.; Souharce, B.; Thiem, H.; Scherf, U. *Angew. Chem. Int. Ed.* **2008**, *47*, 4070-4098.
193. Zaunscil, J.; Sirringhaus, H. *Chem. Rev.* **2007**, *107*, 1296-1323.
194. Sirringhaus, H. *Adv. Mater.* **1998**, *10*, 365-377.
195. Sirringhaus, H. *Adv. Mater.* **2005**, *17*, 2411-2425.
196. Podzorov, V.; Menard, E.; Borissov, A.; Kiryukhin, V.; Rogers, J. A.; Gershenson, M. E. *Phys. Rev. Lett.* **2004**, *93*, 086602.
197. Menard, E.; Podzorov, V.; Hur, S.-H.; Gaur, A.; Gershenson, M. E.; Rogers, J. A. *Adv. Mater.* **2004**, *16*, 2097-2101.

198. Kelley, T. W.; Muryres, D. V.; Baude, P. F.; Smith, T. P.; Jones, T. D. *Mater. Res. Soc. Symp. Proc.* **2003**, *771*, 169-171.
199. Anthony, J. E. *Chem. Rev.* **2006**, *106*, 5028-5048.
200. *Solar Cells and Their Applications*; Partain, L., Ed.; New York, Wiley-Interscience, 1995.
201. Green, M. *Solar Cells: Operating Principles, Technology and Systems Applications*; NJ, Prentice-Hall, 1992.
202. Nunzi, J. M. *C. R. Physique* **2002**, *3*, 523-542.
203. Wöhrle, D.; Meissner, D. *Adv. Mater.* **199**, *3*, 129-138.
204. Yu, G.; Gao, J.; Hummelen, J. C.; Wudl, F.; Heeger, A. J. *Science* **1995**, *270*, 1789-1791.
205. Granstrom, M.; Petritsch, K.; Arias, A. C.; Lux, A.; Anderson, M. R.; Friend, R. H. *Nature* **1998**, *395*, 257-260.
206. Friend, R. H. *Pure Appl. Chem.* **2001**, *73*, 425-430.
207. Tang, C. W. *Appl. Phys. Lett.* **1986**, *48*, 183-185.
208. Xue, J.; Uchida, S.; Rand, B. P.; Forrest, S. R. *Appl. Phys. Lett.* **2004**, *84*, 3013-3015.
209. Xue, J.; Uchida, S.; Rand, B. P.; Forrest, S. R. *Appl. Phys. Lett.* **2004**, *85*, 5757-5759.

210. Reyes-Reyes, M.; Kim, K.; Carroll, D. L. *Appl. Phys. Lett.* **2005**, *87*, 083506.
211. Xue, J.; Rand, B. P.; Uchida, S.; Forrest, S. R. *J. Appl. Phys.* **2005**, *98*, 124903.
212. Kietzke, T. *Advances in Optoelectronics* **2007**, 40285.
213. Sariciftci, N.; Smilowitz, L.; Heeger, A.; Wudl, F. *Science* **1992**, *258*, 1474-1476.
214. Spanggaard, H.; Krebs, F. C. *Solar Energy Materials & Solar Cells* **2004**, *83*, 125-146.
215. Gunes, S.; Neugebauer, H.; Sariciftci, N. S. *Chem. Rev.* **2007**, *107*, 1324-1338.
216. Chamberlain, G. A. *Solar Cells* **1983**, *8*, 47-83.
217. Schulze, K.; Urich, C.; Schüppel, R.; Leo, K.; Pfeiffer, M.; Brier, E.; Reinold, E.; Bäuerle, P. *Adv. Mater.* **2006**, *18*, 2872-2875.
218. Tamayo, A. B.; Walker, B.; Nguyen, T. Q. *J. Phys. Chem. C* **2008**, *112*, 11545-11551.
219. Nierengarten, J.-F.; Gu, T.; Hadziioannou, G.; Tsamouras, D.; Krasnikov, V. *Helv. Chim. Acta*, **2004**, *87*, 2948-2966.
220. Jones, D. E. *New Scientist* **1966**, *35*, 245.
221. Osawa, E. *Kagaku (Kyoto)* **1970**, *25*, 851-863.
222. Brath, W.; Lawton, R. G. *J. Am. Chem. Soc.* **1966**, *88*, 380-381.
223. Davidson, R. A. *Theor. Chim. Acta* **1981**, *58*, 193-231.

224. Stankevich, I. V.; Nikerov, M. V.; Bochkov, D. A. *Uspekhi Khimii* **1984**, *53*, 1101-1124.
225. Rohlfing, E. A.; Cox, D. M.; Kaldor, A. *J. Chem. Phys.* **1984**, *81*, 3322-3330.
226. Haymet, A. D. *J. Chem. Phys. Lett.* **1985**, *122*, 421-424.
227. Kroto, H. W.; Heath, J. R.; O'Brien, S. C.; Curl, R. E.; Smalley, R. E. *Nature* **1985**, *318*, 162-163.
228. Krätscher, W.; Lamb, L.; Fostiropoulos, K.; Huffman, D. R. *Nature* **1990**, *347*, 354-358.
229. Nakamura, E.; Isobe, H. *Acc. Chem. Res.* **2003**, *36*, 807-815.
230. Boorum, M.; Vasilev, Y.; Drewello, T.; Scott, L. *Science* **2001**, *294*, 828-831.
231. Haddon, R.; Raghavachari, K. *Tetrahedron* **1996**, *52*, 5207-5220.
232. Beckhaus, H. D.; Ruchardt, C.; Kao, M.; Diederich, F.; Foote, C. S. *Angew. Chem., Int. Ed. Engl.* **1992**, *31*, 63-64.
233. Balch, A. L.; Olmstead, M. *Chem. Rev.* **1998**, *98*, 2123-2165.
234. Hirsch, A. *Synthesis* **1995**, 895-912.
235. Diederich, F.; Thilgen, C. *Science* **1996**, *271*, 317-323.
236. Prato, M.; Lucchini, V.; Maggini, M.; Stimpff, E.; Scorrano, G.; Eiermann, M.; Suzuki, T.; Wudl, F. *J. Am. Chem. Soc.* **1993**, *115*, 8479-8480.

237. Eiermann, M.; Wudl, F.; Prato, M.; Maggini, M. *J. Am. Chem. Soc.* **1994**, *116*, 8364-8365.
238. Janssen, R. A. J.; Hummelen, J. C.; Wudl, F. *J. Am. Chem. Soc.* **1995**, *117*, 544-545.
239. Hirsch, A.; Brettreich, M. *Fullerenes Chemistry and Reactions*; Wiley-VCH, Weinheim, Germany, 2005.
240. Fagan, P. J.; Krusic, P. J.; Evans, D. H.; Lerke, S. A.; Johnston, E. *J. Am. Chem. Soc.* **1992**, *114*, 9697-9699.
241. Nagashima, H.; Terasaki, H.; Kimura, E.; Nakajima, K.; Itoh, K. *J. Org. Chem.* **1994**, *59*, 1246-1248.
242. Keshavarz-K, M.; Knight, B.; Srdanov, G.; Wudl, F. *J. Am. Chem. Soc.* **1995**, *117*, 11371-11372.
243. Nagashima, H.; Saito, M.; Kato, Y.; Goto, H.; Osawa, E.; Haga, M.; Itoh, K. *Tetrahedron* **1996**, *52*, 5053-5064.
244. Murata, Y.; Komatsu, K.; Wan, T. S. M. *Tetrahedron* **1996**, *52*, 5077-5090.
245. Komatsu, K.; Murata, Y.; Takimoto, N.; Mori, S.; Sugita, N.; Wan, T. S. M. *J. Org. Chem.* **1994**, *59*, 6101-6102.
246. Bucci, N.; Muller, T. J. J. *Tetrahedron Lett.* **2006**, *47*, 8329-8332.
247. Shirai, Y.; Zhao, Y.; Cheng, L.; Tour, J. M. *Org. Lett.* **2004**, *13*, 2129-2132.
248. Bingel, C. *Chem. Ber.* **1993**, *126*, 1957-1959.

249. Lamparth, I.; Hirsch, A. *J. Chem. Soc. Chem. Commun.* **1994**, 1727-1728.
250. Wharton, T.; Wilson, L. *J. Bioorg. Med. Chem.* **2002**, *10*, 3545-3554.
251. Yurovskaya, M. A.; Trushkov, I. V. *Russ. Chem. Bull. Int. Ed.* **2002**, *51*, 367-443.
252. Wilson, S. R.; Schuster, D. I.; Nuber, B.; Meier, M. S.; Maggini, M.; Prato, M.; Taylor, R. *Fullerenes: Chemistry, Physics, and Technology*; Wiley: New York, 2000.
253. Chronakis, N.; Froudakis, G.; Orfanopoulos, M. *J. Org. Chem.* **2002**, *67*, 3284-3289.
254. Kräutler, B.; Maynollo, J. *Tetrahedron* **1996**, *52*, 5033-5042.
255. Wilson, S. R.; Lu, Q. *Tetrahedron Lett.* **1993**, *34*, 8043-8046.
256. Langa, F.; de la Cruz, P.; Espildora, E.; Garcia, J. J.; Perez, M. C.; de la Hoz, A. *Carbon* **2000**, *38*, 1641-1646.
257. Tsuda, M.; Ishida, T.; Nogami, T.; Kurono, S.; Ohashi, M. *J. Chem. Soc., Chem. Commun.* **1993**, 1296-1298.
258. Segura, J. L.; Martín, N. *Angew. Chem. Int. Ed.* **2001**, *40*, 1372-1409.
259. Herranz, M.; Martín, N.; Ramey, J.; Guldi, D. M. *Chem. Commun.* **2002**, 2968-2969.
260. Belik, P.; Gügel, A.; Spickerman, J.; Müllen, K. *Angew. Chem., Int. Ed. Engl.* **1993**, *32*, 78-79.

261. Diederich, F.; Jonas, U.; Gramlich, V.; Herrmann, A.; Ringsdorf, H.; Thilgen, C. *Helv. Chim. Acta* **1993**, *76*, 2445–2453.
262. Tovar, A.; Peña, U.; Hernández, G.; Portillo, R.; Gutiérrez, R. *Synthesis* **2007**, 22–24.
263. Isaacs, L.; Wehrsig, A.; Diederich, F. *Helv. Chim. Acta* **1993**, *76*, 1231–1250.
264. Prato, M.; Bianco, A.; Maggini, M.; Scorrano, G.; Toniolo, C.; Wudl, F. *J. Org. Chem.* **1993**, *58*, 5578–5580.
265. Hummelen, J. C.; Knight, B. W.; LePeq, F.; Wudl, F.; Yao, J.; Wilkins, C. L. *J. Org. Chem.* **1995**, *60*, 532–538.
266. Avent, A. G.; Birkett, P. R.; Paolucci, F.; Roffia, S.; Taylor, R.; Wachter, N. K. *J. Chem. Soc., Perkin Trans. 2* **2000**, 1409–1414.
267. Cases, M.; Duran, M.; Mestres, J.; Martín, N.; Solà, M. *J. Org. Chem.* **2001**, *66*, 433–442.
268. Prato, M.; Li, Q. C.; Wudl, F. *J. Am. Chem. Soc.* **1993**, *115*, 1148–1150.
269. Grosser, T.; Prato, M.; Lucchini, V.; Hirsch, A.; F., W. *Angew. Chem., Int. Ed. Engl.* **1995**, *34*, 1343–1345.
270. Nuber, B.; Hampel, F.; Hirsch, A. *J. Chem. Soc., Chem. Commun.* **1996**, 1799–1800.
271. Yashiro, A.; Nishida, Y.; Ohno, M.; Eguchi, S.; Kobayashi, K. *Tetrahedron Lett.* **1998**, *39*, 9031–9034.

272. Maggini, M.; Scorrano, G.; Prato, M. *J. Am. Chem. Soc.* **1993**, *115*, 9798-9799.
273. Tagmatarchis, N.; Prato, M. *Synlett* **2003**, 768-779.
274. Prato, M.; Maggini, M. *Acc. Chem. Res.* **1998**, *31*, 519-526.
275. Bianco, A.; Ros, T. D.; Prato, M.; Toniolo, C. *J. Pept. Sci.* **2001**, *7*, 208-209.
276. Kahnt, A.; Quintiliani, M.; Vázquez, P.; Guldi, D. M.; Torres, T. *ChemSusChem* **2008**, *1*, 97-102.
277. Nakamura, Y.; Takano, N.; Nishimura, T.; Yashima, E.; Sato, M.; Kudo, T.; Nishimura, J. *Org. Lett.* **2001**, *3*, 1193-1196.
278. Schuster, D. I.; Cao, J.; Kaprinidis, N.; Wu, Y.; Jensen, A. W.; Lu, Q.; Wang, H.; Wilson, S. R. *J. Am. Chem. Soc.* **1996**, *118*, 5639-5647.
279. Bemstein, R.; Foote, C. S. *Tetrahedron Lett.* **1998**, *39*, 7051-7054.
280. Vassilikogiannakis, G.; Chronakis, N.; Orfanopoulos, M. *J. Am. Chem. Soc.* **1998**, *120*, 9911-9920.
281. Matsui, S.; Kinbara, K.; Saigo, K. *Tetrahedron Lett.* **1999**, *40*, 899-902.
282. Diederich, F.; Isaacs, L.; Philp, D. *Chem. Soc. Rev.* **1994**, *23*, 243-255.
283. Smith, A. B.; Tokuyama, H. *Tetrahedron* **1996**, *52*, 5257-5262.
284. Zhu, Y.; Bahnmüller, S.; Chisun, C.; Carpenter, K.; Hosmane, N. S.; Maguire, J. A. *Tetrahedron Lett.* **2003**, *44*, 5473-5476.
285. Segura, J.; Martín, N.; Guldi, D. M. *Chem. Soc. Rev.* **2005**, *34*, 31-47.

286. Nierengarten, J.-F. *Sol. Energy Mater. Sol. Cells* **2004**, *83*, 187–199.
287. Roncali, J. *Chem. Soc. Rev.* **2005**, *34*, 483–495.
288. Brabec, C. J.; Sariciftci, N. S.; Hummelen, J. C. *Adv. Funct. Mater.* **2001**, *11*, 15–25.
289. van Duren, J. K. J.; Yang, X.; Loos, J.; Bulle-Lieuwma, C. W. T.; Sieval, A. B.; Hummelen, J. C.; Janssen, R. A. J. *Adv. Funct. Mater.* **2004**, *14*, 425–434.
290. Imahori, H.; Cardoso, S.; Tatman, T.; Lin, S.; Noss, L.; Seely, G. R.; Sereno, L.; de Silber, J. C.; Moore, T. A.; Moore, A. L.; Gust, D. *Photochem. Photobiol.* **1995**, *62*, 1009–1014.
291. Eckert, J.-F.; Nicoud, J.-F.; Nierengarten, J.-F.; Liu, S.-G.; Echegoyen, L.; Barigelletti, F.; Armaroli, N.; Ouali, L.; Krasnikov, V.; Hadzioannou, G. *J. Am. Chem. Soc.* **2000**, *122*, 7467–7479.
292. Narutaki, M.; Takimiya, K.; Otsubo, T.; Harima, Y.; Zhang, H.; Araki, Y.; Ito, O. *J. Org. Chem.* **2006**, *71*, 1761–1768.
293. Atienza, C.; Insuasty, B.; Seoane, C.; Martin, N.; Ramey, J.; Guldi, D. M. *J. Mater. Chem.* **2005**, *15*, 124–132.
294. Cheng, G.; Zhao, Y. *Tetrahedron Lett.* **2006**, *47*, 5069–5073.
295. Sanchez, L.; Herranz, M. A.; Martin, N. *J. Mater. Chem.* **2005**, *15*, 1409–1421.
296. Sanchez, L.; Sierra, M.; Martin, N.; Guldi, D. M.; Wienk, M. W.; Janssen, R. A. J. *Org. Lett.* **2005**, *7*, 1691–1694.

297. Wilson, J. N.; Windscheif, P. M.; Evans, U.; Myrick, M. L.; Bunz, U. H. F. *Macromolecules* **2002**, *35*, 8681–8683.
298. Zhou, N.; Wang, L.; Thompson, D. W.; Zhao, Y. unpublished results.
299. Zhao, Y.; Shirai, Y.; Slepko, A. D.; Cheng, L.; Almeny, L. B.; Sasaki, T.; Heilmann, F. A.; Tour, J. M. *Chem. Eur. J.* **2005**, *11*, 3643–3658.
300. Baughman, R. H.; Yee, K. C. *J. Polym. Sci. Macromol. Rev.* **1978**, *13*, 219–239.
301. Bernasconi, M.; Chiarotti, G. L.; Focher, P.; Parrinello, M.; Tosatti, E. *Phys. Rev. Lett.* **1997**, *78*, 2008–2011.
302. Schmitz, J. V.; Lawton, E. J. *Science* **1951**, *113*, 718–719.
303. Mesrobian, B.; Ander, P.; Ballantine, D. S. *J. Phys. Chem.* **1954**, *22*, 565–566.
304. Henglein, A.; Schulz, R. *Z. Naturforsch. B* **1954**, *9*, 617–618.
305. Lawton, E. J.; Grubb, W. T.; Balwit, J. B. *J. Polym. Sci.* **1956**, *19*, 455–458.
306. Restaino, A. J.; Mesrobian, R. B.; Morawetz, H.; Ballantine, D. S.; Dienes, G. J.; Metz, D. J. *J. Am. Chem. Soc.* **1956**, *78*, 2939–2943.
307. Hlavaty, J.; Kavan, L.; Okabe, K.; Oya, A. *Carbon* **2002**, *40*, 1147–1150.
308. Lagow, R.; Kampa, J.; Wei, H.; Battles, S.; Genge, J.; Lande, D.; Harper, C.; Bau, R.; Stevens, R.; Haw, J.; Munson, E. *Science* **1995**, *267*, 362–367.
309. Ding, L.; Olesik, S. *Nano Lett.* **2004**, *4*, 2271–2276.

310. Nijhoff, M. In *Polydiacetylenes*; Bloor, D., Chance, R. R., Eds.; NATO ASI Series E, Applied Science 102; Dordrecht, The Netherlands, 1985.
311. Enkelmann, V. *Adv. Polym. Sci.* **1984**, *63*, 91-136.
312. Wegner, G. *Z. Naturforsch.* **1969**, *24B*, 824-832.
313. Donovan, K. J.; Wilson, E. G. *Philos. Mag.* **1981**, *B44*, 9-29.
314. Molyneux, S.; Matsuda, H.; Kar, A. K.; Wherett, B. J.; Okada, S.; Nakanishi, H. *Nonlinear Opt.* **1993**, *4*, 299-304.
315. Hattori, T.; T., K. *Chem. Phys. Lett.* **1987**, *133*, 230-234.
316. Matsuda, H.; Nakanishi, H.; Hosomi, T.; Kato, M. *Macromolecules* **1988**, *21*, 1238-1240.
317. Okada, S.; Hayamizu, K.; Matsuda, H.; Masaki, A.; Minami, N.; Nakanishi, H. *Macromolecules* **1994**, *27*, 6259-6266.
318. Shimada, S.; Masaki, A.; Okada, S.; Nakanishi, H. *Nonlinear Opt.* **1995**, *13*, 57-62.
319. Shimada, S.; Masaki, A.; Hayamizu, K.; Matsuda, H.; Okada, S.; Nakanishi, H. *Chem. Commun.* **1997**, 1421-1422.
320. Okada, S.; Hayamizu, K.; Matsuda, H.; Masaki, A.; Nakanishi, H. *Bull. Chem. Soc. Jpn.* **1991**, *64*, 857-863.
321. Sarkar, A.; Okada, S.; Komatsu, K.; Nakanishi, H. *Macromolecules* **1998**, *31*, 5624-5630.

322. Yoshino, K.; Yin, X.; Muro, K.; Kiyomatsu, S.; Morita, S.; Zakhidov, A. A. *Jpn. J. Appl. Phys.* **1993**, *32(3A)*, L357-L360.
323. *Optical and Electronic Properties of Fullerenes and Fullerene-Based Materials*; Shinar, J., Vardeny, Z. V., Kafafi, Z. H., Eds.; New York: Marcel Dekker, 2000.
324. Taylor, R.; Walton, D. R. M. *Nature* **1993**, *363*, 685-693.
325. Hirsch, A. *Angew. Chem., Int. Ed. Engl.* **1993**, *32*, 1138-1141.
326. Diederich, F.; Thilgen, C. *Science* **1996**, *271*, 317-323.
327. Proto, M. *J. Mater. Chem.* **1997**, *7*, 1097-1109.
328. Zhang, F. I.; Svensson, M.; Andersson, M. R.; Maggini, M.; Bucella, S.; Menna, E.; Inganäs, O. *Adv. Mater.* **2001**, *13*, 1871-1874.
329. Ramos, A. M.; Rispens, M. T.; van Duren, J. K. J.; Hummelen, J. C.; Janssen, R. A. J. *J. Am. Chem. Soc.* **2001**, *123*, 6714-6715.
330. Zhao, Y.; McDonald, R.; Tykwinski, R. R. *J. Org. Chem.* **2002**, *67*, 2805-2812.
331. Opsitnick, E.; Lee, D. *Chem. Eur. J.* **2007**, *13*, 7040-7049.
332. Lim, Y.-K.; Jiang, X.; Bollinger, J. C.; Lee, D. *J. Mater. Chem.* **2007**, *19*, 1969-1980.
333. Mossinger, D.; Hornung, J.; Lei, S.; De Feyter, S.; Hoger, S. *Angew. Chem., Int. Ed.* **2007**, *46*, 6802-6806.
334. Lukes, V.; Matuszyna, K.; Raptá, P.; Solc, R.; Dunsch, L.; Aguiar, A. J.; Lischka, H. *J. Phys. Chem. C* **2008**, *112*, 3949-3958.

335. Spitler, E. L.; Shirtcliff, L. D.; Haley, M. M. *J. Org. Chem.* **2007**, *72*, 86-96.
336. Ito, S.; Akimoto, K.; Kawakami, J.; Tajiri, A.; Shoji, T.; Satake, H.; Morita, N. *J. Org. Chem.* **2007**, *72*, 162-172.
337. Samori, S.; Tojo, S.; Fujitsuka, M.; Spitler, E. L.; Haley, M. M.; Majima, T. *J. Org. Chem.* **2007**, *72*, 2785-2793.
338. Marsden, J. A.; Miller, J. J.; Shirtcliff, L. D.; Haley, M. M. *J. Am. Chem. Soc.* **2005**, *127*, 2464-2476.
339. He, F.; Tian, L.; Tian, X.; Xu, H.; Wang, Y.; Xie, W.; Hanif, M.; Xia, J.; Shen, F.; Yang, B.; Li, F.; Ma, Y.; Yang, Y.; Shen, J. *Adv. Funct. Mater.* **2007**, *17*, 1551-1557.
340. Fratiloiu, S.; Senthilkumar, K.; Grozema, F. C.; Christian-Pandya, H.; Niazimbetova, Z. I.; Bhandari, Y. J.; Galvin, M. E.; Siebbeles, L. D. A. *Chem. Mater.* **2006**, *18*, 2118-2129.
341. Masunov, A.; Tretiak, S.; Hong, J. W.; Liu, B.; Bazan, G. C. *J. Chem. Phys.* **2005**, *122*, 224505.
342. Sun, X.; Liu, Y.; Chen, S.; Qiu, W.; Yu, G.; Ma, Y.; Qi, T.; Zhang, H.; Xu, X.; Zhu, D. *Adv. Funct. Mater.* **2006**, *16*, 917-925.
343. Bilge, A.; Zen, A.; Forster, M.; Li, H.; Galbrecht, F.; Nehls, B. S.; Farrell, T.; Neher, D.; Scherf, U. *J. Mater. Chem.* **2006**, *16*, 3177-3182.
344. Zen, A.; Bilge, A.; Galbrecht, F.; Alle, R.; Meerholz, K.; Grenzer, J.; Neher, D.; Scherf, U.; Farrell, T. *J. Am. Chem. Soc.* **2006**, *128*, 3914-3915.

345. Hauck, M.; Schönhaber, J.; Zuccherro, A. J.; Hardcastle, K. I.; Müller, T. J. J.; Bunz, U. H. F. *J. Org. Chem.* **2007**, *72*, 6714–6725.
346. McGrier, P. L.; Soltsev, K. M.; Schönhaber, J.; Brombosz, S. M.; Tolbert, L. M.; Bunz, U. H. F. *Chem. Commun.* **2007**, 2127–2129.
347. Zuccherro, A. J.; Wilson, J. N.; Bunz, U. H. F. *J. Am. Chem. Soc.* **2006**, *128*, 11872–11881.
348. Gerhardt, W. W.; Zuccherro, A. J.; Wilson, J. N.; South, C. R.; Bunz, U. H. F.; Weck, M. *Chem. Commun.* **2006**, 2141–2143.
349. Wilson, J. N.; Bunz, U. H. F. *J. Am. Chem. Soc.* **2005**, *127*, 4142–4125.
350. Grunder, S.; Huber, R.; Horhoiu, V.; Gonzalez, M. T.; Schonenberger, C.; Calame, M.; Mayor, M. *J. Org. Chem.* **2007**, *72*, 8337–8344.
351. Yi, Y.; Zhu, L.; Shuai, Z. *Macromol. Theory Simul.* **2008**, *17*, 12–22.
352. Slepko, A. D.; Hegmann, F. A.; Tykwinski, R. R.; Kamada, K.; Ohta, K.; Marsden, J. A.; Spitler, E. L.; Miller, J. J.; Haley, M. M. *Opt. Lett.* **2006**, *31*, 3315–3317.
353. Meier, H.; Holst, H. C.; Oehlhof, A. *Eur. J. Org. Chem.* **2003**, 4173–4180.
354. Wurthner, F.; Thalacker, S.; Dicke, S.; Tschierske, C. *Chem. Eur. J.* **2001**, *7*, 2245–2253.
355. Veenstra, S. C.; van Hutten, P. F.; Post, A.; Wang, G.; and Hadziioannou; Jonkman, H. T. *Thin Solid Films* **2002**, *422*, 104–111.

356. Samori, S.; Tojo, S.; Fujitsuka, M.; Spitler, E. L.; Haley, M. M.; Majima, T. *J. Org. Chem.* **2008**, *73*, 3551–3558.
357. Karabunarliev, S.; Baumgarten, M.; Bittner, E. R.; Müllen, K. *J. Chem. Phys.* **2000**, *113*, 11372–11381.
358. James, T. D.; Sandanayake, K. R. A. S.; Shinkai, S. *Angew. Chem., Int. Ed. Engl.* **1996**, *35*, 1910–1922.
359. Wiskur, S. L.; Ait-Haddou, H.; Lavigne, J. J.; Anslyn, E. V. *Acc. Chem. Rev.* **2001**, *34*, 963–972.
360. Wang, W.; Gao, X.; Wang, B. *Curr. Org. Chem.* **2002**, *6*, 1285–1317.
361. Gamsey, S.; Miller, A.; Olmstead, M. M.; Beavers, C. M.; Hirayama, L. C.; Pradhan, S.; Wessling, R. A.; Singaram, B. *J. Am. Chem. Soc.* **2007**, *129*, 1278–1286.
362. Berube, M.; Dowlut, M.; Hall, D. G. *J. Org. Chem.* **2008**, *73*, 6471–6479.



